R loop resolution reverses DNA instability associated with SMN deficiency and protects against neurodegeneration in SMA

EVANGELIA KARYKA

Submitted for the degree of Doctor of Philosophy (PhD)

Sheffield Institute for Translational Neuroscience
University of Sheffield

September 2017

ABSTRACT

Spinal muscular atrophy (SMA) is a devastating genetic childhood neurodegenerative disorder characterised by progressive loss of lower motor neurons due to reduced levels of the ubiquitously expressed survival motor neuron (SMN) protein. SMN is a multifunctional protein and it is still unclear which of the numerous functions of SMN is essential for the survival of motor neurons. Emerging evidence suggests that SMN may have a role as a guardian of genome integrity. Interestingly, DNA damage and genome instability have been linked to numerous neurodegenerative diseases. Therefore, the main aim of this project is to examine DNA damage in SMA and to address whether DNA damage is a contributing factor for the neurodegenerative process of SMA, and if so to introduce new therapeutic targets for treating SMA. The data collected during this PhD project are described under four chapters. Firstly, established DNA repair assays were used to show accumulation of endogenous DNA breaks in SMA experimental models including fibroblasts derived for SMA type I patients, embryonic cortical and motor neurons isolated from SMNΔ7 mice, murine spinal cord and brain tissue as well as human post-mortem tissue. Secondly, the increased DNA damage seen in SMA was shown to be transcription-dependent and associated to the formation of R loops. In addition, a significant reduction in DNA damage after lentiviral-mediated overexpression of SMN, revealed that the observed DNA damage could be a direct consequence of SMN deficiency. Moreover, adenoviral-mediated overexpression of senataxin (SETX), an R loop resolution helicase, reversed the DNA damage caused by SMN-deficiency and also ameliorated the neurodegenerative phenotype in model systems of SMA. Finally, nucleolar disruption caused by rDNA damage was observed in SMA

and a novel interaction between SMN and RNA polymerase I was revealed, disruption of which may lead to the observed nucleolar phenotype. In conclusion, these data demonstrate a physiological role for SMN in maintaining transcriptional integrity and highlight the therapeutic potential of senataxin to alleviate neurodegeneration in SMA.

ACKNOWLEDGMENTS

Firstly, I would like to thank my joint supervisors Prof. Mimoun Azzouz and Prof. Sherif El-Khamisy and co-supervisor Dr. Guillaume Hautbergue, without whom this PhD project would not have been possible. I really appreciate their patience, constant encouragement and endless support. My sincere thanks also go to Mr Gareth Davis and Mrs Andrea Davis for funding my research in memory of their daughter Eve.

Secondly, I am grateful to all my colleagues in the Sheffield Institute for Translational Neuroscience (SITraN) as well as the department of Molecular Biology and Biotechnology (MBB) at the University of Sheffield. In particular, I would like to thank Callum Walker, Dr. Jayanth Chandran, Dr. Saul Herranz-Martin, Dr. Katherine Lewis, Dr. Vera Lukashchuk, Dr. Tomasso Iannitti, Ioannis Tsagakis, Ian Coldicott, Dr. Swagat Ray, Dr. Shih-Chieh Chiang and Dr. Chunyan Liao for their continued assistance and support. They managed to create a very pleasant and friendly environment to work in. I would also like to thank anyone else from the Azzouz, El-Khamisy and Hautbergue labs.

Most importantly, I need to thank my family and in particular my husband Suat who has accompanied me with unlimited patience and constant support. I give my heartfelt appreciation to him for looking after our daughter when I was not there. I am also indebted to my parents who have always believed in me and taught me that nothing is impossible and that I should never stop chasing my dreams. Last but not least, special thanks and appreciation are due to my brother Theodoros for always being there for me.

This PhD thesis is dedicated to my parents,

Sofia and Panagiotis

Table of Contents

1. INTRODUCTION 15
1.1 SPINAL MUSCULAR ATROPHY 16
1.1.1 Clinical features of SMA 17
1.1.2 Molecular genetics 18
1.1.3 Experimental models of SMA 21
1.1.4 SMN: a multifunctional protein 25
1.2 DNA damage and neurodegeneration 37
1.2.1 Ataxia telangiectasia as a model of DDR-defective neurodegenerative disorder 40
1.2.2 Transcription as a source of genomic instability 41
1.2.3 R loop-associated DNA damage and neurodegeneration 44
1.3 Treatment of SMA 46
1.3.1 SMN-dependent therapeutic strategies 46
1.3.2 SMN-independent therapeutic strategies 50
1.4 Project aims 51
2. MATERIALS AND METHODS 54
2.1 Materials 55
2.1.1 DNA preparation 55
2.1.2 Expression constructs 55
2.1.3 Viral vectors 55
2.1.4 Antibodies 55
2.1.5 Post-mortem tissue 57
2.1.6 Reagents and chemicals 57
2.1.7 Equipment 57
2.2 In vitro experimental methods 58
2.2.1 Cells and cell culture maintenance 58
2.2.2 Immunocytochemistry 60
2.2.3 Comet assay 61
2.2.4 DNA/RNA immunoprecipitation (DRIP) followed by qPCR 61

2.2.5 Phenol-chloroform extraction 63
2.2.6 Subcloning of SMN FL and SMN Δ3 64
2.2.7 Production of lentiviral vectors 64
2.2.8 Western blotting 65
2.2.9 Cytoplasmic/Nuclear fractionation 66
2.2.10 Neurite outgrowth assay 67
2.2.11 γH2AX-ChIP 67
2.2.12 RT-qPCR 69
2.3 In vivo experimental methods 70
2.3.1 Breeding and genotyping of transgenic mice 70
2.3.2 Viral vector delivery 72
2.3.3 Behavioural and clinical assessment 73
2.3.4 Tissue collection 73
2.3.5 Neuromuscular analysis 74
2.3.6 Measurement of topoisomerase 1 cleavage complexes (TOP1cc) 74
2.3.7 Immunohistochemistry 75
2.3.8 Randomization and blinding process 77
2.3.9 Experimental repeats and Statistical analysis 78
3. Elevated DNA breaks in human and murine experimental models of SMA 79
3.1 Aim 80
3.2 Cellular models 81
3.2.1 SMA type I fibroblasts display elevated endogenous DNA breaks 81
3.2.2 Smn-depleted cultured neurons develop hallmarks of endogenous DNA instability 84
3.3 In vivo animal models 94
3.3.1 SMA mouse model exhibit increased DNA damage in the spinal cord 94
3.3.2 SMN deficiency results in TOP1cc accumulation in brain tissue 98
3.4 Post-mortem tissue 100
3.4.1 DNA damage is observed in post-mortem tissue from SMA patients 100
3.5 Discussion 102
4. Unravelling the role of SMN protein in genomic integrity 105
4.1 Aim 106
4.2 The accumulation of DNA damage observed in SMA cases is transcription dependent 107
4.3 SMN-deficient cells exhibit increased number of R loops 111

4.4 SMN protein accumulates in the nucleus upon induction of DNA damage 116
4.5 SMN restoration decreases the number of DNA breaks in SMN-deficient cells 119
4.6 SMN Tudor domain is important for DNA damage prevention 122
4.7 Discussion 128
5. Senataxin: A new therapeutic target for treating SMA 131
5.1 Aim 132
5.2 SETX overexpression reverses the elevated levels of DNA breakage 133
5.3 SETX overexpression ameliorates the neurodegenerative phenotype in model systems of SMA 138
5.4 Discussion 151
6. Nucleolar disruption in response to rDNA damage in SMN-deficient cells 153
6.1 Aim 154
6.2 SMN – deficient cells exhibit increased nucleolar disruption 155
6.3 The nucleolar reorganization of SMN-deficient cells could be attributed to rDNA breaks and RNA polymerase I inhibition 158
6.4 RNA polymerase I: a novel SMN-interacting protein 162
6.5 SMN overexpression reduces nucleolar stress 165
6.6 Discussion 168
7. GENERAL DISCUSSION 170
7.1 Project outcomes 172
7.2 Future work 175
8. BIBLIOGRAPHY 178
9. APPENDIX 208

LIST OF FIGURES

Figure 1-1: Splicing of *SMN1* and *SMN2* genes. 21
Figure 1-2: Schematic diagram of SMN. 25
Figure 1-3: The role of SMN protein in the biogenesis of snRNPs. 29
Figure 1-4: R-loop structure. 41
Figure 1-5: Mechanism of action of Spinraza. 48
Figure 3-1: γH2AX staining in SMA type I fibroblasts. 82
Figure 3-2: 53BP1 staining in SMA type I fibroblasts. 84
Figure 3-3: Cortical neuron cultures stained with neuronal marker MAP2. 86
Figure 3-4: 53BP1 and SMN dual staining in SMA cortical neurons. 87
Figure 3-5: γH2AX staining in embryonic cortical neurons. 88
Figure 3-6: Comet assay in cortical neurons. 90
Figure 3-7: Motor neuron culture prepared using p75 immunopanning method. 92
Figure 3-8: γH2AX staining in murine embryonic motor neurons. 93
Figure 3-9: γH2AX staining in SMNΔ7 mouse spinal cords. 95
Figure 3-10: γH2AX and CGRP dual staining in SMNΔ7 mouse spinal cords. 96
Figure 3-11: 53BP1 and NeuN double staining in SMNΔ7 mouse spinal cords. 97
Figure 3-12: TOP1-cc accumulation in SMA mouse brain tissue. 100
Figure 3-13: γH2AX staining in human SMA post-mortem spinal cords. 101
Figure 4-1: Transcription inhibition in SMA type I fibroblasts. 108
Figure 4-2: Transcription inhibition in SMA motor neurons. 110
Figure 4-3: S9.6 staining in SMA cultured motor neurons. 112
Figure 4-4: RNA/DNA hybrids accumulate in actively transcribed genes in SMN-deficient cells. 113
Figure 4-5: S9.6 staining in SMA mouse spinal cords. 114
Figure 4-6: S9.6 staining in human SMA post-mortem spinal cords. 115
Figure 4-7: Acute accumulation of SMN protein in the nucleus upon induction of DNA damage. 118
Figure 4-8: LV-SMN mediated transduction efficiency in SMA fibroblasts. 120
Figure 4-9: Lentiviral-mediated restoration of SMN in SMA type I fibroblasts reduces the number of DSBs. 122
Figure 4-10: LV-SMNΔ3 transduction efficiency in human fibroblasts. 125
Figure 4-11: Lentiviral-mediated overexpression of SMNΔ3 in SMA type I fibroblasts fails to reduce DSBs. 127
Figure 5-1: Ad-SETX mediated transduction of MRC-5 cells. 134
Figure 5-2: Ad-RFP transduction efficiency in spinal cord mixed cultures. 135
Figure 5-3: R loop (S9.6) staining of Ad-SETX transduced SMA motor neurons. 136
Figure 5-4: γH2AX staining of Ad-SETX transduced SMA motor neurons. 137
Figure 5-5: Ad-SETX gene transfer mediates neurite outgrowth improvement. 139
Figure 5-6: Retrograde transport of adenoviral vector when peripherally administered. 140
Figure 5-7: Overexpression of SETX in muscle of Ad-SETX injected mice. 141
Figure 5-8: Retrograde transport of Ad-RFP. 142
Figure 5-9: Ad-SETX mediates transduction of spinal motor neuron by retrograde transport. 143

Figure 5-10: SETX overexpression reduces DSBs as revealed by γH2AX staining of spinal cords derived from Ad-SETX and Ad-RFP injected mice. 144
Figure 5-11: Ad-SETX mediates neuroprotection of lumbar spinal motor neurons. 146
Figure 5-12: Rescue of NMJ pathology in Ad-SETX injected SMA mice. 147
Figure 5-13: Survival analysis and body weight assessment of SMNΔ7 mice after unilateral i.m. injections. 150
Figure 6-1: R loop staining in SMA type I fibroblasts. 156
Figure 6-2: Nucleolin staining in experimental cell models of SMA. 157
Figure 6-3: Nucleolus structure. 158
Figure 6-4: SMA type I fibroblasts form nucleolar caps containing DSBs. 159
Figure 6-5: γH2AX-ChIP followed by qPCR analysis of ribosomal genes. 160
Figure 6-6: Analysis of rRNA synthesis. 161
Figure 6-7: SMN protein interacts with RNA polymerase I. 163
Figure 6-8: SMN-RNA polymerase I interaction is RNA-independent. 164
Figure 6-9: Lentiviral-mediated SMN replacement restores normal nucleolar morphology in SMN-deficient cells. 167

LIST OF TABLES

Table 1-1: Classification of Spinal Muscular Atrophy 18
Table 1-2: Major DNA damage repair pathways in mammalian cells 38
Table 1-3: SMA therapy pipeline 51
Table 2-1: List of viral vectors used 55
Table 2-2: List of primary antibodies used 56
Table 2-3: List of secondary antibodies used 56
Table 2-4: Human tissue information 57
Table 2-5: List of equipment used 57
Table 2-6: Primers used for DRIP-qPCR 62
Table 2-7: Titres of lentiviral vectors 65
Table 2-8: Primers used for γH2AX ChIP-qPCR 69
Table 2-9: Primers used for RT-qPCR 70
Table 2-10: Wild type (WT) reaction setup 71
Table 2-11: Mutant (MT) reaction setup 71

LIST OF ABBREVIATIONS

AAV	Adeno-associated virus
Ad	Adenovirus
ANOVA	Analysis of variance
AP	Apurinic/apyrimidinic sites
APE1	AP endonuclease 1
APOE	Apolypoprotein E
ASO	Antisense oligonucleotide
AT	Ataxia telangiectasia
ATLD	Ataxia telangiectasia-like disorder
BCA	Bicinchoninic acid
BDNF	Brain-derived neurotrophic factor
BRCA1	Breast cancer gene 1
BSA	Bovine serum albumin
BTBD19	BTB domain containing 19
C	Cytosine
C. elegans	*Caenorhabditis elegans*
CB	Cajal bodies
CGRP	Calcitonin gene-related peptide
CMV	Cytomegalovirus
CNS	Central nervous system
CNTF	Ciliary neurotrophic factor
coSMN	Codon-optimised SMN
CsCl	Caesium chloride
CTD	COOH-terminal domain
DIV	Day *in vitro*
DMEM	Dulbecco's Minimum Essential Medium
DNA	Deoxyribonucleic acid
DSBs	Double-strand breaks
EDTA	Ethylenediaminetetraacetic acid
EGR1	Early growth response 1
eIFs	eukaryotic initiation factors
EMA	European Medicines Agency
EMEM	Eagle's minimum essential medium
ENS	Enteric nervous system
FBS	Fetal bovine serum
FDA	Food and Drug Administration
FUS	Fused in sarcoma
G3BP	GTPase activating protein binding protein
Gap43	Growth-associated protein 43
GAR1	G protein-linked acetylcholine receptor 1
GDNF	Glial cell line-derived neurotrophic factor
H_2O_2	Hydrogen peroxide
HDACs	Histone deacetylases
HEK	Human embryonic kidney
HeLa	Henrietta Lacks

hnRNP	heterogeneous ribonucleoprotein particle
HR	Homologous recombination
iMNs	induced motor neurons
IMP1	Inner Membrane Peptidase Subunit 1
iPSCs	induced pluripotent stem cells
KSRP	K-homology splicing regulatory protein
LV	Lentivirus
MAP2	Microtubule associated protein 2
MDC1	mediator of DNA damage checkpoint 1
MRC5	Medical research council cell-strain 5
Mre11	Meiotic recombination 11a homolog
MRN	Mre11-Rad50-Nbs1
MYADM	Myeloid-associated differentiation marker
NAF1	Nuclear Assembly Factor 1 Ribonucleoprotein
Nbs1	Nijmegan breakage syndrome 1
NeuN	Neuronal-specific nuclear protein
NHEJ	Non-homologous end joining
Nhp2	H/ACA ribonucleoprotein complex subunit 2
Nop10	Nucleolar protein 10
Nop56	Nucleolar protein 56
Nop58	Nucleolar protein 58
OCT	Optimum cutting temperature medium
PABP	poly[A]$^+$ mRNA binding protein
PBS	Phosphate buffered saline
PCR	Polymerase chain reaction
PDBs	protein-linked DNA breaks
PFA	Paraformaldehyde
PGK	Phosphoglycerate kinase
PIKK	phosphatidylinositol 3-kinase-related kinase
PLS3	Plastin 3
POLβ	DNA polymerase β
PVDF	Polyvinylidene difluoride
qPCR	Quantitative polymerase chain reaction
Rad50	Radiation-sensitive 50
RFP	Red fluorescent protein
RIPA	Radioimmunoprecipitation
RNA	Ribonucleic acid
RNF168	RING finger protein 168
RNF8	RING finger protein 8
RNP	Ribonucleoprotein
ROS	Reactive oxygen species
RPL32	Ribosomal protein L32
rRNAs	Ribosomal ribonucleic acid
RT-qPCR	Reverse transcription quantitative polymerase chain reaction
scaRNPs	CB-specific RNPs
SCGE	Single-cell gel electrophoresis
SETX	Senataxin
SGs	Stress granules
SMA	Spinal Muscular Atrophy
SMN	Survival motor neuron

SMNΔ7	SMN deleted exon7
snoRNPs	small nucleolar ribonucleoproteins
snRNPs	small nuclear ribonucleoproteins
SNRPN	Small nuclear ribonucleoprotein polypeptide N
SSBs	Single-strand breaks
T	Thymine
TDP1	Tyrosyl-DNA phosphodiesterase 1
TE	Tris-EDTA buffer solution
TIA-1	T-cell internal antigen-1
TIAR	TIA-1-related protein
TOP1	Topoisomerase I
TOP1cc	TOP1-DNA cleavage complex
TTP	Tristetraprolin
Unrip	Unr-interacting protein
WPRE	Woodchuck hepatitis virus posttranscriptional regulatory element
WRAP53	WD40 encoding RNA Antisense to p53
XPF	Xeroderma pigmentosum group F
XPG	Xeroderma pigmentosum group G

1. INTRODUCTION

1.1 SPINAL MUSCULAR ATROPHY

Spinal muscular atrophy (SMA) is a fatal, autosomal recessive neurodegenerative disorder characterised by selective loss of lower alpha motor neurons in the anterior horn of the spinal cord leading to muscle atrophy and weakness. The proximal voluntary muscles of the limbs and the trunk, in some cases, are predominantly affected (Wang *et al.*, 2007). It is considered the most common genetically inherited neurological disorder resulting in infant mortality (Nash *et al.*, 2016). There is a carrier frequency of 1 in 40-60 and an incidence of 1 in 6,000-10,000 live births in the human population (Ogino *et al.*, 2002; Prior *et al.*, 2010). In most severe cases, patients die before reaching 2 years of age, usually because of respiratory failure.

SMA is caused by homozygous mutations or deletion of the *Survival Motor Neuron 1* gene (*SMN1*). That loss of function leads to reduced levels of the ubiquitously expressed SMN protein (Lefebvre *et al.*, 1995). Although, motor neurons are the most severely affected cells, emerging evidence suggests that additional cell types in the central nervous system (CNS), such as sensory neurons, astrocytes and microglial; cells in the enteric nervous system (ENS) as well as liver, muscle and heart are also vulnerable in SMA, indicating that SMA could be a multi-system disorder rather than a cell autonomous one (Arnold *et al.*, 2004; Braun *et al.*, 1995; Gombash *et al.*, 2015; Imlach *et al.*, 2012; Lotti *et al.*, 2012; Martinez-Hernandez *et al.*, 2009; McGivern *et al.*, 2013; Mentis *et al.*, 2011; Rindt *et al.*, 2015; Rudnik-Schoneborn *et al.*, 2003; Rudnik-Schoneborn *et al.*, 2008; Shababi *et al.*, 2010; Tarabal *et al.*, 2014; Vitte *et al.*, 2004). However, some of these findings were generated in pre-clinical models and would need confirmation clinically in SMA patients.

1.1.1 Clinical features of SMA

The clinical symptoms of SMA involve progressive muscle weakness, leading to muscular atrophy. The proximal voluntary muscles are primarily affected, and patients lose or never acquire motor skills during disease progression. The observed muscle wasting is a result of degeneration of the alpha motor neurons of the spinal cord (Lunke *et al.*, 2013). SMA is clinically classified into four main types based on the age of onset and maximum function achieved as presented in **Table 1-1** (Markowitz *et al.*, 2012; Russman, 2007; Wang *et al.*, 2007). Patients with SMA type I (Weirdnig-Hoffman disease or 'acute' SMA), which is the most common form, are characterised by severe muscular problems in infancy (< 6 months of age), they are never able to sit and with rare exceptions death occurs before the age of two, mainly because of respiratory insufficiency if ventilator support is not provided. Patients with SMA type II (intermediate or chronic SMA) have onset between 6 months and 18 months of age but may manifest earlier. Even though they can sit, SMA type II cases are not able to walk unsupported. These patients are expected to live for decades but they face aggressive respiratory problems. The symptoms of patients suffering from type III SMA (juvenile SMA or Kugelberg-Welander disease) make their first appearance usually after the age of 18 months. The patients with this form of SMA manage to stand and walk without any support at least initially but as they age and the disease worsens these motor abilities are lost, and the patients become wheelchair bound. Type IV is a rare form, with symptoms very similar to type III but with onset in adulthood (around 20-30 years old). The life expectancy of this group is normal. Another type of SMA has also been reported, SMA type 0 which is an embryonic form of the disease. It is a very severe form of SMA characterised by diminished movement of the foetus in utero presenting at birth with severe weakness

and asphyxia requiring immediate ventilator support. The life expectancy of this group is very short (Dubowitz, 1999; Zerres *et al.*, 1995).

Table 1-1: Classification of Spinal Muscular Atrophy

Type	Age at onset	Motor milestones	Life expectancy
SMA type 0	Prenatal	Need respiratory support from birth	Limited
SMA type I	<6 months	Never sit	<2 years
SMA type II	6-18 months	Sit with assistance	>2 years
SMA type III	>18 months	Stand and walk	Adulthood
SMA type IV	20-30 years	Walk normally	Normal

(Markowitz *et al.*, 2012; Russman, 2007; Wang *et al.*, 2007).

1.1.2 Molecular genetics

SMN is an evolutionarily conserved gene. However, humans, unlike other species, carry two very similar copies of the gene located in a duplicated region of chromosome 5 (5q13) (DiDonato *et al.*, 1997). There is a telomeric copy (*SMN1*) and a centromeric copy (*SMN2*); these two genes differ by only 5 bases. One of these base changes, a silent C to T substitution at position +6 of exon 7 affects the splicing of the SMN2 transcript causing exclusion of exon 7, resulting in SMNΔ7 mRNA and production of a truncated unstable protein (**Figure 1-1**). It is worth noting that this mutation is in close proximity to the 3' splicing site. The presence of C in *SMN1* exon 7 is believed to form an exonic splicing enhancer (ESE) recognised by the SR protein AS/SF2 and promotes exon 7 inclusion. The C to T substitution in *SMN2*

disrupts this ESE motif resulting in exon 7 exclusion (Cartegni *et al.*, 2006; Cartegni *et al.*, 2002b). Furthermore, the presence of T in *SMN2* exon 7 also creates an exonic splicing silencer (ESS) that is recognised by hnRNP A1 and Sam68 resulting in enhanced skipping of exon 7 (Kashima *et al.*, 2003; Pedrotti *et al.*, 2010). The protein product of the SMN2 transcript with exon 7 exclusion lacks the usual 16 C-terminal amino acids of SMN but has instead 4 amino acids, EMLA, encoded by exon 8 (Le *et al.*, 2005). Despite the high SMNΔ7 mRNA abundance, SMNΔ7 protein is barely detectable in SMA cases (Vitte *et al.*, 2007). The mechanism behind the instability of SMNΔ7 protein is not clear yet. One potential explanation could be the inability of SMNΔ7 protein to self-oligomerize and form complexes with its 'partner' proteins (Cartegni *et al.*, 2002a; Lorson *et al.*, 1999). It has been shown that incorporation of SMN protein into complexes dramatically increases its stability (Burnett *et al.*, 2009). Moreover, the instability of SMNΔ7 protein could also be attributed to the formation of a protein degradation signal (degron) at the C-terminal region of the protein (Cho *et al.*, 2010).

In SMA patients the *SMN1* gene is either missing (95% of cases) or mutated (5% of cases). Homozygous deletions of *SMN2* gene have also been reported with no clinical phenotype though (Wirth, 2000). *SMN1* functional loss leads to reduced levels of SMN protein (Lefebvre *et al.*, 1995).

The 5q13 chromosomal area is very unstable and *SMN1* gene is usually converted to *SMN2*, causing the *SMN2* copy number to vary among populations. For instance, patients with SMA type I have been reported to have either one or two *SMN2* copies, patients with type II have been shown to have three or more copies of *SMN2*, whereas patients with type III, a milder form of the disease, have up to 8 copies (Simic, 2008). The severity of the disease is therefore influenced by the copy number

of the *SMN2* gene (D'Amico *et al.*, 2011). However, *SMN2* is not the only disease modifier for SMA; in fact plastin 3 (*PLS3*), a gene encoding for an actin-binding protein important for axonogenesis, has been shown to influence the phenotype of SMA. In rare cases asymptomatic *SMN1*-depleted individuals were reported to have higher levels of PLS3 compared to their affected siblings, indicating that PLS3 is a modifier of disease severity in SMA (Oprea *et al.*, 2008). Notably, PLS3 overexpression in cultured primary motor neurons from SMA mice or in zebrafish embryos, *Caenorhabditis elegans* and *Drosophila melanogaster* SMA models appears to ameliorate disease severity and rescue axon growth defects associated with SMN deficiency (Dimitriadi *et al.*, 2010b; Hao le *et al.*, 2012; Oprea *et al.*, 2008). However, the mechanism underlying PLS3-mediated SMA protection is still unclear. Data derived from a PLS3 overexpressing mouse model has led to the hypothesis that PLS3 may rescue the SMA phenotype by stabilising neuromuscular connectivity and improving the synapse architecture of motor neurons (Ackermann *et al.*, 2013). To investigate the therapeutic potential of PLS3 in treating SMA, preclinical studies have been conducted utilising adeno-associated virus serotype 9 (AAV9) mediated overexpression of PLS3 protein. PLS3 overexpression appears to extend survival and reduce severity in SMA mouse models (Alrafiah *et al.*; Kaifer *et al.*, 2017).

The identification and characterisation of novel disease modifiers is essential for the development of new therapeutic strategies to treat SMA.

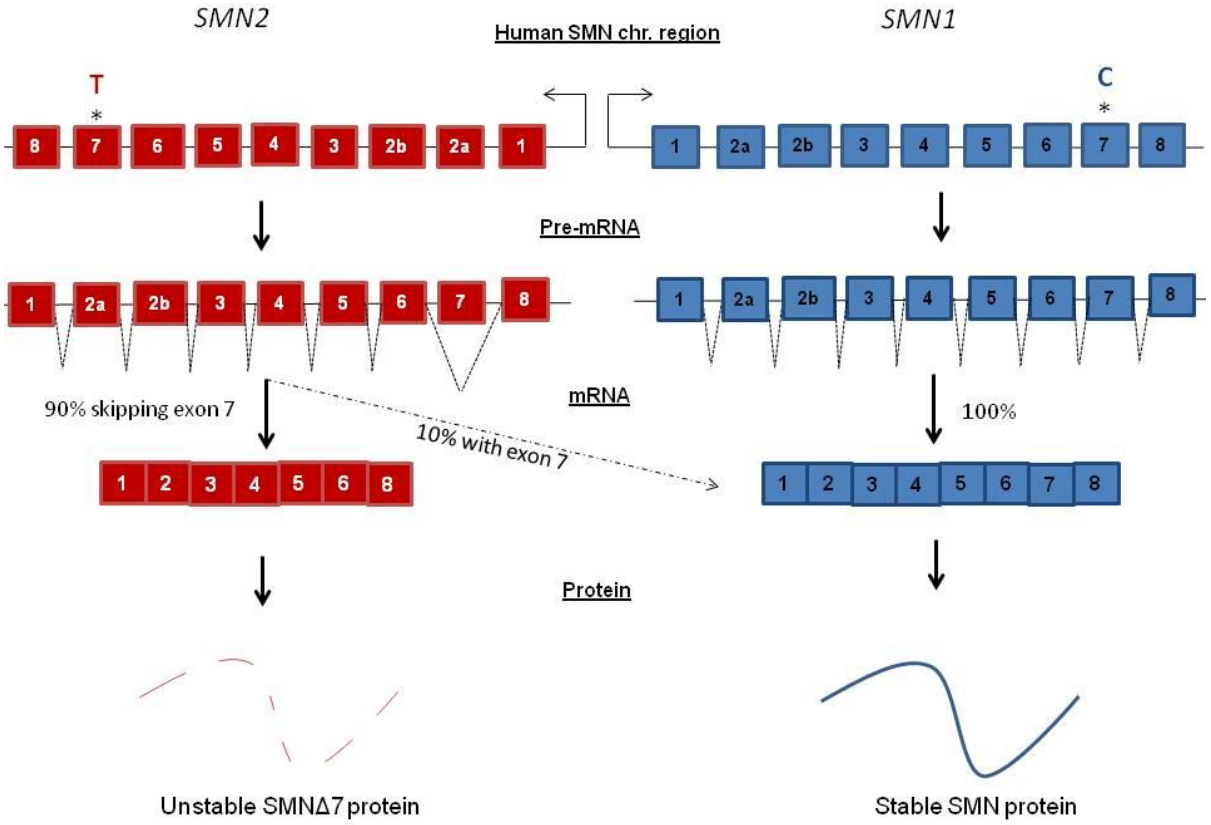

Figure 1-1: Splicing of *SMN1* and *SMN2* genes.

A silent C to T substitution in exon 7 affects the splicing of the SMN2 transcript causing exclusion of exon 7 which leads to production of a truncated and unstable protein. However a small amount (10%) of full-length and fully functional protein is still produced by *SMN2* gene. Adapted from (Sendtner, 2010).

1.1.3 Experimental models of SMA

In order to broaden our knowledge about the pathogenesis of SMA the development and usage of animal models that recapitulate the pathology observed in humans appears to be essential. A wide range of animal models for the disease has been developed so far. The model systems, in general, need to be small in size,

affordable, easy to manipulate, and have short life cycles. SMN has been disrupted in different model organisms such as fly, worm, zebrafish, and mouse, however it is difficult to generate a model that closely resembles the human disease due to the fact that only humans carry multiple copies of the *SMN* gene (Schmid *et al.*, 2007).

One of the best and widely used invertebrate systems as a tool to study neurodegenerative diseases because of its easily detectable and rapid genetics is *Drosophila melanogaster* (Lee *et al.*, 2008; Rossoll *et al.*, 2009). Hypomorphic mutations in *Smn* gene have been shown to cause defects in Drospophila motor neurons resulting in reduced locomotive ability (Rajendra *et al.*, 2007). Motor neurons innervating flight muscles exhibit striking axon routing and arborisation defects resulting in atrophy of the flight muscles in mutants.

Another invertebrate with tractable neuromuscular system is the nematode worm *Caenorhabditis elegans*. *C. elegans* has been exploited to model a wide spectrum of neurological disorders and it is commonly used as a tool for large scale screening of chemical compound libraries (Dimitriadi *et al.*, 2010a; Sleigh *et al.*, 2010; Vistbakka *et al.*, 2012). RNAi library screening can also be achieved relatively easy by feeding the worms with small interfering RNAs (siRNAs). RNAi-mediated knockdown of *smn-1* gene leads to larval lethality, suggesting that *smn-1* gene plays a vital role for the survival of *C.elegans* animals (Miguel-Aliaga *et al.*, 1999). There are two *smn-1* alleles that have been generated to study SMA in *C. elegans*. The first one and most severe, *smn-1* (ok355) is characterised by larval arrest, reduced lifespan, sterility and progressive decline in neuromuscular function (Briese *et al.*, 2009). This deletion allele lacks most of the *smn-1* gene including the translation start codon. *smn-1(*cb131) is the second *smn-1* allele. It was isolated from a library of randomly

chemically-mutagenized animals. These animals carry a missense mutation in a highly conserved residue of exon 2 also seen in SMA type III patients. It is a milder allele with the ability to reproduce facilitating screening. The *smn-1(*cb131) worms display minor motor defects and slightly reduced lifespan (Sleigh *et al.*, 2011a).

The fresh water zebrafish, *Dario rerio*, is an important model for studying vertebrate developmental biology (Beattie *et al.*, 2007). Zebrafish have a short life cycle, external development and embryo transparency. These features, in addition to their well-characterized neuromuscular system, have enabled scientists to analyse the developing motor neurons in living embryos (Schmid *et al.*, 2007). Zebrafish have been used to model SMA by antisense morpholinos-mediated reduction of Smn protein levels (McWhorter *et al.*, 2003). Morpholinos are essentially modified antisense oligonucleotides usually designed against the translation start site of specific RNA aiming to inhibit protein translation. Smn-deficient zebrafish embryos exhibit motor axon defects. More specifically, motor neuron axons from the spinal cord of these fish are truncated and display increased branching suggesting a defect in axonal growth (McWhorter *et al.*, 2003). Moreover, Smn-deficient fish with severe motor axon defects have been shown to exhibit decreased survival (Carrel *et al.*, 2006). More recently, zebrafish genetic models of SMA have been generated that resemble the human disease more closely. These fish have their endogenous smn1 gene mutated while expressing a human *SMN2* transgene and exhibit severe axon defects (Hao le *et al.*, 2011).

Mouse models are the most important and commonly used models of human diseases. Complete loss of mouse *Smn* gene is embryonically lethal. Various strategies have therefore been developed to allow for partial expression of the SMN protein (Schrank *et al.*, 1997). One way of overcoming the lethality of *Smn* knockout

in mice is to introduce a human *SMN2* gene. Following this line, a transgenic mouse has been generated which expresses human *SMN2* transgene in the *Smn* knockout background (m*Smn*$^{-/-}$; *SMN2*$^{+/+}$) also known as Taiwanese SMA mouse model. These mice live on average 5 days and are shown to have reduced number of motor neurons. Intriguingly, *SMN2* copy number can influence the severity of this mouse model, in a similar manner that it does in humans (Hsieh-Li *et al.*, 2000; Monani *et al.*, 2000). Mice with 1 copy of SMN2 gene are stillborn, mice with 2 copies of *SMN2* gene die between 4 to 6 days while mice with 8 copies of the gene can reach adulthood. Moreover, mice carrying the human *SMN* gene without exon 7 (*SMNΔ7*) have been generated. These mice were crossed onto a severe SMA background (m*Smn*$^{-/-}$; *SMN2*$^{+/+}$) which resulted in mice with both the *SMN2* and *SMNΔ7* genes but lacking mouse *Smn* gene (m*Smn*$^{-/-}$; *SMN2*$^{+/+}$*; SMNΔ7*$^{+/+}$*)* (Le *et al.*, 2005). Addition of *SMNΔ7* has been shown to extend the survival of SMA mice from 5 to 14 days, displaying a slightly less severe SMA-like phenotype. Multiple SMA mouse models have been generated to study SMA as reviewed by (Sleigh *et al.*, 2011b), however the Taiwanese and the SMNΔ7 are the most commonly used ones.

Despite having vastly contributed to the understanding of SMA, one could argue that these animal models cannot fully represent the human disease, especially with regard to the neural phenotype as their physiology and anatomy are different from humans. Alternatively, the development of cellular reprogramming technology has helped scientists in the field to establish *in vitro* model systems for SMA. Patient derived induced pluripotent stem cells (iPSCs) or induced motor neurons (iMNs) have been used for SMA studies related to drug screening or basic research (Ebert *et al.*, 2010; Sareen *et al.*, 2012; Zhang *et al.*, 2017).

1.1.4 SMN: a multifunctional protein

SMN is a highly conserved ubiquitously expressed protein with a predicted molecular weight of 38 kDa. It consists of 294 amino acids and contains several functional domains including the Gemin 2 and nucleic acid-binding domain at the N-terminal part (basic domain), the central Tudor domain that mediates protein-protein interactions and is often found in RNA-binding proteins, the proline rich (P-rich) domain as well as the C-terminal tyrosine/glycine-rich domain (YG box) which is a common motif of many RNA-binding proteins (**Figure 1-2**). Interestingly, mutations in all the above domains have been linked to SMA (Rossoll *et al.*, 2009).

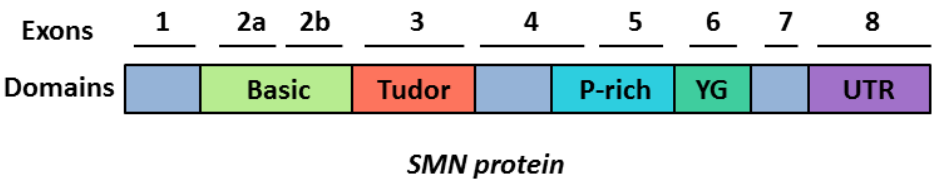

Figure 1-2: Schematic diagram of SMN.

SMN protein is depicted with a highly basic lysine-rich domain in exons 2a and 2b, a Tudor domain in exon 3, a poly-proline (P-rich) domain in exon 5 and part of exon 4 and several YG boxes in exon 6. There is a stop codon on exon 7; therefore exon 8 is not translated. UTR = untranslated region.

SMN expression is developmentally regulated; its levels appear to be high during gestational and early neonatal stages followed by a decrease to basal levels later in development (Burlet *et al.*, 1998). Interestingly, high expression of SMN protein in spinal motor neurons, in particular, has been reported from the second trimester of

life into adulthood possibly due to a higher demand for SMN protein in these cells (Tizzano *et al.*, 1998).

SMN is present in both the cytoplasm and nucleus of the cells. In the nucleus, it is concentrated in nuclear bodies called gems (gemini of coiled bodies due to their close proximity to the Coiled or Cajal bodies) which are structures resembling small dots (foci) (Liu *et al.*, 1996). In fact in the majority of cell types gems and coiled bodies are undistinguishable (Matera *et al.*, 1998). Coiled bodies or Cajal bodies (CBs) as they are widely known in honour of their discoverer Ramon y Cajal, are subnuclear compartments responsible for the storage and maturation of many ribonucleoprotein (RNP) complexes such as small nuclear RNPs (snRNPs), small nucleolar RNPs (snoRNPs) and small CB-specific RNPs (scaRNPs) (Machyna *et al.*, 2013). Cajal bodies and gems are two distinct structures in fetal tissues, however they predominantly co-localize in adult tissues (Young *et al.*, 2000). The number of gems is reduced in SMA patients with the lowest number observed in tissues derived from SMA type I patients (Coovert *et al.*, 1997).

Another sub-nuclear compartment where SMN has been shown to localise is the nucleolus (Wehner *et al.*, 2002). The nucleolus is a membrane-less intranuclear organelle where the transcription and processing of ribosomal RNAs (rRNAs) as well as the assembly of ribosomes take place (Olson *et al.*, 2002).

Within the cytoplasm the SMN protein localises in the perinuclear cytoplasm, where the assembly of snRNPs takes places but it can also be found in the stress granules, the Golgi apparatus and the microtubules (Zou et al., 2011; Ting et al., 2012; Torres-Benito et al., 2011). In motor neurons in particular, SMN is seen in dendritic and

axonal compartments in association with cytoskeletal elements (Bechade *et al.*, 1999; Pagliardini *et al.*, 2000).

According to the literature, SMN protein appears to have numerous functions and interacts with various other proteins; it has been reported to play roles in mRNA splicing, mRNA transport, stress granule formation, transcription regulation and DNA repair (Singh *et al.*, 2017b). However, despite the plethora of functions, it is still unclear how SMN deficiency leads to SMA pathogenesis.

1.1.4.1 Assembly of ribonucleoproteins

The earliest reported and best characterized role for SMN is in the assembly of snRNPs. snRNPs are initially assembled in the cytoplasm and then translocated to the nucleus, in order to initiate the splicing of pre-mRNA as part of the spliceosome (Hamilton *et al.*, 2013; Workman *et al.*, 2012). The spliceosome is an essential RNP complex that removes introns in a regulated and precise manner that also allows for alternative splicing events, providing accurate control of gene expression (Chari *et al.*, 2009; Coady *et al.*, 2011). There are two types of spliceosomes in eukaryotic cells; the major spliceosome which catalyses the vast majority of splicing reactions and the minor spliceosome which is responsible for a smaller portion. Their composition is very similar (Chari *et al.*, 2009). Each spliceosomal snRNP consists of one of U small-nuclear RNA (U1, U2, U4, U5, and U6 for the major spliceosome and U4atac, U5 and U6atac, U11, and U12 for the minor spliceosome), seven Smith-antigen (Sm) proteins (B, D1, D2, D3, E, F and G) and a set of additional proteins specific for each snRNP. All U snRNAs, with the only exemption of U6, are exported to the cytoplasm, after their transcription, and there the seven Sm proteins are

assembled into a ring around the Sm site which is present on all snRNAs, in a controlled manner co-ordinated by the SMN complex. The SMN complex includes SMN protein, Gemins 2–8, and Unr-interacting protein (Unrip) and it binds both snRNAs and Sm proteins, facilitating the attachment of the Sm core onto the snRNA (Coady *et al.*, 2011). The Sm core assembly is considered as the most important step in snRNP biogenesis (**Figure 1-3**).

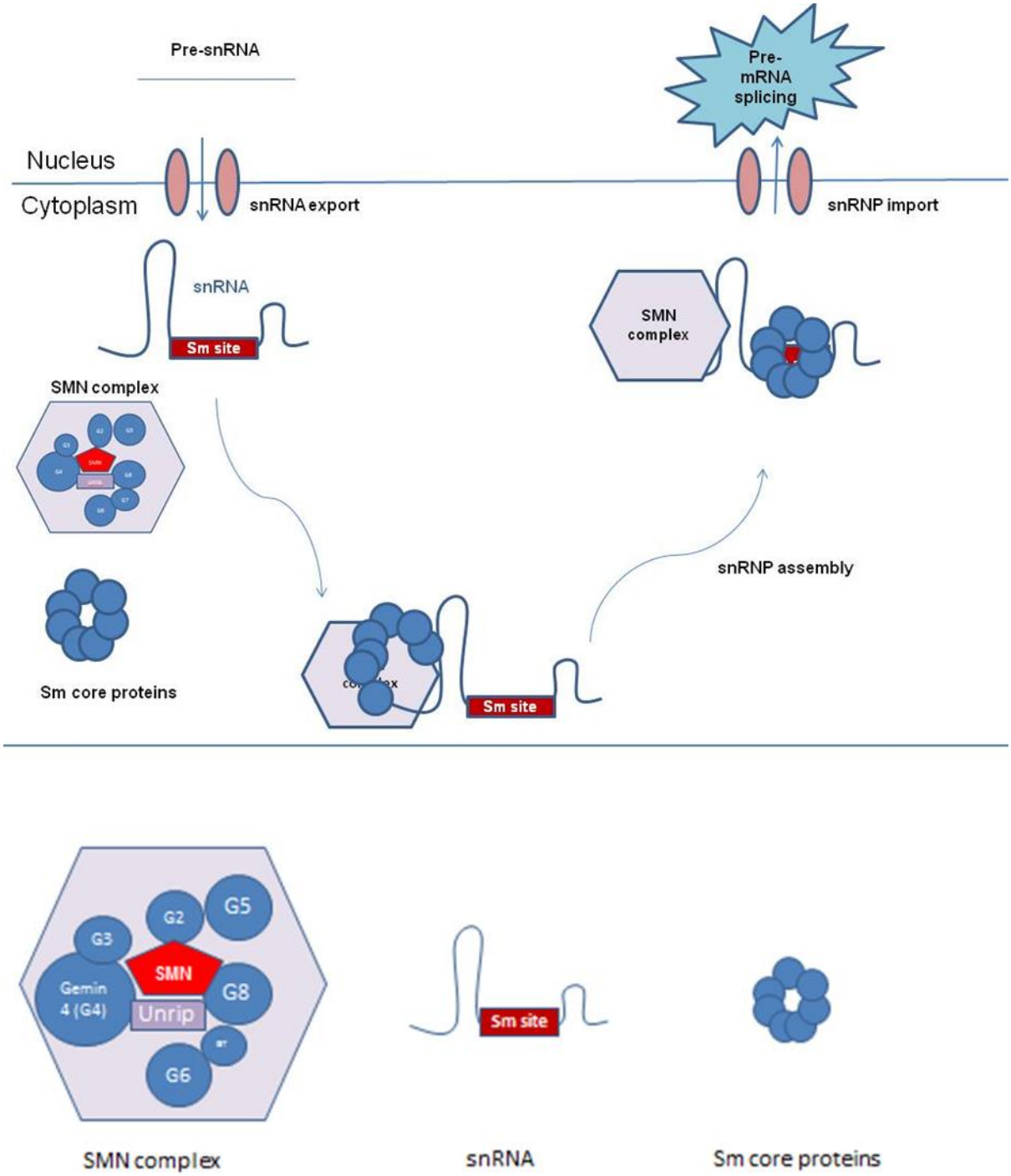

Figure 1-3: The role of SMN protein in the biogenesis of snRNPs.

The SMN complex consisting of SMN protein, Gemins 2-8 and Unrip protein facilitates the binding of Sm core proteins onto the small nuclear RNAs (snRNAs) to assemble snRNPs, the major component of spliceosome.

The snRNPs are then translocated into the nucleus for further maturation steps and initiation of the pre-mRNA splicing. Before snRNPs are ready for splicing, important modification steps take place in the Cajal bodies, such steps include pseudouridylation and ribose methylation of snRNA (mainly the RNA polymerase II-derived U1, U2, U4 and U5 snRNAs). These modifications are important for complete functionality of the snRNPs and are conducted by small Cajal body specific RNPs (scaRNPs), another type of RNPs. scaRNPs are essentially a subset of small nucleolar RNPs (snoRNPs) that will be described in more details below. Three classes of scaRNPs have been reported so far based on the sequence and structural motifs of the scaRNAs; box C/D scaRNPs catalyse 2'-O-methylation and contain the core proteins fibrillarin (a conserved methyltransferase), nucleolar protein 56 (Nop56), nucleolar protein 58 (Nop58) and a 15.5kDa, box H/ACA scaRNPs catalyse pseudouridylation and contain the core proteins dyskerin (the pseudouridylase), G protein-linked acetylcholine receptor 1 (GAR1), nucleolar protein 10 (Nop10) and H/ACA ribonucleoprotein complex subunit 2 (Nhp2), finally there is also a third chimeric class of scaRNPs that has both box C/D and box H/ACA motifs.

Similar to snRNA, ribosomal RNA (rRNA) is also subjected to post-transcriptional modifications. Pseudouridylation and 2′-*O*-methylation of rRNAs as well as RNA polymerase III-derived U6 snRNA are conducted by snoRNPs in the nucleolus. There are only two classes of snoRNPs: box C/D and box H/ACA. The main differences between scaRNPs and snoRNPs are their location of action; Cajal bodies for the former and nucleolus for the latter, and their RNA. scaRNAs, unlike snoRNAs, contain the Cajal body localisation box (CAB box) that leads these RNAs

to Cajal bodies. WD40 encoding RNA antisense to p53 (WRAP53) protein interacts with the CAB box and facilitates the transport of scaRNAs to the CBs.

The fact that SMN localises in the Cajal bodies and the nucleolus and interacts with GAR1, dyskerin and fibrillarin suggests its involvement in snoRNP/scaRNP assembly and/or function (Jones *et al.*, 2001; Poole *et al.*, 2016; Whitehead *et al.*, 2002). Supporting this hypothesis, SMN has also been shown to interact with Nuclear Assembly Factor 1 Ribonucleoprotein (NAF1), a box H/ACA assembly factor (Poole *et al.*, 2016).

1.1.4.2 Pre-mRNA splicing

Apart from being an essential assembly machine for RNPs, SMN has been shown to play a major role in splicing regulation. Splicing is catalysed by the spliceosome that consists of five snRNPs (U1, U2, U4, U5, and U6 snRNPs) and a number of non-snRNP auxiliary factors as reviewed by (Wahl *et al.*, 2009). The assembly of spliceosome takes place in a series of consecutive steps that produce complexes E, A, B and C. E complex forms early and brings the 5'- and 3'- splice sites of introns in close proximity. Interestingly, a recent study showed that one of the components of the E complex is SMN protein and that depletion of SMN inhibits the formation of this complex (Makarov *et al.*, 2012). SMN also interacts with several splicing factors such as fused in sarcoma (FUS), heterogeneous ribonucleoprotein particle (hnRNP) R and hnRNP U all of which are associated with complex E (Liu *et al.*, 1996; Makarov *et al.*, 2012; Rossoll *et al.*, 2002; Yamazaki *et al.*, 2012). Furthermore, SMN interacts with RNA polymerase II; therefore it may modulate co-transcriptional splicing by recruiting splicing factors such as FUS (Munoz *et al.*, 2010; Pellizzoni *et al.*, 2001;

Saldi *et al.*, 2016). In line with all this, Zhang and colleagues have shown that SMN deficiency leads to numerous splicing defects (Zhang *et al.*, 2008).

1.1.4.3 mRNA transport and local translation

Additionally, a more neuron-specific function for SMN supported by accumulating evidence has been proposed. Immunocytochemical studies have shown that SMN is localised in dendrites and axons of motor neurons and that is also associated with cytoskeletal filaments and polyribosomes (Bechade *et al.*, 1999; Pagliardini *et al.*, 2000) which implies that SMN protein may be actively transported into neuronal processes. The first indication of the function of SMN in axons came when reduced levels of β-actin mRNA and protein were observed at the axonal terminals of motor neurons derived from a SMA mouse model (Rossoll *et al.*, 2003). More recently, defects in the axonal localisation of other transcripts such as poly (A) mRNAs, neuritin/cpg15 and Growth-associated protein 43 (Gap43) have also been reported in SMA experimental models (Akten *et al.*, 2011; Fallini *et al.*, 2016; Fallini *et al.*, 2011). In addition, SMN has been found to bind RNA (Lorson *et al.*, 1998). That suggests that SMN may facilitate the transport of the aforementioned mRNAs. Furthermore, it has been reported that SMN interacts with a plethora of RNA-binding proteins (RBPs) such as hnRNP R/Q, HuD, Inner Membrane Peptidase Subunit 1 (IMP1) and K-homology splicing regulatory protein (KSRP) in cytoplasmic granules formed in axonal and dendritic compartments. These granules exhibit bidirectional and rapid movements and are associated with microtubules (Fallini *et al.*, 2014). Furthermore, SMN granules have been associated with the Golgi apparatus. SMN has been shown to interact with α-COP, a Golgi-associated subunit of COPI protein

(Coat Protein I) and to co-traffic with it in motor axons, delivering possibly mRNA or other cargoes to the axonal or dendritic compartments (Li *et al.*, 2015; Peter *et al.*, 2011). Interestingly SMN deficiency seems to decrease the localization of the aforementioned RBPs in the neuronal processes and growth cones of developing neurons (Akten *et al.*, 2011; Fallini *et al.*, 2014; Hubers *et al.*, 2011; Rossoll *et al.*, 2002; Tadesse *et al.*, 2008). These findings indicate that SMN may play a role in neuronal mRNA trafficking by facilitating the interaction of RBPs with their mRNA targets.

SMN does not only modulate mRNA transport but it can also regulate local translation. For instance, it has been reported to interact with fragile X mental retardation protein (FMRP) which is another RBP that associates with polyribosomes and activates or represses translation (Bechara *et al.*, 2007; Darnell *et al.*, 2012; Sanchez *et al.*, 2013; Wang *et al.*, 2012).

Identifying the full set of axonal mRNAs affected by SMN deficiency will lead to a better understanding of SMA and also to the development of complementary therapies.

1.1.4.4 Stress granule assembly

In addition to its presence in axonal RNA granules, SMN has also been shown to localise in cytoplasmic stress granules (Hua *et al.*, 2004). Stress granules (SGs) are dynamic membrane-less organelles formed in the cytoplasm under stress conditions when translation initiation is inhibited. Stress granules act essentially as a shelter for mRNAs whose translation has been brought to a halt due to priority in transcription

and translation of cytoprotective genes such as heat shock genes. After stress release, the SGs disassemble and the stalled mRNAs become translationally active again. SGs typically contain stalled mRNAs, RNA-binding proteins TIA-1 (T-cell internal antigen-1), TIAR (TIA-1-related protein), tristetraprolin (TTP), GTPase activating protein binding protein (G3BP), and PABP (poly[A]$^{+}$ mRNA binding protein), 40S ribosomal subunits, as well as a subset of eIFs (eukaryotic initiation factors) such as eIF2, eIF3, eIF4A, eIF4B, eIF4E and eIF4G (Kedersha *et al.*, 2000; Kedersha *et al.*, 1999; Kimball *et al.*, 2003). SGs are initially small in size, but as they mature they recruit additional RNA binding proteins linked to neurodegeneration such as hnRNPA1, TDP43, FUS, ataxin-2 or SMN, which in turn bring with them more transcripts for sequestration in SG forming in the end a larger body (Dormann *et al.*, 2011; Guil *et al.*, 2006; Hart *et al.*, 2012; Hua *et al.*, 2004; Liu-Yesucevitz *et al.*, 2010). SG assembly is dysregulated in neurodegenerative disorders (Monahan *et al.*, 2016; Vanderweyde *et al.*, 2013). Interestingly, SMN deficiency has been shown to reduce the ability of cells to form SGs making the cells more vulnerable to stress (Zou *et al.*, 2011). Consistent with the latter observation, SMN has been shown to co-localise with TIAR and G3BP, SG assembler proteins and physically interact with the former. The recruitment of SMN in the granules precedes the accumulation of TIAR, suggesting that SMN may act as a facilitator of SG assembly (Hua *et al.*, 2004).

1.1.4.5 Transcriptional regulation

SMN has also been suggested to play a role in transcription as it was found to interact with the COOH-terminal domain (CTD) of RNA polymerase II (pol II)

(Pellizzoni *et al.*, 2001). Additionally, SMN is associated with a number of transcription factors further suggesting its role in transcription initiation. One of these factors is the nuclear transcription activator E2 of papillomavirus. Interestingly, SMN expression has been shown to enhance E2-dependent transcriptional activation, while SMN mutations linked to SMA reduce E2 gene expression (Strasswimmer *et al.*, 1999). Another transcription factor that binds SMN is the tumour suppressor p53 multifunctional protein (Young *et al.*, 2002). p53 protein serves a role in cell cycle control (Sherr *et al.*, 2000), apoptosis (Vousden, 2000) and DNA repair (Huang *et al.*, 1996), however the most well studied function of p53 is in transcriptional activation (Beckerman *et al.*, 2010). Conversely, SMN could mediate transcriptional silencing through its interaction with Sin3A, a transcription co-repressor. Sin3A acts as a scaffold for histone deacetylases (HDACs) which are associated with gene silencing (Grzenda *et al.*, 2009; Zou *et al.*, 2004). Furthermore, SMN has been implicated in transcriptional termination. It interacts with senataxin (SETX), a DNA/RNA helicase that facilitates the resolution of R loops formed by RNA polymerase II, as a part of a pause mechanism at the transcription termination sites (Zhao *et al.*, 2016). SMN directly interacts with the CTD of pol II and recruits SETX that in turn resolves R loops releasing the RNA molecule and promoting efficient transcription termination (Proudfoot, 2016; Skourti-Stathaki *et al.*, 2011; Zhao *et al.*, 2016). Loss of either SMN or SETX leads to R loop accumulation causing increased DNA damage (Jangi *et al.*, 2017; Mischo *et al.*, 2011). Therefore, SMN could also be considered as guardian of genome integrity. The transcription-associated genome instability will be described in more details in a separate section below.

1.1.4.6 DNA repair

Not only is SMN critical for DNA damage prevention as mentioned above but recent reports also highlight its role in the repair of DNA once the breaks have already occurred. SMN binds tightly to Gemin 2 forming the core of a larger complex, the 'SMN complex' that also contains Gemins 3-8 and unrip (Sarachan *et al.*, 2012). Gemin 2 interacts with RAD51, an essential protein for double-strand break (DSB) repair and stimulates RAD51-mediated homologous recombination (HR) (Takizawa *et al.*, 2010). Intriguingly, SMN-Gemin 2 fusion protein enhances the RAD51-mediated HR more efficiently than Gemin 2 alone (Takaku *et al.*, 2011). In addition to HR, SMN has also been implicated in non-homologous end joining (NHEJ) DNA repair. SMN is well known to interact with coilin, a Cajal body marker (Hebert *et al.*, 2001) which interacts with Ku proteins to inhibit NHEJ (Velma *et al.*, 2010). Ku proteins are nucleoplasmic and do not localise in CBs, therefore the interaction between Ku proteins and coilin must take place in the nucleoplasm. In line with this, 70% of coilin has been shown to be nucleoplasmic (Lam *et al.*, 2002). The initial step of NHEJ is the rapid recognition of DSBs by the Ku70-Ku80 heterodimer. SMN competes with Ku proteins for coilin-interaction sites; therefore when SMN binds coilin, the Ku proteins are released and are able to perform their NHEJ DNA repair function (Velma *et al.*, 2010). SMN has also been reported to interact with FUS, an RNA/DNA binding protein (Mirra *et al.*, 2017; Yamazaki *et al.*, 2012). Mutations in FUS cause ALS and are linked to DNA damage (Wang *et al.*, 2013b; Zhou *et al.*, 2014). Despite the studies presented here, the role of SMN deficiency in DNA damage is still poorly understood. Given that DNA damage has been considered as a contributing factor in the pathogenesis of various neurodegenerative diseases, it is

therefore important to unravel the significance of SMN protein in the maintenance of genome integrity.

1.2 DNA damage and neurodegeneration

Mammalian cells are constantly exposed to DNA damage in the form of DNA strand breaks (single-strand breaks or double-strand breaks), base damage (base loss, base mismatch, alkylation, deamination, oxidation), helical distortions (thymine dimers) and DNA-protein crosslinks (stalled TOP1ccs as described below) (Iyama *et al.*, 2013). The integrity of DNA can be threatened by endogenously spontaneous reactions such as hydrolytic deamination and depurination and by products or by-products formed during cellular metabolism such as reactive oxygen species (ROS) and alkylating agents. DNA can also be damaged by environmental sources such as radiation and mutagens (Dexheimer, 2013; Hoeijmakers, 2009; Jackson *et al.*, 2009). It has been estimated that every cell in the human body could experience up to 10^5 DNA lesions per day (Hoeijmakers, 2009). To counteract DNA damage and maintain genomic integrity, all cells contain various DNA damage repair (DDR) machineries including base excision repair (BER), nucleotide excision repair (NER), mismatch repair (MMR), and double-strand break (DSB) repair that includes homologous recombination (HR) and non-homologous end joining (NHEJ) as outlined in **Table 1-2** (Ashour *et al.*, 2015a; Jackson *et al.*, 2009). Compromising genomic integrity can lead to a spectrum of diseases including cancer, immunodeficiency and neurodegenerative disorders.

Table 1-2: Major DNA damage repair pathways in mammalian cells

Source of damage	Type of lesion	Repair pathway
- Hydrolysis - Oxygen radicals - Alkylating agents - X-ray	- Abasic sites (AP) - DNA single-strand breaks (SSBs) - Oxidised, deaminated or alkylated bases	Base excision repair (BER)
- UV - Chemicals	- Helical distortions - Bulky adducts	Nucleotide excision repair (NER)
- DNA replication errors	- DNA mismatches - Insertions - Deletions	Mismatch repair (MMR)
- Ionising radiation (IR) - X-rays - UV - Anti-cancer drugs	DNA double-strand breaks (DSBs)	Double strand break repair (DSDR) - Homologous recombination (HR) - Non-homologous end joining (NHEJ)
- Abortive activity of DNA topoisomerases	Protein-linked DNA breaks (PDBs)	Protein-linked DNA break repair

Among the various types of DNA lesions, DSBs are considered the most toxic form of DNA damage. Two major mechanistically distinct pathways exist in mammalian cells for mediating DSB repair: the homologous recombination (HR) and non-homologous end joining (NHEJ). HR allows error free repair of DSBs by using the intact sister chromatin as a template, therefore HR can operate during S and G2/M phases of the cell cycle (Brandsma *et al.*, 2012; Helleday *et al.*, 2007; West, 2003). On the contrary, NHEJ provides an error-prone DSB repair by directly ligating the two broken DNA termini and it is active throughout the cell cycle (Davis *et al.*, 2013; Lees-Miller *et al.*, 2003; Lieber *et al.*, 2003). NHEJ is the predominant DSB repair machinery for non-cycling cells such as post-mitotic neurons (Lee *et al.*, 2007).

In response to DSBs, a signalling cascade of multiple events is triggered. Immediately after their formation, DSBs are recognised by the MRE11-RAD50-NBS1

(MRN) and the Ku70/80 complexes which recruit ataxia telangiectasia mutated (ATM) protein and DNA-dependent protein kinase catalytic subunit (DNA-PKcs), respectively (Bohgaki *et al.*, 2010; Stewart *et al.*, 2003). ATM and DNA-PK belong to the phosphatidylinositol 3-kinase-related kinase (PIKK) protein family (Falck *et al.*, 2005). One of the earliest targets of these kinases is the histone variant H2AX which is phosphorylated on its serine 139 and it is then referred to as γH2AX (Burma *et al.*, 2001). The phosphorylated H2AX is directly recognised by the mediator of DNA damage checkpoint 1 (MDC1) and it binds to it (Stucki *et al.*, 2005). The MDC1, in turn, interacts with the Nijmegan breakage syndrome 1 (NBS1) component of the MRN complex promoting the retention of ATM-MRN complex at chromatin near the DSB sites (Chapman *et al.*, 2008). Then, MDC1 phosphorylated by ATM recruits the RING finger protein RNF8, an ubiquitin E3-ligase which ubiquitinates H2A and H2AX. The recruitment of RNF168, another ubiquitin E3-ligase, is followed. RNF168 further propagates the ubiquitination of histones H2A and H2AX. The polyubiquitinated H2A/H2AX histones trigger the accumulation of proteins involved in DNA damage checkpoints and DNA repair proteins such as p53-binding protein 1 (53BP1) and breast cancer gene 1 (BRCA1) proteins (Doil *et al.*, 2009; Mailand *et al.*, 2007).

The repair of DSBs is essential for neural homeostasis given that defects in DSB repair can lead to neurodegeneration. Ataxia telangiectasia (AT), Ataxia telangiectasia-like disorder (ATLD) and Nijmegen breakage syndrome (NBS) all result from defective repair in DSBs (McKinnon, 2009). Furthermore, age-associated neurodegenerative diseases such as Parkinson’s disease, Alzheimer’s disease and Amyotrophic lateral sclerosis have also been linked with defects in DNA repair (Carroll *et al.*, 2015; Jeppesen *et al.*, 2011; Madabhushi *et al.*, 2014).

1.2.1 Ataxia telangiectasia as a model of DDR-defective neurodegenerative disorder

Ataxia telangiectasia (AT), a rare neurodegenerative disease caused by mutations in the *ATM* gene, represents a key example of how defects in DNA repair capacity can lead to neurodegeneration. AT is an autosomal recessive childhood disease characterised by progressive degeneration of the cerebellum, genome instability, cancer predisposition, immunodeficiency and radiosensitivity (Biton *et al.*, 2008). The ATM protein as mentioned above functions to regulate an extensive network of downstream double strand breaks (DSBs) repair factors. Mutations in *ATM* gene cause the accumulation of DNA breaks and abortive DNA topoisomerase I (TOP1) cleavage complexes and protein-linked DNA breaks in neuronal cells (Alagoz *et al.*, 2013; Katyal *et al.*, 2014a). TOP1 relaxes DNA supercoiling generated by transcription by nicking one strand of the DNA duplex forming a transient TOP1 cleavage complex (TOP1cc). At the end of a normal catalytic cycle, TOP1cc is rapidly released. However, TOP1cc can be trapped in the presence of endogenous DNA base modifications (AP sites, base mismatch, oxidation, and alkylation), DNA nicks or carcinogenic adducts, resulting in TOP1-SSBs or TOP1-DSBs generally known as protein-linked DNA breaks (PDBs). The threat posed by PDBs to the central nervous system (CNS) is also well illustrated by the spinocerebellar ataxia SCAN1, a rare neurological disease which exhibits cerebellar degeneration as its most notable clinical feature (Ashour *et al.*, 2015b; El-Khamisy *et al.*, 2005a). SCAN1 is caused by a mutation in the gene encoding for tyrosyl-DNA phosphodiesterase 1 (*TDP1*) which promotes the resolution of stalled TOP1ccs (Takashima *et al.*, 2002).

1.2.2 Transcription as a source of genomic instability

The two major sources of genome instability are aberrant replication and defects in DNA damage response (DDR). However, a number of studies over the last decade have provided evidence that transcription could also be considered as a source of genome instability. R loops are RNA/DNA hybrids generated during transcription by hybridization of the nascent RNA with the DNA template strand, leaving the non-template DNA single-stranded and forming that way a very stable three-stranded nucleic acid structure (Thomas *et al.*, 1976) (**Figure 1-4**).

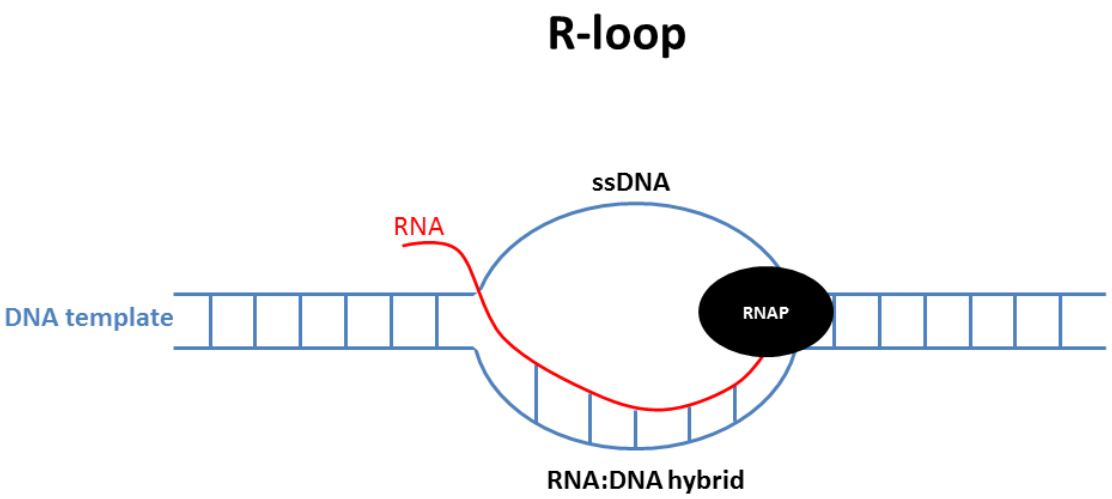

Figure 1-4: R-loop structure.

R loops are three-stranded nucleic acid structures consisted of an RNA:DNA hybrid and the resultant displaced single-stranded DNA (ssDNA).

R loops form naturally and are implicated in a wide range of cellular processes in several organisms from bacteria to mammals. They play essential role in DNA

replication, generation of antibody diversity through immunoglobulin class switch recombination, chromatin architecture, gene expression and transcription termination and also DNA repair (Chen *et al.*, 2015; Ginno *et al.*, 2013; Keskin *et al.*, 2014; Lombrana *et al.*, 2015; Zarrin *et al.*, 2004).

Despite their beneficial roles, R loops are considered as an important source of DNA damage and genome instability (Skourti-Stathaki *et al.*, 2014). For this reason, the formation of R loops is tightly regulated and cells have developed several mechanisms to resolve them or prevent their formation and/or accumulation. R loops can be resolved by degradation of the RNA moiety in the RNA/DNA hybrid. R loop resolution can be achieved by RNAse H enzymes (Wahba *et al.*, 2011). Alternatively, R loops are resolved by DNA/RNA helicases such as senataxin (SETX) that unwinds RNA/DNA hybrids (Skourti-Stathaki *et al.*, 2011). Additionally, R loop formation can be prevented by topoisomerase I (TOP1). TOP1 resolves the negative DNA supercoiling behind RNA polymerase II and by doing so it prevents annealing of the nascent RNA with the DNA template (Sordet *et al.*, 2009; Tuduri *et al.*, 2009). Furthermore, factors involved in RNA processing and RNA export appear to protect against R loop formation presumably due to their binding with the newly synthetized RNA which precludes the hybridization of the latter with the DNA template (Li *et al.*, 2007).

Interestingly, perturbation of factors that resolve R loops or preclude their formation can lead to increased DNA damage and genome instability. However it is still unclear how R loops lead to genome instability. It is possible that the displaced ssDNA is more vulnerable to DNA damage, leading to DSBs. Additionally, R loops can be converted into DSBs via NER pathway. It has recently been shown that R loops can be processed into DSBs by the NER endonucleases xeroderma pigmentosum group

F (XPF) and xeroderma pigmentosum group G (XPG) (Sollier *et al.*, 2014). However the exact mechanism by which NER acting in a non-canonical manner converts R loops to DSBS remains unknown.

The first indication of R loops as a source of genome instability was shown in R loop forming THO/TREX yeast mutants. THO/TREX, is a complex involved in transcription and RNA export and plays a central role in coating the nascent RNA with several RBPs. These mutants exhibit a transcription-associated hyper recombination phenotype and increased plasmid and chromosomal loss. Intriguingly, this phenotype can be ameliorated after overexpression of RNAse H1 (Huertas *et al.*, 2003). Additionally, a genome-wide siRNA screen in human cells identified numerous proteins involved in RNA processing whose depletion led to increased genome instability as revealed by γH2AX foci analysis. The observed DNA damage appeared to be R loop-associated given that RNAse H overexpression reduced the levels of γH2AX foci in those cells (Paulsen *et al.*, 2009).

Furthermore, mutations in the yeast SETX homologue, Sen1, exhibit accumulation of R loops which gives rise to transcription-associated recombination and genome instability (Mischo *et al.*, 2011). The depletion of SETX in human cells is also associated with increased DNA damage (Hatchi *et al.*, 2015; Roda *et al.*, 2014). Moreover, *Setx* knock-out mice have been shown to accumulate R loops and DSBs (Becherel *et al.*, 2013). Similarly to SETX data, RNAse H depletion has been reported to promote chromosomal rearrangements (Zimmer *et al.*, 2016).

1.2.3 R loop-associated DNA damage and neurodegeneration

R loops have recently drawn much attention in the field of neuroscience as they were found to be associated with numerous neurological disorders. Mutations in proteins involved in R loop biology are often related to neurodegeneration. This is the case of mutations in the DNA/RNA helicase SETX leading to Ataxia with Oculomotor Apraxia type 2 (AOA2) and Amyotrophic Lateral Sclerosis type 4 (ALS4). AOA2 is a rare but severe autosomal recessive cerebellar ataxia. Its main clinical features include progressive cerebellar atrophy, peripheral neuropathy and oculomotor apraxia with onset between 10-20 years of age. Nearly 120 *SETX* mutations causing AOA2 have been reported so far, the majority of which are missense, nonsense, frameshift, splice site mutations as well as insertions and deletions as reviewed by (Groh *et al.*, 2016). In contrast, ALS4 is caused by dominant missense *SETX* mutations. It is a rare juvenile form of motor neuron disease characterised by distal muscle weakness and atrophy, absence of bulbar involvement, pyramidal signs with onset occurring the first two decades of life (Chen *et al.*, 2004). Therefore, it can be speculated that loss of function leads to AOA2 phenotype, whereas toxic gain of function leads to ALS4. However, the exact mechanism by which *SETX* mutations result in AOA2 or ALS4 is still unknown.

Other neurodegenerative diseases associated with accumulation of R loops are Friedreich's ataxia (FRDA), fragile X-associated tremor/ataxia syndrome (FXTAS) and C9orf72 linked ALS, all of which are nucleotide expansion disorders. FRDA, the most common inherited form of ataxia, is an autosomal recessive fatal neurodegenerative disease caused by a GAA trinucleotide repeat expansion in intron 1 of *Frataxin* (*FXN*) gene. It has been shown that extensive formation of R loops on

GAA templates inhibits FXN transcription leading to decreased levels of *FXN* protein, the hallmark of FRDA (Butler *et al.*, 2015; Campuzano *et al.*, 1996; Grabczyk *et al.*, 2007). Similarly, FXTAS is a neurodegenerative disorder caused by a CGG trinucleotide repeat expansion in the 5' untranslated region (5' UTR) of the fragile X mental retardation 1 gene (*FMR1*) leading to reduced FMR1 expression. It is characterised by cerebellar ataxia, intension tremor, parkinsonian features and cognitive deficits. Transcription-associated R loops are formed across the CGG repeat region of *FMR1* gene and it has been hypothesised that they mediate its silencing (Colak *et al.*, 2014; Hagerman *et al.*, 2016; Loomis *et al.*, 2014). The R loop-mediated DNA damage observed at the CGG repeat region has also been proposed to contribute to the disease pathogenesis (Hoem *et al.*, 2011; Iwahashi *et al.*, 2006).

An expanded hexanucleotide GGGGCC in the chromosome 9 open reading frame 72 (C9orf72) is the most common genetic cause of ALS and frontotemporal dementia (FTD). The expanded repeats promote the formation of R loops both *in vitro* and *in vivo* (Haeusler *et al.*, 2014; Walker *et al.*, 2017), and it was recently shown that R loop-mediated DNA damage could be one of the factors contributing to C9orf72-linked neurodegeneration (Walker *et al.*, 2017). Motor neurons being post-mitotic cells are very vulnerable to DSBs since the only DSB repair mechanism in those neurons is the error-prone NHEJ. Accumulation of DNA damage in motor neurons could lead to cell death and eventually ALS.

Understanding more how DNA damage leads to neurodegeneration and unravelling the involved mechanisms could offer new therapeutic opportunities for several neurodegenerative disorders including SMA.

1.3 Treatment of SMA

For a long time the treatment of SMA was restricted to clinical management of the disease through physiotherapy, orthopaedic care, nutritional support and respiratory care. However, this supportive and lenitive care has no effect on the basic neuropathological process of SMA and is unable to modify the natural history of the disease. A fundamental change to the so far history of SMA occurred in December 2016 when Spinraza, a drug that alters the way in which SMN2 pre-mRNA is processed resulting in increased amount of SMN protein, was approved by the American Food and Drug Administration (FDA). Spinraza is the first and, currently, the only approved treatment for SMA. The European Medicines Agency (EMA) following FDA has also given the green light to this therapy. Spinraza that will be described in more details below is one of a wide range of therapeutic strategies that are currently in the pipeline for SMA. These strategies can be divided into two major categories: i) SMN-dependent approaches that focus on increasing the level of full-length SMN protein either by regulating the expression of *SMN2* gene or by replacing the entire *SMN1* gene, and ii) SMN-independent approaches that do not affect the SMN protein but instead have neuroprotective, antiapoptotic or myotrophic effects.

1.3.1 SMN-dependent therapeutic strategies

The discovery of *SMN1* as the disease-causing gene (Lefebvre *et al.*, 1995) and the development of animal models able to accurately mimic the symptoms of the disease for preclinical studies have yielded several promising options for treatment strategies

in the last two decades. The monogenic nature of SMA makes the *SMN* gene an obvious target for therapy development.

All SMA patients have at least one copy of *SMN2* gene. As it has already been mentioned in **1.1.2 Molecular genetics** section, *SMN2* gene is virtually identical to *SMN1* gene except a single nucleotide change which excludes exon 7 from the SMN2 transcript resulting to the formation of a truncated and unstable SMN protein. Therefore, an increase in exon 7 inclusion in *SMN2* transcripts could increase the levels of SMN full-length protein and theoretically ameliorate the disease phenotype. One such therapeutic approach utilises splice switching antisense oligonucleotides, which are essentially synthetic RNA molecules designed to alter splicing patterns of specific pre-mRNAs. Spinraza (also known as nusinersen and Ionis SMN_{rx}) is an antisense oligonucleotide (ASO) that binds to an intronic splicing silencer in intron 7 of the SMN2 pre-mRNA prohibiting the negative splicing factors hnRNP A1 and A2 from interacting with the SMN2 pre-mRNA. As a consequence, exon 7 is included in SMN2 mRNA transcripts during splicing, resulting in the production of full-length and functional SMN protein (**Figure 1-5**) (Hache *et al.*, 2016; Singh *et al.*, 2006; Singh *et al.*, 2017a). Given that ASOs do not cross the blood brain barrier (Smith *et al.*, 2006); Spinraza delivery to the central nervous system could be a challenge. However, it has been shown that intrathecal injections via lumbar puncture result in widespread delivery of ASOs to the central nervous system (Smith *et al.*, 2006 (Passini *et al.*, 2011). Therefore, Spinraza is administered intrathecally by means of repeated doses. The treatment commences with four loading doses followed by a maintenance dose every four months (Tabet *et al.*, 2017).

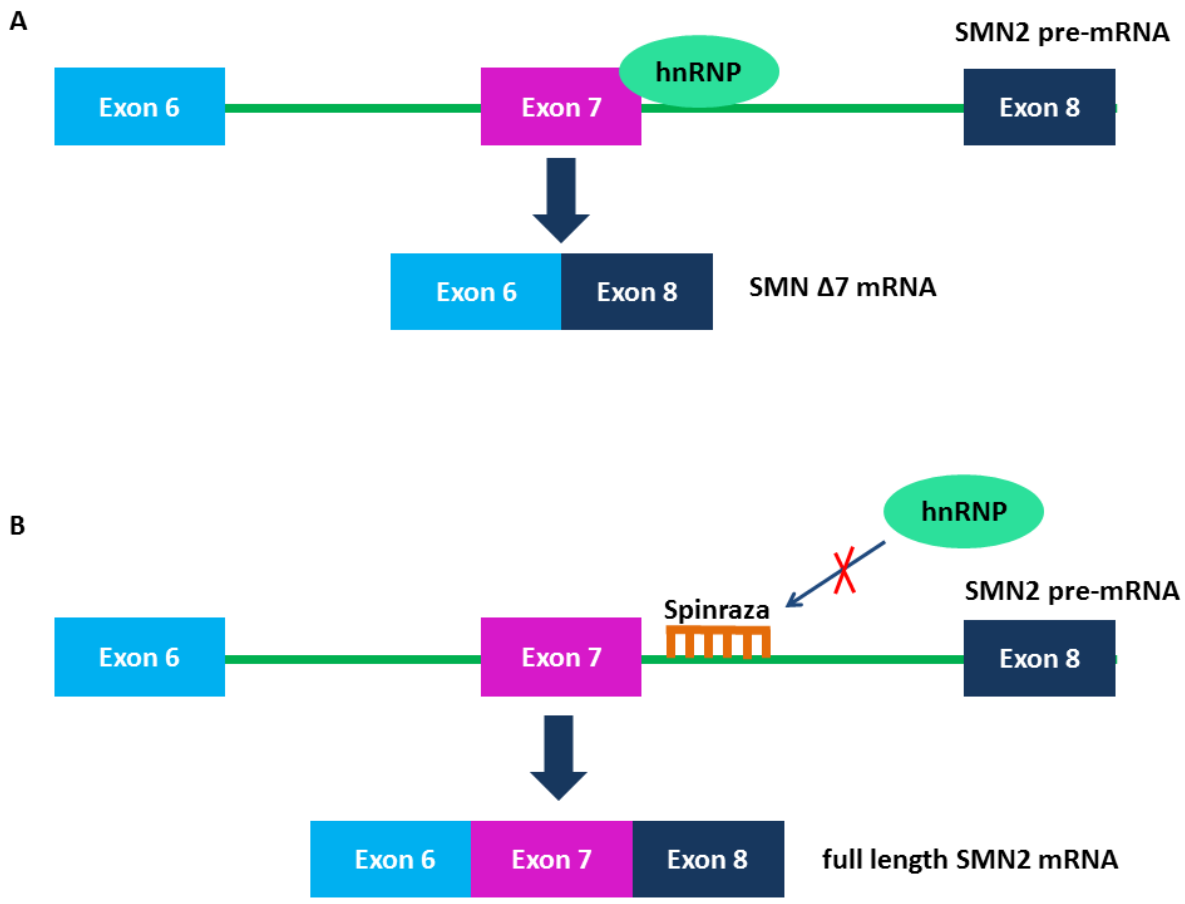

Figure 1-5: Mechanism of action of Spinraza.

(A) Splicing of SMN2 pre-mRNA where exon 7 is usually skipped. (B) In the presence of Spinraza, hnRNP negative splicing factors are displaced from the SMN2 pre-mRNA allowing the inclusion of exon 7 in the mature transcript.

Similar advanced therapies including low molecular weight drugs are also showing promising results in early clinical trials. Roche in collaboration with PTC Therapeutics have recently initiated two phase I/IIa clinical trials to assess the safety and efficacy of an orally administered small molecule RG7916 in SMA type I infants (FIREFISH trial) and in SMA type II and III patients (SUNFISH trial). This compound like

Spinraza increases the production of full-length SMN protein by modifying the splicing of SMN2 transcript.

Another approach is viral vector mediated gene therapy. The monogenic nature of SMA makes *SMN1* gene replacement the most direct approach to treating the disease. Viral-mediated gene replacement therapy has been remarkably successful in preclinical studies (Armbruster *et al.*, 2016; Benkhelifa-Ziyyat *et al.*, 2013; Dominguez *et al.*, 2011; Foust *et al.*, 2010; Glascock *et al.*, 2012; Meyer *et al.*, 2015; Valori *et al.*, 2010). An open-label, dose-escalation clinical trial of AVXS-101 has been currently conducted by AveXis. It is the first ever phase I/IIa gene transfer clinical trial to assess the safety and efficacy of intravenous delivery of self-complementary adeno-associated viral vector serotype 9 carrying the human *SMN* gene (scAAV9-SMN) in infants suffering from SMA type I. As of January 2017, AVXS-101 appeared to be a safe and well-tolerated treatment. Also, 100% of patients receiving AVXS-101 had reached 13.6 months of age event-free, where the expected event-free rate based on natural history of SMA type I patients is only 25%. Event is defined as death or time until a patient requires at least 16 hours per day of ventilation support for 2 consecutive weeks. Furthermore, an improvement in motor function was also observed; the natural history of SMA type I shows that SMA type I babies are unable to achieve or maintain motor milestones (i.e. head control, ability to sit, roll, crawl, stand or walk), interestingly AVXS-101-treated babies achieved developmental milestones not seen in the natural history of the disease (Mendell *et al.*, 2017).

The main advantage of this therapy over Spinraza is the ability of AAV9 to cross the blood brain barrier due to its capsid and efficiently transduce neuronal cells allowing systemic administration (Foust *et al.*, 2009). Another element of AVXS-101

necessary for optimal function is its self-complementarity; the human *SMN* gene contained within the recombinant AAV9 capsid shell forms an intramolecular double-stranded (self-complementary) DNA template that enables rapid onset of effect. The canonical AAV vectors need to convert the single-stranded DNA into double-stranded DNA prior to gene expression. However, self-complementary AAV vectors like AVXS-101 overcome this rate-limiting step allowing rapid expression of the transgene (McCarty, 2008). In addition to the self-complementary feature of the vector, the presence of a continuous promoter such as the hybrid cytomegalovirus enhancer-chicken beta actin (CAG) promoter that drives the expression of the human *SMN* transgene enables rapid but also sustained expression.

1.3.2 SMN-independent therapeutic strategies

In addition to impressive results of SMN-dependent therapies, there are also numerous SMN-independent therapeutic approaches that could potentially benefit SMA. Among these a neuroprotective compound (olesoxime) and a skeletal muscle activator (CK-2127107) have entered clinical trials. Olesoxime is a small cholesterol-like molecule studied by Trophos that had demonstrated neuroprotective properties in motor neurons in numerous *in vitro* and *in vivo* studies prior entering clinical trials as reviewed by (Bordet *et al.*, 2010). A Phase II clinical trial in patients suffering from SMA type II or type III has been completed with treated patients showing improvements in motor functions (Bertini *et al.*, 2017). Another small molecule currently in phase II clinical trial for SMA is CK-2127107, a novel fast skeletal muscle troponin activator that sensitises the sarcomere, the contractile unit of skeletal muscles. Based on this mechanism, CK-2127107 has been hypothesized to be

capable of improving muscle function and physical performance when administered in SMA patients. The promising preclinical data along with the safe profile of this compound demonstrated by 5 phase I clinical trials led to the ongoing phase II clinical trial in patients with SMA type II, III and IV (Hwee *et al.*, 2015). All the promising drugs that are currently used in SMA clinical trials are summarised below (**Table 1-3**).

Table 1-3: SMA therapy pipeline

		Pre-clinical development	Clinical trials			FDA approval
			Phase I	Phase II	Phase III	
SMN-dependent strategies	Ionis/Biogen **Spinraza**	→	→	→	→	→
	Roche/PTC **RG7916**	→	→	→		
	Avexis **AVXS-101**	→	→	→		
SMN-independent strategies	Roche/Trophos **Olesoxime**	→	→	→	→	
	Cytokinetics **CK-2127107**	→	→	→		

1.4 Project aims

The mechanisms by which SMN deficiency leads to SMA pathogenesis are still not known, making the development of effective treatment very challenging. In an attempt to shed more light on the pathobiology of SMA, this PhD project was focused on the emerging yet, currently, obscure role of genome instability in the neurodegeneration linked to SMA. Fayzullina and colleagues were the first to report

increased DNA damage in SMA (Fayzullina *et al.*, 2014). Generally, accumulation of DNA damage can be a result of either impaired DNA repair machinery or increased number of DNA breaks that exceed the capacity of repair systems to remove them efficiently. In a following up study, Fayzullina and colleagues reported that DNA repair is not faulty in SMA leading to the hypothesis that the observed DNA damage could be due to excessive formation of DNA breaks in SMN-deficient cells (Fayzullina *et al.*, 2016). In the same vein, Zhao and colleugues showed that SMN-deficiency leads to R loop accumulation in the termination region of genes and given that R loop accumulation is a source of genome instability, they hypothesized that increased number of R loops may lead to excessive DNA damage seen in SMA (Zhao *et al.*, 2016). Moreover, Jangi and collegues further reinforced the hypothesis of R loop-driven DNA damage in SMA (Jangi *et al.*, 2017). The primary aim of our study is to confirm that the genomic instability observed in SMA is R loop-mediated and to determine whether R loop resolution and the resultant prevention of DNA damage could rescue the disease phenotype and eventually lead to a novel therepautic approach to treat SMA.

Very briefly, the main aims of the project can be summarised as follows: we began by investigating endogenous DNA breaks in a range of SMA experimental models, including post-mortem tissue from SMA patients. It is worth highlighting that none of the studies listed above tested the clinical relevance of increased DNA damage to human disease and it will be presented here for the first time. After establishing that SMN deficiency can lead to accumulated DNA damage, the next goal was to provide a mechanistic understanding of how that happens. Having confirmed that the genomic instability observed in SMA is R loop-mediated in accordance to so far literature; a novel gene therapy approach with an adenovirus vector carrying the

senataxin gene (Ad-SETX) was utilised for *in vitro* and *in vivo* studies to determine the impact of R loop resolution on DNA instability and neurodegeneration in SMA. Furthermore, the role of SMN protein in rDNA integrity was also examined during this project as we discovered an interaction between SMN and RNA polymerase I protein. To our knowledge, this is a novel finding as this protein-protein interaction has not been reported before.

2. MATERIALS AND METHODS

2.1 Materials

2.1.1 DNA preparation

pLV-SMN FL, pLV-SMN Δ3, pRSV-Rev, pCMV ΔR8.92 and pMD.G were prepared using Qiagen mega prep kit (QIAGEN) prior to lentiviral production.

2.1.2 Expression constructs

The plasmid maps and sequences of LV-SMN FL and LV-SMN Δ3 used in this project are available in **Appendix 1**.

2.1.3 Viral vectors

The lentiviral vectors used in this project were generated in house, while the production of the adenoviral vectors used for our *in vitro* and *in vivo* studies was out-sourced:

Table 2-1: List of viral vectors used

Viral vector	Promoter	Produced by
Ad-SETX	CMV	Vector Biolabs
Ad-RFP	CMV	Vector Biolabs
LV-SMN FL	PGK	In house
LV-SMN Δ3	PGK	In house

2.1.4 Antibodies

All antibodies both primary and secondary utilised in this study are listed below:

Table 2-2: List of primary antibodies used

Target Protein	Host	Supplier	Application-Dilution
SMN	Mouse	BD	WB (1:5000), ICC (1:1000)
53BP1	Rabbit	Bethyl	ICC (1:800), IHC (1:500)
γH2AX	Mouse	Merk Millipore	ICC(1:1000), IHC (1:500)
RNA/DNA hybrids [S9.6]	Mouse	Kerafast	ICC (1:2000), IHC (1:1000)
SETX	Rabbit	Bethyl	ICC (1:500)
Tau	Mouse	ThermoFisher Scientific	ICC (1:500)
Nucleolin	Rabbit	Abcam	ICC (1:2000)
NeuN	Mouse	MERK MILLIPORE	IHC (1:500)
SETX	Rabbit	Novus Biologicas	IHC (1:500)
SMI32	Mouse	Biolegend	ICC (1:2000), IHC (1:2000)
RFP	Rabbit	Genetex	IHC (1:500)
γH2AX	Rabbit	R&D systems	IHC (1:500)
α-tubulin	Mouse	SIGMA	WB (1:10000)
SSRP1	Mouse	Biolegend	WB (1:5000)
RNA polymerase I	Rabbit	Bethyl	WB(1:1000)
RNA polymerase II	Rabbit	Santa Cruz	WB (1:250)

Table 2-3: List of secondary antibodies used

Target Protein	Host	Supplier	Application	Dilution
Mouse-A568	Goat	Invitrogen	IF	1:1000
Rabbit-A488	Goat	Invitrogen	IF	1:1000
Rabbit-A568	Goat	Invitrogen	IF	1:1000
Mouse-A488	Goat	Invitrogen	IF	1:1000
Rabbit-HRP	Goat	Thermo Scientific	WB	1:3000
Mouse-HRP	Goat	Bio-Rad	WB	1:3000

2.1.5 Post-mortem tissue

Human spinal cord sections were kindly provided by Brain UK Committee and Newcastle Brain Tissue Resource. Detailed information of each case is included in **Table 2-4**.

Table 2-4: Human tissue information

Subject code	Type	Age	Sex	Diagnosis/Symptoms
143/94	Control	50 days	M	Sceletal muscular atrophy/hypoplasia
R1220	Control	3 months	M	Non ketotic hyperglycinemia
NA44/92	SMA patient	4 months	F	Werdning Hoffman disease
NA132/95	SMA patient	6 months	M	Werdning Hoffman disease
177/90P	SMA patient	16 days	M	Werdning Hoffman disease
NN37/78	SMA patient	6 days	F	Werdning Hoffman disease

2.1.6 Reagents and chemicals

All the analytical grade chemicals, solvents and reagents were supplied by Sigma (Cambridge, UK) or Thermo Fisher Scientific Inc. (Loughborough, UK), unless otherwise stated.

2.1.7 Equipment

The main equipment used in this project is listed below

Table 2-5: List of equipment used

Equipment	Manufacture
NanoDrop 1000	Labtech
G: Box gel imaging system	Syngene

GENi imaging machine	Syngene
FLUOstar Omega plate reader	BMG Labtech
Optima L-100K Ultracentrifuge	Beckman Coulter
CFX96 Real-Time System C1000 Touch Thermal Cycler	BIO-RAD
Confocal microscope	Leica SP5 microscope system
Nikon microscope	Nikon
Bioruptor	Diagenode

2.2 In vitro experimental methods

2.2.1 Cells and cell culture maintenance

Primary fibroblast cell lines from SMA type I patients (GM03813, GM09677 and GM00232) and age and gender–matched healthy individuals (GM00498, GM05658, GM08680) were obtained from Coriell Cell Repositories. They were grown in Eagle's minimum essential medium (EMEM, SIGMA) containing 10% (v/v) fetal bovine serum (FBS, BIOSERA), 1 mM sodium pyruvate (SIGMA), 1x MEM vitamins (Lonza), 50 µg/ml uridine and 100 U/ml of penicillin and 100 µg/ml streptomycin (Lonza).

For primary cortical neuron culture, E16 embryos were dissected from carrier pregnant females (m*Smn*$^{+/-}$; *SMN2*$^{+/+}$*; SMNΔ7*$^{+/+}$*)* essentially as described by (Krichevsky *et al.*, 2001). Details about the SMNΔ7 mice are provided in **2.3.1 Breeding and genotyping of transgenic mice** section. DNA was isolated from embryos for genotyping. Very briefly, the cortices were dissected and digested in 0.25% trypsin in HBSS without calcium or magnesium (GIBCO) at 37°C for 15 minutes and dissociated manually in triturating medium by using three fire-burnt Pasteur pipettes with successively smaller openings. Dissociated cortical neurons were then plated on poly-D-lysine (SIGMA) coated plates and maintained in

Neurobasal medium (Life Technologies) supplemented with 2% B27 (Life Technologies), 0.5 mM GlutaMax (Life Technologies) and 100 U/ml of penicillin and 100 µg/ml streptomycin (Lonza).

For primary spinal motor neuron cultures, E13 embryos were dissected from carrier pregnant females (m*Smn*$^{+/-}$; *SMN2*$^{+/+}$*; SMNΔ7*$^{+/+}$*)* and the genotype of the embryos was determined by PCR. Cultures of embryonic lower motor neurons were prepared as described in (Weise *et al.*, 2010). Briefly, spinal motor neurons were isolated using the p75 immunopanning method. Cells were plated on poly-D-ornithine (SIGMA) and laminin (SIGMA) coated coverslips and maintained in Neurobasal medium (SIGMA) supplemented with 2% B27 (Life Technologies), 2% horse serum (SIGMA), 0.5 mM Glutamax (Life Technologies), 25 µM 2-mercaptoethanol (SIGMA), 5 ng/ml ciliary neurotrophic factor (CNTF) (Biotechne), 1 ng/ml glial cell line-derived neurotrophic factor (GDNF) (Biotechne), 5 ng/ml brain-derived neurotrophic factor (BDNF) (SIGMA) and 100 U/ml of penicillin and 100 µg/ml streptomycin.

For mixed spinal cord cultures, cells were plated in poly-D-ornithine and laminin coverslips, immediately after the dissection of spinal cords and dissociation of the cells without any further purification. Cells were maintained in Neurobasal medium supplemented with 2% B27, 2% horse serum, 0.5 mM Glutamax, 25µM 2-mercaptoethanol, 5 ng/ml CNTF, 1 ng/ml GDNF, 5 ng/ml BDNF and 100 U/ml of penicillin and 100 µg/ml streptomycin.

HEK293T cells (Human embryonic kidney cell line immortalized by the adenoviral E1A/E1B protein expressing the SV40 large T antigen) were obtained from ATCC and used for lentiviral productions. HEK293T cells were maintained in Dulbecco's Minimum Essential Medium (DMEM with 4.5 g/L Glucose, L-glutamine, without

sodium pyruvate, SIGMA), supplemented with 10% FBS and 100 U/ml of penicillin and 100 µg/ml streptomycin.

HeLa cells (a cell line derived from human cervical cancer cells) were obtained from ATCC and used for lentiviral titration assays. HeLa cells were maintained in DMEM, supplemented with 10% FBS and 100 U/ml of penicillin and 100 µg/ml streptomycin.

The human lung fibroblast cell line, MRC-5 (Medical research council cell-strain 5) was obtained from ATCC and used for Ad-SETX transduction validation studies. MRC-5 cells were maintained in EMEM supplemented with 10% FBS and 100 U/ml of penicillin and 100 µg/ml streptomycin.

2.2.2 Immunocytochemistry

Cells cultured on glass coverslips were fixed in 4% paraformaldehyde (PFA) (or 1:1 Methanol: Acetone for R-loops staining) for 10 minutes, washed with phosphate buffered saline (PBS) and permeabilised with 0.5% Triton X-100 in PBS. Cells were then blocked with 3% bovine serum albumin (BSA) in PBS for 30 minutes at room temperature and incubated with primary antibodies diluted in blocking buffer for 2 hours at room temperature. The primary antibodies utilised in this study included SMN (1:1000, BD), 53BP1 (1:800, Bethyl), γH2AX (1:1000, Merk Millipore), RNA/DNA hybrids [S9.6] (1:2000, Kerafast), SETX (1:500, Bethyl) and Tau (1:500, ThermoFisher Scientific). Finally, the cells were counter-stained with secondary Alexa-Fluor® conjugated antibodies (1:1000, Invitrogen) diluted in blocking buffer and incubated for 1 hour at room temperature. Hoechst stain was used to visualize nuclei. Images were captured using a Leica SP5 confocal microscope.

2.2.3 Comet assay

Alkaline comet assays were performed as previously described (Alagoz *et al.*, 2013). Briefly, day *in vitro* 7 (DIV7) primary cortical neurons were treated with accutase (SIGMA) for 10 minutes at room temperature for cell detachment. A five-minute centrifugation step at 400 g and 4°C was followed. The supernatant was discarded and the cells were re-suspended in pre-chilled PBS at a density of $3x10^5$ cells/ml and fixed with 1.4% low-melting agarose and layered onto pre-coated with 0.6% agarose glass microscope slides. The cells were then lysed and electrophoresis was conducted for DNA unwinding. Finally, samples stained with SYBR green were observed under microscope and tail moments from 50 cells/sample were quantified using Comet Assay IV software.

2.2.4 DNA/RNA immunoprecipitation (DRIP) followed by qPCR

The contents of 2 T175 flasks of healthy and SMA type I fibroblasts (roughly $5x10^6$ cells) were transferred to a 15 ml falcon tube, respectively, and the cells were pelleted gently. The cell pellet was washed with PBS and re-suspended in 1.6 ml Tris-EDTA (TE) buffer solution with addition of 41.5 µl 20% SDS and 5 µl Proteinase K and incubated overnight at 37°C. The genomic DNA was isolated with phenol/chloroform followed by ethanol (EtOH) precipitation, as described in the next section. The DNA was eluted in 150 µl TE. 100 µl of extracted DNA was digested overnight using a cocktail of restriction enzymes (Hind III, EcoRI, BsrGI, XbaI and SspI) according to supplier's instruction adding 2 mM spermidine and 1xBSA. After incubation, the digested DNA was cleaned up with phenol/chloroform followed by EtOH precipitation. For the negative control, half of the DNA was treated with RNAse

H overnight and cleaned up with phenol/chloroform followed by EtOH precipitation. For the DNA:RNA immunoprecipitation, 4 µg of digested DNA were diluted in 450 µl TE, with addition of 51 µl 10x binding buffer (100 mM NaPO4 pH 7.0 , 1.4 M NaCl, 0.5% Triton X-100) and 10 µl of S9.6 antibody (Kerafast) and incubated overnight at 4°C while gently inverting on a rotating shaker. The DNA/antibody complexes were added to prewashed (with 1x binding buffer) protein G magnetic beads (Invitrogen) and incubated for 2 hours at 4°C. After the incubation the beads were washed twice with 1x binding buffer and resuspended in 250 µl Elution buffer (50 mM Tris pH 8.0, 10 mM EDTA, 0.5% SDS) and 7 µl Proteinase K and incubated at 55°C for 45 minutes with inversion. Cleanup elution with phenol/chloroform and EtOH precipitation was followed. The concentration of DNA was measured with NanoDrop 1000 and the enrichment was analysed with real-time quantitative PCR (qPCR) using QuantiFast SYBR Green PCR kit (QIAGEN). 5 ng of immunoprecipitated DNA was added to 5 µl 2x QuantiFast SYBR Green PCR Master Mix along with the appropriate forward and reverse primers (the final concentration of each primer was 1 µM) and H_20 to make a final volume of 10 µl. Real-time PCR was performed by CFX96 Real-Time System C1000 Touch Thermal Cycler (Bio-Rad) following the program below:

- 95°C 5 minutes
- 95°C 10 seconds
- 60°C 30 seconds

39 cycles

Table 2-6: Primers used for DRIP-qPCR

Primer	Sequence
Positive primers	
MYADM F	CGTAGGTGCCCTAGTTGGAG
MYADM R	TCCATTCTCATTCCCAAACC

APOE F	CCGGTGAGAAGCGCAGTCGG
APOE R	CCCAAGCCCGACCCCGAGTA
EGR1 F	CATAGGGAAGCCCCTCTTTC
EGR1 R	CTTGTGGTGAGGGGTCACTT
BTBD19 F	GGCTGCTCAGGAGAGCTAGA
BTBD19 R	ACCAGACTGTGACCCCAAAG
Negative primers	
SNRPN Negative F	GCCAAATGAGTGAGGATGGT
SNRPN Negative R	TCCTCTCTGCCTGACTCCAT

2.2.5 Phenol-chloroform extraction

Phenol-chloroform extractions were performed in cases when DNA was required to be purified from a solution that might have also been mixed with proteins. One volume of phenol:chloroform:isoamylalcohol (25:24:1) (Merck Millipore) was added to DNA solution. The solution was mixed gently and centrifuged for 5 minutes at maximum speed. The top aqueous layer was collected and an equal volume of chloroform (Acros Organics) was added to it. After a centrifugation step for 2 minutes at maximum speed, the top aqueous layer was isolated and subjected to ethanol precipitation. More specifically, the aqueous phase was mixed with sodium acetate to final concentration 0.3 M, 1 μl Glycogen (5 μg) and 2 volumes of ice cold 100% ethanol. The sample was centrifuged at maximum speed for 30 minutes at 4°C. The supernatant was completely removed and the pellet was resuspended in 750 μl 70% ethanol. It was centrifuged at maximum speed for 2 minutes at 4°C. The wash step was repeated once again. At the end of the centrifugation the supernatant was carefully removed, the pellet was then air dried for 20 minutes at room temperature and dissolved in 20 μl H_20.

2.2.6 Subcloning of SMN FL and SMN Δ3

Codon – optimised SMN (coSMN) (generated by Geneart AG) was subcloned into a self-inactivating lentiviral (SIN-W-PGK) vector using standard cloning methods by Dr. Chiara Valori, prior to starting this project. I then generated coSMNΔ3 by an inverse PCR deletion method (Wang *et al.*, 2001) with inverse primers 5'-CACTTTCCACTGCTGCAGGCTG-3' and 5'-GTCGACCTGTCCCCCATCTGCGAAGTG-3' using SIN-W-PGK-coSMN as a template. Inverse PCR is a site-directed DNA mutagenesis technique using primers oriented in the reverse direction and allowing the amplification of the entire plasmid lacking the fragment of DNA that needs to be deleted. In our case, one of the primers was binding the exon 2 of SMN gene while the other one was binding exon 4. After the amplification, the PCR product was ligated and an enzymatic step to remove the background template was followed. The plasmid maps of LV-SMN FL and LV-SMN Δ3 are available in **Appendix 1**.

2.2.7 Production of lentiviral vectors

Lentiviruses were propagated in HEK293T cells using calcium phosphate transfection method (Deglon *et al.*, 2000). 13 µg pCMVΔR8.92 (packaging plasmid), 3.75 µg pMD.G (envelope plasmid), 3 µg pRSV-Rev (accessory protein rev plasmid) and 13 µg pLV-SMN FL or pLV-SMN Δ3 were transfected to HEK293T cells. Cells were allowed to produce the virus for 72 hours, then the supernatant was collected, filtered using a 0.45 µm filter (SIGMA) and centrifuged at 19,000 g for 90 minutes at 4°C. The supernatant was discarded and the viral pellet was resuspended in 1% BSA in PBS and stored at -80°C. Viral titres were measured by qPCR. Genomic

DNA isolated from transduced with serial dilutions (10^{-2}, 10^{-3} and 10^{-4}) HeLa cells was used as a template for qPCR with WPRE primers to assess the number of copies of stably integrated lentiviruses. WPRE (Woodchuck Hepatitis Virus Posttranscriptional Regulatory Element) is a substantial element carried by both oncoretroviral or lentiviral vectors and increases the levels of their transgene expression. A lentiviral vector carrying GFP of known biological titre (FACS titration) was used as a reference.

Table 2-7: Titres of lentiviral vectors

Virus	Titre
LV- SMN FL	0.4×10^{7} TU/mL
LV-SMN Δ3	1.9×10^{7} TU/mL

2.2.8 Western blotting

Unless otherwise indicated, total cellular protein was extracted as follows: cells were rinsed in ice-cold PBS and lysed with a nuclear and cytoplasmic RIPA (radioimmunoprecipitation) lysis buffer [5% Tris-HCl (pH 7.4), 1% NP-40, 0.5% Sodium deoxycholate, 0.01% SDS, 150 mM NaCl, 0.2 mM EDTA] supplemented with 1% Protease Inhibitor Cocktail (SIGMA). Protein concentration was determined by BCA (Bicinchoninic acid) protein assay (Thermo Scientific) as per the manufacturer's guidelines using PHERAstar FS spectrophotometer plate reader (BMG Labtech). Protein equivalents from each sample were subjected to SDS-PAGE following by immunoblotting. More specifically, protein samples were denatured in SDS protein sample buffer (10% Glycerol, 60 mM Tris/HCl pH 6.8, 2% SDS, 0.01% bromophenol blue, 1.2% beta-mercaptoethanol) by heating at 95°C for 5 minutes before being loaded on to a 8%, 10% or 12% SDS-polyacrylamide gel.

The gels were electrophoresed in Tris/Glycine/SDS running buffer at 50V for 30 minutes then 1-1.5 hours at 110 V. For immunodetection proteins were transferred onto a Polyvinylidene difluoride (PVDF) membrane in cold transfer (Tris/Glycine/Methanol) buffer at 250mA for 2 hours, or at 30mA overnight for high molecular weight proteins. 5% milk in TBST (0.137 M NaCl, 25.92 mM Tris base, 0.1% Tween20) (SIGMA) was used for blocking and incubation with antibodies. The proteins were visualized using the ECL Plus chemiluminescence detection kit (GE Healthcare) and images were captured using the G: Box gel imaging system (Syngene).

2.2.9 Cytoplasmic/Nuclear fractionation

Cells were harvested by trypsin-EDTA, collected by centrifugation (400 g, 5 minutes) and washed two times in ice-cold PBS, to remove traces of trypsin and growth media. The cell pellet was then slowly resuspended in hypotonic lysis buffer (10 mM HEPES, 1.5 mM MgCl2, 10 mM KCl, 0.5 mM DTT) supplemented with 2% Protease Inhibitor Cocktail (SIGMA) and 0.4% Ribosafe RNAse inhibitor (Bioline) and incubated for 15 minutes on ice. The lysates were homogenized by passing through a 19G (BD Microlance 3) needle 15 times; a small amount of lysates was stained with Trypan blue and microscopically examined for number of lysed cells, purity and integrity. Nuclei were pelleted by centrifugation at 1,500 g for 3 minutes at 4°C and supernatant containing the cytoplasmic fraction was collected. The supernatant was then centrifuged two more times, firstly at 3,500 g for 8 minutes and then at 17,000 g for 1 minute at 4°C. The supernatant of the final spin containing pure cytoplasmic fraction was collected. The pellet consisting of nuclei was re-suspended in IP lysis

buffer (50 mM HEPES, 150 mM NaCl, 1 mM DTT, 1% Triton, 1% sodium deoxycholate, 1 mM EDTA) supplemented with 2% Protease Inhibitor Cocktail, 0.1% Ribosafe RNAse inhibitor (Bioline) and passed through a 21G and a 23G needle for 10 times respectively, then it was incubated on ice for 30 minutes before centrifugation at 17,000 g for 4 minutes at 4°C. The supernatant was collected. Protein concentration of both fractions was determined by BCA assay and equal amounts of cytoplasmic and nuclear fractions were analyzed by western blotting as described previously.

2.2.10 Neurite outgrowth assay

For axon length measurements, motor neurons were immunolabelled for Tau (ThermoFisher Scientific, 1:500), images were taken with Leica SP5 confocal microscope and the neurite length was calculated using the ImageJ plugin NeurphologyJHT as described previously (Ho *et al.*, 2011). The quantification was kindly performed by Dr. Laura Ferraiuolo in a blinded fashion.

2.2.11 γH2AX-ChIP

Pelleted SMA type I and healthy fibroblasts (roughly $5x10^6$ cells/group) were re-suspended in 10 ml PBS and chemically crosslinked by the addition of 270µl 37% PFA while rotated for 10 minutes on ice. The cross-link reaction was then stopped by the addition of 1ml 1.25 M glycine and a further incubation at 4°C for 5 minutes. The cross-linked cells were pelleted by centrifugation at 500 g for 5 minutes at 4°C, washed once with PBS and re-suspended in 500 µl ChIP lysis buffer (50 mM

HEPES-KOH pH 7.5, 140 mM NaCl, 1 mM EDTA pH 8, 1% Triton X-100, 0.1% Sodium Deoxycholate, 0.1% SDS). The cells were lysed for 30 minutes while shaking in a thermomixer set at 4°C. The lysed cells were then sonicated at 4°C for 55 cycles (30 seconds on, 30 seconds off) using a Diagenode's Bioruptor to solubilize and shear crosslinked DNA. After the sonication the samples were centrifuged at 4°C for 10 minutes at maximum speed and the supernatant was collected. 10% of each sample was kept as input. The remaining 90% was then subjected to immunoprecipitation (IP). Briefly, 30 µl of protein G magnetic beads (Invitrogen) were washed two times with PBS/0.02% Tween-20 and incubated for 1 hour at 4°C with 5 µg of γH2AX (Merk Millipore) or mouse IgG antibody. Beads were washed two times with RIPA buffer. Meanwhile, 400 µl of the cell lysates were diluted 1:1 with 400 µl of RIPA lysis buffer and then loaded onto the beads. Two-hour incubation at 4°C was followed. At the end of the incubation, beads were washed four times with RIPA buffer and once with elution buffer (1% SDS, 0.1 M $NaHCO_3$). Bound complexes were eluted from the beads by heating at 65°C in a thermomixer and crosslinking was reversed by overnight incubation at the same temperature. Immunoprecipitated DNA and 10% input samples were then purified by treatment with RNase A, proteinase K and phenol/chloroform extraction. The DNA samples were then subjected to qPCR as described in section **2.4. DNA/RNA immunoprecipitation (DRIP) followed by qPCR**. The primer pairs used are listed below:

Table 2-8: Primers used for γH2AX ChIP-qPCR

Primer	Sequence
Human RPL32 F	GAAGTTCCTGGTCCACAACG
Human RPL32 R	GCGATCTCGGCACAGTAAG
Human 18 S F	ATGGCCGTTCTTAGTTGGTG
Human 18S R	CGCTGAGCCAGTCAGTGTAG
Human 5.8S F	GACTCTTAGCGGTGGATCACTC
Human 5.8S R	GACGCTCAGACAGGCGTAG
Human 28S F	CAGGGGAATCCGACTGTTTA
Human 28S R	ATGACGAGGCATTTGGCTAC

2.2.12 RT-qPCR

Cells were harvested and RNA was extracted using RNeasy Mini kit (QIAGEN) or Direct-zol RNA Miniprep (Zymo Research) according to the manufacturer's guidelines. The concentration of extracted RNA was then measured using NanoDrop1000 and the RNA was then subjected to quantitative reverse transcription PCR (RT-qPCR) using QuantiFast SYBR Green RT-PCR kit (QIAGEN). 10 ng of RNA (or 1 ng of RNA for rRNA analysis) was added to 5 µl 2x QuantiFast SYBR Green RT-PCR Master Mix along with the appropriate forward and reverse primers (the final concentration of each primer was 1 µM), 1 µl QuantiFast RT Mix and H_2O to make a final volume of 10 µl. RT-qPCR was performed by CFX96 Real-Time System C1000 Touch Thermal Cycler (Bio-Rad) using the program below:

- 50°C 10 minutes
- 95°C 5 minutes
- 95°C 10 seconds
- 60°C 30 seconds

39 cycles

Table 2-9: Primers used for RT-qPCR

Primer	Sequence
mouse 45S F	CTCTTCCCGGTCTTTCTTCC
mouse 45S R	TGATACGGGCAGACACAGAA
mouse 18S F	CGCGGTTCTATTTTGTTGGT
mouse 18S R	AGTCGGCATCGTTTATGGTC
mouse 5.8S F	TCGTGCGTCGATGAAGAA
mouse 5.8S R	CGCTCAGACAGGCGTAGC
mouse 28S F	CCCGACGTACGCAGTTTTAT
mouse 28S R	CCTTTTCTGGGGTCTGATGA

2.3 In vivo experimental methods

2.3.1 Breeding and genotyping of transgenic mice

All *in vivo* experiments were approved by the University of Sheffield Ethical Review Sub-Committee, the UK Animal Procedures Committee (London, UK) and performed according to the Animal (Scientific Procedures) Act 1986, under the Project License 40/3739. SMNΔ7 mice were purchased from The Jackson Laboratory (stock #005025) and were maintained in a controlled facility in a 12 h dark/12 h light photocycle (on at 7 am/ off at 7 pm) with free access to food and water. SMNΔ7 are triple mutant mice on a FVB background; they carry the human *SMN2* gene, human *SMN* gene without exon 7 (*SMNΔ7*) and lack the mouse *smn* gene. This mouse model was generated by Le and colleagues (Le *et al.*, 2005). Carrier (m$Smn^{+/-}$; $SMN2^{+/+}$; $SMN\Delta7^{+/+}$) animals were used for breeding and the offspring were tattooed (for identification) and genotyped immediately after birth at postnatal day 1 (P1) by PCR amplification of the transgenes according to the protocols provided by The Jackson Laboratory. Very briefly, tail clips were taken from P1 pups, submerged in 20µl DNA extraction solution (QuickExtract DNA Extraction Solution 1.0, Epicentre

Biotechnologies) and incubated for 15 minutes at 65°C, then for 2 minutes at 98°C in a thermocycler. The isolated DNA was then used for two PCR reactions as demonstrated below:

Table 2-10: Wild type (WT) reaction setup

Component	**Volume**	**Final concentration**
FIREPol 5x Master Mix	4 µl	1x
Smn forward primer (CTCCGGGATATTGGGATTG)	Variable	1.34 µM
Smn WT reverse primer (TTTCTTCTGGCTGTGCCTTT)	Variable	1.34 µM
Template DNA	1µl of quick extracted DNA	
H_2O	Variable	
Total reaction volume	20 µl	

Table 2-11: Mutant (MT) reaction setup

Component	**Volume**	**Final concentration**
FIREPol 5x Master Mix	4 µl	1x
Smn forward primer (CTCCGGGATATTGGGATTG)	Variable	1.34 µM
Smn MT reverse primer (GGTAACGCCAGGGTTTTCC)	Variable	0.5 Mm
Template DNA	1µl of quick extracted DNA	
H20	Variable	
Total reaction volume	20 µl	

Both reactions were run simultaneously under the following conditions:

- 94°C 3 minutes
- Start cycle 35 times
- 94°C 30 seconds
- 50°C 1 minute
- 72°C 1 minute and 30 seconds

- End cycle
- 72°C 7 minutes
- 10°C Hold

At the end of the reaction, the PCR products were loaded onto a 2% agarose gel with 0.5 µg/µL ethidium bromide and subjected to electrophoresis for 25 minutes at 120 V in a standard TAE buffer (40 mM Tris, 20 mM Acetate and 1 mM EDTA). The gel was visualised on a GENi imaging system (Syngene). Wild-type animals (WT) were expected to have one band at 800 bp, hemizygous (Hemi) carriers were expected to have two bands, one at 800 bp and one at 500 bp and finally homozygous transgenic animals (m*Smn*$^{-/-}$; *SMN2*$^{+/+}$; *SMNΔ7*$^{+/+}$ or KO) were expected to have one band at 500 bp.

2.3.2 Viral vector delivery

KO offsprings (m*Smn*$^{-/-}$; *SMN2*$^{+/+}$; *SMNΔ7*$^{+/+}$) from the same breeding pair were allocated randomly to the experimental groups. For Ad-SETX study, animals were injected intramuscularly the day after birth (postnatal day 1) under isoflurane anaesthesia with 30 µl (1x10^{9} PFU) of Ad-SETX or control vector Ad-RFP. The animals were left to recover before being rolled in sawdust from their cage and returned to the cage with their mother. Pups were sacrificed when they reached postnatal day 11 or they were euthanized when they were deemed ready for sacrifice based on animal welfare. The latter applied for mice included in the survival study.

2.3.3 Behavioural and clinical assessment

Animals were monitored daily for normal behavior as well as disease onset and progression. They were weighed every other day to minimize handling that could trigger an aggressive behaviour from their mother. After postnatal day 7, the mice were closely checked for grooming, respiration, gait, activity levels, and motor skills such as righting reflex as indicators of disease onset. When mice showed reduced mobility, loss of righting reflex, severe respiratory distress or being neglected by their mother, they were considered as end-stage mice and they were sacrificed.

2.3.4 Tissue collection

Mice were sacrificed by administration of 500 µg/g pentobarbital via intraperitoneal injection (sodium pentobarbital, 20% w/v solution for injections, JML). Intracardiac perfusion of cold PBS was immediately followed. Spinal cords were collected and incubated with 4% PFA for exactly 24 hours, they were washed thrice with PBS and then they were either incubated in 30% sucrose in PBS for at least one day before being cryoembedded in optimum cutting temperature medium (OCT, Dako) or dehydrated through a series of graded ethanol baths (from 70% to absolute ethanol), infiltrated with wax using Leica TP1020 tissue processor and then embedded in paraffin blocks. OCT–embedded lumbar spinal cords were sectioned at 20µm using a Leica CM3050s cryostat and placed onto slides, while paraffin-embedded lumbar spinal cords were sectioned at 5µm using a Leica RM2245 microtome. Spinal cord sections were then subjected to immunostaining as described below. Brains used for the TOP1cc experiment were collected immediately after PBS perfusion and snap frozen in liquid nitrogen. For neuromuscular analysis, the right back legs of Ad-SETX or Ad-RFP injected mice were isolated after PBS perfusion and immersed in 4% PFA

for 30 minutes then washed thrice with PBS and FBS muscles of those legs were then subjected to neuromuscular analysis. Finally, gastrocnemius muscles of Ad-SETX and Ad-RFP injected were snap frozen in isopentane: liquid nitrogen baths immediately after PBS perfusion.

2.3.5 Neuromuscular analysis

Analysis of neuromuscular pathology was performed on Ad-RFP and Ad-SETX injected SMA P11 mice [n=12 muscles, N=7 mice (Ad-RFP injected); n=6 muscles, N=3 mice (Ad-SETX injected). Spinal motor neuron cell body counts were performed as previously described in (http://www.treat-nmd.eu/downloads/file/sops/sma/SMA_M.1.2.004.pdf). NMJ pathology was assessed on whole-mount immunohistochemically-labelled preparations of FDB (flexor digitorum brevis) muscles as previously described (Powis *et al.*, 2016b; Wishart *et al.*, 2014). Example images were taken using a Nikon A1R confocal system combined with a Ti:E inverted microscope (×60 objective). NMJ analysis was kindly performed by members of Professor Gillingwater's lab at the University of Edinburgh. The investigators were blinded to the treatment groups.

2.3.6 Measurement of topoisomerase 1 cleavage complexes (TOP1cc)

TOP1 protein–DNA complexes (TOP1cc) were purified using caesium chloride density gradients. Cortical tissues from SMA mice described above (100mg) were homogenised using a piston-type pestle homogeniser and cells (2×10^6) were lysed in

1% sarcosyl, 8 M guanidine HCl, 30 mM Tris pH 7.5 and 10 mM EDTA. Tissue lysates were then incubated at 70°C for 15 minute to remove all non-covalently bound proteins from DNA. Cell lysates were then loaded on a caesium chloride density (CsCl) step gradient (5 ml total volume); a stock solution of caesium chloride was made by dissolving 63.2 g of CsCl (Affymetric-USB Corporation) in 36.8 ml of TE buffer (10 mM Tris, 1 mM EDTA [pH 8.0]). This stock solution with a density of 1.86 g/ml was used to prepare four CsCl solutions with densities of 1.82 g/ml, 1.72 g/ml, 1.50 g/ml, and 1.37 g/ml. The tissue lysates were loaded on top of the gradient and centrifuged at 75,600 × g at 25°C for 24 hour to separate free proteins from DNA. Ten consecutive 0.5 ml fractions were collected and slot blotted onto Hybond-C membrane (Amersham). To ensure equal DNA loading, the DNA concentration in each extract was determined fluorimetrically using PicoGreen (Molecular Probes/Invitrogen). Covalent TOP1–DNA complexes were then detected by immunoblotting with anti-TOP1 anti- bodies (sc-32736, Santa Cruz) and visualised by chemiluminescence. The TOP1 cc experiments were kindly performed by Dr. Liao from Prof. El-Khamisy's lab.

2.3.7 Immunohistochemistry

Mice were terminally anesthetized and transcardially perfused as previously described (Ning *et al.*, 2010a). Spinal cord sections were washed 3 times with PBS, blocked with 10% goat serum in PBS/0.2% Triton X-100 solution for 1 hour and double stained for 53BP1 (1:500, Bethyl) and NeuN (1:500, MERK MILLIPORE). The sections were incubated overnight at 4°C with primary antibodies diluted in PBS/0.2% Triton X-100 supplemented with 5% goat serum. On the second day,

sections were washed three times with PBS and incubated with secondary Alexa-Fluor® conjugated antibodies (1:2000, Invitrogen) diluted in PBS/0.2% Triton X-100 for 1 hour at room temperature. Hoechst stain was used to visualize the nuclei. Images were taken with Leica SP5 confocal microscope. For R loop staining, S9.6 (1:1000, Kerafast) antibody was used. Before primary antibody incubation, antigen retrieval was performed in 10 mM Tris for 30 minutes in a pressure cooker. Visualisation of the primary antibodies was enabled by use of the intelliPATH FLX™ Detection Kit, according to the manufacturer's protocol. Similarly, human spinal cords were stained with γH2AX (1:500 R&D systems), or S9.6 (1:1000, Kerafast), respectively. Visualisation of the primary antibodies was enabled by use of the intelliPATH FLX™ Detection Kit, according to the manufacturer's protocol.

Furthermore, immunofluorescence of paraffin-embedded tissue was performed using Vectastain ABC Kit as follows: for deperaffinization and antigen retrieval the slides were placed in a pressure cooker with citrate-based pH 6 solution and heated for 15 minutes. The slides were then incubated in Glycine/PBS for 15 minutes; they were washed briefly with TBS and blocked for 30 minutes using diluted normal blocking serum. An overnight incubation with the first primary antibody was followed. The slides were then washed with TBS and incubated for 30 minutes with biotinylated secondary antibody. After a brief wash with TBS, the slides were incubated with Alexa Fluor 488 (or 555) Streptravidin. Next, the slides were blocked using Avidin/Biotin Blocking kit (SP – 2001, Vector Laboratories) as per the manufacturer's guidelines and the incubation with the second primary antibody was followed as described above. At the end, the slides were dried and mounted with Vectashield (Hard set) mounting medium with DAPI (H-1500, Vector Laboratories).

For Nissl staining, the spinal cord sections were defatted with xylene for 5 minutes and hydrated through washes with 100%, 96%, 70% and 50% ethanol. They were then washed with H_2O and incubated for 5 minutes in 0.1% Cresyl Fast Violet solution. They were quickly rinsed in H_2O, incubated for 15 minutes in 95% ethanol and then dehydrated in 100% ethanol for 1 minute. Finally, the slides were incubated in xylene for 5 minutes and then mounted with permanent mounting medium.

These experiments were performed with help from members of the histology lab.

2.3.8 Randomization and blinding process

For our *in vivo* study, we employed a double-blind randomization process in which experimental groups were blinded to the person conducting viral delivery and another blinded person analysed the data (e.g. motor neuron counts or NMJ analysis). In addition, our collaborator in Edinburgh received coded muscle tissues for NMJ analysis and the codes were released to the supervisor once the quantification was completed.

For R loop, 53BP1 and Top1cc assays, data were obtained from spinal cords and brains harvested from SMA (mSmn-/-; SMN2+/+; SMNΔ7+/+) and control (mSmn+/+; $SMN2^{+/+}$; $SMN\Delta7^{+/+}$) mice sacrificed at postnatal P2 (R loops) or P10 (53BP1 and Top1cc). We similarly employed a double-blind process in which the person undertaking the assays was blinded to the condition assigned. A separate person analysed the data was similarly unaware of the genotype of the mice.

2.3.9 Experimental repeats and Statistical analysis

All data are presented as mean ± standard error of the mean (s.e.m.) of 3 experimental replicates, unless otherwise stated. Statistical analysis was performed using GraphPad Prism 6. Statistical differences were analysed using a Student's t-test, one way or two way Anova, with $p < 0.05$ considered to be statistically significant.

3. Elevated DNA breaks in human and murine experimental models of SMA

3.1 Aim

DNA damage and genome instability have been linked to several neurodegenerative diseases such as Alzheimer's disease, Parkinson's disease as well as Amyotrophic Lateral Sclerosis (Anderson *et al.*, 1996; Bender *et al.*, 2006; Hill *et al.*, 2016a; Lu *et al.*, 2004; Walker *et al.*, 2017). Fayzullina and colleagues were the first to report excessive accumulation of DNA breaks in tissue isolated from an SMA mouse model; however their research was predominantly focused on skeletal muscle (Fayzullina *et al.*, 2014). The increased DNA damage observed in Smn-deficient muscles could be attributed to increased number of DNA breaks or faulty DNA repair. Interestingly, during the course of this PhD several publications came out linking SMN protein with DNA repair or prevention of DNA damage as described in Chapter 1 (Fayzullina *et al.*, 2016; Jangi *et al.*, 2017; Zhao *et al.*, 2016).

The aim of this project was to examine DNA damage in SMA and to address whether DNA damage is a contributing factor for the SMA neurodegenerative process, and if so to introduce new therapeutic targets for treating SMA. Using established DNA repair assays the formation of endogenous DNA breaks was investigated in SMA experimental models including fibroblasts derived for SMA type I patients, embryonic cortical and motor neurons isolated from SMNΔ7 mice, murine spinal cord and brain tissue as well as human post-mortem tissue.

3.2 Cellular models

3.2.1 SMA type I fibroblasts display elevated endogenous DNA breaks

As an initial step towards the correlation between SMA and DNA damage, endogenous DNA breaks were investigated in SMA experimental models, starting with fibroblasts cultured from either healthy controls or SMA type I patients. The main advantage of using skin fibroblasts as an *in vitro* model of SMA is their easy availability from patients and matched controls. Phosphorylation of histone H2AX (γH2AX) is an early marker to DNA double-strand breaks (DSBs) and leads to the formation of γH2AX foci at the sites of DSBs (Modesti *et al.*, 2001; Rogakou *et al.*, 1999). Assessment of DSBs, indicative of genomic instability, achieved using γH2AX immunoreactivity revealed a striking increase in γH2AX foci in SMA type I fibroblasts compared to healthy controls (**Figure 3-1**), suggesting that SMN deficiency might lead to DNA instability in SMA.

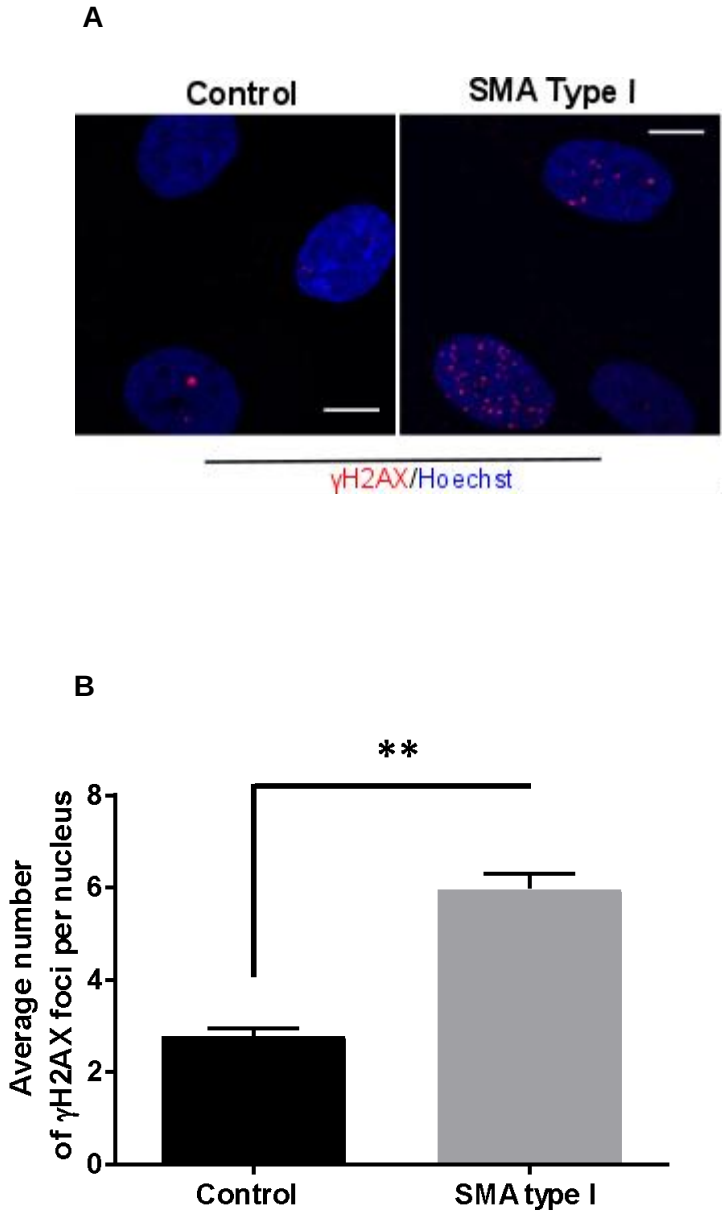

Figure 3-1: γH2AX staining in SMA type I fibroblasts.

(A) Immunofluorescence detection of γH2AX foci (red) and Hoechst (blue) in SMA type I fibroblasts and healthy controls. Scale bars represent 10 µm. (B) Average number of γH2AX foci per nucleus. Nuclei counted = 50 per line. Data are presented as mean ± s.e.m. ** $P < 0.01$, paired two-tailed *t* test; p= 0.0068. *t* test was selected as only two groups (control vs SMA type I) were compared for statistical differences. The data were collected from 3 biological independent replicates (n=3) and were normally distributed.

To further confirm DNA instability as a function linked to SMN deficiency, 53BP1 immunostaining was examined in control and SMA patient fibroblasts. 53BP1 (also called TP53BP1), is a mediator of DNA double-strand break (DSB) repair and accumulates at the sites of DSB forming nuclear bodies/foci. When SMA type I fibroblasts derived from 3 different patients (GM08318, GM09677, and GM00232) and healthy controls (GM00498, GM08680, and GM05658) were probed for 53BP1 immunoreactivity, a significant increase in the number of 53BP1 foci was observed in all three SMA patient fibroblast cell lines (**Figure 3-2**) compared to healthy controls, indicating that this phenotype is more likely to be disease - related than cell line specific.

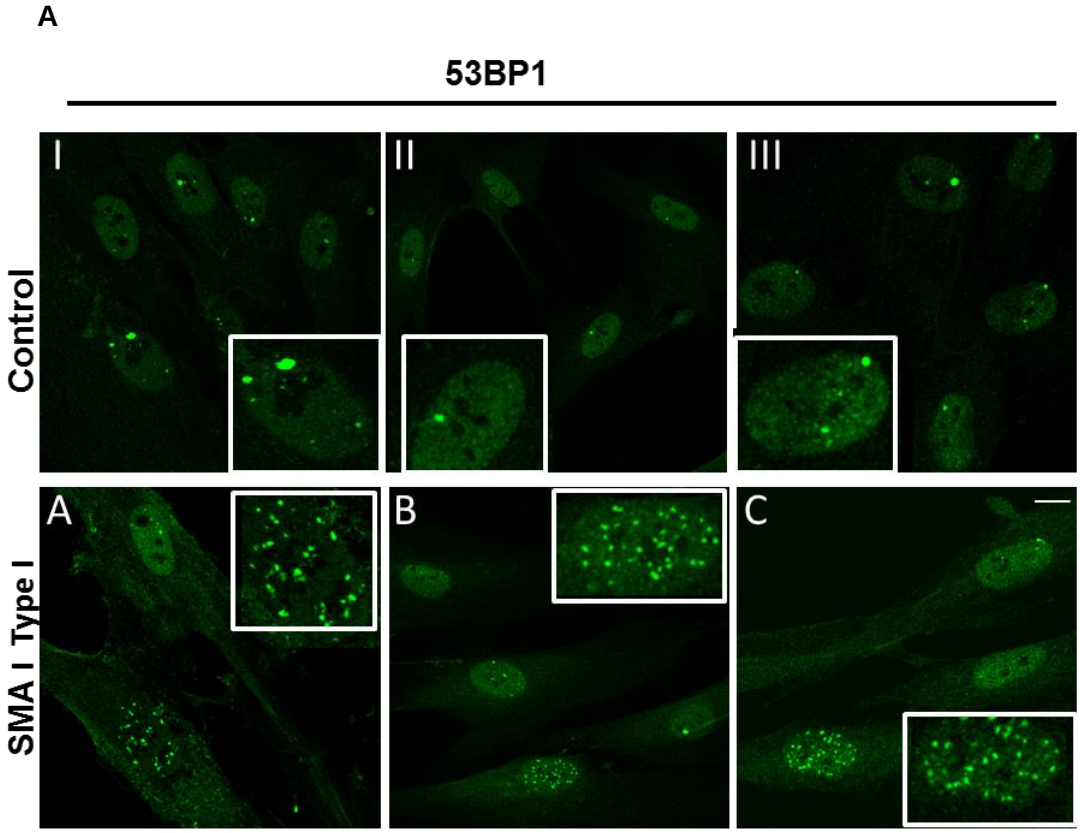

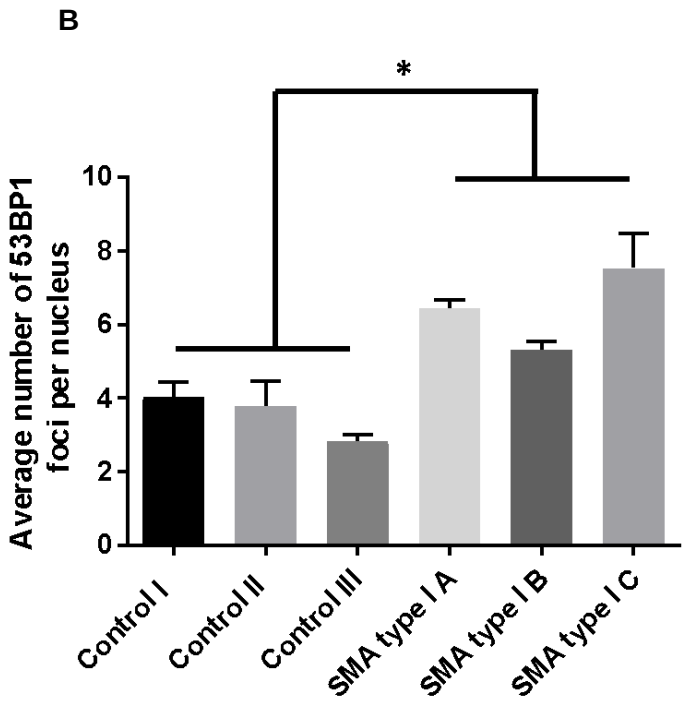

Figure 3-2: 53BP1 staining in SMA type I fibroblasts.

(A) 53BP1 immunoreactivity in fibroblasts derived from 3 different SMA type I patients (A = GM08318, B = GM09677, C = GM00232) and healthy controls (I = GM00498, II = GM08680, III = GM05658). Scale bars of all images represent 10 µm**.** (B) Quantification of the number of 53BP1 foci in control and SMA type I fibroblasts. Nuclei counted =50. Data are presented as mean ± s.e.m. * $P < 0.05$; paired two-tailed *t* test comparing the average of control group with the average of SMA type I group; p= 0.0176. The data were collected from 3 biological independent replicates (n=3).

3.2.2 Smn-depleted cultured neurons develop hallmarks of endogenous DNA instability

It was next investigated whether the phenotype observed in SMA type I fibroblasts can be replicated in post-mitotic neurons derived from SMNΔ7 mice (Le *et al.*, 2005),

a widely used mouse model of SMA (Sleigh et al., 2011). Initially, cortical neurons isolated from E16 control (m*Smn*$^{+/+}$; *SMN2*$^{+/+}$; *SMNΔ7*$^{+/+}$, referred to as wild type littermate) and SMA (m*Smn*$^{-/-}$; *SMN2*$^{+/+}$; *SMNΔ7*$^{+/+}$, referred to as SMNΔ7 knock out) embryos were immunostained with an antibody to the neuronal marker MAP2. It was revealed that over 85% of cells are MAP2 positive (**Figure 3-3**). Consistently with our findings in fibroblasts, there was an increase of endogenous DNA breaks in SMNΔ7 cortical neurons compared to controls; with cells lacking nuclear SMN gems appeared to have elevated 53BP1 foci, confirming a correlation between lack of SMN expression and DNA damage (**Figure 3-4**).

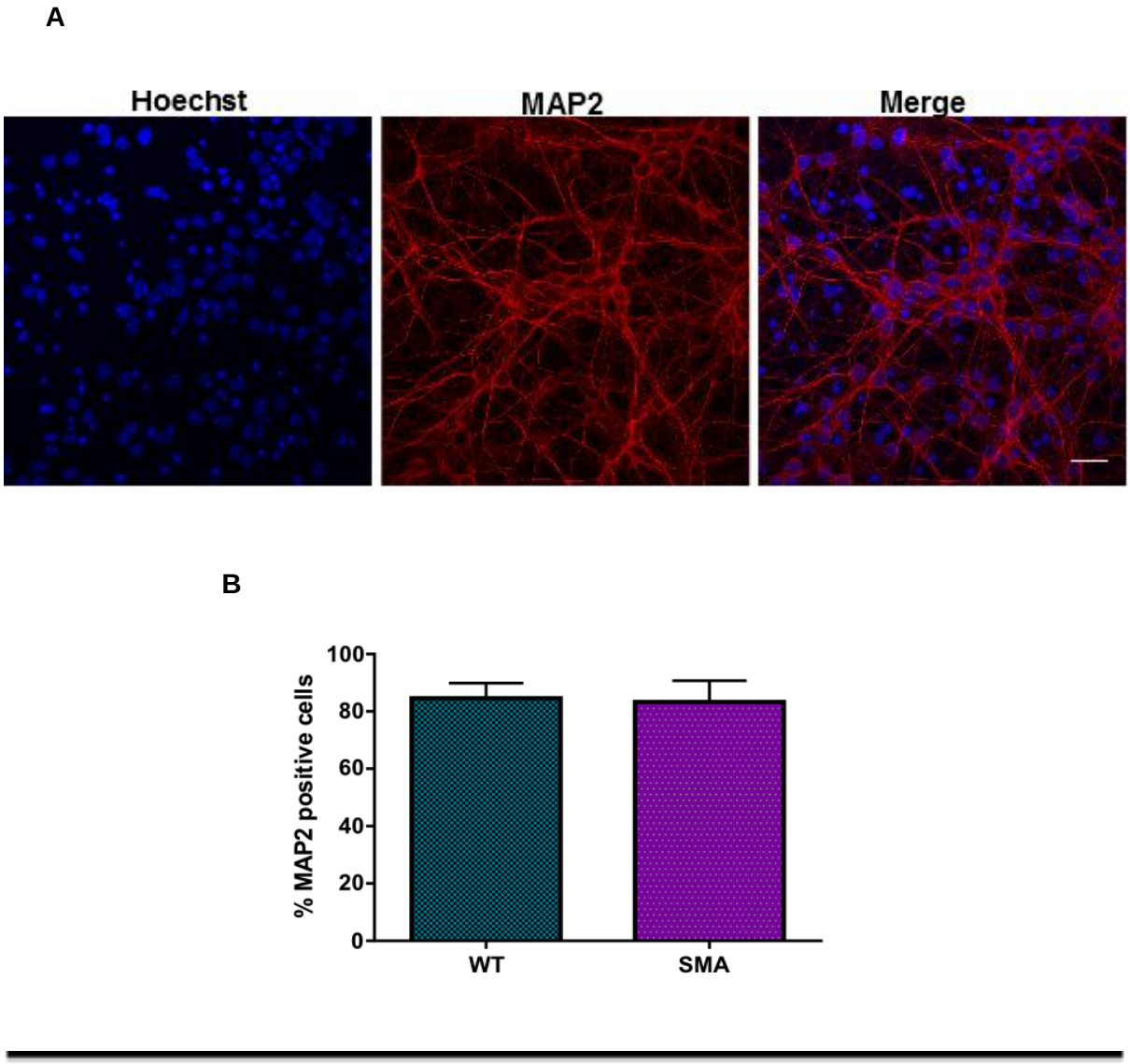

Figure 3-3: Cortical neuron cultures stained with neuronal marker MAP2.

(A) Dissociated cells from E16 mouse cortex were immunostained for the neuronal marker MAP2 after being in culture for 7 days (DIV7). Representative images are shown. Scale bar represents 25 µm. (B) The percentage of MAP2-positive cells in culture is presented as mean ± s.e.m. (C) The percentage of MAP2-positive cells isolated from WT embryonic cortices is compared to SMA. Data are presented as mean ± s.e.m.

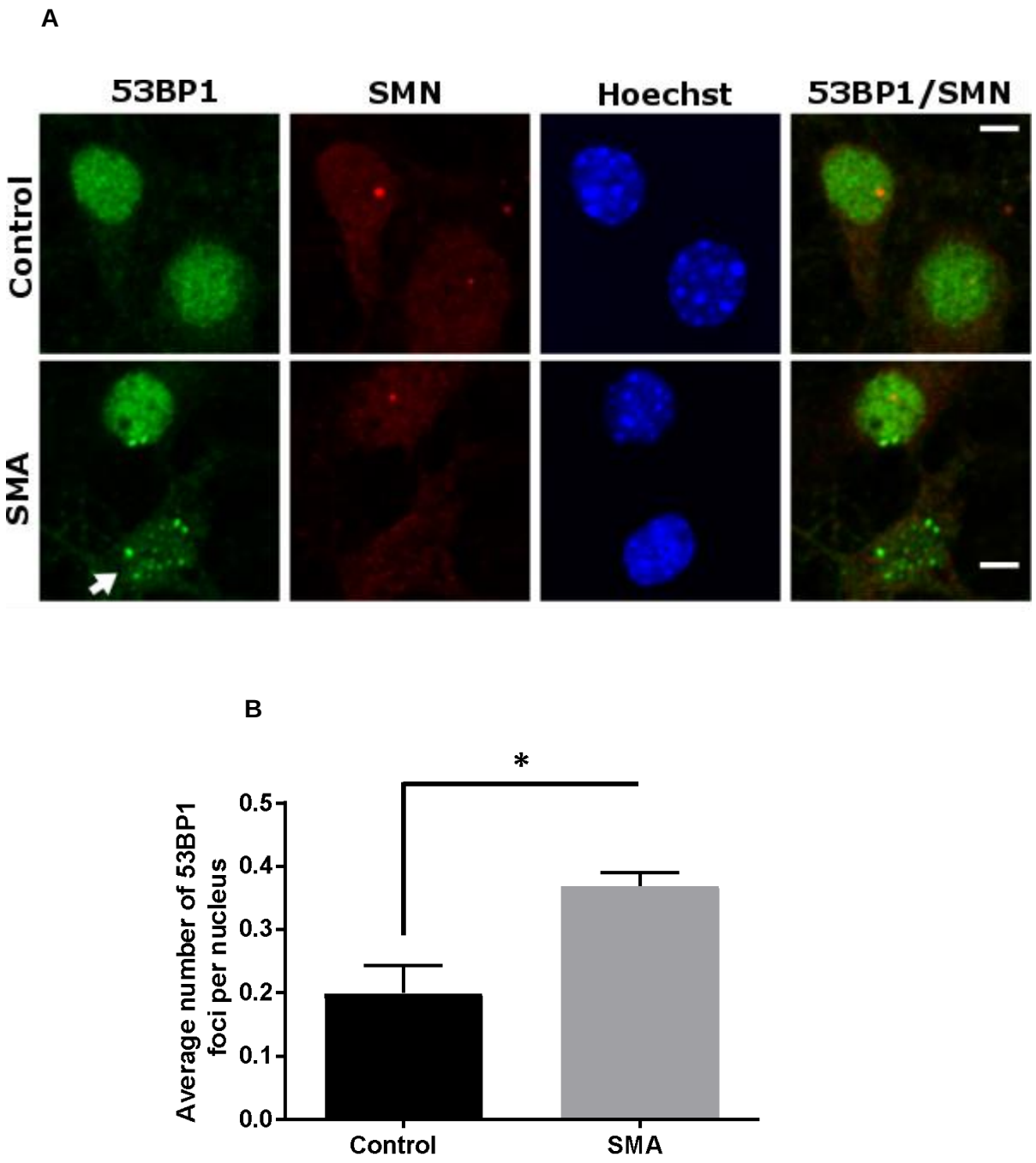

Figure 3-4: 53BP1 and SMN dual staining in SMA cortical neurons.

(A) Embryonic cortical neurons isolated from SMNΔ7 mice were double immunolabelled for 53BP1 (green) and SMN (red). Smn deficiency leads to elevation of 53BP1 nuclear foci (Arrow). Scale bars represent 5 µm. (B) Average number of 53BP1 foci per nucleus. Data are presented as mean ± s.e.m. * $P < 0.05$; paired two-tailed *t* test, p=0.0256. The data were collected from 3 independent neuronal cultures (biological replicates). Nuclei counted = 150/replicate.

Consistent with previous data, depletion of Smn in cortical neurons also led to a significant increase in γH2AX foci, in comparison to cells derived from healthy mouse embryos (**Figure 3-5**).

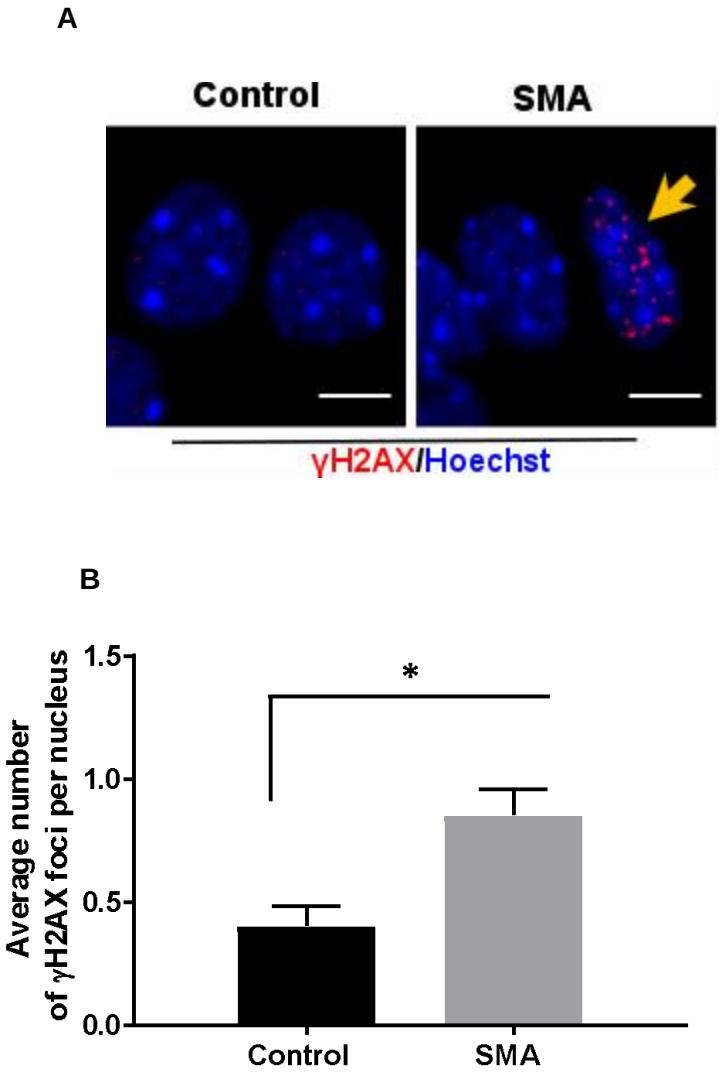

Figure 3-5: γH2AX staining in embryonic cortical neurons.

(A) Cortical neurons (DIV7) derived from SMNΔ7 mice were labelled for γH2AX (red). Nucleus is labelled with Hoechst (blue). Scale bars represent 5 μm. (B) Quantification of the number of γH2AX foci in control and SMA embryonic cortical neurons. Data are presented as mean ± s.e.m. * $P < 0.05$; paired two-tailed t test, p=0.0234. The data were collected from 3 biological independent replicates (n=3).

To further confirm the presence of DSBs in experimental models of SMA, DNA breaks were measured using the alkaline comet assay, a sensitive and rapid single-cell gel electrophoresis assay widely used to assess total DNA breakage in eukaryotic cells at the single cell level (Alagoz *et al.*, 2013; Meisenberg *et al.*, 2016). In these assays cells are immobilized in agarose and lysed to form nucleoids, which are supercoiled DNA loops attached to the nuclear matrix. The principle is that DNA containing breaks loses its supercoiling and migrates towards the anode during electrophoresis forming a comet-like appearance (Azqueta *et al.*, 2014; Collins, 2004; Olive *et al.*, 2006). Analysis of Comet assay data further confirmed DNA damage in Smn-depleted neurons (**Figure 3-6**), therefore supporting our previous data (**Figures 3-4 & 3-5**).

A

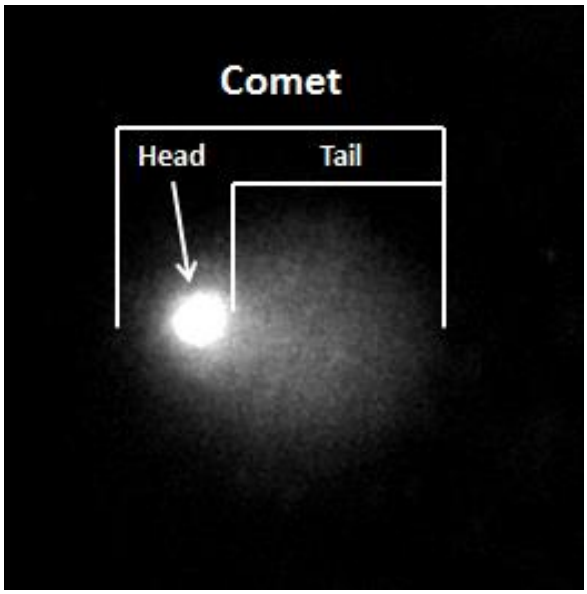

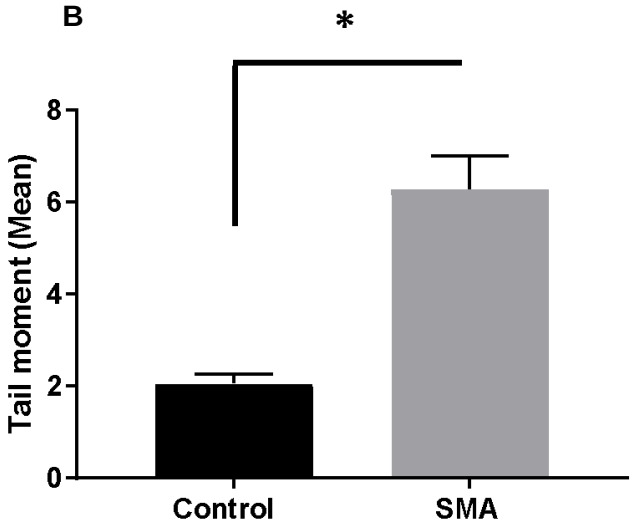

Figure 3-6: Comet assay in cortical neurons.

(A) Microscopy visualization of comets. The comet 'head' represents the cell nucleus containing undamaged DNA. Damaged and fragmented DNA migrates from the cell nucleus towards the anode forming the comet 'tail'. (B) Cortical neurons were harvested at DIV7 and subjected to comet assay. DNA damage was quantified as the comet tail moment which is defined as the product of tail length and the fraction of total DNA in tail. Tail moment = Tail length x % DNA in tail. Data presented as mean ± s.e.m. * $P < 0.05$, paired two-tailed t test, p=0.0364. Data were collected from 3 biological independent replicates (n=3). Nuclei analysed = 100/replicate.

It was then examined whether increased DNA instability can also be observed in SMN-deficient motor neurons, the cells that primarily degenerate in SMA. To test this point, spinal motor neurons derived from E13 SMNΔ7 embryos, a well-established animal model of SMA, and cultured using the p75 immunopanning method (Weise *et al.*, 2010) (**Figure 3-7**) were labelled with anti-γH2AX antibodies (**Figure 3-8**). Analysis of this labelling revealed significant increase in the number of γH2AX foci in

Smn-deficient motor neurons compared to wildtype controls (**Figure 3-8**). The faint cytoplasmic signal of γH2AX stained motor neurons could be attributed to either presence of mitochondrial DNA damage in these neurons or non-specific signal due to the fact that the γH2AX is a mouse antibody used on mouse cells. However, the cytoplasmic staining was very faint compared to the bright nuclear signal and it is worth highlighting that only nuclear foci were counted in the figures presented here.

A

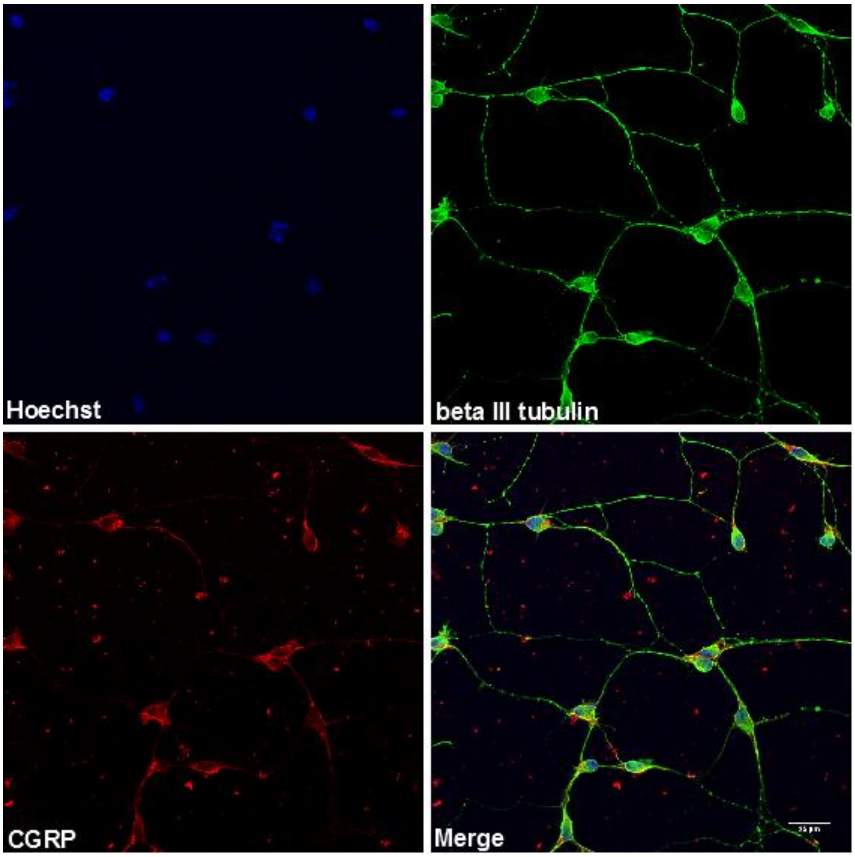

B

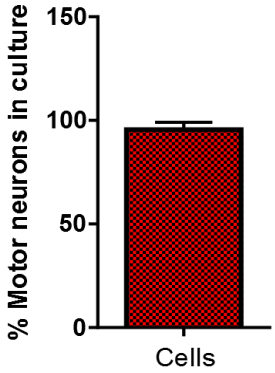

Figure 3-7: Motor neuron culture prepared using p75 immunopanning method.

(A) DIV7 cultures were immunostained for the motor neuron marker CGRP and the pan-neuronal marker beta III tubulin. Scale bar represents 25 µm. (B) The percentage of motor neurons was estimated based on the CGRP immunolabelling. Data are presented as mean ± s.e.m.

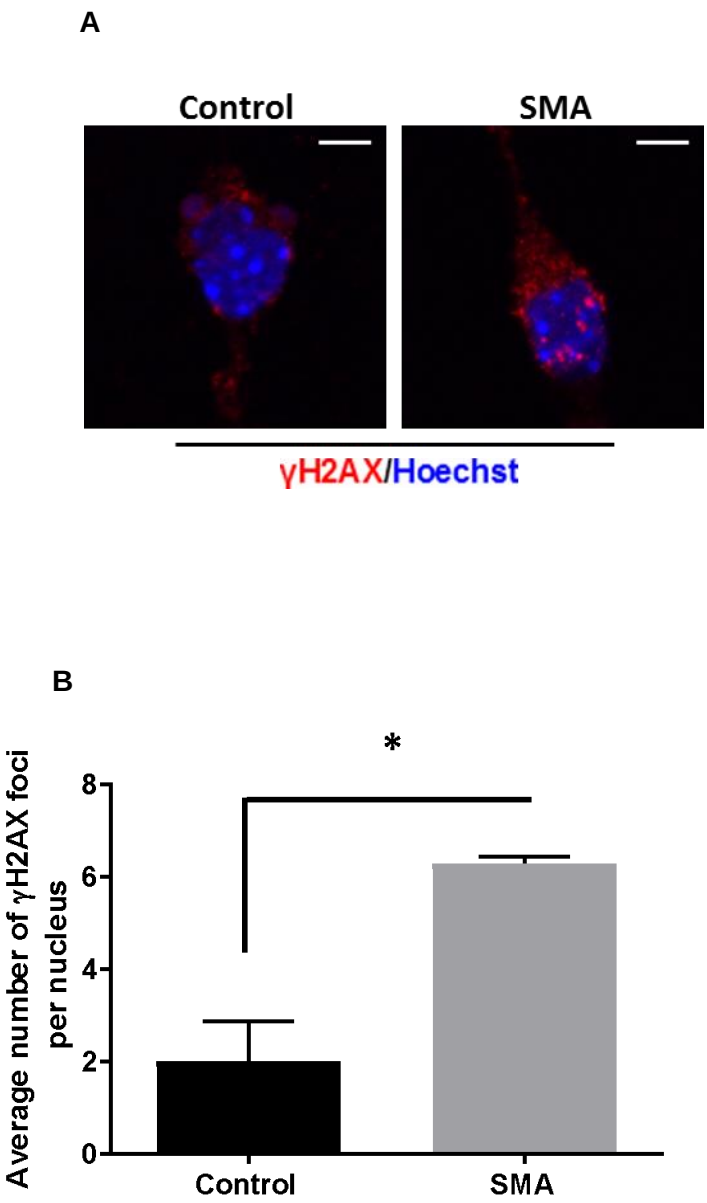

Figure 3-8: γH2AX staining in murine embryonic motor neurons.

(A) p75 enriched motor neurons (DIV7) derived from SMNΔ7 embryos were labelled for γH2AX. (B) Average number of γH2AX foci per nucleus of motor neurons. Data presented as mean ± s.e.m. * $P < 0.05$; paired two-tailed t test, $p=0.0284$. The data were collected from 3 biological independent replicates (n=3). Nuclei counted = 10-20/replicate.

3.3 In vivo animal models

3.3.1 SMA mouse model exhibit increased DNA damage in the spinal cord

Having established a link between SMN deficiency and DNA instability in SMA cellular models, the so far findings were next tested in whole organisms based on the SMNΔ7 mouse model. Spinal cord sections from P10 symptomatic SMA (m*Smn*$^{-/-}$; *SMN2*$^{+/+}$; *SMNΔ7*$^{+/+}$) and control (m*Smn*$^{+/+}$; *SMN2*$^{+/+}$; *SMNΔ7*$^{+/+}$) mice were first immunolabeled with γH2AX antibody, and elevated γH2AX immunoreactivity was observed in the SMA mice when compared to controls (**Figure 3-9**). Interestingly, H2AX phosphorylation produces pan-nuclear γH2AX in SMA spinal cord sections instead of foci, which was observed in motor neurons cultured from the mice. The cells with pan-nuclear γH2AX staining may represent apoptotic cells with compact chromatin (de Feraudy *et al.*, 2010; Leist *et al.*, 2001). One potential way of showing that these γH2AX positive cells are indeed apoptotic would be by dual immunohistochemistry alongside an apoptotic marker such as cleaved Poly(ADP-ribose) Polymerase (PARP) (Boulares *et al.*, 1999; Chaitanya *et al.*, 2010; Walker *et al.*, 2017). However, due to time constrains that was not investigated further.

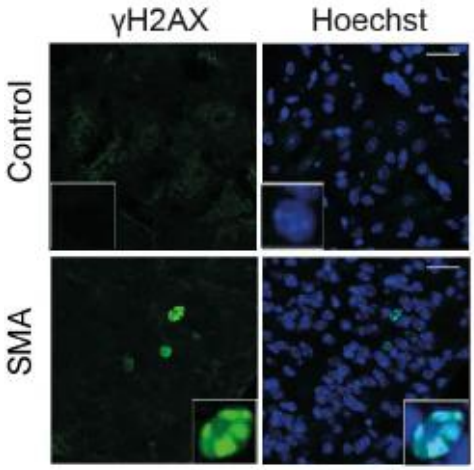

Figure 3-9: γH2AX staining in SMNΔ7 mouse spinal cords.

Representative images of γH2AX (green) and Hoechst (blue) staining in the lumbar spinal cord sections of post-natal day 10 SMA (n=5) and control (n=5) mice. Scale bars represent 25 µm. High power images (insets) indicate abnormal nuclear morphology (Hoechst) in γH2AX positive cells.

A double immunostaining of spinal cord sections with γH2AX and Calcitonin gene-related peptide (CGRP), a marker for motor neurons (Azzouz *et al.*, 2004b; Ralph *et al.*, 2005), revealed that all γH2AX – immunopositive cells were motor neurons. CGRP is predominantly located in the cytoplasm forming a ring around the nucleus that likely corresponds to its localization to the Golgi apparatus (Marvizon *et al.*, 2002). It was observed, however, that CGRP distribution in Smn-deficient/γH2AX^{+} motor neurons is different than in controls (**Figure 3-10**) and is similar to spinal cords of DNA repair-deficient excision repair cross-complementing 1 (Ercc1)$^{\Delta/-}$ mice (de Waard *et al.*, 2010). The abnormal CGRP distribution observed in both animal models could be a sign of motor neuron degeneration.

ERCC1 protein forms a complex with xeroderma pigmentosum group F (XPF) that acts as a nuclease in the NER pathway (Houtsmuller *et al.*, 1999). ERCC1-XPF is also required for the repair of interstand crosslinks as well as DSB repair (Ahmad *et al.*, 2008; Bhagwat *et al.*, 2009). Therefore, Ercc1$^{\Delta/-}$ mice are impaired in several DNA repair systems and interestingly, exhibit progressive motor abnormalities with impaired neuromuscular junctions, degeneration of motor neurons as well as reduced lifespan (de Waard *et al.*, 2010), similar to SMA. This similarity of SMA phenotype to (Ercc1)$^{\Delta/-}$ is very important as it indicates that accumulation of DNA damage may contribute to motor neuron vulnerability in neuromuscular disorders like SMA.

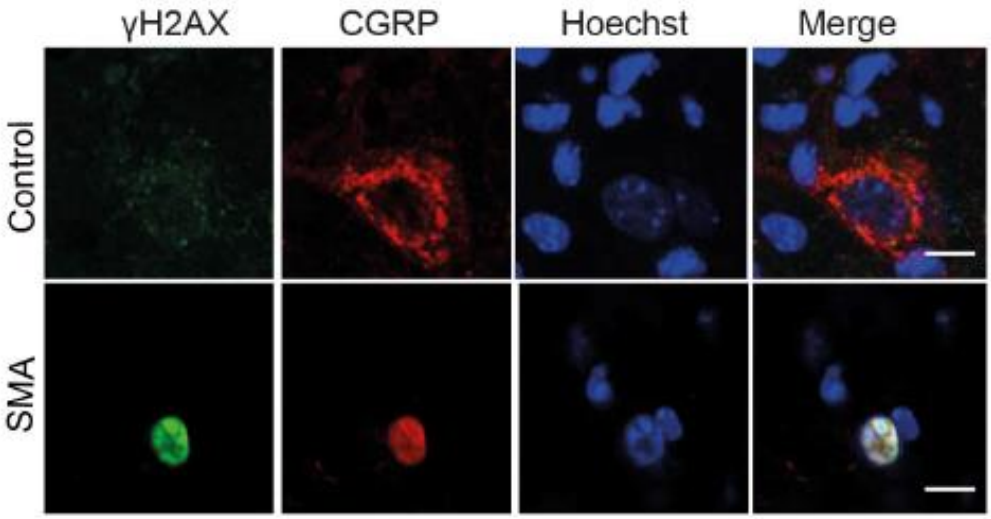

Figure 3-10: γH2AX and CGRP dual staining in SMNΔ7 mouse spinal cords.

Representative images of γH2AX (green) and CGRP (red) double-labeled lumbar spinal cord sections of P10 SMA and control mice. Scale bar represent 10 μm.

Labelling with 53BP1, another marker for DSBs, of the spinal cord sections also confirmed a remarkable increase in DNA breaks in SMA mice as revealed by elevated 53BP1 expression with co-localisation of nuclear foci in NeuN-positive neurons (**Figure 3-11**). Interestingly, most of neurons with numerous 53BP1 foci exhibited abnormal nuclear morphology and diminished NeuN expression, suggesting that accumulation of DNA damage could be an early sign of neuronal degeneration in SMA. Diminished NeuN expression could also suggest that neurons lose their post mitotic state trying to re-enter cell cycle as part of DNA damage response (Kruman *et al.*, 2004; Lavin *et al.*, 2006).

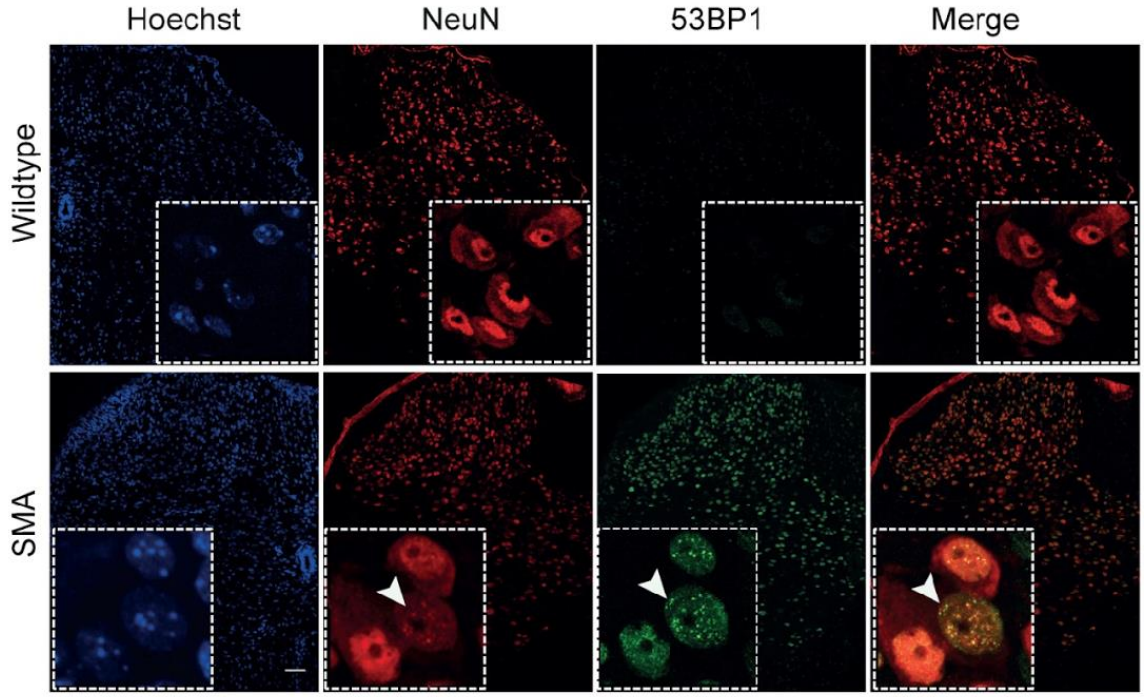

Figure 3-11: 53BP1 and NeuN double staining in SMNΔ7 mouse spinal cords.

Representative images of 53BP1 (green), NeuN (red) and Hoechst (blue) immunoreactivity in lumbar spinal cord sections of controls and SMA mice. White arrowheads point to accumulation of 53BP1 foci in neurons, leading to reduced levels of NeuN labelling. Scale bar in low power images represent 50 µm.

3.3.2 SMN deficiency results in TOP1cc accumulation in brain tissue

Accumulation of endogenous DNA breaks has been shown to trap DNA topoisomerase I (TOP1), causing elevated levels of TOP1-DNA cleavage complexes (TOP1cc) (Alagoz *et al.*, 2013; Katyal *et al.*, 2014b; Walker *et al.*, 2017). TOP1 is an essential enzyme that relaxes DNA supercoiling by incising one DNA strand and forming a transient and reversible intermediate called a TOP1-cleavage complex when it is covalently attached to the 3' end of the nick. TOP1cc can be converted to irreversible intermediates in the presence of DNA lesions (Ashour *et al.*, 2015a). To test if this is also the case in SMA pathogenesis, the levels of TOP1cc were quantified in the brain of SMA (n=3) and wild type (n=3) animals (Alagoz *et al.*, 2013). TOP1cc were purified using CsCl gradients and visualized by anti-TOP1 immunoblotting with help from Dr. Chunyan Liao (El-Khamisy Lab) (**Figure 3-12 A,B**). A 4-fold TOP1cc increase in the brain of SMNΔ7 mice was observed when compared to controls (p=0.02) (**Figure 3-12** C and D) that was independent of total TOP1 levels as shown by immunoblotting (**Figure 3-12** C inset). These data provide further *in vivo* evidence for a link between genome instability and SMN deficiency.

A

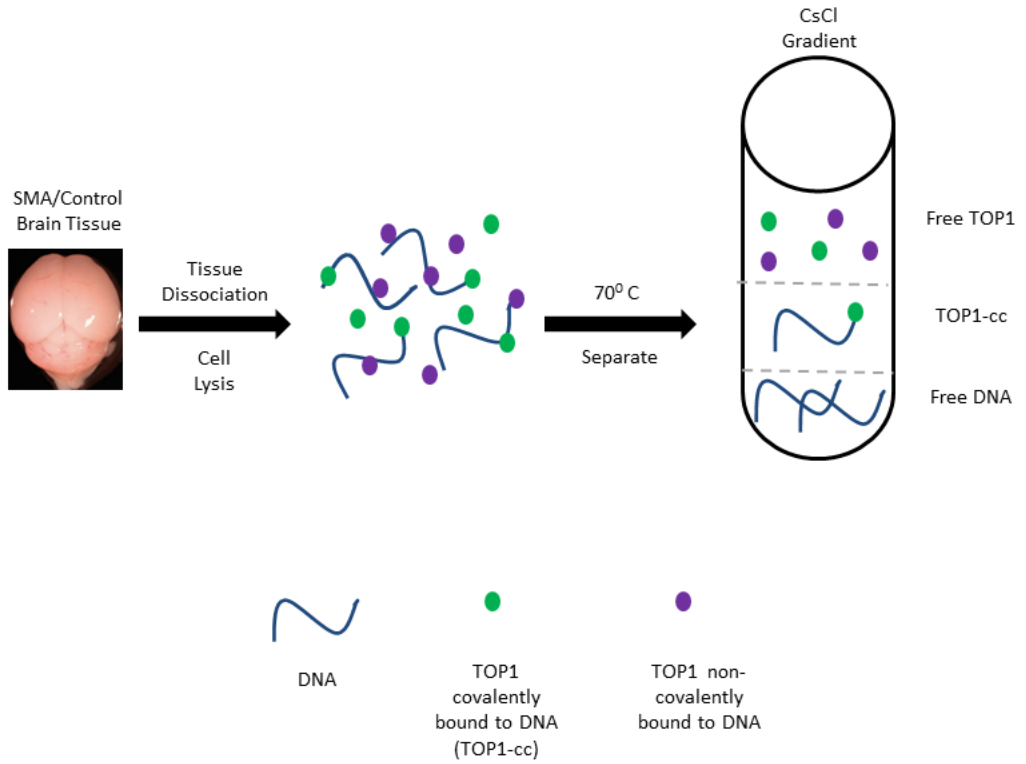
CsCl
Gradient
SMA/Control
Brain Tissue
Tissue
Dissociation
Cell
Lysis
70⁰ C
Separate
Free TOP1
TOP1-cc
Free DNA
DNA
TOP1
covalently
bound to DNA
(TOP1-cc)
TOP1 non-
covalently
bound to DNA

B

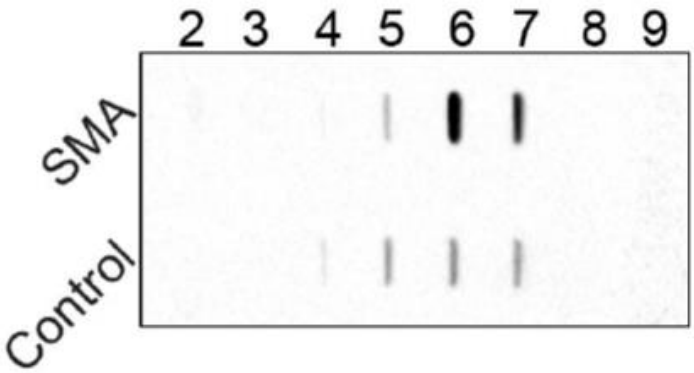
2 3 4 5 6 7 8 9
SMA
Control

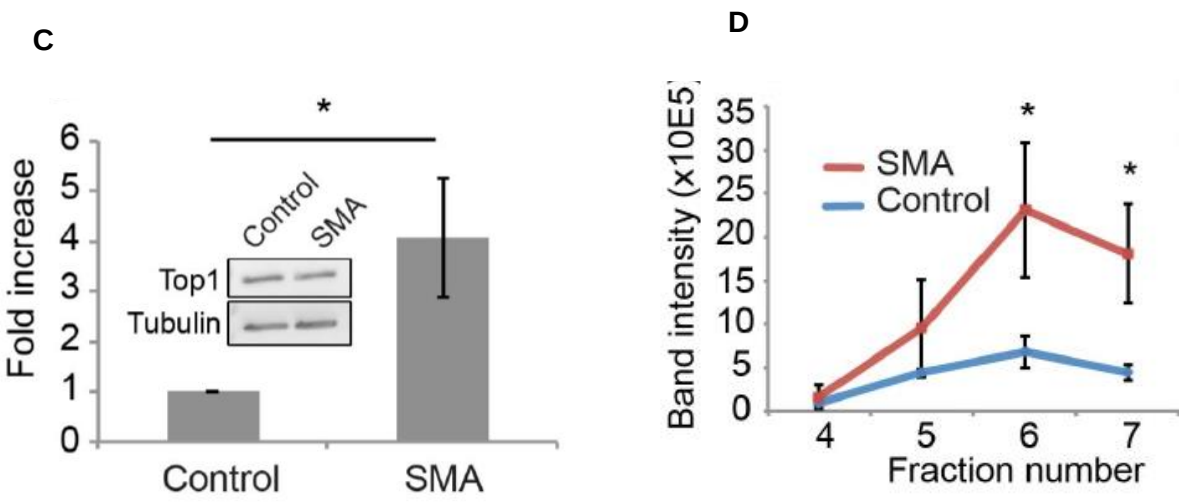

Figure 3-12: TOP1-cc accumulation in SMA mouse brain tissue.

(A) Schematic depecting the biochemical fractionation of TOP1-ccs. Adapted from (Katyal et al., 2014; Alagoz et al., 2013). (B) Genomic DNA isolated from SMA and control brains was slot-blotted. TOP1-ccs were immunodetected with antibody to TOP1. Fractions 2 and 3 are expected to contain free TOP1 proteins, fractions 4-7 contain TOP1cc, while fractions 8 and 9 contain free DNA. (C) TOP1 cleavage complexes (fold-increase over background) were quantified for fractions 4-7 showed in (B) and the mean value plotted (± s.e.m.). Insert shows immunoblotting of total TOP1 levels. (D) The intensity of each separate band (4-7) is presented. * $P < 0.05$, paired two-tailed *t* test (p=0.02). The data were collected from 3 biological independent replicates (n=3).

3.4 Post-mortem tissue

3.4.1 DNA damage is observed in post-mortem tissue from SMA patients

Given that SMN deficiency results in DNA damage in cell and rodent SMA models examined in the current study, the clinical relevance of these findings was assessed by investigating the presence of DNA breaks in sections of spinal cord of SMA

patients and controls. Consistent with the data presented here so far, it was observed an increase in DNA instability in spinal motor neurons from SMA patients compared with controls as revealed by γH2AX labelling (**Figure 3-13**).

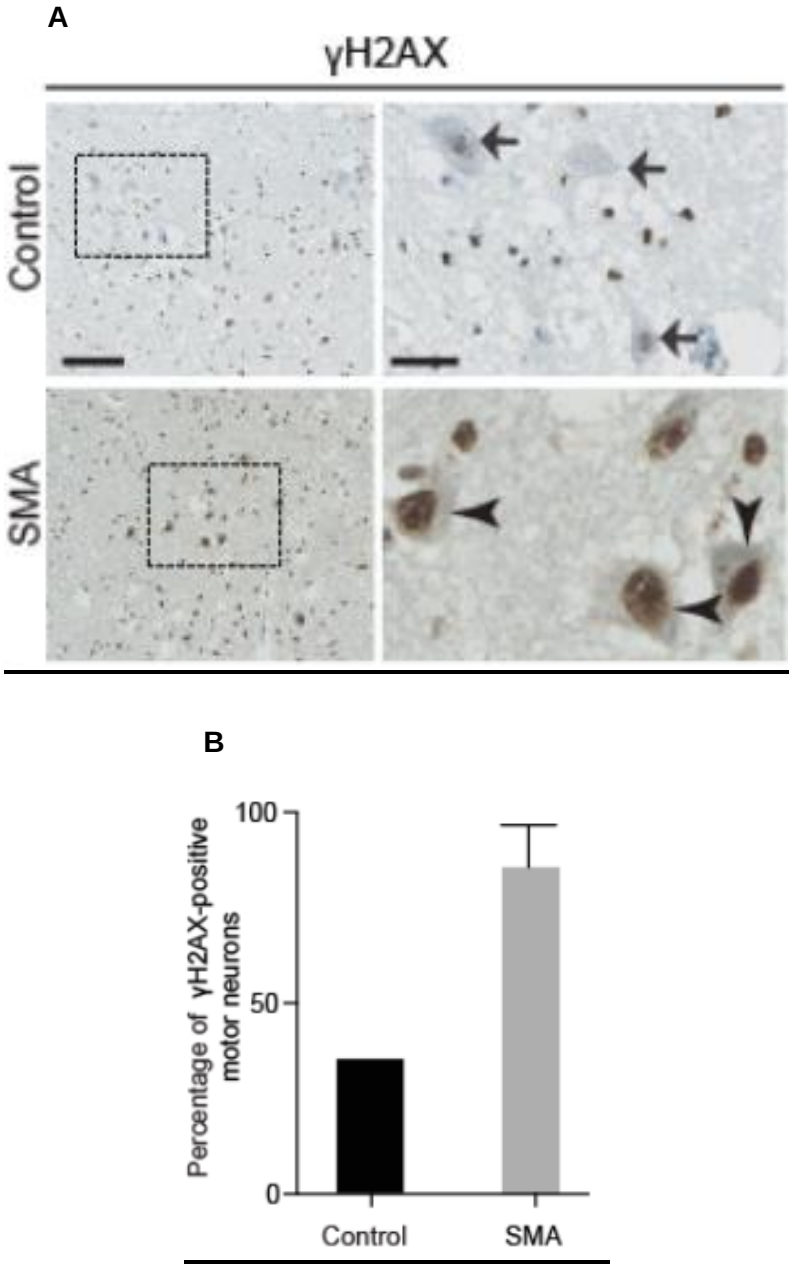

Figure 3-13: γH2AX staining in human SMA post-mortem spinal cords.

(A) Representative images of γH2AX staining in human post-mortem spinal cord sections from control (n=2) and SMA patients (n=4). Increased DNA breaks in SMA (arrowheads)

compared to control motor neurons (arrows). Higher magnification images show motor neurons indicated by arrows. Scale bar represent 50 μm (left image) and 10 μm (right image), respectively. (B) Percentage of γH2AX positive motor neurons. Data presented as mean ± s.e.m. P-value analysis was not performed as only 2 controls were analysed due to the difficulty in having post-mortem tissue from healthy young children.

3.5 Discussion

SMA is caused by mutations in *SMN1* gene that encodes the ubiquitously expressed and multifunctional SMN protein. The widely reported and characterised role for SMN is its involvement in the assembly of small nuclear ribonucleoproteins (snRNPs), the major component of the spliceosome. Therefore, SMN is critical for pre-mRNA splicing; however, it remains unclear if this defective splicing function is a causative factor of the disease. There is also emerging evidence that SMN may have a role as a guardian of genome integrity. It has been shown that SMN is implicated in the resolution of R loops, a transcription-associated source of genome instability (Zhao *et al.*, 2016). Furthermore, it appears to play a role in DNA repair pathways as described in chapter 1 (Takaku *et al.*, 2011; Velma *et al.*, 2010). Cumulative DNA damage and perturbations in DNA repair pathways have been linked to numerous neurodegenerative disorders (Jeppesen *et al.*, 2011; Madabhushi *et al.*, 2014).

A link between DNA damage and SMA has been reported previously in skeletal muscle (Fayzullina *et al.*, 2016; Fayzullina *et al.*, 2014). However, the clinical relevance of DNA damage in SMA was assessed for the first time here. Data obtained during this PhD project complement previous observations in SMA mouse model (Fayzullina *et al.*, 2016; Fayzullina *et al.*, 2014). Here, a significant increase in DNA breaks in neurons derived from murine experimental models of SMA and in

patients' fibroblasts and post-mortem tissue is reported. Based on these findings it was hypothesized that DNA damage accumulation may contribute to the pathogenesis of SMA and that SMN may have a role in maintenance of DNA integrity.

Previous studies have reported several DNA repair genes linked to neurodegenerative diseases (Date *et al.*, 2001; El-Khamisy *et al.*, 2005a; Walker *et al.*, 2017; Wang *et al.*, 2013a). For example, Ataxia telangiectasia (AT), a rare neurodegenerative disease caused by mutations in the ATM gene, represents a key example of how defects in DNA repair capacity can lead to neurodegeneration. ATM functions to regulate an extensive network of downstream double strand breaks (DSBs) repair factors. Mutations in ATM cause the accumulation of abortive DNA topoisomerase I (TOP1) cleavage complexes and protein-linked DNA breaks (PDBs) in neuronal cells (Alagoz *et al.*, 2013; Katyal *et al.*, 2014b). Interestingly, an accumulation of abortive TOP1ccs was also observed in neuronal tissue from SMA mice (**Figure 3-12**).

Furthermore, Smn-deficient/γH2AX^{+} motor neurons exhibit abnormal CGRP staining as presented in **Figure 3-10**. Surprisingly, similar phenotype has been observed in motor neurons of Ercc1$^{\Delta/-}$ mice (de Waard *et al.*, 2010). Major DNA repair pathways such as nucleotide excision repair, interstrand crosslink repair, and double strand break repair are impaired in Ercc1$^{\Delta/-}$ mice. Failure to repair DNA damage, severely affects the motor neurons of these mice which generally exhibit progressive motor abnormalities with impaired neuromuscular junctions, degeneration of motor neurons as well as reduced lifespan (de Waard *et al.*, 2010). Interestingly the phenotype of Ercc1$^{\Delta/-}$ mice is so similar to SMA mice, which even further reinforces our hypothesis that the increased DNA damage observed in SMA could contribute to disease

pathogenesis.

DNA damage and genome instability have also been linked to age-related neurodegenerative diseases such as Alzheimer's disease (AD), Parkinson's disease (PD) and, Amyotrophic Lateral Sclerosis (ALS) (Anderson *et al.*, 1996; Bender *et al.*, 2006; Lu *et al.*, 2004; Qiu *et al.*, 2014). The main source of DNA damage in the most common neurodegenerative diseases such as AD and PD is mainly attributed to oxidative stress (Carroll *et al.*, 2015; Lovell *et al.*, 2007; Sanders *et al.*, 2014). However, Jangi and colleagues have recently demonstrated that oxidative stress is unlikely to be the cause of DNA damage observed in SMA (Jangi *et al.*, 2017). The question that is raised now is how SMN deficiency leads to increased DNA damage, which I will try to address in the following chapter.

4. Unravelling the role of SMN protein in genomic integrity

4.1 Aim

Having shown that SMN deficiency can lead to elevated DNA damage in SMA experimental models, a mechanistic understanding of how that happens was attempted to be provided. Therefore, the aim of this chapter is to establish mechanistic understanding on how low levels of SMN leads to increased DNA damage.

DSBs are generated by cell-intrinsic processes such as DNA replication and transcription, as well as by by-products formed during cellular metabolism such as reactive oxygen species (ROS), the main source of oxidative stress (Aguilera *et al.*, 2013; Kim *et al.*, 2012; van Gent *et al.*, 2001). It was hypothesized that the DSBs seen in several SMA experimental models, are all formed in a similar manner. The potential of replication-induced DNA damage as an underlying cause of DSB formation in SMA was excluded since neurons are non-dividing cells. Oxidative stress is another source of DNA damage and has a central role in the pathogenesis of neurodegenerative diseases such as Alzheimer's disease and Parkinson's disease (Lovell *et al.*, 2007; Sanders *et al.*, 2014). However, oxidative stress is unlikely to be the cause of DNA damage observed in SMA according to a recent study (Jangi *et al.*, 2017). It is well known that ROS activate p38 pathways (Katagiri *et al.*, 2010). Jangi and colleagues, however, failed to detect activation of p38 MAPK in experimental models of SMA. Therefore, transcription appears to be the most prominent player responsible for the DNA damage observed in SMA. It is worth mentioning that the TOP1cc accumulation observed in SMNΔ7 brain tissue and reported in the previous chapter supports the hypothesis that the DNA breaks seen in SMA cases are transcription-associated.

One major transcription-associated structure that can potentially harm the integrity of DNA is R loop formation. R loop accumulation is an emerging source of genome instability and has been linked with a number of neurodegenerative disorders (Groh *et al.*, 2014; Sollier *et al.*, 2015). This section describes that the increased DNA damage seen in SMA is transcription-dependent and R loop-associated. It is also reported in this chapter that lentiviral-mediated SMN overexpression reduces the number of DNA breaks in SMN-deficient cells suggesting its direct role in genome integrity. Furthermore, the Tudor domain of SMN protein was shown to be essential for the maintenance of genome stability.

4.2 The accumulation of DNA damage observed in SMA cases is transcription dependent

In an attempt to reinforce the hypothesis that DSB induction is transcription-dependent in SMA, fibroblasts cells from SMA type I patients and healthy controls were treated with α-amanitin, a transcription inhibitor that primarily inhibits RNA polymerase II. The cells were treated with 5 μM of the drug for 18 hours (El-Khamisy *et al.*, 2005b)). Strikingly, inhibition of transcription suppressed the number of 53BP1 foci in SMN-deficient cells to nearly background levels observed in control cells (**Figure 4-1**). Someone may argue that the reduced number of 53BP1 after treatment with α-amanitin could be a result of reduced expression of this protein due to RNA polymerase II inhibition. One way to address this point would be by collecting cell lysates before and after treatment and analyse 53BP1 levels by immunoblotting.

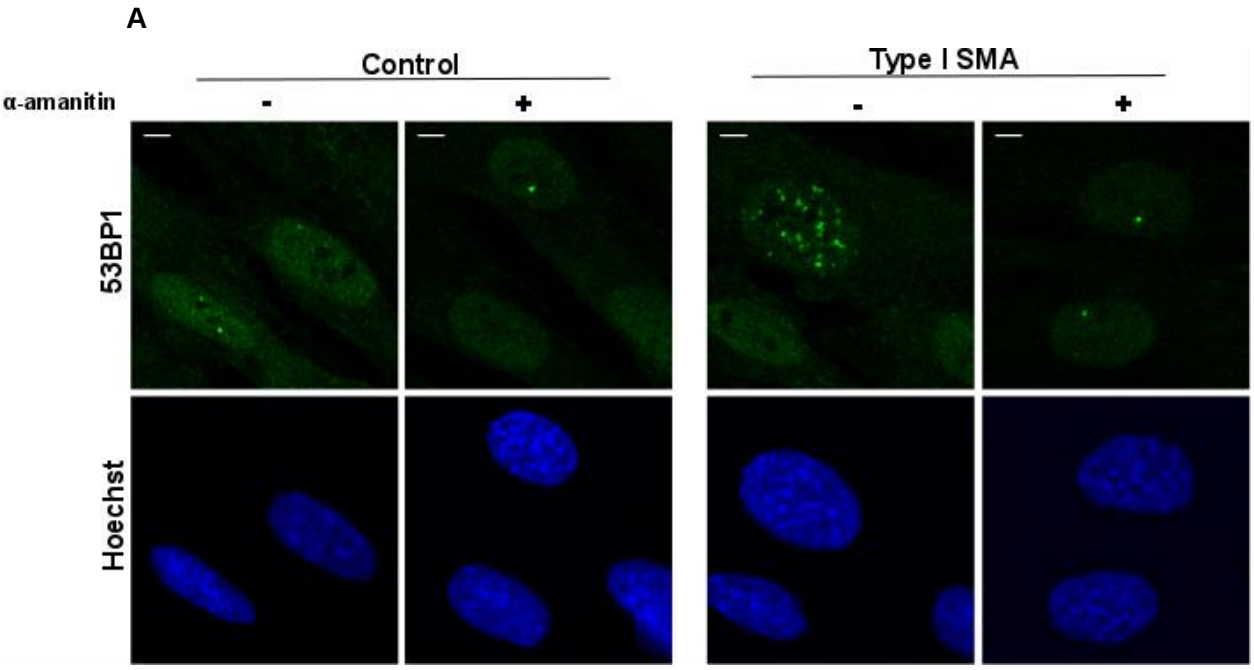

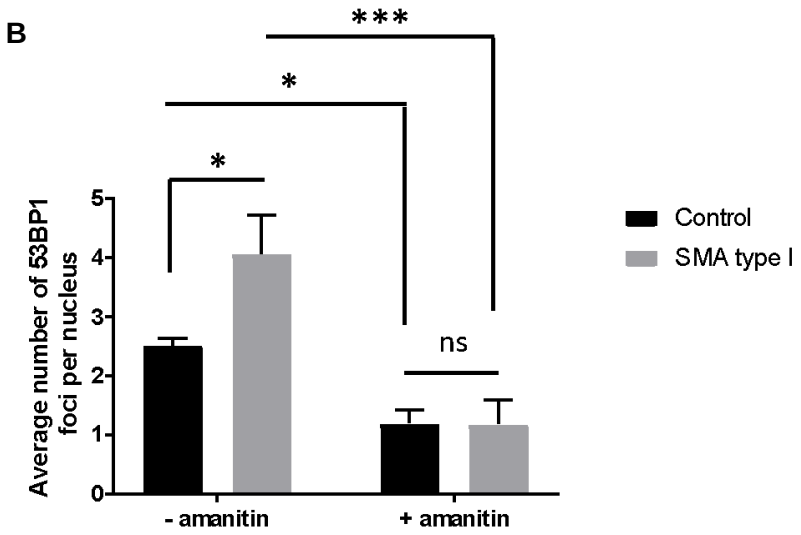

Figure 4-1: Transcription inhibition in SMA type I fibroblasts.

(A) SMA type I fibroblasts and healthy controls were pre-treated with α-amanitin (5 µM, 18h); a transcription inhibitor that primarily inhibits RNA polymerase II. DNA damage was analysed by 53BP1 immunolabeling. Scale bar represents 5 µm. (B) The number of 53BP1 foci per nucleus (average of 100 nuclei) was determined for each condition. Data are presented as

mean ± s.e.m. * $P < 0.05$, *** $P < 0.001$, ns: no significant difference, two-way ANOVA followed by Tukey's multiple comparisons test; F (3,6) = 30.54. p=0.0005. The data were collected from 3 biological independent replicates (n=3) and were normally distributed.

A similar result using γH2AX to label DSBs was observed in embryonic spinal motor neurons derived from SMA mice (SMNΔ7) compared to control after α-amanitin treatment (**Figure 4-2**). As previously stated, γH2AX and 53BP1 are widely used markers for DNA DSBs. The reason for using γH2AX for motor neuron immunostaining instead of 53BP1 is purely technical. Incubation of motor neurons with 53BP1 antibody produced a strong non-specific cytoplasmic staining that prevented us from its use.

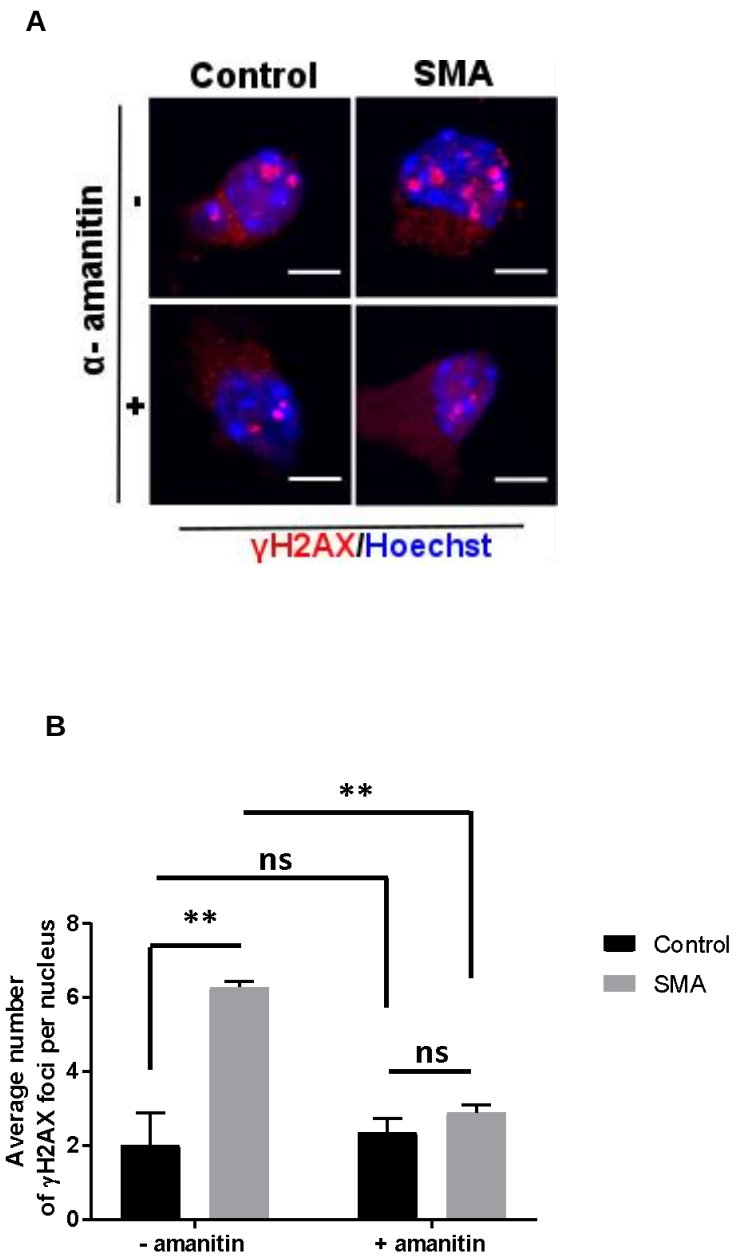

Figure 4-2: Transcription inhibition in SMA motor neurons.

(A) SMA and control motor neurons were pre-treated with α-amanitin (5μM, 18h); an inhibitor of RNA polymerase II. DNA damage was analysed by γH2AX immunolabeling. Scale bar represents 10 μm. (B) The average number of γH2AX foci was determined. Nuclei counted = 10-20. Data are presented as mean ± s.e.m. $^{**}P < 0.001$, two-way ANOVA followed by Tukey's multiple comparisons test; F (3,6) = 13.3. p=0.0046. The data were collected from 3 biological independent replicates (n=3) and were normally distributed.

4.3 SMN-deficient cells exhibit increased number of R loops

Having confirmed that the increased number of DSBs observed in SMA is transcription-dependent; it was next investigated whether these DNA breaks are associated with R loop formation. R loops form naturally during transcription and are essentially RNA/DNA hybrids generated by hybridization of the nascent RNA with the DNA template strand, leaving the non-template DNA single-stranded and forming that way a very stable three-stranded nucleic acid structure (Thomas *et al.*, 1976). These structures can be 'hazardous' for the cells because if they are not properly resolved, they can lead to DNA damage, as their exposed ssDNA is susceptible to lesions (Skourti-Stathaki *et al.*, 2014). To address this, spinal motor neurons derived from E13 SMNΔ7 embryos, a well-established animal model of SMA, and cultured using the p75 immunopanning method (Wiese *et al.*, 2010) were labelled with the R loop specific S9.6 antibody (Boguslawski *et al.*, 1986) (**Figure 4-3**). Pre-treatment of fixed cells with RNAse H was performed to confirm the specificity of S9.6 for endogenous RNA/DNA hybrids. S9.6 antibody is used extensively in our group for R loop staining and RNAse H treatment has been shown to reduce the fluorescence intensities to background levels (Walker *et al.*, 2017). Similar reduction in S9.6 signal upon RNAse H treatment of human post-mortem tissue and human primary fibroblasts is also presented here **(Figure 4-6** and **Figure 6-1**).

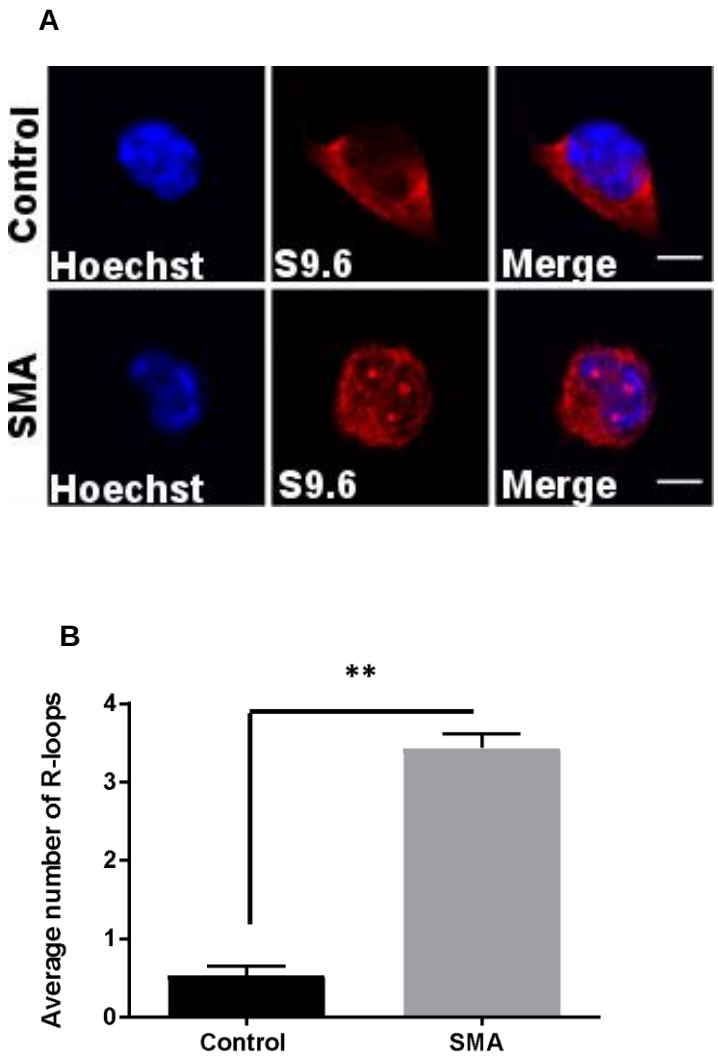

Figure 4-3: S9.6 staining in SMA cultured motor neurons.

(A) p75 enriched motor neurons derived from SMNΔ7 and wild type E13 embryos were labelled with RNA:DNA heteroduplex specific antibody, S9.6 at DIV7. Scale bars represent 5 µm B) Quantification of the number of R-Loops in SMA and wild type motor neurons. Data presented as mean ± s.e.m. ** $P < 0.01$; paired two-tailed t test, $p=0.0016$. The data were collected from 3 biological independent replicates (n=3). Nuclei counted = 10/replicate.

Smn depletion in motor neurons caused a significant increase in R loop levels when compared to control cells (**Figure 4-3**). It is worth highlighting that only nuclear foci were counted. As an extra confirmation of R loop accumulation in SMN-deficient

cells a DNA/RNA immunoprecipitation (DRIP) was then performed in SMA type I fibroblasts and healthy controls, using S9.6 antibody as a bait to pull down R loops followed by qPCR for 4 actively transcribed genes (MYADM, APOE, EGR1 and BTBD19) that have been identified as regions prone to R loop formation (Bhatia *et al.*, 2014; Ginno *et al.*, 2013; Herrera-Moyano *et al.*, 2014). SMA Type I fibroblasts showed an enrichment of R loops at the regions of the selected genes compared to control cells (**Figure 4-4**), however the difference was not statistically significant. To confirm the specificity of the S9.6 antibody, samples treated with RNase H prior to immunoprecipitation were also included. RNAse H is an enzyme that removes the R loops by specifically degrading the RNA moiety from the RNA/DNA hybrids. RNase H treatment nearly abolished the R-loop signals (**Figure 4-4**).

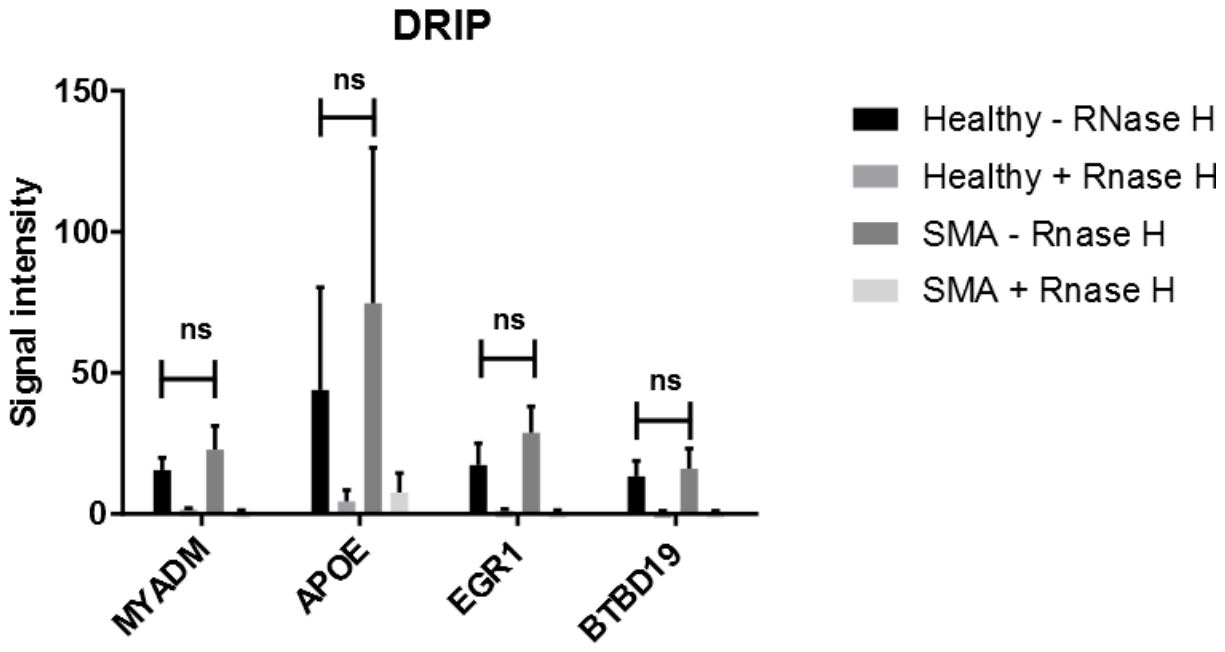

Figure 4-4: RNA/DNA hybrids accumulate in actively transcribed genes in SMN-deficient cells.

(A) DNA/RNA immunoprecipitation performed on RNase H treated or not treated genomic DNA isolated from SMA type I and healthy fibroblasts. The immunoprecipitates were then

subjected to qPCR using primers specific for MYADM, APOE, EGR1 and BTBD19 genes. Data are presented as mean ± s.e.m. ns = not significant, two-way ANOVA followed by Tukey's multiple comparisons test; F (9, 32) = 0.4504. p= 0.8964. The data were collected from 3 biological independent replicates (n=3) and were normally distributed.

Consistent with the cellular findings, labelling of spinal cord sections from postnatal day 2 SMNΔ7 pups with S9.6 antibodies revealed a significant R loop accumulation in motor neurons compared to wild type littermates (**Figure 4-5**).

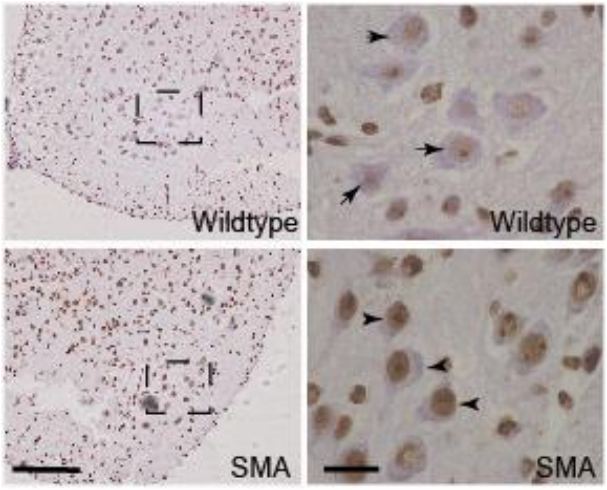

Figure 4-5: S9.6 staining in SMA mouse spinal cords.

Lumbar spinal cord sections from postnatal day 2 SMNΔ7 and wild type mice labelled with the S9.6 antibody show increased R loop formation in SMA mice (arrowheads) compared to wild type controls (arrows). Scale bars represent 100 µm (left image) and 10 µm (right image).

Whether the R loop accumulation in SMA experimental models is clinically relevant is still unknown. To test this post-mortem spinal cord sections from controls and SMA patients were stained with the S9.6 antibody. Consistent with the cell and mouse

data, a significant increase in the number of R loop-positive motor neurons in SMA sections compared to controls was revealed (**Figure 4-6**). The specificity of S9.6 signal was confirmed by prior treatment with RNAse H (**Figure 4-6** B).

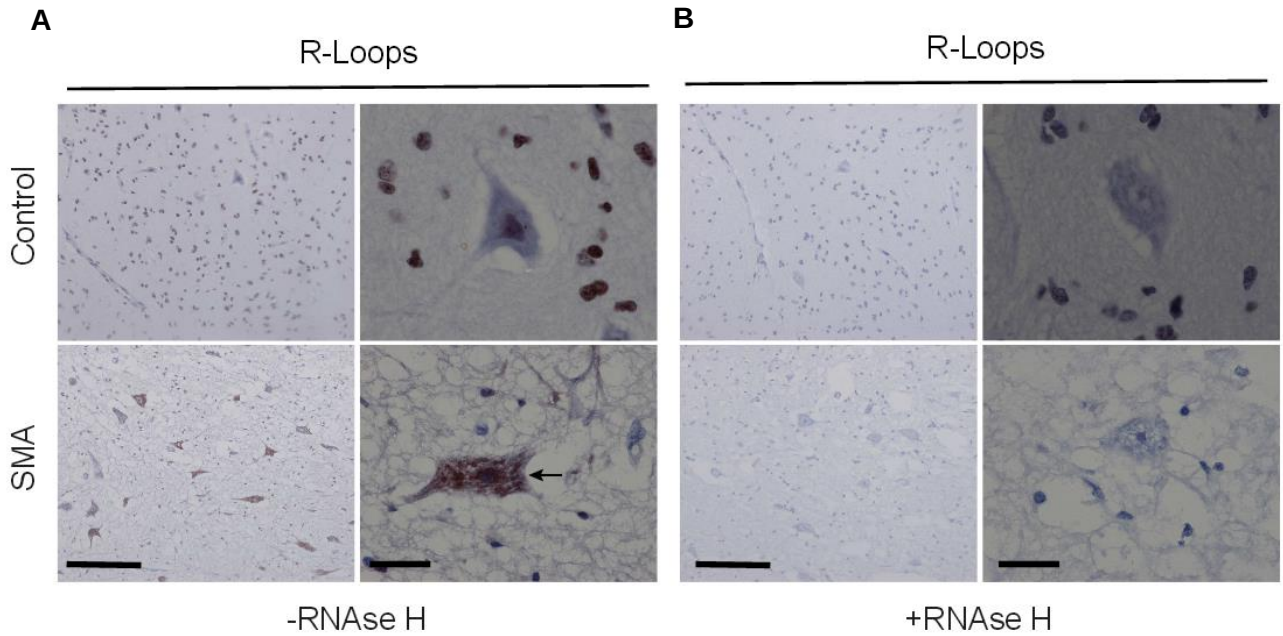

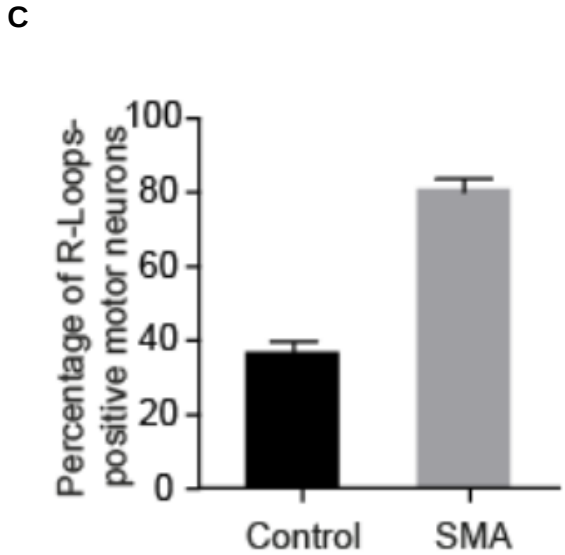

Figure 4-6: S9.6 staining in human SMA post-mortem spinal cords.

(A) Sections of post-mortem spinal cord from SMA patients and control individuals subjected to S9.6 immunoreactivity. (B) Specificity of S9.6 staining confirmed by treating sections with

RNAse H prior R-loop labeling. Scale bar represents 10 μm (C) Percentage of R loops-positive motor neurons in spinal cord sections from SMA patients and control individuals. Data presented as mean ± s.e.m. SMA, n=4; controls, n=2. P-value analysis was not performed as only 2 controls were analysed due to the difficulty in having post-mortem tissue from healthy young children.

It is worth mentioning that cytoplasmic staining of R loops does not imply non-specificity of the S9.6 antibody. Nucleolar and extranuclear signals for R loops have been observed in cells stained with S9.6 antibody showing that R loops can occur both in the nucleolus and mitochondria too (El Hage *et al.*, 2010; Marinello *et al.*, 2013).

4.4 SMN protein accumulates in the nucleus upon induction of DNA damage

The increased number of DNA breaks in all experimental SMN-deficient models studied here, implies that SMN may have a role in mechanisms that maintain DNA integrity. In order to examine the behaviour of cellular SMN protein during DNA damage induction, cortical neurons isolated from E16 wild type mice were treated with a DNA damaging agent; the topoisomerase I inhibitor camptothecin (CPT) for 1 hour and then the cells were subjected to dual labels for 53BP1 and Smn. CPT treatment of wild type neurons led to increased number of DNA DSBs as indicated by the formation of 53BP1 foci and enrichment of Smn in the nucleus forming increased number of gem-like structures (foci) (**Figure 4-7**). Mobilization of DNA repair proteins in response to DNA damage is a well-established measure for a putative role in DNA damage response (Hudson *et al.*, 2012). The acute

accumulation of Smn protein into the neuronal nuclei upon DNA damage induction is consistent with the TOP1-cc data that was presented in Chapter 3 and suggests that SMN is rapidly recruited to sites of protein-linked DNA breaks (PDBs). Since cortical neurons are bona fide non-dividing cells thus it was reasoned that the rapid accumulation of SMN to sites of PDBs would be associated with transcription. These data are in accordance with the results of α-amanitin experiments that were presented above. Because CPT also contributes to stabilization of R loops (Marinello *et al.*, 2016), these results suggest that SMN rushes into the nucleus in an attempt to assist in R loop resolution and prevent DNA damage.

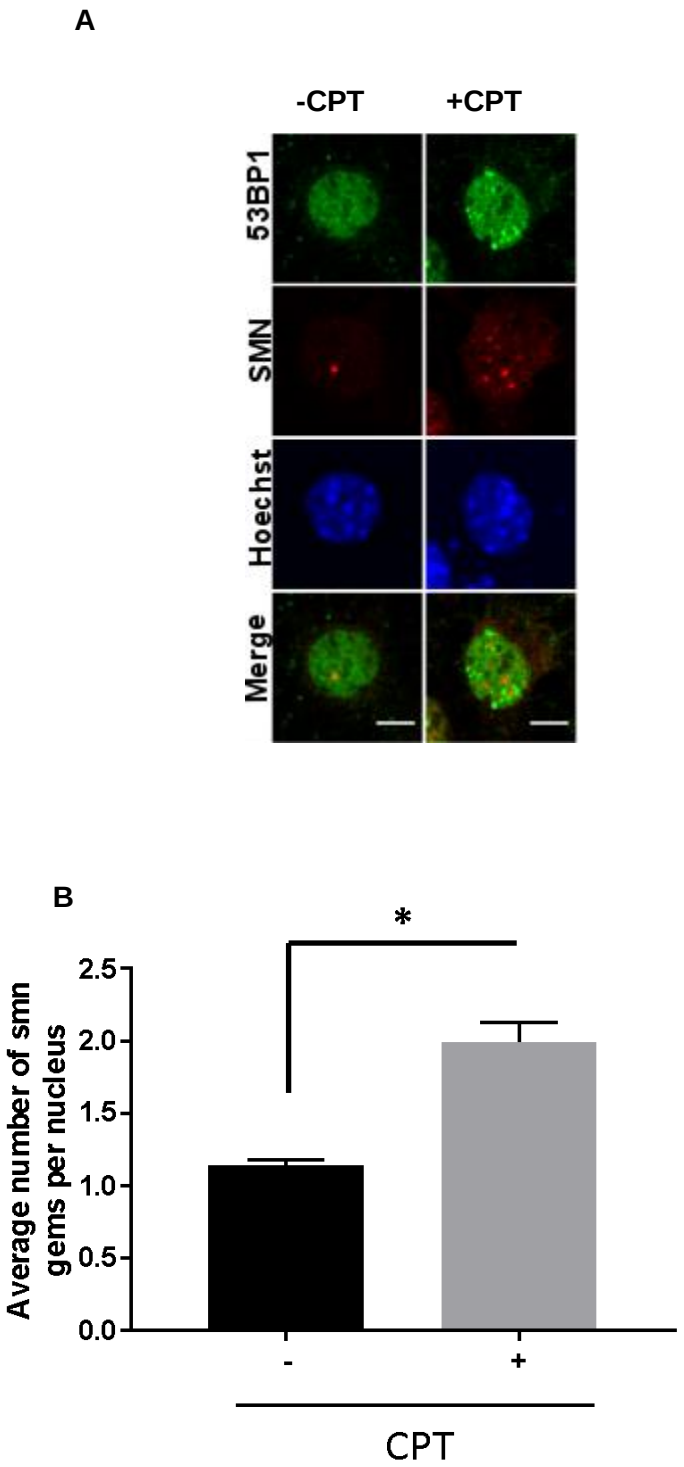

Figure 4-7: Acute accumulation of SMN protein in the nucleus upon induction of DNA damage.

(A) Embryonic cortical neurons (*DIV7*) purified from E16 wild type embryos were treated with 10μM CPT for 1 hour then dual-labelled for 53BP1 and SMN. Scale bars represent 5 μm. (B) Average number of SMN gems per nucleus. Data presented as mean ± s.e.m. * $P <$

0.05; paired two-tailed *t* test, p=0.0395. The data were collected from 3 biological independent replicates (n=3). Nuclei counted = 50/replicate.

4.5 SMN restoration decreases the number of DNA breaks in SMN-deficient cells

If SMN does have a role in maintaining DNA integrity, one would expect to detect a reduction in DNA breaks after restoring SMN protein levels in SMN-deficient cells. In order to test that, a lentiviral vector that encodes for the full-length SMN protein was generated. Firstly, it was tested whether the viral vector is functional by transducing SMA type I fibroblasts, which are deficient in SMN, with increasing amount of virus and assessed the level of SMN overexpression (**Figure 4-8**).

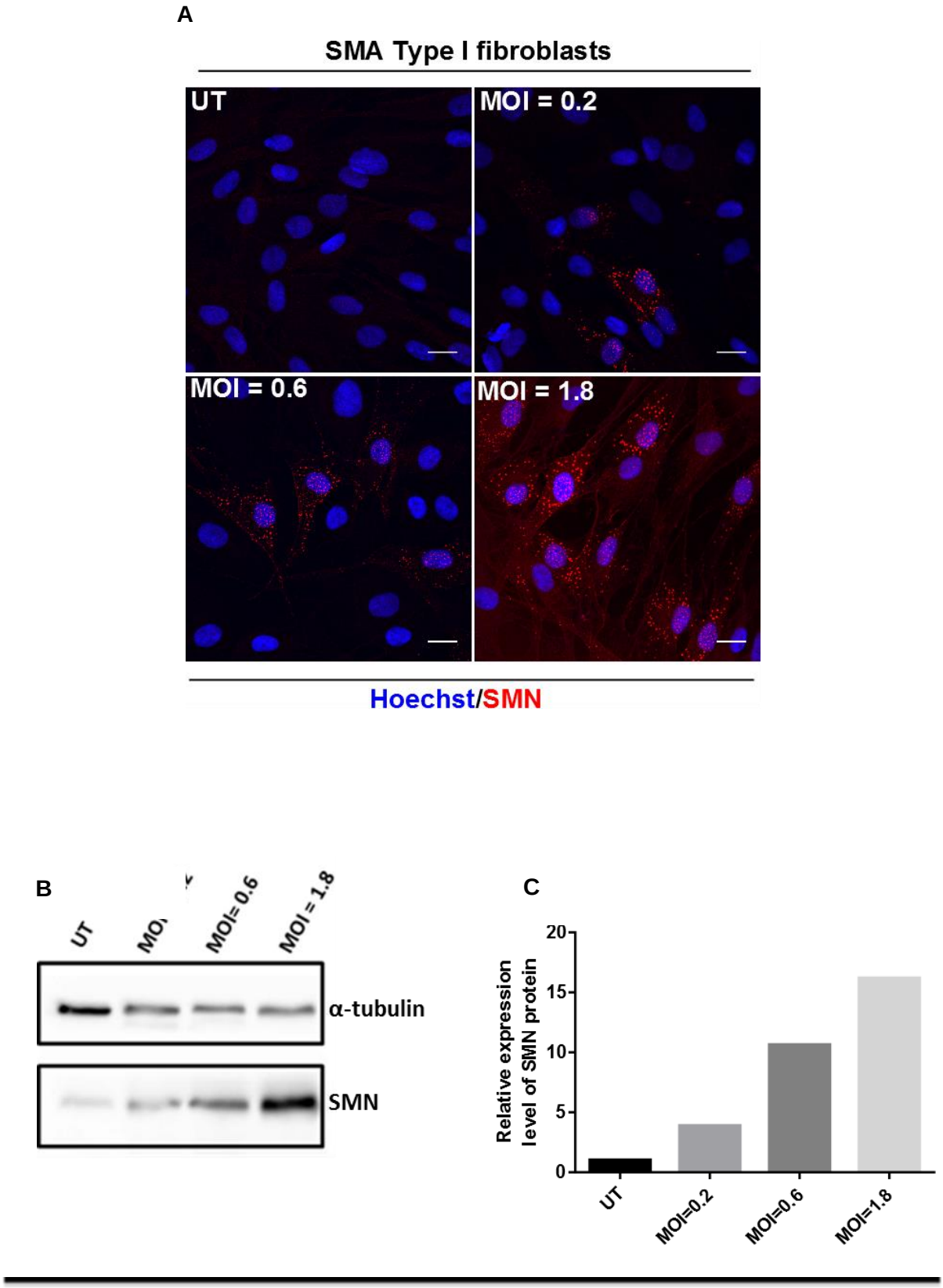

Figure 4-8: LV-SMN mediated transduction efficiency in SMA fibroblasts.

SMA type I fibroblasts were transduced with 3 different Multiplicity of Infection (MOI) of LV-

SMN (MOI=0.2, MOI=0.6 and, MOI=1.8). SMN levels were assessed by immunolabeling (A) and western blotting (B) 96 hours post LV transduction. (C) Densitometric analysis revealed that SMN protein levels were increased 5-fold, 10-fold and 15-fold respectively following transduction with LV-SMN virus. Scale bars represent 20 µm. MOI = (Volume of virus x Titre of virus)/Number of cells.

SMA type I fibroblasts were then transduced with LV-SMN MOI = 0.6 and cells were probed for SMN and 53BP1 immunoreactivity (**Figure 4-9A**). As expected, SMN overexpression significantly reduced the elevated number of DNA breaks previously observed in SMN-deficient cells (**Figure 4-9B**).

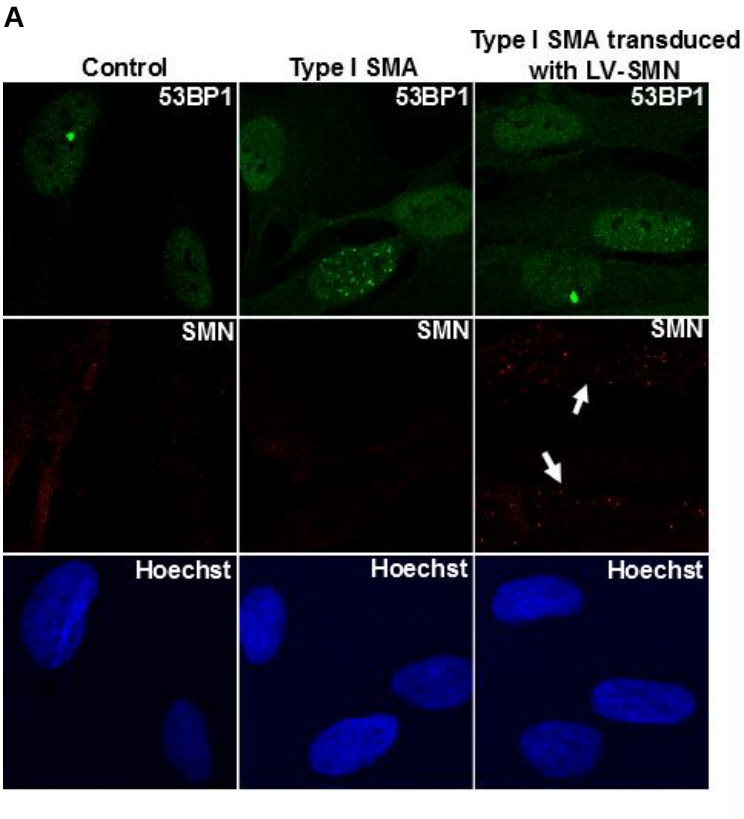

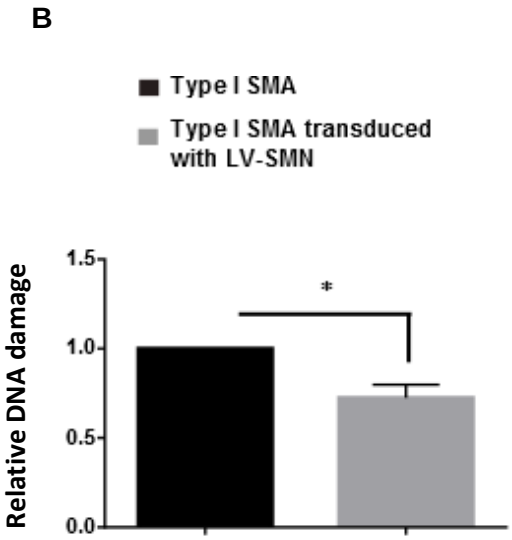

Figure 4-9: Lentiviral-mediated restoration of SMN in SMA type I fibroblasts reduces the number of DSBs.

(A) SMA type I fibroblasts transduced with a lentiviral vector carrying SMN cDNA were labelled for 53BP1 and SMN. White arrows indicate cells with restored SMN protein levels. (B) Relative DNA damage. The average number of 53BP1 foci per nucleus in SMA type I fibroblasts transduced with LV-SMN was normalised to the un-transduced SMA type I fibroblasts. 50 nuclei were counted (n=3). The relative DNA damage in un-transduced SMA type I fibroblasts was set as 1. Data are presented as mean ± s.e.m. *P<0.05; paired two-tailed t test, p=0.0202. The data were collected from 3 biological independent replicates (n=3).

4.6 SMN Tudor domain is important for DNA damage prevention

The next goal was to determine which domain in SMN is critical for DNA damage prevention. Of particular note is the SMN Tudor domain, a conserved structural motif

originally identified as a region of 50 amino acids found in the Tudor protein encoded in *Drosophila*. The structurally characterized tudor domain in human SMN is a strongly bent anti-parallel β-sheet that specifically recognizes symmetrically dimethylated arginine (Zhao *et al.*, 2016). To evaluate the importance of the SMN Tudor domain in the regulation of DNA damage prevention, a SMN construct lacking exon 3 (SMNΔ3) was generated as described in Materials and Methods. Exon 3 of the *SMN* gene encodes for the SMN Tudor domain. A lentiviral vector expressing SMNΔ3 (LV-SMNΔ3) under the PGK promoter was then produced. We first tested the efficacy of LV-SMN FL and the LV-SMNΔ3 on SMA type I fibroblasts with increasing MOIs. The transgene SMN level was assessed by immunostaining and western blotting (**Figure 4-10**).

A

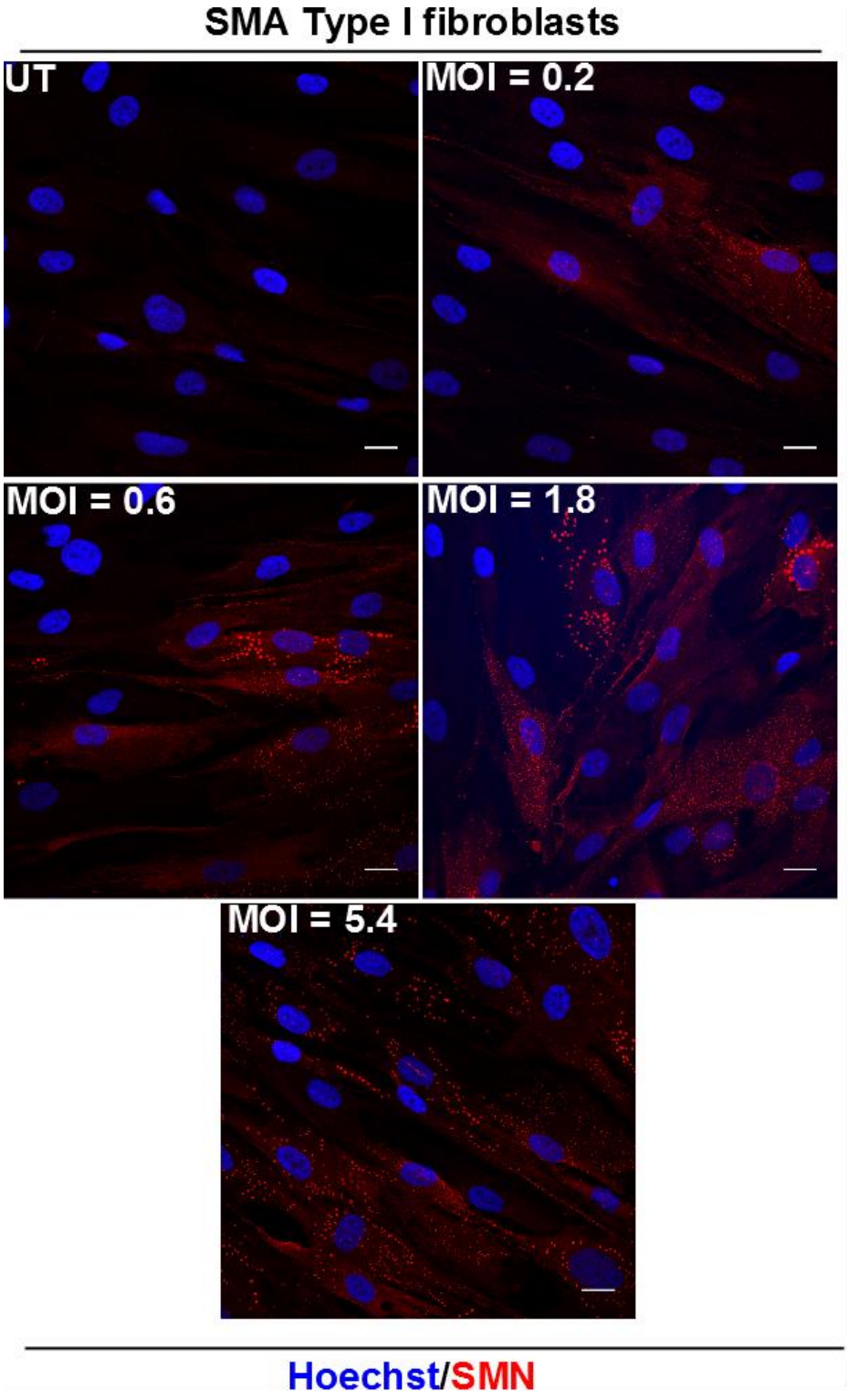
SMA Type I fibroblasts
UT
MOI = 0.2
MOI = 0.6
MOI = 1.8
MOI = 5.4
Hoechst/SMN

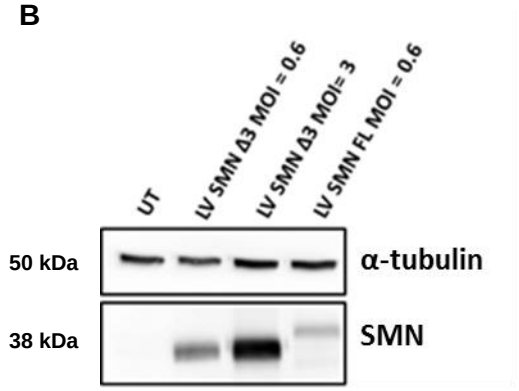

Figure 4-10: LV-SMNΔ3 transduction efficiency in human fibroblasts.

(A) SMA type I fibroblasts were transduced with 4 different MOIs of LV-SMNΔ3 (MOI=0.2, MOI=0.6 and, MOI=1.8 and MOI=5.4) and 96 hours post-transduction SMN levels were assessed by immunolabeling. Scale bars represent 20 µm. (B) SMA type I fibroblasts were transduced with 2 different MOIs of LV-SMN Δ3 (MOI=0.6 and MOI=3) and SMN level were assessed by Western blot. LV-SMN FL was used as a control (MOI=0.6).

Having confirmed that both viral vectors (LV SMN FL and LV SMN Δ3) express SMN, the ability of each viral construct to reduce the DNA damage observed in SMN-deficient cells was tested next. Consistent with the results presented in **Figure 4-9**, overexpression of full-length SMN protein reduced the number of DNA breaks in SMA type I fibroblasts. Interestingly, lentiviral-mediated overexpression of SMN protein that lacked the Tudor domain failed to repair or prevent DSB formation, as demonstrated by a higher number of 53BP1 foci (**Figure 4-11**). The readouts of γH2AX and 53BP1 in SMN-deficient cells are very similar as presented above (Chapter 3). Therefore, the utilisation of either marker is sufficient to assess DNA damage in cells. SMN protein expressed by truncated version (LV-SMNΔ3) failed to form gems-like structures in the nucleus and formed instead a diffuse nuclear

expression pattern. In an effort to exclude the potential scenario that SMNΔ3 fails to ameliorate the DNA damage phenotype of SMN-deficient cells because it localizes predominantly in the cytoplasm, cellular fractionation in SMA type I fibroblasts transduced with LV-SMN FL or LV-SMNΔ3 viral vectors was performed. It was observed that transduction with either vector produced significant expression of both cytoplasmic and nuclear SMN protein levels (**Figure 4-11 C**).

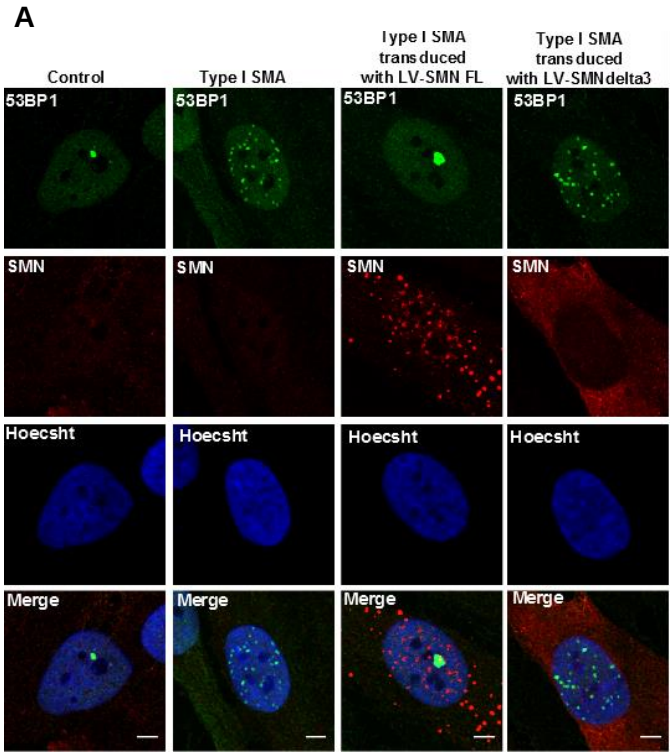

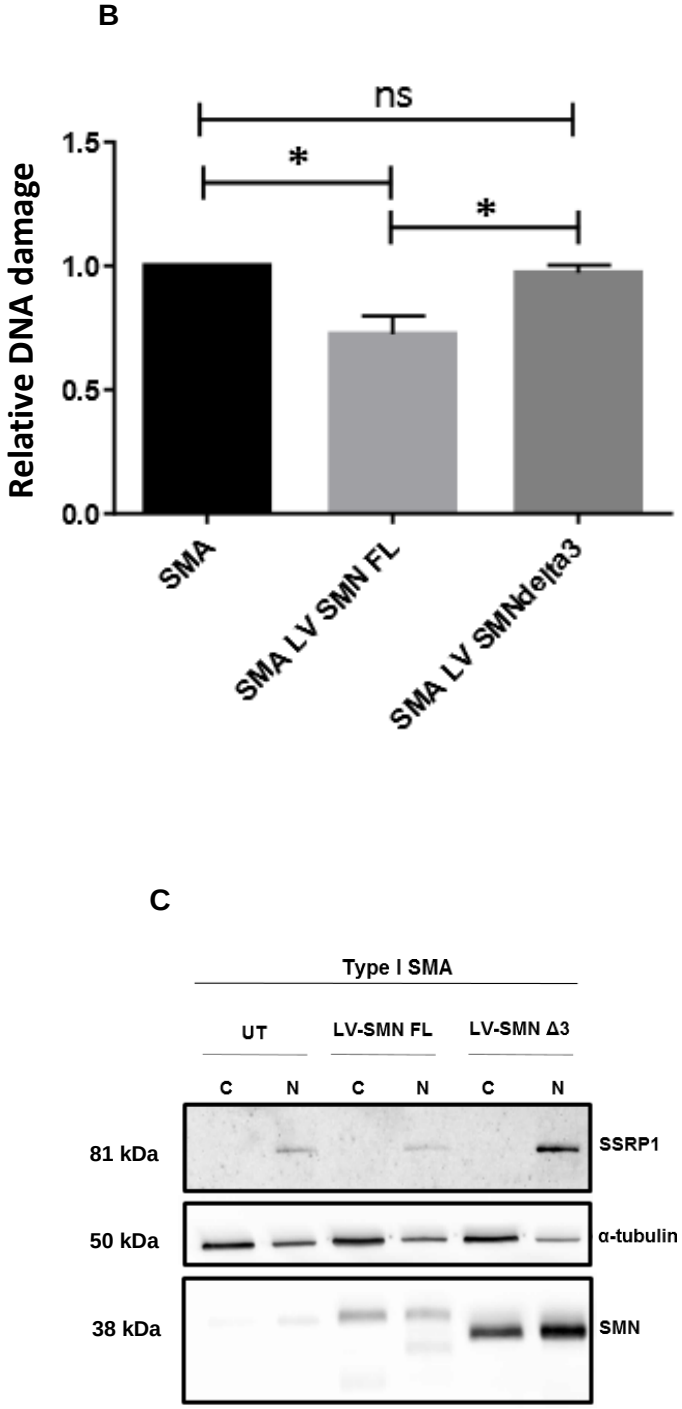

Figure 4-11: Lentiviral-mediated overexpression of SMNΔ3 in SMA type I fibroblasts fails to reduce DSBs.

(A) SMA type I fibroblasts were transduced with lentiviral vectors carrying either full SMN gene (LV-SMN FL) or SMN lacking exon 3 (LV-SMNΔ3) that encodes for Tudor domain. The cells were double labelled for 53BP1 and SMN 96 hour after LV-mediated transduction. The number of 53BP1 foci per nucleus (average of 100 nuclei) was assessed. Scale bars

represent 5 µm. (B) Quantification of 53BP1 data is presented as mean ± s.e.m. * $P < 0.05$, One way ANOVA analysis followed by Tukey's multiple comparisons test; F (2,6) = 10.72. p= 0.0105. The data were collected from 3 biological independent replicates (n=3) and were normally distributed. Nuclei counted=100/replicate. (C) Cytoplasmic and nuclear fractionation of transduced fibroblasts. Analysis of nuclear fractions of LV-transduced cells confirming localisation of LV-SMNΔ3 mediated protein expression to the nucleus. SSRP1 was used as a nuclear marker.

These data are consistent with a recent report by Zhao and colleagues (Zhao *et al.*, 2016), showing that SMN physically interacts with RNA POL II through its Tudor domain and facilitates the recruitment of senataxin, forming an R loop resolution complex.

4.7 Discussion

The current chapter provides evidence that SMN has a transcription-dependent role in the DNA damage response by assessing DNA damage in control and SMN-deficient cells pre-treated with the transcriptional inhibitor α-amanitin. α-amanitin, a toxin isolated from Amanita mushrooms, irreversibly binds to RPB1, the largest subunit of RNA polymerase II (RNAP II) leading to its degradation. RNA polymerase III is 100-fold less sensitive, while RNA polymerase I is insensitive to the drug (Bushnell *et al.*, 2002).

It was then established that the transcription-mediated DNA breaks observed in SMA cases are associated with R loops. A significant R loop accumulation in SMN-deficient cells was detected when compared to controls utilising two different techniques; S9.6 immunostaining and DRIP. Importantly, RNAse H treatment

decreased the S9.6 signal to background levels in both experiments, indicating that S9.6 antibody specifically recognises endogenous RNA/DNA hybrids. Interestingly, loss of other spliceosome-associated proteins (e.g. ASF/SF2, Nrl1) has also been reported to induce the formation of R loops (Aronica *et al.*, 2016; Li *et al.*, 2005). R loops are three-stranded nucleic acid structures formed by an RNA/DNA hybrid and a displaced single-strand DNA (ssDNA) (Aguilera *et al.*, 2012). They form naturally during transcription, but if they are not resolved properly, they can induce DNA damage and genome instability (Hamperl *et al.*, 2014). In this vein, loss of numerous proteins involved RNA processing that has been linked with excessive R loop formation, has also been shown to lead to increased genome instability (Paulsen *et al.*, 2009).

Furthermore, mutations in proteins implicated in R loop resolution, such as senataxin (SETX) and RNAse H can cause neurodegenerative disorders (Anheim *et al.*, 2009; Chen *et al.*, 2004; Crow *et al.*, 2006; Moreira *et al.*, 2004). SETX, an DNA/RNA helicase in particular, is of great interest as it has been reported to interact with SMN and RNA polymerase II forming an R loop resolution complex at the transcription termination sites (Zhao *et al.*, 2016). Mutations in SETX gene have been associated with a dominant juvenile form of amyotrophic lateral sclerosis (ALS4) and a recessive form of ataxia oculomotor apraxia (AOA2). Similar to SMA, ALS4 is characterised by progressive motor neuron degeneration, muscle weakness and atrophy (Anheim *et al.*, 2009; Chen *et al.*, 2004; Crow *et al.*, 2006).

It was also demonstrated that exposing cells to the topoisomerase I inhibitor CPT induces DNA damage and leads to the accumulation of nuclear SMN. Given that CPT contributes to stabilization of R loops (Marinello *et al.*, 2016), these results reinforce even more the hypothesis that SMN protects genome integrity by

preventing R loop mediated DNA damage. Perhaps an interesting experiment to do that would prove this hypothesis would be a dual staining of SMN with R loops after CPT treatment.

This chapter of the thesis also reports that the Tudor domain of SMN protein is crucial for DNA damage prevention. These results complement a recent study which demonstrated that SMN interacts with RNAP II and senataxin (SETX) through its Tudor domain to form an R loop resolving complex (Zhao *et al.*, 2016).

Our data so far suggest that SMN-deficiency leads to R loop accumulation resulting in increased DNA damage that may contributes to the neurodegenerative phenotype of SMA. In the following chapter, we test the hypothesis that SETX overexpression can prevent the build-up of excess R loops in SMN deficient models and protect against neurodegeneration.

5. Senataxin: A new therapeutic target for treating SMA

5.1 Aim

Having established that SMN deficient neurons are prone to R loop accumulation and DNA breakage (Chapters 3 & 4), it was hypothesized that the DNA instability contributes to neurodegeneration in SMA. If so, one would predict that promoting the resolution of R loops would delay or even prevent neuronal loss associated with SMN deficiency. To test this possibility, it was examined whether the elevated levels of DNA breakage in model systems of SMA could be reversed by adenovirus mediated overexpression of the R loop resolution helicase, senataxin (SETX) (Mischo *et al.*, 2011; Skourti-Stathaki *et al.*, 2011). The rationale behind using adenovirus is its large cloning capacity and efficient gene transfer in motor neurons. The size of senataxin open reading frame (ORF) is 8033bp, which means that a simple gene transfer option is technically challenging and not amenable to typical viral delivery approaches using attractive viral vector systems for CNS applications such as adeno-associated virus (AAV) which has a packaging capacity of ~ 4,000 bp (Grieger *et al.*, 2005). The most promising therapeutic strategies, including survival studies, in SMA mouse model so far were performed using AAV serotype 9 (AAV9) (Kaifer *et al.*, 2017; Meyer *et al.*, 2015; Powis *et al.*, 2016a; Valori *et al.*, 2010).

AAV and more specifically AAV9 is considered a vector of choice for central nervous system gene delivery due to its ability to efficiently cross the blood brain barrier and it has been extensively used for *in vivo* studies in SMA as it appears to show high affinity for motor neurons (Benkhelifa-Ziyyat *et al.*, 2013; Dominguez *et al.*, 2011; Foust *et al.*, 2010; Valori *et al.*, 2010). Despite the fact that adenoviral vectors lack the ability to cross the blood brain barrier, it has been reported that they can however permit binding and uptake by nerve terminals and retrograde transport to deliver

transgene to spinal motor neurons when injected in muscles (Acsadi *et al.*, 2002; Millecamps *et al.*, 2002). Exploiting this property of adenoviral vectors, we conducted our *in vivo* studies.

After assessing the transduction efficiency of our adenoviral vectors, the effect of SETX expression on axonal growth was evaluated in cultured spinal motor neurons. Having confirmed the ability of SETX overexpression to ameliorate the neurodegenerative phenotype of SMA *in vitro*, we then moved forward to undertake *in vivo* studies using the SMNΔ7 animal model. The efficiency of the adenoviral mediated SETX gene transfer to the spinal motor neurons after intramuscular administration is described in this section. This section also details the assessment of the therapeutic potential of SETX gene through this approach.

5.2 SETX overexpression reverses the elevated levels of DNA breakage

Adenoviral vector efficacy was first evaluated by transducing MRC5 cells with adenoviruses expressing either a control red fluorescent protein (RFP) or SETX for 3 days, and assessing protein transgene levels by Western blot (**Figure 5-1**). Both adenoviral vectors were produced by Vector Biolabs.

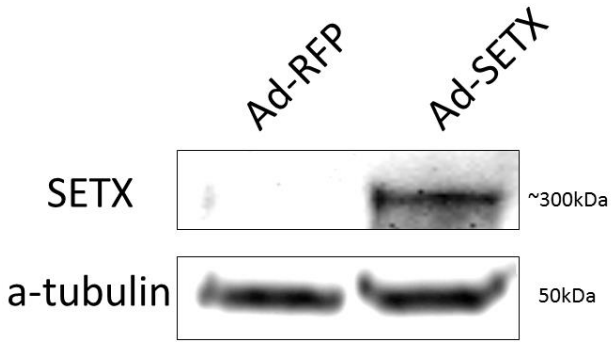

Figure 5-1: Ad-SETX mediated transduction of MRC-5 cells.

Immunoblotting of SETX levels in MRC5 alpha cells 3 days after transduction with Ad-SETX. Ad-RFP was used as a control virus. a- tubulin was used as a loading control.

Even though, it is well known that recombinant adenoviruses transduce a wide variety of cell types (Lee *et al.*, 2002), the ability of Ad-RFP vector to transduce spinal motor neurons was examined. Spinal cord cultures purified from E13 mouse embryos, were transduced with 8.4×10^6 PFU/ml Ad-RFP two days after cell plating (DIV2) and analysed after 5 days. Note that these are mixed cultures containing motor neurons, interneurons as well as glia. 100% of the cells were transduced with Ad-RFP (**Figure 5-2**). Morphologically, motor neurons are relatively distinguishable in a mixed culture, as their processes are seen to extend from their cell body and form very long axons; they also appear to grow on the top of non-neuronal (glial) cells as shown below.

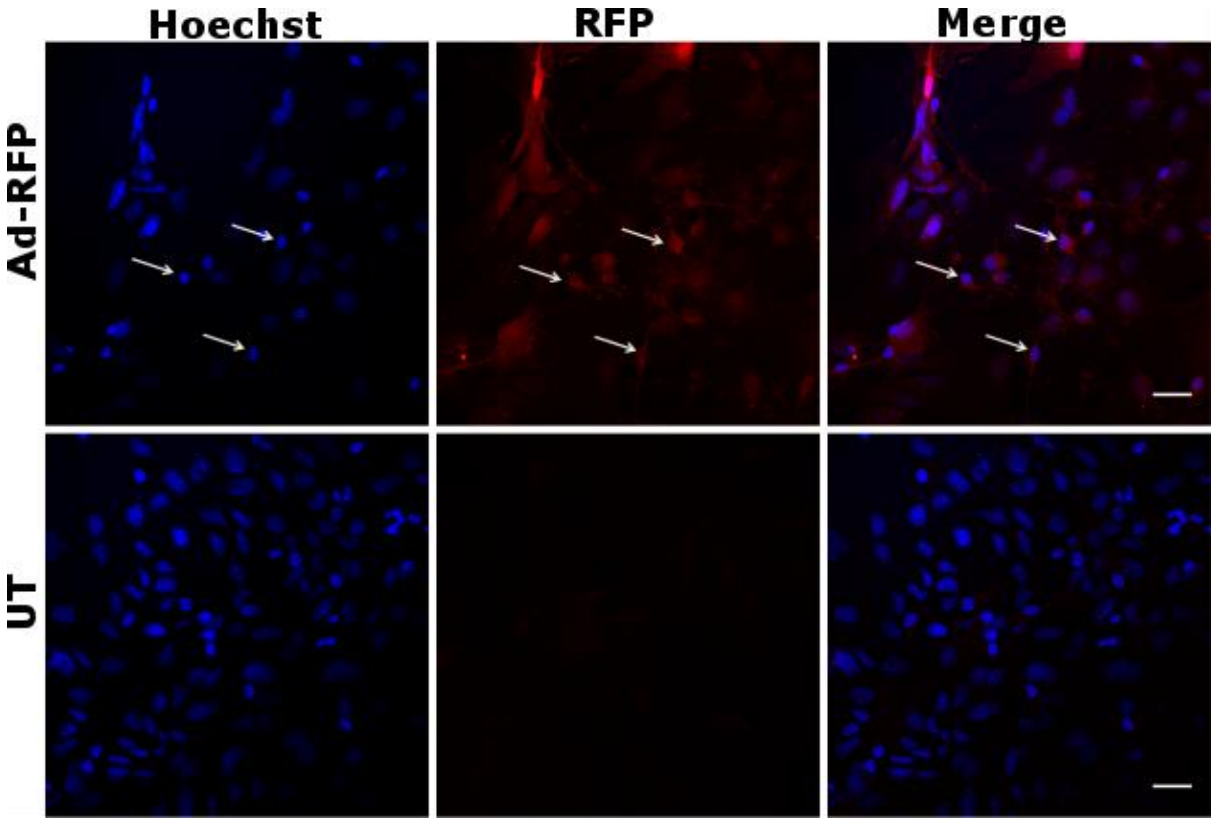

Figure 5-2: Ad-RFP transduction efficiency in spinal cord mixed cultures.

Mixed spinal cord cultures were transduced with Ad-RFP ($8.4x10^6$ PFU/ml) at DIV2 and collected at DIV7 when the expression of RFP was assessed by immunolabelling. All cell types appear to be transduced with high efficiency. Arrows indicate transduced motor neurons (identified based on their morphology). Scale bar represents 25 µm.

Having confirmed that adenoviral vectors can efficiently transduce spinal cord cultures, I then proceeded to a meticulous isolation of pure motor neurons from E13 embryos (Ning *et al.*, 2010b) (using the same protocol as described in Materials and Methods chapter). Ad-mediated gene transfer of SETX in spinal motor neurons cultured from SMNΔ7 mouse embryos (m*Smn*$^{-/-}$; *SMN2*$^{+/+}$*; SMNΔ7*$^{+/+}$) led to a significant decrease in R loop levels as revealed by S9.6 labelling (**Figure 5-3**). However, no obvious changes in R loops were observed in Ad-RFP control cells (**Figure 5-3**). Notably, overexpression of SETX also reduced the DSBs as assessed

by a decline in the number of γH2AX foci (**Figure 5-4**), indicating that the DSBs elevation associated with SMN deficiency was attributable to R loop formation.

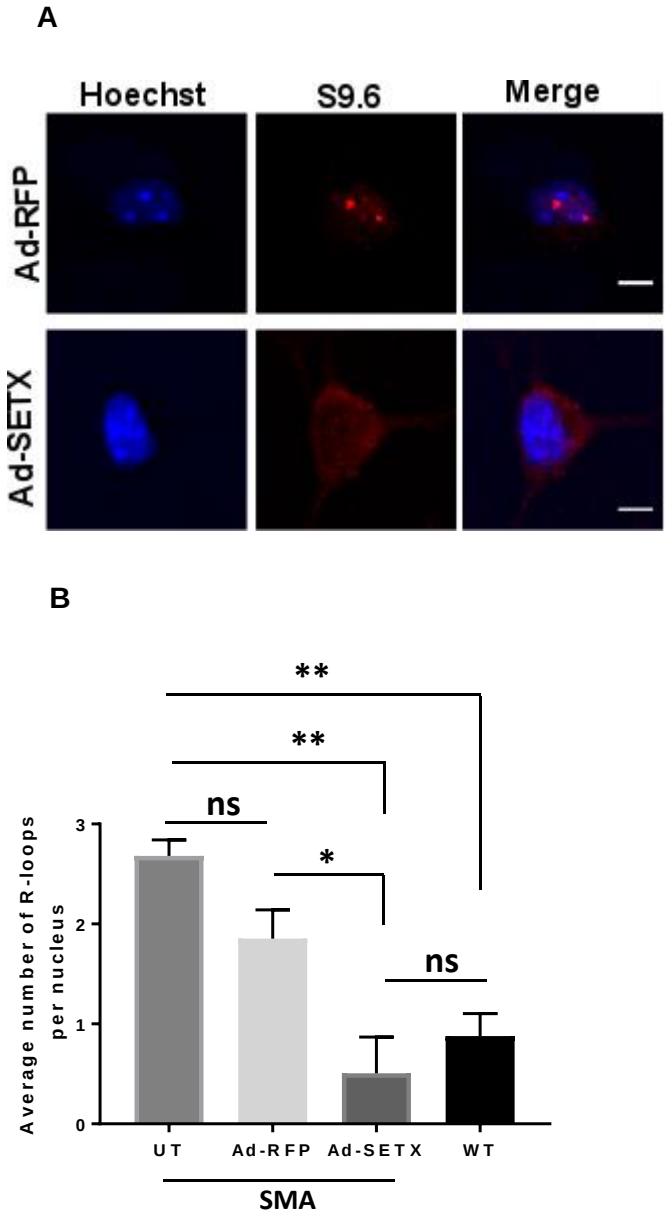

Figure 5-3: R loop (S9.6) staining of Ad-SETX transduced SMA motor neurons.

(A) Spinal motor neuron cultures from SMNΔ7 embryos transduced with adenoviral vectors carrying either RFP or SETX genes. Cells were labelled for RNA/DNA hybrids (S9.6). Scale bars represent 5 μm. (B) Average number of R loops per nucleus. (n=3). Data presented as mean ± s.e.m. * $P < 0.05$; ** $P < 0.01$, one-way ANOVA followed by Tukey's multiple

comparisons test; F (3,8)=13.35, p=0.0018. ns= not significant. The data were collected from 3 biological independent replicates (n=3) and were normally distributed. Nuclei counted = 25/replicate.

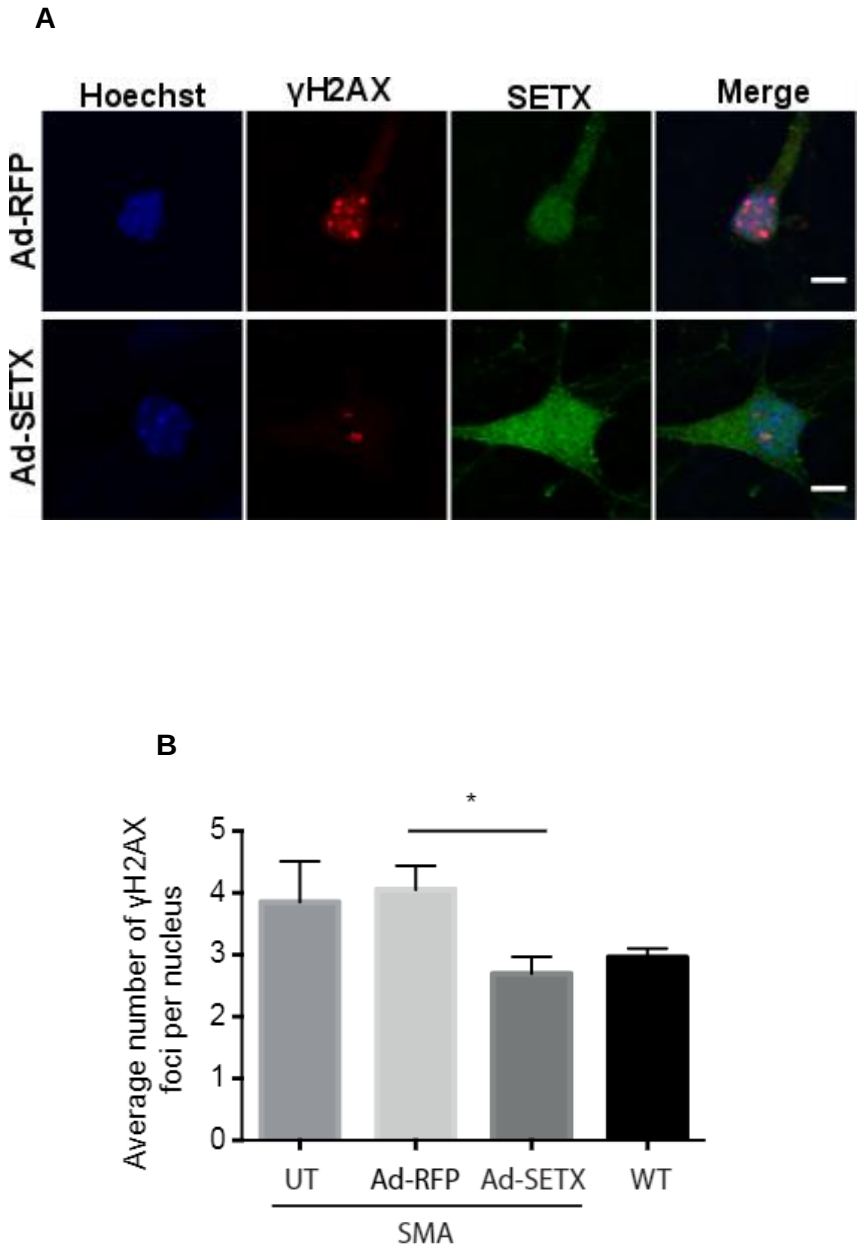

Figure 5-4: γH2AX staining of Ad-SETX transduced SMA motor neurons.

(A) Ad-SETX transduced motor neuron cultures immunolabelled for γH2AX (red) and SETX (green). Ad-RFP was used as a control. Hoechst stain (blue) was used to visualize nuclei

Scale bars represent 5 μm. (B) Average number of γH2AX foci in the experimental groups. Data presented as mean ± s.e.m. Firstly, a one-way ANOVA followed by Tukey's multiple comparisons test was performed [F(3,8)=2.61, p=0.1236]. Thinking that we may lose power after correcting for multiple comparisons, we then performed 4 individual *t* tests and Ad-RFP vs Ad-SETX is presented here. * $P < 0.05$, paired two-tailed *t* test comparing Ad-RFP and Ad-SETX transduced SMA motor neurons. (p=0.0305). The data were collected from 3 biological independent replicates (n=3) and were normally distributed. Nuclei counted = 25/replicate.

5.3 SETX overexpression ameliorates the neurodegenerative phenotype in model systems of SMA

Having confirmed that overexpression of SETX can reverse the DNA damage phenotype of SMA; it was then tested whether it can also rescue the neurodegenerative phenotype of SMA. Rossoll and colleagues first reported that spinal motor neurons isolated from SMA mouse embryos exhibit normal survival but show impaired axonal growth (Rossoll *et al.*, 2003). Adenoviral-mediated overexpression of SETX significantly improved the axonal growth of SMNΔ7 motor neurons when compared to untransduced and Ad-RFP transduced motor neurons (**Figure 5-5**). Motor neurons derived from wild type embryos were used as unaffected controls of normal axonal growth (**Figure 5-5**).

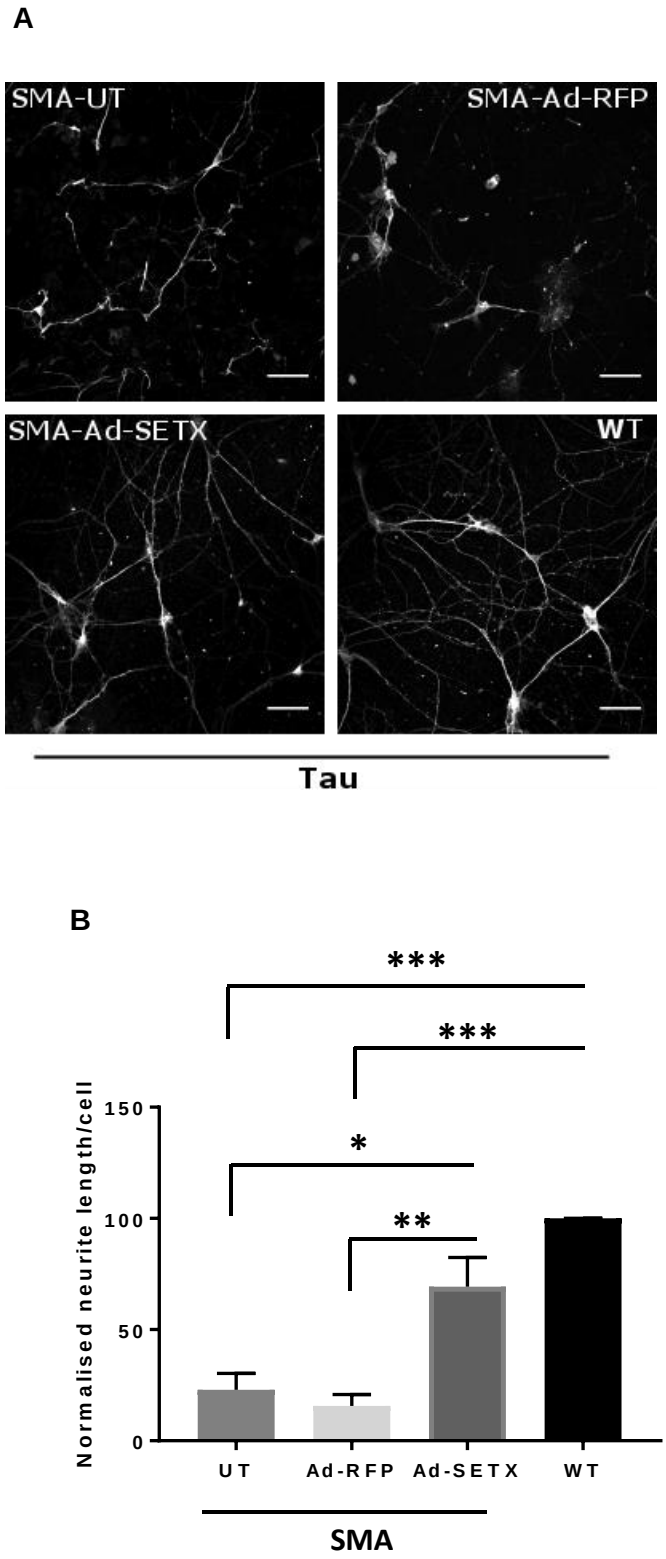

Figure 5-5: Ad-SETX gene transfer mediates neurite outgrowth improvement.

(A) Tau labelling of cultured motor neurons. Scale bars represent 20 µm. (B) Neurite length measurement based on Tau labelling. 25-30 cells were analysed per mouse (n=3). Data

presented as mean ± s.e.m. * $P < 0.05$, ** $P < 0.01$, *** $P < 0.001$; one-way ANOVA followed by Tukey's multiple comparisons test; $F(3, 8) = 25.17$. $p = 0.0002$. Data were normally distributed.

It was next examined whether Ad-SETX could mitigate motor neuron phenotypes in a mouse model of SMA *in vivo*. SMNΔ7 mice display progressive muscle weakness, motor neuronal loss, neuromuscular junction (NMJ) deficits and die on average 2 weeks after birth (Le *et al.*, 2005). To achieve this aim, viral vectors encoding SETX or RFP reporter gene were administered intramuscularly in P1 neonate pups. The rationale of using this route of delivery is that adenoviruses can retrogradely transduce spinal motor neurons when peripherally administered (Acsadi *et al.*, 2002; Millecamps *et al.*, 2002) (**Figure 5-6**).

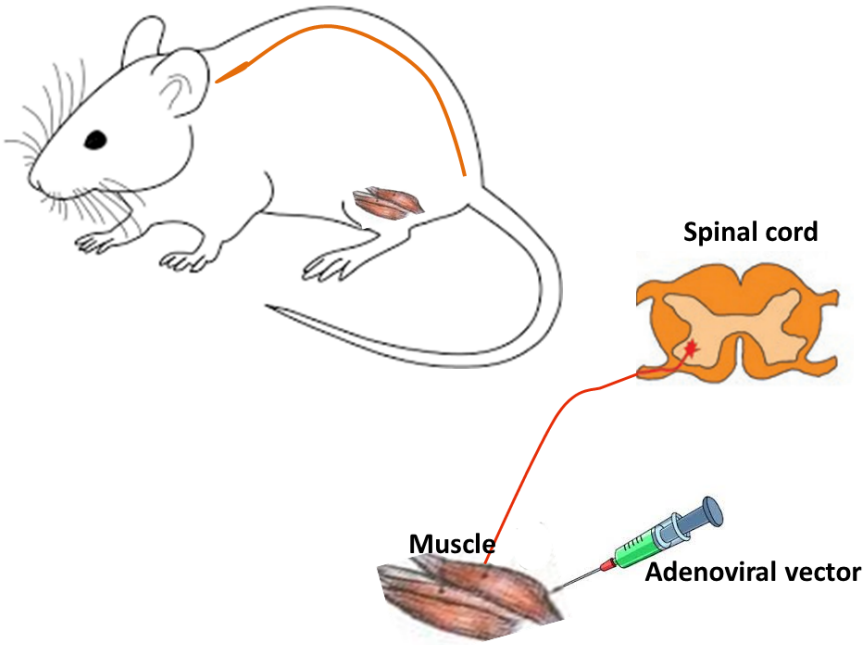

Figure 5-6: Retrograde transport of adenoviral vector when peripherally administered. Schematic representation of intramuscular injection of an adenoviral vector to achieve retrograde transport to the spinal cord motor neurons.

To maximize gene transfer, 30µl of high titre Ad-SETX or Ad-RFP control vector solutions, corresponding to ~ 1.26×10^9 PFU (Plaque Formation Unit) were injected intramuscularly into the right leg muscles of SMNΔ7 mice at postnatal day 1 (P1). Mice were sacrificed at postnatal day 11. Western blots of muscle tissue collected from these animals revealed an elevation of SETX in Ad-SETX injected animals when compared to Ad-RFP controls (**Figure 5-7**).

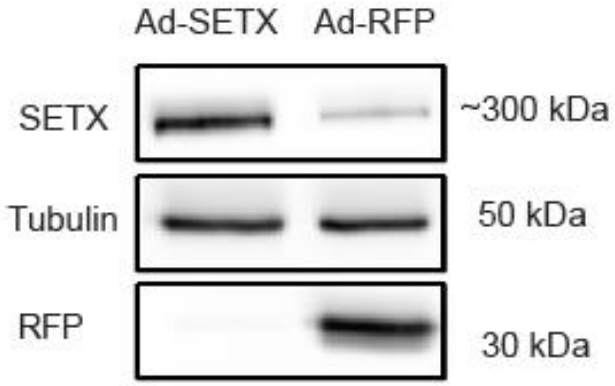

Figure 5-7: Overexpression of SETX in muscle of Ad-SETX injected mice.
Immunoblotting of SETX and RFP levels in SMNΔ7 muscle tissue after intramuscular injections with Ad-SETX and Ad-RFP, respectively. α- tubulin was used as a loading control.

In order to confirm that the adenoviral vector can be retrogradely transported from the injected muscles to spinal motor neurons, spinal cords of the RFP- treated mice were first dissected and sections examined under a fluorescence microscope. A robust RFP signal could be detected unilaterally to the injected side (**Figure 5-8**).

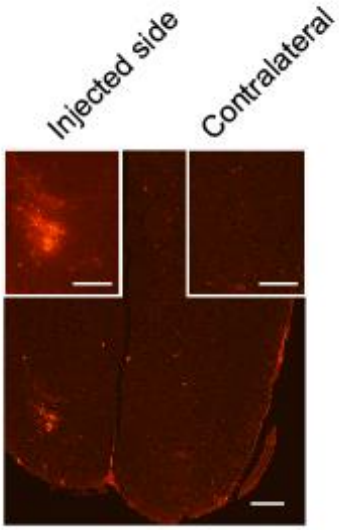

Figure 5-8: Retrograde transport of Ad-RFP.

Ad-RFP delivered unilaterally to leg muscles can transduce motor neurons in SMNΔ7 mice. Scale bar represents 100 μm.

Then spinal cord sections derived from Ad-SETX injected mice were immunostained with SETX and SMI32 (a widely used motor neuron marker) antibodies, and a strong SETX signal was observed in motor neurons located unilaterally to the injected side (**Figure 5-9**).

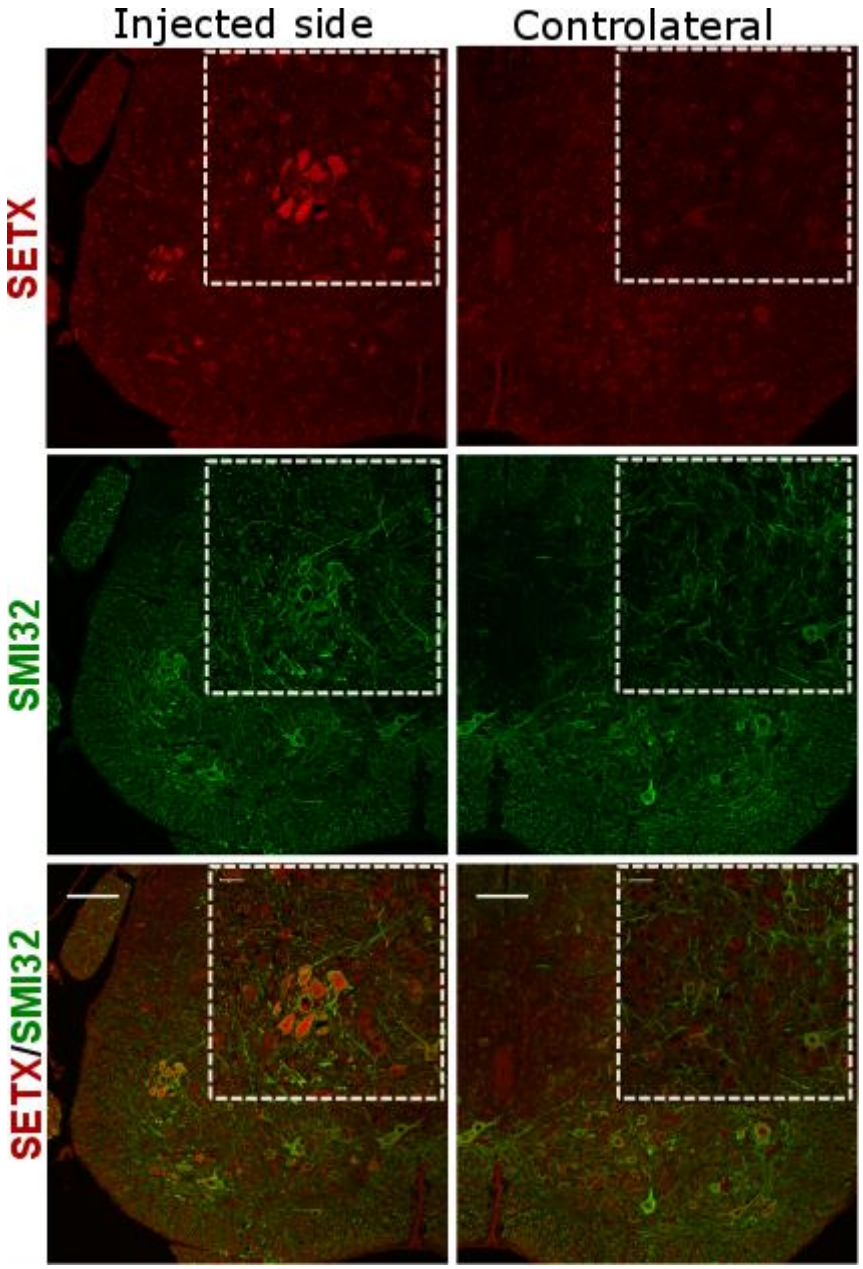

Figure 5-9: Ad-SETX mediates transduction of spinal motor neuron by retrograde transport.

Ad encoding SETX delivered unilaterally to leg muscles led to elevated SETX protein levels in spinal motor neurons. SETX expression was co-localised with neuronal marker SMI32. Scale bars represent 100 µm and 25 µm (for insets), respectively.

Consistent with our *in vitro* data in cultured motor neurons, Ad-mediated SETX expression in motor neurons reduced DNA breaks as revealed by a decline of

γH2AX-positive cells (**Figure 5-10**). Due to time constrains, only a qualitative assessment of γH2AX staining was performed. The stained cells were evaluated by eye using a fluorescence microscope and representative images were taken. All Ad-RFP treated cells that were examined were stained with γH2AX, while the majority of Ad-SETX treated cells were not stained. However, we do acknowledge the importance of quantitative evaluation of the data.

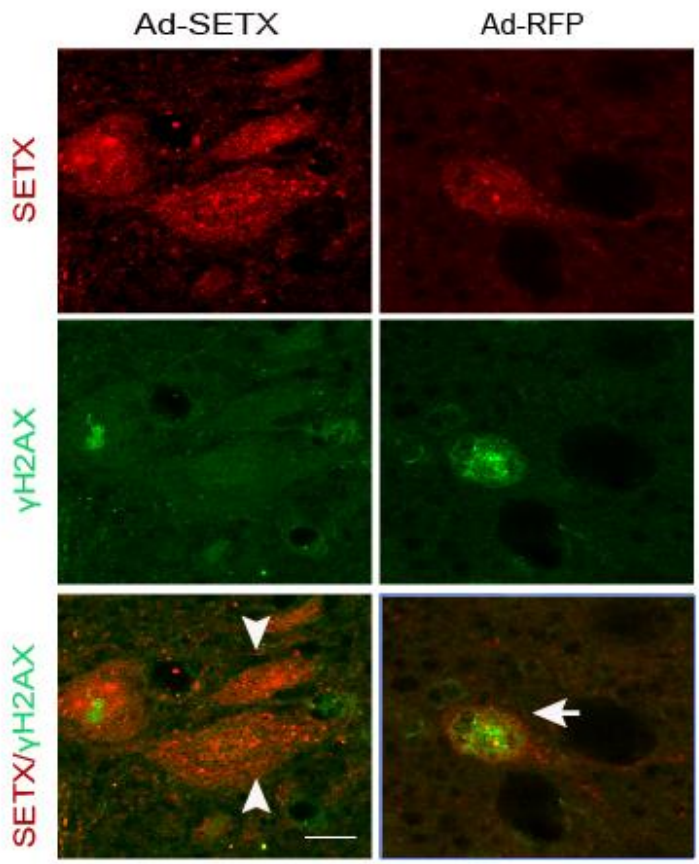

Figure 5-10: SETX overexpression reduces DSBs as revealed by γH2AX staining of spinal cords derived from Ad-SETX and Ad-RFP injected mice.

Spinal cord sections were double-labelled with SETX and γH2AX or RFP and γH2AX revealing a loss of γH2AX staining in Ad-SETX treated motor neurons (arrowheads) compared to Ad-RFP controls (arrows). Scale bar represents 10 μm.

Next step was to examine if SETX overexpression could have an impact on motor neuron survival. Spinal cord motor neuron numbers are normally reduced in SMNΔ7 mice around postnatal day 9 (Le *et al.*, 2005). Histological evaluation of spinal cord sections subjected to Nissl staining revealed that Ad-SETX intramuscular delivery in SMNΔ7 mice promoted motor neuron survival compared to Ad-RFP controls (**Figure 5-11**).

A

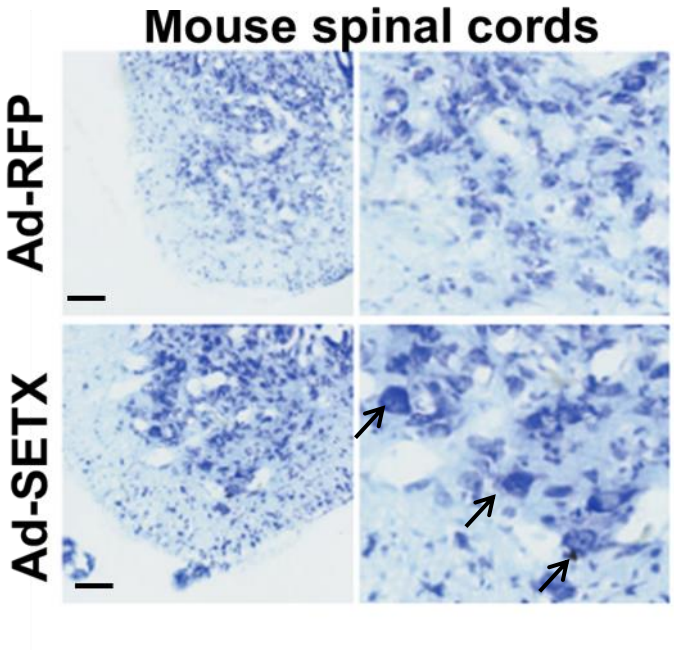

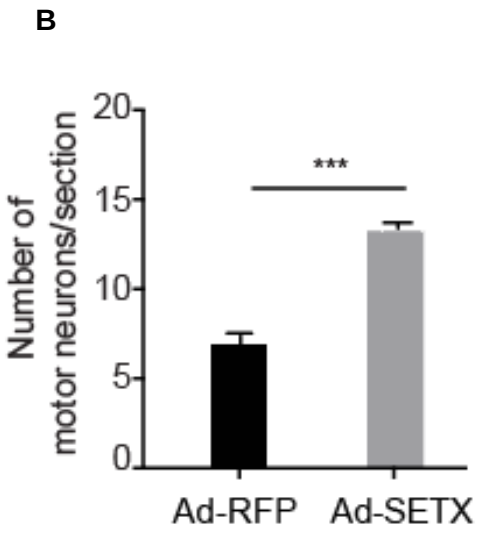

Figure 5-11: Ad-SETX mediates neuroprotection of lumbar spinal motor neurons.

(A) Lumbar spinal cord sections of Ad-SETX and Ad-RFP injected SMA mice were stained with Nissl and (B) the number of motor neurons per section counted. Data presented mean ± s.e.m from N=5 mice per group. *** $P < 0.001$, paired *t* test. Scale bars represent 100 µm. Arrows indicate motor neurons, the number of which is reduced in Ad-RFP treated spinal cords.

Changes at the neuromuscular junction (NMJ) are a key early pathological event in SMA (Murray *et al.*, 2008). Muscles collected from these animals were therefore immunohistochemically processed to label the motor neuron proteins 2H3 and SV2 (medium weight neurofilament and synaptic vesicle protein, respectively) and AChRs, on skeletal muscle fibres, allowing morphological assessment of the impact of SETX treatment on NMJ pathology (**Figure 5-12**). SETX gene transfer robustly ameliorated NMJ pathology in flexor digitorum brevis (FDB) muscles, as revealed by greater numbers of vacant and partially occupied endplates in RFP-injected SMA mice, compared with higher numbers of fully occupied endplates and poly-innervated endplates in SETX-treated mice (**Figure 5-12**). Quantification of these findings

demonstrated statistically significant rescue of NMJ pathology in the Ad-SETX treated group compared with the controls (**Figure 5-12**), thereby preserving neuromuscular connectivity. NMJ analysis was kindly performed by members of Professor Gillingwater's lab at the University of Edinburgh, a research group with extensive experience in investigating neuromuscular junction pathology.

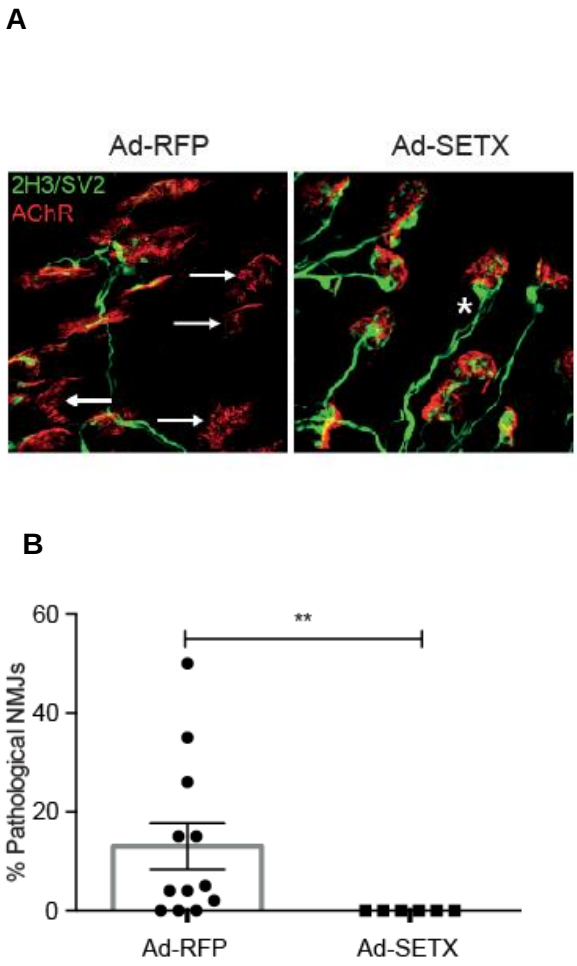

Figure 5-12: Rescue of NMJ pathology in Ad-SETX injected SMA mice.

(A) Confocal micrographs illustrating vacant (arrows) and partially occupied endplates at NMJs in Ad-RFP treated SMA mice (left), compared with fully occupied endplates and poly-innervated endplates (asterisk) at NMJs in Ad-SETX injected SMA mice (right). Scale bar represent 30 µm. B) Statistically significant ($p < 0.01$) rescue of NMJ pathology in Ad-SETX injected SMA mice compared with Ad-RFP injected controls. Pathological NMJs included

both vacant and partially occupied endplates. [n=12 muscles, N=7 mice (Ad-RFP); n=6 muscles, N=3 mice (Ad-SETX); Mann-Whitney test].

Taken together, our *in vitro* and *in vivo* studies provide compelling evidence of a causative link between R loop-driven DNA damage and neurodegeneration in SMA. Given that Ad-SETX treatment had a beneficial effect on SMA mice by rescuing neuromuscular pathology and motor neuron loss; it was then investigated whether Ad-SETX administration can also have an effect on SMNΔ7 mouse survival. Due to the fact that there was not enough virus for multiple muscle injections a small number of SMA (SMNΔ7) and WT mice were injected intramuscularly into the right leg muscles as described above. SMNΔ7 and WT untreated mice were also included in the study as controls. Understanding that it is extremely optimistic to have an impact on survival by targeting one group of muscles the survival and body weight of the animals participated in the study were assessed nonetheless. The body weight of all mice was monitored every two days as a measure of overall health. As expected, under these circumstances, there was no significant difference in the bodyweight or survival between Ad-SETX treated, Ad-RFP treated or untreated SMA mice (**Figure 5-13**).

A

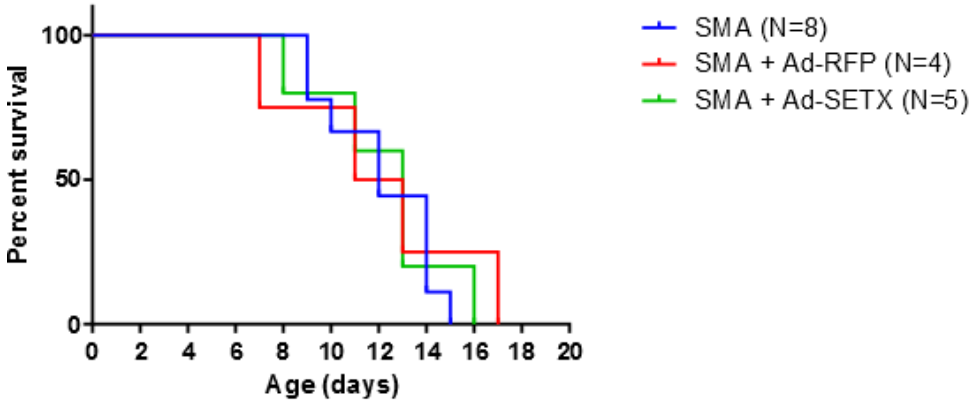
Percent survival
100
50
0
0 2 4 6 8 10 12 14 16 18 20
Age (days)
SMA (N=8)
SMA + Ad-RFP (N=4)
SMA + Ad-SETX (N=5)

B

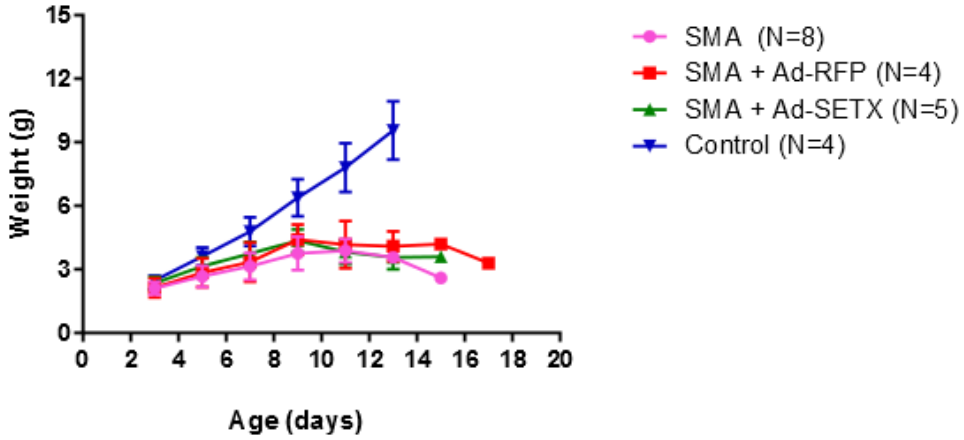
Weight (g)
15
12
9
6
3
0
0 2 4 6 8 10 12 14 16 18 20
Age (days)
SMA (N=8)
SMA + Ad-RFP (N=4)
SMA + Ad-SETX (N=5)
Control (N=4)

C

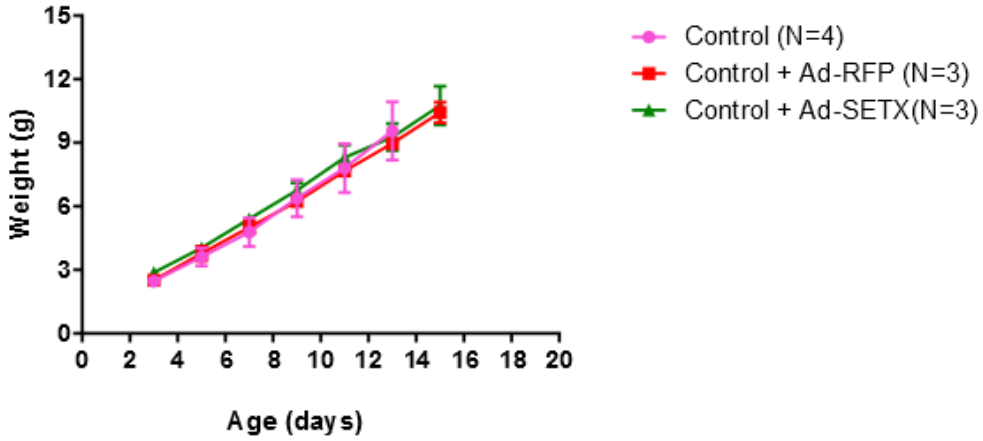
Weight (g)
15
12
9
6
3
0
0 2 4 6 8 10 12 14 16 18 20
Age (days)
Control (N=4)
Control + Ad-RFP (N=3)
Control + Ad-SETX(N=3)

Figure 5-13: Survival analysis and body weight assessment of SMNΔ7 mice after unilateral i.m. injections.

(A) Kaplan-Meier survival curves comparing lifespan of Ad-SETX injected mice, Ad-RFP injected mice and uninjected SMNΔ7 mice. (B) Body weight growth in SMNΔ7 injected mice with Ad-SETX, Ad-RFP or uninjected mice. (C) Body weight growth in WT mice injected with Ad-SETX, Ad-RFP or uninjected mice.

The inability of SETX administration to prolong survival does not necessarily understate the therapeutic potential of SETX to treating SMA. As it was shown earlier in this chapter, SETX overexpression significantly improves motor neuron survival, however the transduction of motor neurons is limited to the motor neurons connected to the injected muscles. Possibly, motor neurons that innervate muscles essential for the survival of mice (for example muscles responsible for breathing) are not efficiently transduced and degenerate. There are two ways to overcome the limited transduction of spinal motor neurons; firstly, to inject more muscle sites. Ascadi and colleagues reported an increased survival and function of SOD1 mice after adenoviral mediated transfer of GDNF gene to the spinal cord of those mice (Acsadi *et al.*, 2002). Anterior tibialis, gastrocnemious, quadriceps and paraspinal muscles were injected bilaterally in their study. We could therefore inject the same muscle groups along with the diaphragm muscle in an attempt to increase the transduction efficiency of spinal motor neurons. However, it is worth noting that GDNF and SETX transgenes are not comparable. GDNF, being a neurotrophic factor, can be excreted by the cells and in principle can exhibit a therapeutic effect through the following routes: it can be either released by injected muscles and transferred via bloodstream everywhere in the body, it can also be released by

muscle cells, be uptaken by NMJs and be retrogradely transported to MNs, additionally the adenoviral vector carrying GDNF can be retrogradely transported to MNs and finally adenoviral-transduced MNs can also release GDNF facilitating its wide spread within spinal cord. Conversely, SETX lacks the ability to be excreted by the cells. Therefore, the current plan is to use our group's well-established design based on previous multiple muscle delivery proof-of concepts as reported in the following papers (Azzouz *et al.*, 2004a; Azzouz *et al.*, 2004b; Ralph *et al.*, 2005). Alternatively, we could assess which domain of SETX protein is essential for its neuroprotective role and utilise the more favourable AAV delivery system for its transfer. AAV vectors are very promising viral systems for gene delivery in the CNS as they can transduce post-mitotic neuronal cell types and express genes for long periods without associated immunological complications (Bessis *et al.*, 2004; Terzi *et al.*, 2008). Due to time constraints, it was not possible to assess these possibilities.

5.4 Discussion

Here we revealed that R loop resolution by adenoviral- mediated overexpression of senataxin, a DNA/RNA helicase involved in R loop resolution, reduced DNA breaks and rescued neurodegenerative phenotypes in a SMA mouse model.

Recently, Zhao and colleagues conducted elegant biochemical experiments showing that SMN interacts with RNA polymerase II and recruits senataxin to resolve RNA/DNA hybrids at transcription termination site (Zhao *et al.*, 2016). Interestingly, mutations in the senataxin gene have been associated with a juvenile-onset form of

amyotrophic lateral sclerosis (*ALS4*), which results in motor neuron loss in early childhood similarly to SMA (Bennett *et al.*, 2015; Chen *et al.*, 2004). Furthermore, mutations in the gene encoding the immunoglobulin mu-binding protein 2 (IGHMBP2) have been linked to spinal muscular atrophy with respiratory distress (SMARD), a variant form of SMA (Grohmann *et al.*, 2001; Tachi *et al.*, 2005). IGHMBP2 is a 5' to 3' helicase that unwinds RNA/DNA hybrids in an ATP-dependent manner (Fukita *et al.*, 1993; Grishin, 1998; Mizuta *et al.*, 1993). Taken together, there is a link between R loop accumulation and motor neuron degeneration. In this chapter we showed that resolution of R loops by SETX overexpression can protect motor neurons against cell death.

Our data demonstrate a role for SMN in maintaining transcriptional integrity and establish senataxin as a potential therapeutic target to alleviate neurodegeneration associated with SMA. We showed that Ad-SETX administration in SMNΔ7 mice dramatically improved the neuromuscular phenotype observed in SMA and rescued motor neurons from cell death; however we did not detect any effect on mouse survival. This inability of Ad-SETX to extend life expectancy could be attributed to the viral vector per se and its ability to transduce only the motor neurons connected to the injected muscle. The most promising therapeutic strategies, including survival studies, in SMA mouse model so far were performed using AAV serotype 9 (AAV9) that can cross the blood brain barrier (Benkhelifa-Ziyyat *et al.*, 2013; Glascock *et al.*, 2012; Kaifer *et al.*, 2017; Powis *et al.*, 2016a; Valori *et al.*, 2010). As it was mentioned above, it is important to unravel the exact domain of SETX which is responsible for its neuroprotective role in order to be able to use the more suitable therapeutic viral vectors such as AAV.

6. Nucleolar disruption in response to rDNA damage in SMN-deficient cells

6.1 Aim

The nucleolus is a dynamic nuclear membrane-less organelle in which ribosomal DNA (rDNA) transcription and ribosomal assembly take place. rDNA is transcribed by RNA polymerase I in a cell cycle phase-dependent manner (Sirri *et al.*, 2008). The size and the number of nucleoli in each cell depend on the rate of RNA polymerase I – mediated transcription, which in turn, depends on cell growth and metabolism (Russell *et al.*, 2005). Motor neurons usually have very prominent nucleoli due to their high energy demands that require high levels of ribosome synthesis. The nucleolus is not only the ribosome factory of a cell; it is also a stress sensor. The nucleolus adjusts its activity enabling cellular homeostasis under stress conditions (Boulon *et al.*, 2010; Olson, 2004; Pederson *et al.*, 2009). Perturbation of nucleolar activity and integrity, also known as nucleolar stress has been linked to several neurodegenerative diseases such as Parkinson's disease, Huntington's disease, Alzheimer's disease and Amyotrophic Lateral Sclerosis (Iacono *et al.*, 2008; Lee *et al.*, 2014; Parlato *et al.*, 2014; Rieker *et al.*, 2011).

Nucleolar disruption could be caused by increased rDNA damage among other factors (van Sluis *et al.*, 2017). The repetitive nature of rDNA coupled with its high transcription rates could lead to improper recombination and potential rDNA deletions or rearrangements as well as excessive formation of R loops leading to rDNA DSBs (Tsekrekou *et al.*, 2017). rDNA DSBs have been shown to result in an ATM-dependent inhibition of RNA polymerase I transcription (Kruhlak *et al.*, 2007) and nucleolar reorganization with the formation of nucleolar caps (Harding *et al.*, 2015). Perturbations in any step of ribosomal biogenesis such as rDNA transcription, rRNA processing and ribosomal assembly can cause nucleolar disruption and p53-

mediated cell cycle arrest or apoptosis (James *et al.*, 2014; Rubbi *et al.*, 2003). Therefore, it is apparent that normal nucleolar function is important for cell survival.

Here, I hypothesized that potential DSBs into rDNA could lead to disruption of the nucleolus. I also hypothesized that SMN may play a role in the resolution of R loops formed during the transcription of rDNA and that SMN deficiency may lead to accumulation of R loops in the nucleolus and resultant rDNA damage. The identification of a complex consisting of SMN, SETX and RNA polymerase I reinforced this hypothesis.

6.2 SMN – deficient cells exhibit increased nucleolar disruption

In chapter 4, it was shown that SMN deficient motor neurons displayed high number of R loops when compared to healthy controls (**Figure 4-4**). To extend this finding to other cell types, SMA type I fibroblasts and healthy controls were labelled with an antibody against R loops (S9.6). Interestingly the morphology of R loop-enriched nuclear structures in SMA type I patient was abnormal when compared to control cells (**Figure 6-1**). Usually, when cells are stained with S9.6 antibody nuclear round foci are detected similar to those seen in control fibroblasts (**Figure 6-1**).

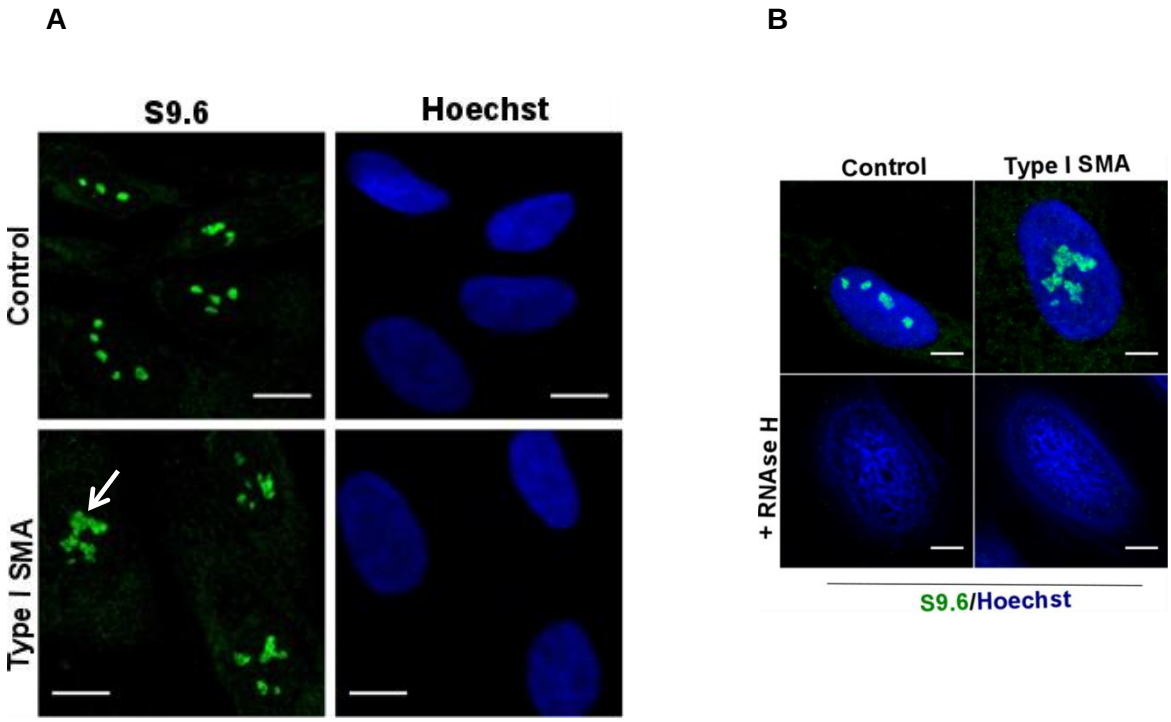

Figure 6-1: R loop staining in SMA type I fibroblasts.

(A) Fibroblasts derived from SMA type I child (GM08318) and healthy control (GM00498) were labelled for RNA/DNA hybrids (S9.6). Scale bars represent 10 µm. Arrow indicates an abnormal structure (B) Specificity of the R loop (S9.6) antibody. Fixed cells were either pre-incubated with RNAse H enzyme or left untreated and subsequently stained for R-loops. Scale bars represent 5 µm.

Given that R loops are specifically formed at highly transcribed regions such as R loop prone rDNA arrays (El Hage *et al.*, 2010), it was hypothesized that the observed R loop staining is primarily nucleolar and that the abnormal phenotype of R loops in SMN-deficient cells could be due to nucleolar disruption. To confirm this hypothesis SMA type I fibroblasts and healthy controls were stained with nucleolin, a major nucleolar protein of the DFC compartment. As expected, nucleolin staining confirmed changes in nucleolar morphology of SMA type I fibroblasts compared to controls

(**Figure 6-2A**). Similar phenotype was observed in motor neurons isolated from SMA embryos (**Figure 6-2B**). Both the shape and texture of nucleoli in SMA type I patient cells appear to be much different when compared to the control cells. In SMA cells adjacent nucleoli seem to have been fused or collapsed forming a large structure.

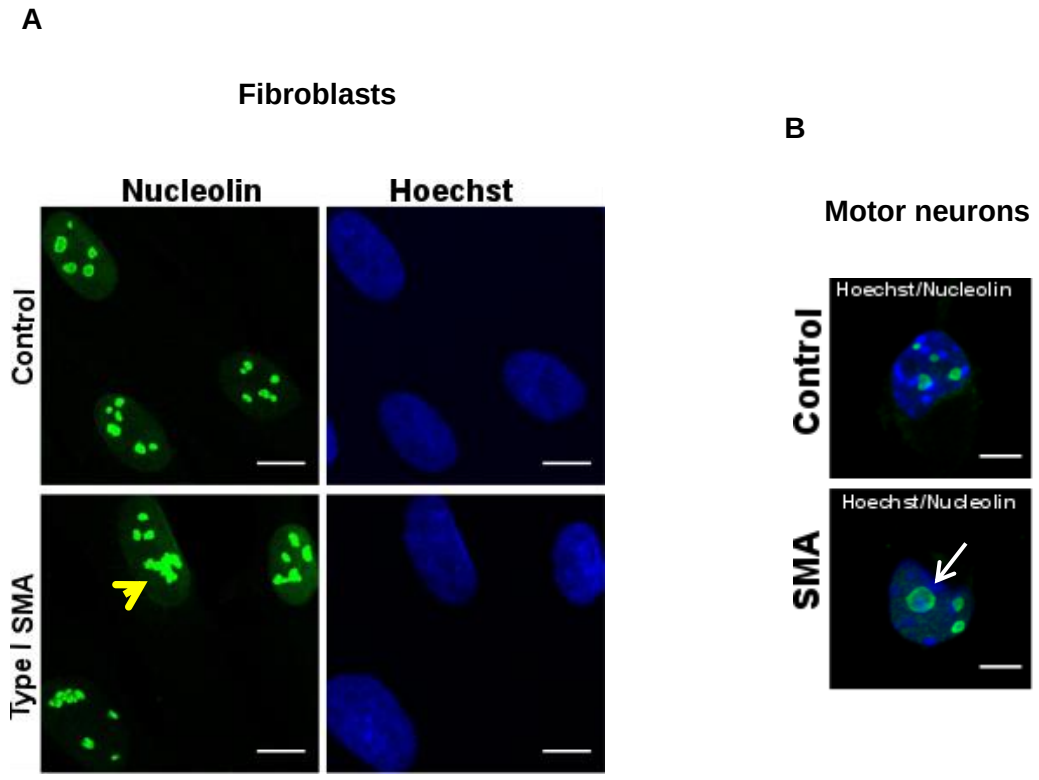

Figure 6-2: Nucleolin staining in experimental cell models of SMA.

(A) Fibroblasts derived from SMA type I child and healthy control were stained with nucleolin (green). Yellow arrowhead shows disrupted nucleoli (B) E13 motor neurons derived from SMA and wild type mouse embryos were stained with nucleolin (green) antibody and Hoechst (blue). White arrow shows an enlarged (disrupted) nucleolus. Scale bars represent 10 µm (A) and 5 µm (B), respectively.

6.3 The nucleolar reorganization of SMN-deficient cells could be attributed to rDNA breaks and RNA polymerase I inhibition

The nucleolus consists of 3 distinct components: the fibrillary centre (FC), the surrounding dense fibrillary component (DFC), which in turn, is surrounded by the granular component (GC) (**Figure 6-3**). These three layers exhibit liquid like properties and their distinct organization is a consequence of liquid phase immiscibility (Feric *et al.*, 2016).

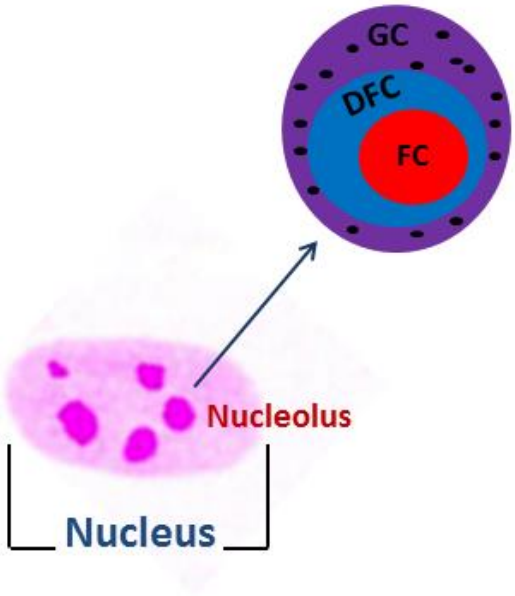

Figure 6-3: Nucleolus structure.

Many diploid cells have a range from 1 to 6 nucleoli per nucleus. Each nucleolus is composed of the fibrillary centre (FC, red), the dense fibrillary component (DFC, blue) and the granular component (GC, purple).

It is believed that pre-rRNA synthesis takes place in the interphase between FC and DFC, and then pre-rRNA processing begins in DFC and is completed in the GC. The latter is also the compartment where the ribosomal assembly occurs (Boisvert *et al.*, 2007; Melese *et al.*, 1995). Inhibition of RNA polymerase I – mediated transcription has been shown to lead to nucleolar reorganization, in which FCs and DFCs migrate along with rDNA to the periphery of the nucleolus, forming nucleolar caps (Shav-Tal *et al.*, 2005). Interestingly, a similar formation of nucleolar caps was detected in SMA type I fibroblasts. These structures resemble cap-like formations situated on the outer part of the segregated nucleolus (**Figure 6-4 white arrows**). Notably, these nucleolar caps are associated with γH2AX signals, suggesting that the rDNA that is exposed to the periphery contains DSBs (**Figure 6-4**).

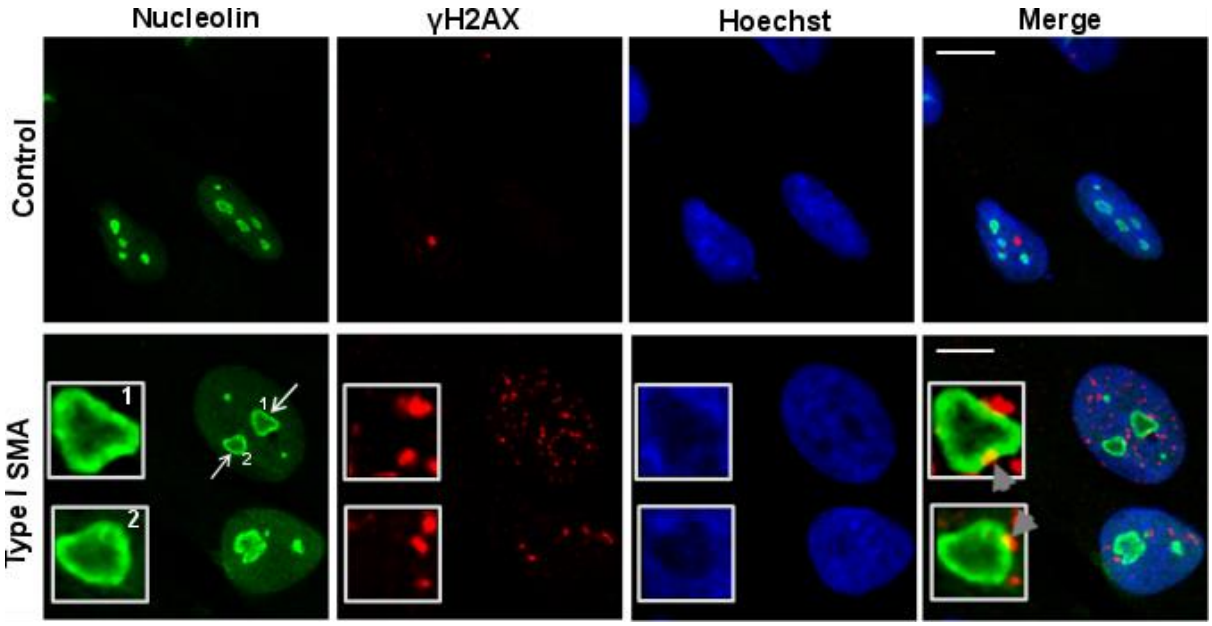

Figure 6-4: SMA type I fibroblasts form nucleolar caps containing DSBs.

Dual immunostaining with nucleolin and γH2AX performed on SMA type I and control fibroblasts. SMA type I fibroblasts form nucleolar caps (white arrows) that are shown to co-localise with γH2AX foci (grey arrowheads). Scale bars represent 5 μm.

Further suggestion of the presence of DSBs in the rDNA comes from a preliminary ChIP (chromatin immunoprecipitation) analysis for γH2AX, followed by a qPCR using primers specific for ribosomal genes (RPL32, 18S, 5.8S and 28S). ChIP was performed to select γH2AX-enriched chromatin fractions (**Figure 6-5**). Unfortunately, due to time constraints it was not possible to repeat this experiment more than once, but it looks very promising as a preliminary data.

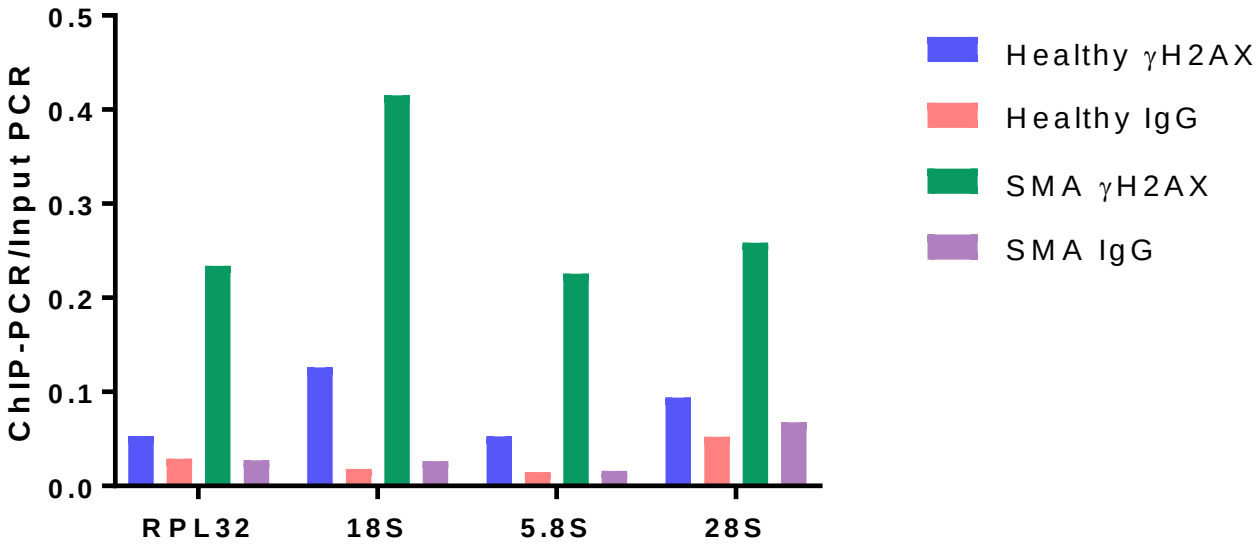

Figure 6-5: γH2AX-ChIP followed by qPCR analysis of ribosomal genes.

Quantified RPL32, 18S, 5.8S and 28S gene qPCR data from γH2AX- ChIP experiment in SMA type I fibroblasts and healthy controls. IgG was used as a background control.

According to van Sluis and colleagues, DSBs in rDNA induce nucleolar reorganization with cap formation and inhibition of RNA polymerase I transcription (van Sluis *et al.*, 2015). To investigate whether RNA polymerase I –mediated transcription is also affected in SMN-deficient cells, total RNA from SMA and control

embryonic (E16) cortical neurons was isolated and real time quantitative reverse transcriptase PCR (qRT-PCR) was performed for the 45S precursor as well as the 5.8S, 18S and 28S mature rRNAs (**Figure 6-6**).

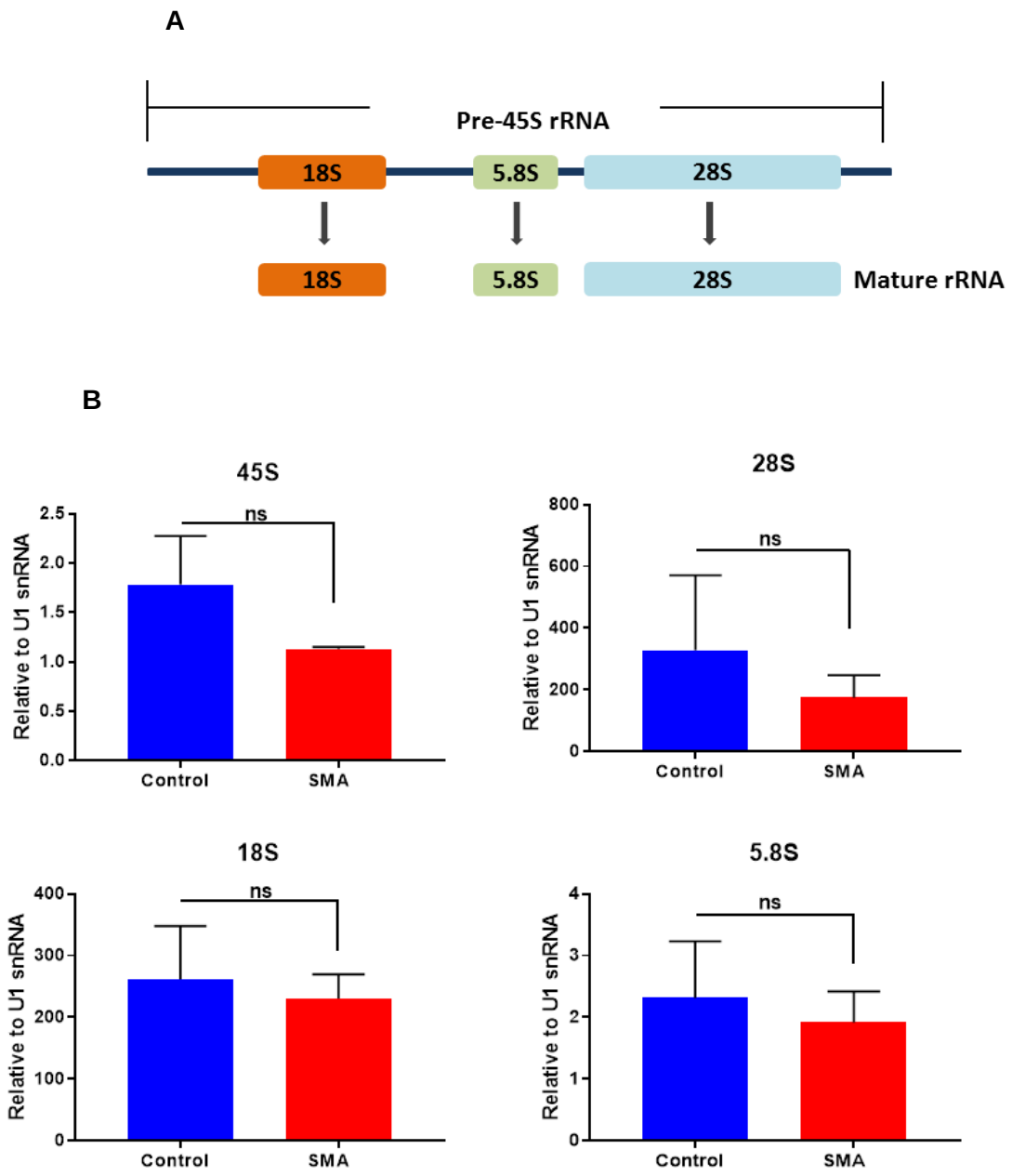

Figure 6-6: Analysis of rRNA synthesis.

(A) Schematic depicting the processing of the 45S pre-rRNA into the mature 5.8S, 18S, and 28S rRNA species. (B) Total RNA was extracted from SMA and control embryonic cortical

neurons. The levels of 45S pre-rRNA along with 5.8S, 18S, and 28S mature rRNAs were determined by real-time quantitative PCR (RT-qPCR) and normalized to U1 snRNA levels. Data are presented as mean ± s.e.m. ns = not significant. paired two-tailed *t* test; p=0.308 (45S), p=0.406 (28S), p=0.689 (18S), p=0.446 (5.8S). The data were collected from 3 biological independent replicates (n=3).

The 45S precursor rRNA is believed to be more sensitive indicator for variations in the rate of rRNA synthesis due to its short life, whereas the levels of the accumulating mature rRNA forms can be influenced by several factors such as rRNA processing rate and degradation (Uemura *et al.*, 2012). The levels of all rRNA species appeared to be lower in SMA cortical neurons compared to wildtype controls suggesting impairment in rRNA biogenesis. However, this reduction was not statistically significant. Perhaps qPCR is a crude way to investigate alterations in expression levels of newly synthesized rRNAs. A more sensitive and accurate way to follow rRNA synthesis and processing would be by radiolabels such as tritiated uridine (^{3}H-uridine) that is taken up by cells and incorporated into highly abundant transcripts such as rRNAs. Newly synthesized labelled transcripts can then be detected by autoradiography (Pestov *et al.*, 2008; Ray *et al.*, 2013).

6.4 RNA polymerase I: a novel SMN-interacting protein

Having shown data which suggest that SMN-deficient cells may have impaired rRNA synthesis and given that SMN is reportedly localised in the nucleolus (Francis et al., 1998), it was hypothesised that SMN may interact with RNA polymerase I. Therefore immunoprecipitation (IP) experiments were performed by using antibodies against RNA polymerase II, RNA polymerase I or rabbit IgG (**Figure 6-7**). In the nucleoplasm

SMN forms a complex with RNA polymerase II and senataxin facilitating the resolution of R loops that occur naturally during transcription (Zhao *et al.*, 2016), so RNA polymerase II was used as a positive control that interacts with SMN, whereas rabbit IgG was used as a negative control. Our results revealed that a novel complex exists which contains RNA polymerase I, SMN and senataxin (**Figure 6-7**).

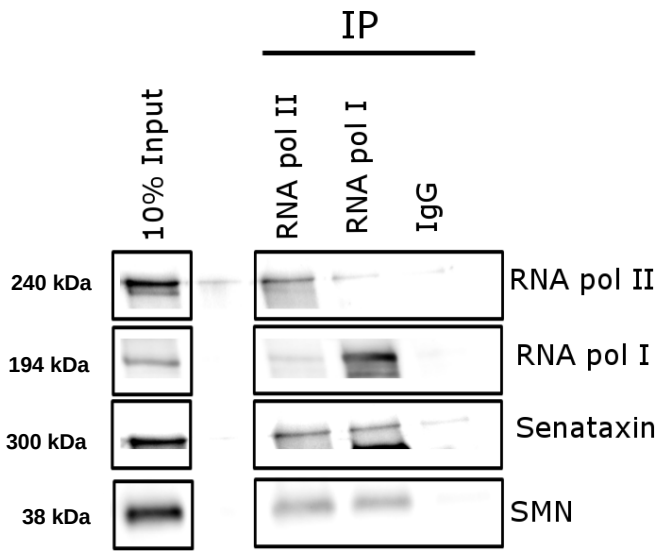

Figure 6-7: SMN protein interacts with RNA polymerase I.

(A) Immunoprecipitation (IP) experiments were carried out in HEK293T cell nuclear extract using anti- RNA polymerase II, anti-RNA polymerase I or control rabbit (IgG) antibodies. Immunoprecipitates were analysed by SDS-PAGE and Western blotting with antibodies against RNA polymerase II, RNA polymerase I, SMN and senataxin.

It was next tested whether the association between SMN and RNA polymerase I is RNA – mediated. For this reason half of the cell nuclear extract was incubated with RNAse A that hydrolyses single-stranded RNA (ssRNA) and then an IP was

performed by incubating the samples with antibodies against RNA polymerase I or rabbit IgG (**Figure 6-8**).

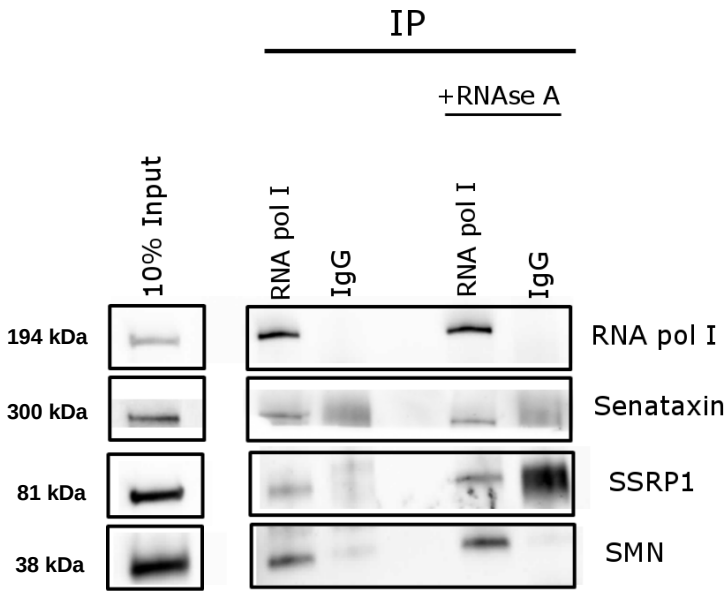

Figure 6-8: SMN-RNA polymerase I interaction is RNA-independent.

(A) Immunoblot analyses of RNA polymerase I, senataxin, SSRP1 and SMN on immunoprecipitations with RNA polymerase I (RNA polymerase I IP) from nuclear extracts of HEK293T cells without and with RNAse A treatment respectively. Rabbit IgG was used as negative control.

Since RNAse A treatment did not interfere with the precipitation of SMN by the RNA polymerase I antibody, it was concluded that RNA is not required for SMN – RNA polymerase I interaction. The SSRP1 protein was used as a positive control because of its known association with RNA polymerase I (Birch *et al.*, 2009). Indeed, immunoprecipitation with RNA polymerase I antibody, but not control IgG, co-precipitated SSRP1. However, there was a strong background in IgG control after

RNAse A treatment that we speculate to be due to some contaminants as the band appeared to be smeared rather than sharp.

These results even though they are still very preliminary, they are really important because they could explain the phenotypes observed in the nucleolus of SMN-deficient cells. Based on these results, it was hypothesised that SMN might form an R loop resolution complex in the nucleolus similar to the one observed in the nucleoplasm. Therefore, SMN deficiency may lead to accumulation of R loops in the nucleolus and resultant rDNA damage that in turn leads to nucleolar disorganisation and impairment in RNA polymerase I – mediated transcription.

6.5 SMN overexpression reduces nucleolar stress

The data described under chapter 4 of this thesis revealed that lentiviral (LV)-mediated SMN replacement in SMN-deficient cells led to significant reduction in DSBs (**Figures 4-9 & 4-11**). To determine whether SMN overexpression could also rescue nucleolar stress observed in SMA cases, we transduced SMA type I fibroblasts with LV vector encoding human SMN cDNA (LV-SMNFL) and immunostained the cells with nucleolin antibody. LV-SMN FL reduced the levels of disrupted nucleoli when compared to control cells (**Figure 6-9**). Interestingly, lentiviral mediated overexpression of SMNΔ3, the truncated version of SMN protein that lacks the Tudor domain, did not have any effect on the increased nucleolar stress observed in SMA (**Figure 6-9**). As it has already been mentioned above, nucleolar stress can be defined as perturbation of nucleolar activity and/or integrity. In **Figure 6-9**, we present the number of disrupted nucleoli as a measure of

nucleolar stress. Qualitative monitoring of nucleolar morphology was based on shape and textural features of nucleoli, in order to distinguish normal from altered (disrupted) nucleoli. The manual classification was based on the visual inspection of representative images and the assignment of nucleolar disruption phenotypes to two categories: normal and disrupted. Small individual nucleoli with round shape (yellow arrowhead) were classified as normal, whereas large and fused nucleoli with usually coarse texture were classified as disrupted (orange arrowhead) in **Figure 6-9**.

A

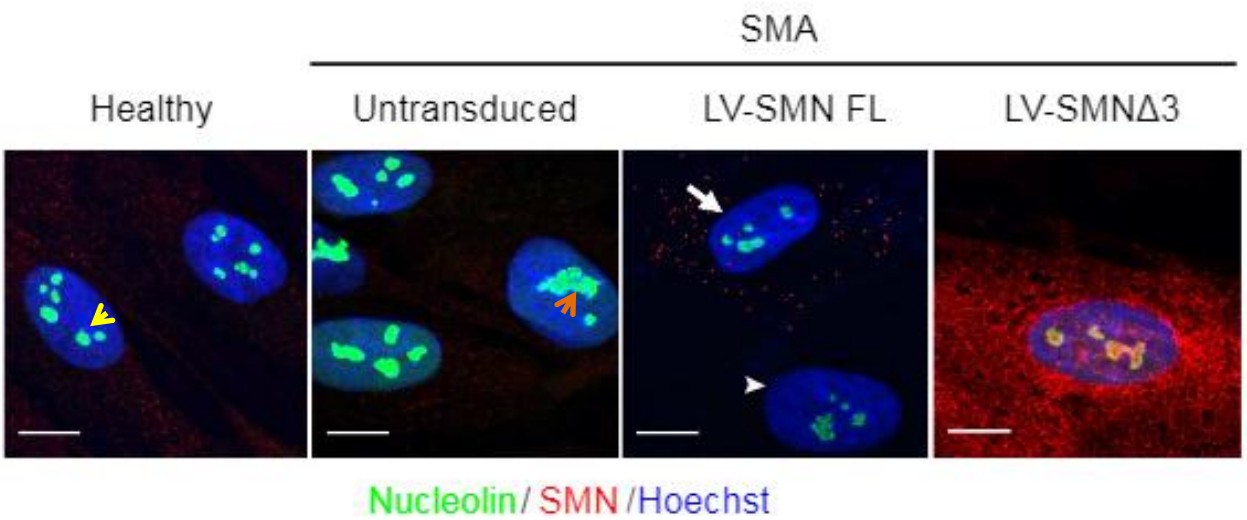

B

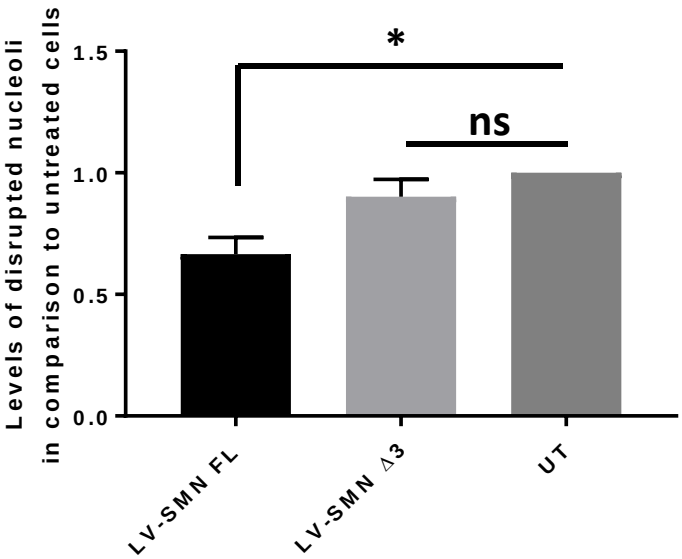

Figure 6-9: Lentiviral-mediated SMN replacement restores normal nucleolar morphology in SMN-deficient cells.

(A) SMA type I fibroblasts were transduced with lentiviral vectors carrying either full SMN gene (LV-SMN FL) or SMN lacking exon 3 (LV-SMNΔ3) that encodes for Tudor domain. The cells were double labelled for nucleolin and SMN 96 hour after transduction. Healthy fibroblasts were used as a control. Scale bars represent 5 µm. White arrow indicates a SMN overexpressing cell, white arrowhead indicates an untransduced cell, yellow arrowhead

indicated a normal nucleolus and orange arrowhead indicated a disrupted nucleolus. (B) Quantification of disrupted nucleoli. Relative reduction of nucleolar stress in presented as mean ± s.e.m. * $P < 0.05$. One way ANOVA analysis followed by Tukey's multiple comparisons test; $F(2,6) = 9.034$. $p = 0.0155$. The data were collected from 3 biological independent replicates (n=3) and were normally distributed. Nuclei counted=50/replicate.

6.6 Discussion

Here we report that SMN-deficient cells exhibit increased rDNA damage that leads to nucleolar disruption which is coupled with inhibition of RNA polymerase I – mediated transcription. Impaired nucleolar activity has been shown to be responsible for the pathogenesis of numerous genetic disorders, such as dyskeratosis congenita, Werner syndrome and Treacher Collins syndrome (Heiss *et al.*, 1998; Isaac *et al.*, 2000; Marciniak *et al.*, 1998). It has also been associated with some types of cancer (Hannan *et al.*, 2013; Johnson *et al.*, 1998; Montanaro *et al.*, 2008). Impaired rRNA transcription and altered nucleolar integrity were reported in neurodegenerative diseases such as PD, AD, HD and ALS (Iacono *et al.*, 2008; Lee *et al.*, 2014; Parlato *et al.*, 2014; Rieker *et al.*, 2011).

According to Hetman and Pietrzak, nucleolar disruption is a consequence of RNA polymerase I inhibition following DNA damage or oxidative injury (Hetman *et al.*, 2012). Consistent with their claims, we also observed increased rDNA damage in SMN-deficient cells and reduced rRNA synthesis that could be attributed to RNA polymerase I inhibition.

Furthermore, the finding presented here of an interaction between SMN and RNA polymerase I is of great interest. Zhao and colleagues have recently showed that SMN interacts with RNA polymerase II and recruits SETX to resolve RNA/DNA

hybrids at transcription termination sites (Zhao *et al.*, 2016). Loss of either SMN or SETX leads to R loop accumulation causing increased DNA damage (Jangi *et al.*, 2017; Mischo *et al.*, 2011). Studies in yeast have shown that Sen1 protein is involved in transcription termination of the 35S pre-rRNA (Kawauchi *et al.*, 2008; Ursic *et al.*, 2004). In addition to this, mutations of Sen1 gene in yeast cells lead to R loop accumulation over rDNA genes (Chan *et al.*, 2014). In line with this, our immunoprecipitation results demonstrate that SMN, RNA polymerase I and SETX are all parts of one complex; therefore it is tempting to hypothesize that SMN interacts with RNA polymerase I and recruits SETX to resolve R loops occurring during the transcription of rDNA. SMN-deficient cells, recruit SETX less efficiently, with a result the R loops to be accumulated, inhibiting the rRNA synthesis and resulting in increased rDNA damage.

However, more work needs to be done in order to confirm that the interaction between SMN and RNA polymerase I is real and not just an artefact of cell lysis. Glutathione-S-transferase (GST) pull down assay could be an alternative method to analyse this protein-protein interaction *in vitro* (Sambrook *et al.*, 2006).

7. GENERAL DISCUSSION

Spinal muscular atrophy is a devastating genetic childhood onset neurodegenerative disorder characterised by progressive loss of lower motor neurons due to reduced levels of the ubiquitously expressed SMN protein. SMN is a multifunctional protein and it is still unclear which of the numerous functions of SMN is essential for the survival of motor neurons. However, despite this uncertainty, enormous systematic research on SMA since the identification of *SMN1* as the disease-causing gene in 1995 (Lefebvre *et al.*, 1995) has revealed the exact molecular genetic mechanisms that give rise to SMA. The great understanding of the molecular genetic basis of SMA has led to recent advances in the treatment of the disease. The most successful therapeutic strategies focus on increasing the levels of SMN protein either by regulating the expression of *SMN2* gene or by replacing the entire *SMN1* gene.

Spinraza, the only currently licenced drug to treat SMA belongs to the first category of SMN-dependent therapeutic strategies. However, despite the dramatic effect of Spinraza in SMA patients there are still some issues that need to be considered. It is important to highlight that treated SMA patients may have shown significant progress but they did not manage to achieve completely normal function during the phase III clinical trial (Hache *et al.*, 2016). Therefore it is apparent that even though it is a very promising treatment it cannot be considered as the ultimate cure for SMA. Furthermore, despite the fact that it was tested only on SMA type I patients it has been approved for all types of SMA. For an effective treatment, SMN needs to be restored as early as possible, even at a pre-symptomatic level as studies in SMA mouse models have indicated (Foust *et al.*, 2010; Valori *et al.*, 2010), therefore it is likely that SMN restoration may not be equally beneficial for the older children (SMA type II and III) or young adults (SMA type IV) where SMN-dependent neuromuscular

decline might have already been established and been irreversible at the time of diagnosis (Mercuri *et al.*, 2016). For these reasons, a combinatorial therapeutic approach may appear to be more beneficial. Combining SMN-dependent with therapies that target dysregulated pathways downstream of SMN over the lifespan of individual may be more effective than SMN-directed treatments alone. It is clear then that the identification of key pathways, dysregulation of which contributes to SMA pathogenesis is essential for designing effective therapeutic approaches for SMA. In line with this, this PhD project was mainly aimed at elucidating the emerging role of DNA damage in the pathogenesis of SMA and introducing new therapeutic targets.

7.1 Project outcomes

A significant increase of endogenous DNA breaks was observed in SMA experimental models after utilising established DNA repair assays. Fibroblasts derived from SMA type I patients, embryonic SMNΔ7 cortical and motor neurons, postnatal mouse SMNΔ7 spinal cord and brain tissue as well as human post-mortem tissue were analysed, all of which exhibited elevated DNA damage compared to control samples. Similar results were demonstrated by Fayzullina and colleagues; however their study was focused on skeletal muscles from an SMA mouse model (Fayzullina *et al.*, 2014). The inclusion and analysis of human post-mortem tissue from SMA and healthy individuals was of great significance as no one before had tested the clinical relevance of increased DNA damage to human disease. The increased number of DSBs in SMA was hypothesized to be a direct consequence of SMN deficiency and not a secondary event during the disease progression. That was

proven after a lentiviral-mediated restoration of SMN protein in SMN-deficient cells that managed to reduce the increased DNA damage. As shown in Chapter 4, the observed DNA damage in SMA experimental models is transcription – driven since it appeared to be decreased after transcriptional arrest mediated by alpha-amanitin (a transcriptional inhibitor) treatment. It is well reported that transcription – associated DNA damage can arise from the formation and accumulation of R loops (Aguilera *et al.*, 2012; Skourti-Stathaki *et al.*, 2014). This seems to be the case in SMA as well; an increased number of R loops was demonstrated in SMN-deficient cells and interestingly overexpression of the R loop resolution helicase, SETX, led to a marked decrease of R loops but also reduced the number of DSBs as examined by immunostaining for γH2AX.

In parallel to this project, two independent studies have recently proposed how SMN deficiency may lead to R loop accumulation and result in genome instability. According to the first report, SMN has a direct role in R loop resolution by recruiting SETX at transcription termination sites. Defects in SMN, SETX or any other component of the R loop resolution pathway can lead to R loop accumulation (Zhao *et al.*, 2016). The second study suggests that the well reported spliceosome malfunction due to SMN deficiency causes defects in intron removal leading to increased intron retention. The retained introns are GC-rich and therefore prone to R loop formation (Jangi *et al.*, 2017). One important implication of our study was the investigation of a potential involvement of defective R-loop resolution, reported by the two aforementioned studies, in the pathogenesis of SMA by utilising SMNΔ7 mouse model, a well-established animal model of SMA.

R loop accumulation and DNA damage have been involved in several neurodegenerative disorders but more profoundly in motor neuron diseases (Hill *et*

al., 2016b; Walker *et al.*, 2017; Wang *et al.*, 2015). Motor neurons are exceptionally large cells; therefore they require huge amount of energy for their maintenance. The high energy demands of motor neurons coupled to high transcription rates may lead to increased number of R loops and a resultant DNA damage. Motor neurons are non-dividing postmitotic cells where the repair of DSBs is restricted to the more error-prone NHEJ. Accumulation of DSBs in these neurons can eventually lead to cell death (El-Khamisy, 2011) and contribute in this way to the pathogenesis of motor neuron diseases.

It was demonstrated here that R loop mediated - DNA damage does indeed contribute to the pathogenesis of SMA. R loop resolution by adenoviral- mediated overexpression of SETX reduced DSBs and rescued the neurodegeneration linked to SMA both *in vitro* and *in vivo*. More specifically, overexpression of SETX significantly improved the axonal growth of SMN-deficient motor neurons *in vitro*. It also rescued motor neurons from cell death and dramatically improved the neuromuscular phenotype *in vivo*. Thus, it is apparent that manipulation of R loop accumulation and subsequent DNA damage can potentially be a good and novel therapeutic approach for SMA.

In addition to its role in resolution of R loops formed by RNA polymerase II, SETX may play a similar role in RNA polymerase I – mediated transcription. Studies in yeast have shown that Sen1 protein interacts with Rnt1 protein, a double-strand RNA nuclease and facilitates the transcription termination of the 35S pre-rRNA (Kawauchi *et al.*, 2008; Ursic *et al.*, 2004). In this context, results from this PhD project demonstrate for the first time that a novel complex exists which contains RNA polymerase I, SMN and SETX in mammalian cells. Therefore, it can be hypothesised that SMN and SETX may be responsible for the resolution of R loops formed during

RNA polymerase I – mediated transcription and that mutations in either component may lead to accumulation of R loops during transcription of rDNA genes and subsequent rDNA damage. In this vein, mutations of Sen1 gene in yeast cells lead to R loop accumulation over rDNA genes (Chan *et al.*, 2014). Interestingly, it was also shown in Chapter 6 that SMN-deficient cells exhibit increased DSBs in rDNA. Numerous studies have shown that rDNA DSBs result in ATM-dependent inhibition of RNA polymerase I transcription and formation of nucleolar caps (Harding *et al.*, 2015; Kruhlak *et al.*, 2007; van Sluis *et al.*, 2015). Noteworthy, both phenotypes were also present in SMN – deficient cells as presented in chapter 6. Despite this promising preliminary data presented here, it is apparent that the role of SMN protein in prevention/repair of RNA polymerase I – associated rDNA damage is far from clear.

7.2 Future work

Although the *in vitro* and *in vivo* studies of SETX viral delivery demonstrated its ability to ameliorate the neurodegenerative phenotype of SMA the exact mechanism by which SMN deficiency induces aberrant R loop accumulation and consequent DNA damage that leads to neurodegeneration is still unclear. Therefore more work needs to be done for a clear mechanistic understanding. To maximise the therapeutic potential of SETX, an AAV9 vector, which is considered an ideal vector for SMA treatment, should be utilised. The only limitation is the size of SETX gene that exceeds the packaging capacity of AAV vectors. One way to address this issue is by identifying the domain of SETX that is essential for its neuroprotective role and

sub-clone it in an AAV vector genome. Manipulation of R loop resolution accumulation in SMN-deficient cells might lead to a new avenue for future SMA combinatorial therapies that target both SMN-dependent and SMN-independent pathways in order to generate robust treatments.

Furthermore, the so far data presented here suggests that R loop – mediated genome instability contributes to the pathogenesis of the disease. One experiment to reinforce even further this hypothesis would be a time course experiment that includes several time points in SMA pups and test whether R loop accumulation and the resultant DNA damage precede the motor neuron degeneration. More specifically, tissue from SMA mice and age-matched controls at three different time points, for instance, could be collected and stained with the following markers: S9.6 antibody in order to determine the number of R loops, γH2Ax or 53BP1 as markers of DNA damage and caspase-3 or cleaved PARP in order to assess cell death of motor neurons. It is also important to include a motor neuron – specific marker such as ChAT.

Another exciting data obtained through this project but needs further work is the role of SMN in the nucleolus and RNA polymerase I – mediated transcription. Given that nucleolar dysfunction has been linked to a number of neurodegenerative disorders and is presented as one of the main nuclear hallmarks of DNA damage - induced neurodegeneration, it is apparent how important it is to shed more light on this field. The questions that need to be answered are numerous: Is SMN-RNA polymerase I interaction mediated through the Tudor domain of SMN similarly to SMN-RNA polymerase II interaction? Are the R loops in the nucleolus also formed predominantly at the termination sites of the ribosomal genes? If there is indeed an

accumulation of R loop-driven rDNA, which one is more detrimental for the cell the nucleoplasmic or nucleolic?

Despite the plethora of questions that still remain to be answered, it is important to highlight that the current study led us to findings of great interest and significance that may contribute to the development of a new therapeutic avenue for SMA treatment. To sum up, we confirmed that the genomic instability observed in SMA is R loop-mediated. We also showed that after utilising a gene therapy approach to resolve R loops by overexpressing SETX, a DNA/RNA helicase not only did we prevent DNA damage in SMA but we also managed to ameliorate the disease phenotype. Finally, we discovered a novel interaction between SMN and RNA polymerase I and a potential new R loop resolution complex in the nucleolus.

8. BIBLIOGRAPHY

Ackermann B, Kröber S, Torres-Benito L, Borgmann A, Peters M, Hosseini Barkooie SM*, et al.* (2013). Plastin 3 ameliorates spinal muscular atrophy via delayed axon pruning and improves neuromuscular junction functionality. *Human Molecular Genetics* **22**(7)**:** 1328-1347.

Acsadi G, Anguelov RA, Yang H, Toth G, Thomas R, Jani A*, et al.* (2002). Increased survival and function of SOD1 mice after glial cell-derived neurotrophic factor gene therapy. *Human gene therapy* **13**(9)**:** 1047-1059.

Aguilera A, Garcia-Muse T (2013). Causes of genome instability. *Annu Rev Genet* **47:** 1-32.

Aguilera A, Garcia-Muse T (2012). R loops: from transcription byproducts to threats to genome stability. *Molecular cell* **46**(2)**:** 115-124.

Ahmad A, Robinson AR, Duensing A, van Drunen E, Beverloo HB, Weisberg DB*, et al.* (2008). ERCC1-XPF endonuclease facilitates DNA double-strand break repair. *Molecular and cellular biology* **28**(16)**:** 5082-5092.

Akten B, Kye MJ, Hao le T, Wertz MH, Singh S, Nie D*, et al.* (2011). Interaction of survival of motor neuron (SMN) and HuD proteins with mRNA cpg15 rescues motor neuron axonal deficits. *Proceedings of the National Academy of Sciences of the United States of America* **108**(25)**:** 10337-10342.

Alagoz M, Chiang SC, Sharma A, El-Khamisy SF (2013). ATM deficiency results in accumulation of DNA-topoisomerase I covalent intermediates in neural cells. *PLoS One* **8**(4)**:** e58239.

Alrafiah A, Karyka E, Coldicott I, K I, Lewis KE, Ning K*, et al.* Plastin 3 promotes motor neuron axonal growth and extends survival in a mouse model of spinal muscular atrophy. *Molecular Therapy - Methods & Clinical Development*.

Anderson AJ, Su JH, Cotman CW (1996). DNA damage and apoptosis in Alzheimer's disease: colocalization with c-Jun immunoreactivity, relationship to brain area, and effect of postmortem delay. *The Journal of neuroscience : the official journal of the Society for Neuroscience* **16**(5)**:** 1710-1719.

Anheim M, Monga B, Fleury M, Charles P, Barbot C, Salih M*, et al.* (2009). Ataxia with oculomotor apraxia type 2: clinical, biological and genotype/phenotype correlation study of a cohort of 90 patients. *Brain : a journal of neurology* **132**(Pt 10)**:** 2688-2698.

Armbruster N, Lattanzi A, Jeavons M, Van Wittenberghe L, Gjata B, Marais T*, et al.* (2016). Efficacy and biodistribution analysis of intracerebroventricular administration of an optimized scAAV9-SMN1 vector in a mouse model of spinal muscular atrophy. *Molecular therapy. Methods & clinical development* **3:** 16060.

Arnold AS, Gueye M, Guettier-Sigrist S, Courdier-Fruh I, Coupin G, Poindron P*, et al.* (2004). Reduced expression of nicotinic AChRs in myotubes from spinal muscular atrophy I patients. *Laboratory investigation; a journal of technical methods and pathology* **84**(10)**:** 1271-1278.

Aronica L, Kasparek T, Ruchman D, Marquez Y, Cipak L, Cipakova I*, et al.* (2016). The spliceosome-associated protein Nrl1 suppresses homologous recombination-dependent R-loop formation in fission yeast. *Nucleic acids research* **44**(4)**:** 1703-1717.

Ashour ME, Atteya R, El-Khamisy SF (2015a). Topoisomerase-mediated chromosomal break repair: an emerging player in many games. *Nature reviews. Cancer* **15**(3)**:** 137-151.

Ashour ME, Atteya R, El-Khamisy SF (2015b). Topoisomerase-mediated chromosomal break repair: an emerging player in many games. . *Nat Rev Cancer* **15**(3)**:** 137–151.

Azqueta A, Slyskova J, Langie SA, O'Neill Gaivao I, Collins A (2014). Comet assay to measure DNA repair: approach and applications. *Frontiers in genetics* **5:** 288.

Azzouz M, Le T, Ralph GS, Walmsley L, Monani UR, Lee DC*, et al.* (2004a). Lentivector-mediated SMN replacement in a mouse model of spinal muscular atrophy. *The Journal of clinical investigation* **114**(12)**:** 1726-1731.

Azzouz M, Ralph GS, Storkebaum E, Walmsley LE, Mitrophanous KA, Kingsman SM*, et al.* (2004b). VEGF delivery with retrogradely transported lentivector prolongs survival in a mouse ALS model. *Nature* **429**(6990)**:** 413-417.

Beattie CE, Carrel TL, McWhorter ML (2007). Fishing for a mechanism: using zebrafish to understand spinal muscular atrophy. *Journal of child neurology* **22**(8)**:** 995-1003.

Bechade C, Rostaing P, Cisterni C, Kalisch R, La Bella V, Pettmann B*, et al.* (1999). Subcellular distribution of survival motor neuron (SMN) protein: possible involvement in nucleocytoplasmic and dendritic transport. *The European journal of neuroscience* **11**(1)**:** 293-304.

Bechara E, Davidovic L, Melko M, Bensaid M, Tremblay S, Grosgeorge J*, et al.* (2007). Fragile X related protein 1 isoforms differentially modulate the affinity of fragile X mental retardation protein for G-quartet RNA structure. *Nucleic acids research* **35**(1)**:** 299-306.

Becherel OJ, Yeo AJ, Stellati A, Heng EY, Luff J, Suraweera AM*, et al.* (2013). Senataxin plays an essential role with DNA damage response proteins in meiotic recombination and gene silencing. *PLoS genetics* **9**(4)**:** e1003435.

Beckerman R, Prives C (2010). Transcriptional regulation by p53. *Cold Spring Harbor perspectives in biology* **2**(8)**:** a000935.

Bender A, Krishnan KJ, Morris CM, Taylor GA, Reeve AK, Perry RH*, et al.* (2006). High levels of mitochondrial DNA deletions in substantia nigra neurons in aging and Parkinson disease. *Nature genetics* **38**(5)**:** 515-517.

Benkhelifa-Ziyyat S, Besse A, Roda M, Duque S, Astord S, Carcenac R*, et al.* (2013). Intramuscular scAAV9-SMN injection mediates widespread gene delivery to the spinal cord and decreases disease severity in SMA mice. *Molecular therapy : the journal of the American Society of Gene Therapy* **21**(2)**:** 282-290.

Bennett CL, La Spada AR (2015). Unwinding the role of senataxin in neurodegeneration. *Discovery medicine* **19**(103)**:** 127-136.

Bertini E, Dessaud E, Mercuri E, Muntoni F, Kirschner J, Reid C*, et al.* (2017). Safety and efficacy of olesoxime in patients with type 2 or non-ambulatory type 3 spinal muscular atrophy: a randomised, double-blind, placebo-controlled phase 2 trial. *The Lancet. Neurology* **16**(7)**:** 513-522.

Bessis N, GarciaCozar FJ, Boissier MC (2004). Immune responses to gene therapy vectors: influence on vector function and effector mechanisms. *Gene therapy* **11:** S10.

Bhagwat N, Olsen AL, Wang AT, Hanada K, Stuckert P, Kanaar R*, et al.* (2009). XPF-ERCC1 Participates in the Fanconi Anemia Pathway of Cross-Link Repair. *Molecular and cellular biology* **29**(24)**:** 6427-6437.

Bhatia V, Barroso SI, Garcia-Rubio ML, Tumini E, Herrera-Moyano E, Aguilera A (2014). BRCA2 prevents R-loop accumulation and associates with TREX-2 mRNA export factor PCID2. *Nature* **511**(7509)**:** 362-365.

Birch JL, Tan BC, Panov KI, Panova TB, Andersen JS, Owen-Hughes TA*, et al.* (2009). FACT facilitates chromatin transcription by RNA polymerases I and III. *EMBO J* **28**(7)**:** 854-865.

Biton S, Barzilai A, Shiloh Y (2008). The neurological phenotype of ataxia-telangiectasia: Solving a persistent puzzle. *DNA repair* **7**(7)**:** 1028-1038.

Boguslawski SJ, Smith DE, Michalak MA, Mickelson KE, Yehle CO, Patterson WL*, et al.* (1986). Characterization of monoclonal antibody to DNA.RNA and its application to immunodetection of hybrids. *Journal of immunological methods* **89**(1)**:** 123-130.

Bohgaki T, Bohgaki M, Hakem R (2010). DNA double-strand break signaling and human disorders. *Genome Integr* **1**(1)**:** 15.

Boisvert FM, van Koningsbruggen S, Navascues J, Lamond AI (2007). The multifunctional nucleolus. *Nature reviews. Molecular cell biology* **8**(7)**:** 574-585.

Bordet T, Berna P, Abitbol JL, Pruss RM (2010). Olesoxime (TRO19622): A Novel Mitochondrial-Targeted Neuroprotective Compound. *Pharmaceuticals* **3**(2)**:** 345-368.

Boulares AH, Yakovlev AG, Ivanova V, Stoica BA, Wang G, Iyer S*, et al.* (1999). Role of Poly(ADP-ribose) Polymerase (PARP) Cleavage in Apoptosis: CASPASE 3-RESISTANT PARP MUTANT INCREASES RATES OF APOPTOSIS IN TRANSFECTED CELLS. *Journal of Biological Chemistry* **274**(33)**:** 22932-22940.

Boulon S, Westman BJ, Hutten S, Boisvert FM, Lamond AI (2010). The nucleolus under stress. *Molecular cell* **40**(2)**:** 216-227.

Brandsma I, van Gent DC (2012). Pathway choice in DNA double strand break repair: observations of a balancing act. *Genome Integrity* **3**(1)**:** 9.

Braun S, Croizat B, Lagrange MC, Warter JM, Poindron P (1995). Constitutive muscular abnormalities in culture in spinal muscular atrophy. *Lancet* **345**(8951)**:** 694-695.

Briese M, Esmaeili B, Fraboulet S, Burt EC, Christodoulou S, Towers PR*, et al.* (2009). Deletion of smn-1, the Caenorhabditis elegans ortholog of the spinal muscular atrophy gene, results in locomotor dysfunction and reduced lifespan. *Human molecular genetics* **18**(1)**:** 97-104.

Burlet P, Huber C, Bertrandy S, Ludosky MA, Zwaenepoel I, Clermont O*, et al.* (1998). The distribution of SMN protein complex in human fetal tissues and its alteration in spinal muscular atrophy. *Human molecular genetics* **7**(12)**:** 1927-1933.

Burma S, Chen BP, Murphy M, Kurimasa A, Chen DJ (2001). ATM Phosphorylates Histone H2AX in Response to DNA Double-strand Breaks. *Journal of Biological Chemistry* **276**(45)**:** 42462-42467.

Burnett BG, Munoz E, Tandon A, Kwon DY, Sumner CJ, Fischbeck KH (2009). Regulation of SMN protein stability. *Molecular and cellular biology* **29**(5)**:** 1107-1115.

Bushnell DA, Cramer P, Kornberg RD (2002). Structural basis of transcription: alpha-amanitin-RNA polymerase II cocrystal at 2.8 A resolution. *Proceedings of the National Academy of Sciences of the United States of America* **99**(3)**:** 1218-1222.

Butler JS, Napierala M (2015). Friedreich's ataxia--a case of aberrant transcription termination? *Transcription* **6**(2)**:** 33-36.

Campuzano V, Montermini L, Molto MD, Pianese L, Cossee M, Cavalcanti F*, et al.* (1996). Friedreich's ataxia: autosomal recessive disease caused by an intronic GAA triplet repeat expansion. *Science* **271**(5254)**:** 1423-1427.

Carrel TL, McWhorter ML, Workman E, Zhang H, Wolstencroft EC, Lorson C*, et al.* (2006). Survival motor neuron function in motor axons is independent of functions required for small nuclear

ribonucleoprotein biogenesis. *The Journal of neuroscience : the official journal of the Society for Neuroscience* **26**(43)**:** 11014-11022.

Carroll J, Page TK, Chiang SC, Kalmar B, Bode D, Greensmith L*, et al.* (2015). Expression of a pathogenic mutation of SOD1 sensitizes aprataxin-deficient cells and mice to oxidative stress and triggers hallmarks of premature ageing. *Human molecular genetics* **24**(3)**:** 828-840.

Cartegni L, Hastings ML, Calarco JA, de Stanchina E, Krainer AR (2006). Determinants of exon 7 splicing in the spinal muscular atrophy genes, SMN1 and SMN2. *American journal of human genetics* **78**(1)**:** 63-77.

Cartegni L, Krainer AR (2002a). Disruption of an SF2/ASF-dependent exonic splicing enhancer in SMN2 causes spinal muscular atrophy in the absence of SMN1. *Nature genetics* **30**(4)**:** 377-384.

Cartegni L, Krainer AR (2002b). Disruption of an SF2/ASF-dependent exonic splicing enhancer in SMN2 causes spinal muscular atrophy in the absence of SMN1. *Nature Genetics* **30:** 377.

Chaitanya GV, Steven AJ, Babu PP (2010). PARP-1 cleavage fragments: signatures of cell-death proteases in neurodegeneration. *Cell communication and signaling : CCS* **8:** 31.

Chan YA, Aristizabal MJ, Lu PY, Luo Z, Hamza A, Kobor MS*, et al.* (2014). Genome-wide profiling of yeast DNA:RNA hybrid prone sites with DRIP-chip. *PLoS genetics* **10**(4)**:** e1004288.

Chapman JR, Jackson SP (2008). Phospho-dependent interactions between NBS1 and MDC1 mediate chromatin retention of the MRN complex at sites of DNA damage. *EMBO reports* **9**(8)**:** 795-801.

Chari A, Paknia E, Fischer U (2009). The role of RNP biogenesis in spinal muscular atrophy. *Current opinion in cell biology* **21**(3)**:** 387-393.

Chen PB, Chen HV, Acharya D, Rando OJ, Fazzio TG (2015). R loops regulate promoter-proximal chromatin architecture and cellular differentiation. *Nature structural & molecular biology* **22**(12)**:** 999-1007.

Chen YZ, Bennett CL, Huynh HM, Blair IP, Puls I, Irobi J*, et al.* (2004). DNA/RNA helicase gene mutations in a form of juvenile amyotrophic lateral sclerosis (ALS4). *American journal of human genetics* **74**(6)**:** 1128-1135.

Cho S, Dreyfuss G (2010). A degron created by SMN2 exon 7 skipping is a principal contributor to spinal muscular atrophy severity. *Genes & development* **24**(5)**:** 438-442.

Coady TH, Lorson CL (2011). SMN in spinal muscular atrophy and snRNP biogenesis. *Wiley interdisciplinary reviews. RNA* **2**(4)**:** 546-564.

Colak D, Zaninovic N, Cohen MS, Rosenwaks Z, Yang WY, Gerhardt J*, et al.* (2014). Promoter-bound trinucleotide repeat mRNA drives epigenetic silencing in fragile X syndrome. *Science* **343**(6174)**:** 1002-1005.

Collins AR (2004). The comet assay for DNA damage and repair: principles, applications, and limitations. *Molecular biotechnology* **26**(3)**:** 249-261.

Coovert DD, Le TT, McAndrew PE, Strasswimmer J, Crawford TO, Mendell JR*, et al.* (1997). The survival motor neuron protein in spinal muscular atrophy. *Human molecular genetics* **6**(8)**:** 1205-1214.

Crow YJ, Leitch A, Hayward BE, Garner A, Parmar R, Griffith E*, et al.* (2006). Mutations in genes encoding ribonuclease H2 subunits cause Aicardi-Goutieres syndrome and mimic congenital viral brain infection. *Nature genetics* **38**(8)**:** 910-916.

D'Amico A, Mercuri E, Tiziano FD, Bertini E (2011). Spinal muscular atrophy. *Orphanet journal of rare diseases* **6:** 71.

Darnell JC, Richter JD (2012). Cytoplasmic RNA-binding proteins and the control of complex brain function. *Cold Spring Harbor perspectives in biology* **4**(8)**:** a012344.

Date H, Onodera O, Tanaka H, Iwabuchi K, Uekawa K, Igarashi S*, et al.* (2001). Early-onset ataxia with ocular motor apraxia and hypoalbuminemia is caused by mutations in a new HIT superfamily gene. *Nature genetics* **29**(2)**:** 184-188.

Davis AJ, Chen DJ (2013). DNA double strand break repair via non-homologous end-joining. *Translational cancer research* **2**(3)**:** 130-143.

de Feraudy S, Revet I, Bezrookove V, Feeney L, Cleaver JE (2010). A minority of foci or pan-nuclear apoptotic staining of γH2AX in the S phase after UV damage contain DNA double-strand breaks. *Proceedings of the National Academy of Sciences* **107**(15)**:** 6870-6875.

de Waard MC, van der Pluijm I, Zuiderveen Borgesius N, Comley LH, Haasdijk ED, Rijksen Y*, et al.* (2010). Age-related motor neuron degeneration in DNA repair-deficient Ercc1 mice. *Acta neuropathologica* **120**(4)**:** 461-475.

Deglon N, Tseng JL, Bensadoun JC, Zurn AD, Arsenijevic Y, Pereira de Almeida L*, et al.* (2000). Self-inactivating lentiviral vectors with enhanced transgene expression as potential gene transfer system in Parkinson's disease. *Human gene therapy* **11**(1)**:** 179-190.

Dexheimer TS (2013). DNA Repair Pathways and Mechanisms. In: Mathews LA, Cabarcas SM, Hurt EM (ed)^(eds). *DNA Repair of Cancer Stem Cells*, edn. Dordrecht: Springer Netherlands. p^pp 19-32.

DiDonato CJ, Chen XN, Noya D, Korenberg JR, Nadeau JH, Simard LR (1997). Cloning, characterization, and copy number of the murine survival motor neuron gene: homolog of the spinal muscular atrophy-determining gene. *Genome research* **7**(4)**:** 339-352.

Dimitriadi M, Hart AC (2010a). Neurodegenerative disorders: insights from the nematode Caenorhabditis elegans. *Neurobiology of disease* **40**(1)**:** 4-11.

Dimitriadi M, Sleigh JN, Walker A, Chang HC, Sen A, Kalloo G*, et al.* (2010b). Conserved genes act as modifiers of invertebrate SMN loss of function defects. *PLoS genetics* **6**(10)**:** e1001172.

Doil C, Mailand N, Bekker-Jensen S, Menard P, Larsen DH, Pepperkok R*, et al.* (2009). RNF168 binds and amplifies ubiquitin conjugates on damaged chromosomes to allow accumulation of repair proteins. *Cell* **136**(3)**:** 435-446.

Dominguez E, Marais T, Chatauret N, Benkhelifa-Ziyyat S, Duque S, Ravassard P*, et al.* (2011). Intravenous scAAV9 delivery of a codon-optimized SMN1 sequence rescues SMA mice. *Human molecular genetics* **20**(4)**:** 681-693.

Dormann D, Haass C (2011). TDP-43 and FUS: a nuclear affair. *Trends in neurosciences* **34**(7)**:** 339-348.

Dubowitz V (1999). Very severe spinal muscular atrophy (SMA type 0): an expanding clinical phenotype. *European journal of paediatric neurology : EJPN : official journal of the European Paediatric Neurology Society* **3**(2)**:** 49-51.

Ebert AD, Svendsen CN (2010). Stem cell model of spinal muscular atrophy. *Archives of neurology* **67**(6)**:** 665-669.

El-Khamisy SF (2011). To live or to die: a matter of processing damaged DNA termini in neurons. *EMBO molecular medicine* **3**(2)**:** 78-88.

El-Khamisy SF, Saifi GM, Weinfeld M, Johansson F, Helleday T, Lupski JR*, et al.* (2005a). Defective DNA single-strand break repair in spinocerebellar ataxia with axonal neuropathy-1. *Nature* **434**(7029)**:** 108-113.

El-Khamisy SF, Saifi GM, Weinfeld M, Johansson F, Helleday T, Lupski JR*, et al.* (2005b). Defective DNA single-strand break repair in spinocerebellar ataxia with axonal neuropathy-1. *Nature* **434**(7029)**:** 108-113.

El Hage A, French SL, Beyer AL, Tollervey D (2010). Loss of Topoisomerase I leads to R-loop-mediated transcriptional blocks during ribosomal RNA synthesis. *Genes Dev* **24**(14)**:** 1546-1558.

Falck J, Coates J, Jackson SP (2005). Conserved modes of recruitment of ATM, ATR and DNA-PKcs to sites of DNA damage. *Nature* **434**(7033)**:** 605-611.

Fallini C, Donlin-Asp PG, Rouanet JP, Bassell GJ, Rossoll W (2016). Deficiency of the Survival of Motor Neuron Protein Impairs mRNA Localization and Local Translation in the Growth Cone of Motor Neurons. *The Journal of neuroscience : the official journal of the Society for Neuroscience* **36**(13)**:** 3811-3820.

Fallini C, Rouanet JP, Donlin-Asp PG, Guo P, Zhang H, Singer RH*, et al.* (2014). Dynamics of survival of motor neuron (SMN) protein interaction with the mRNA-binding protein IMP1 facilitates its trafficking into motor neuron axons. *Developmental neurobiology* **74**(3)**:** 319-332.

Fallini C, Zhang H, Su Y, Silani V, Singer RH, Rossoll W*, et al.* (2011). The survival of motor neuron (SMN) protein interacts with the mRNA-binding protein HuD and regulates localization of poly(A) mRNA in primary motor neuron axons. *The Journal of neuroscience : the official journal of the Society for Neuroscience* **31**(10)**:** 3914-3925.

Fayzullina S, Martin LJ (2016). DNA Damage Response and DNA Repair in Skeletal Myocytes From a Mouse Model of Spinal Muscular Atrophy. *Journal of neuropathology and experimental neurology* **75**(9)**:** 889-902.

Fayzullina S, Martin LJ (2014). Skeletal muscle DNA damage precedes spinal motor neuron DNA damage in a mouse model of Spinal Muscular Atrophy (SMA). *PLoS One* **9**(3)**:** e93329.

Feric M, Vaidya N, Harmon TS, Mitrea DM, Zhu L, Richardson TM*, et al.* (2016). Coexisting Liquid Phases Underlie Nucleolar Subcompartments. *Cell* **165**(7)**:** 1686-1697.

Foust KD, Nurre E, Montgomery CL, Hernandez A, Chan CM, Kaspar BK (2009). Intravascular AAV9 preferentially targets neonatal neurons and adult astrocytes. *Nature biotechnology* **27**(1)**:** 59-65.

Foust KD, Wang X, McGovern VL, Braun L, Bevan AK, Haidet AM*, et al.* (2010). Rescue of the spinal muscular atrophy phenotype in a mouse model by early postnatal delivery of SMN. *Nature biotechnology* **28**(3)**:** 271-274.

Fukita Y, Mizuta TR, Shirozu M, Ozawa K, Shimizu A, Honjo T (1993). The human S mu bp-2, a DNA-binding protein specific to the single-stranded guanine-rich sequence related to the immunoglobulin mu chain switch region. *The Journal of biological chemistry* **268**(23)**:** 17463-17470.

Ginno PA, Lim YW, Lott PL, Korf I, Chedin F (2013). GC skew at the 5' and 3' ends of human genes links R-loop formation to epigenetic regulation and transcription termination. *Genome research* **23**(10)**:** 1590-1600.

Glascock JJ, Shababi M, Wetz MJ, Krogman MM, Lorson CL (2012). Direct central nervous system delivery provides enhanced protection following vector mediated gene replacement in a severe model of spinal muscular atrophy. *Biochemical and biophysical research communications* **417**(1)**:** 376-381.

Gombash SE, Cowley CJ, Fitzgerald JA, Iyer CC, Fried D, McGovern VL*, et al.* (2015). SMN deficiency disrupts gastrointestinal and enteric nervous system function in mice. *Human molecular genetics* **24**(13)**:** 3847-3860.

Grabczyk E, Mancuso M, Sammarco MC (2007). A persistent RNA.DNA hybrid formed by transcription of the Friedreich ataxia triplet repeat in live bacteria, and by T7 RNAP in vitro. *Nucleic acids research* **35**(16)**:** 5351-5359.

Grieger JC, Samulski RJ (2005). Packaging capacity of adeno-associated virus serotypes: impact of larger genomes on infectivity and postentry steps. *Journal of virology* **79**(15)**:** 9933-9944.

Grishin NV (1998). The R3H motif: a domain that binds single-stranded nucleic acids. *Trends in biochemical sciences* **23**(9)**:** 329-330.

Groh M, Albulescu LO, Cristini A, Gromak N (2016). Senataxin: Genome Guardian at the Interface of Transcription and Neurodegeneration. *Journal of molecular biology*.

Groh M, Gromak N (2014). Out of balance: R-loops in human disease. *PLoS genetics* **10**(9)**:** e1004630.

Grohmann K, Schuelke M, Diers A, Hoffmann K, Lucke B, Adams C*, et al.* (2001). Mutations in the gene encoding immunoglobulin mu-binding protein 2 cause spinal muscular atrophy with respiratory distress type 1. *Nature genetics* **29**(1)**:** 75-77.

Grzenda A, Lomberk G, Zhang JS, Urrutia R (2009). Sin3: master scaffold and transcriptional corepressor. *Biochimica et biophysica acta* **1789**(6-8)**:** 443-450.

Guil S, Long JC, Caceres JF (2006). hnRNP A1 relocalization to the stress granules reflects a role in the stress response. *Molecular and cellular biology* **26**(15)**:** 5744-5758.

Hache M, Swoboda KJ, Sethna N, Farrow-Gillespie A, Khandji A, Xia S*, et al.* (2016). Intrathecal Injections in Children With Spinal Muscular Atrophy: Nusinersen Clinical Trial Experience. *Journal of child neurology* **31**(7)**:** 899-906.

Haeusler AR, Donnelly CJ, Periz G, Simko EA, Shaw PG, Kim MS*, et al.* (2014). C9orf72 nucleotide repeat structures initiate molecular cascades of disease. *Nature* **507**(7491)**:** 195-200.

Hagerman RJ, Hagerman P (2016). Fragile X-associated tremor/ataxia syndrome - features, mechanisms and management. *Nature reviews. Neurology* **12**(7)**:** 403-412.

Hamilton G, Gillingwater TH (2013). Spinal muscular atrophy: going beyond the motor neuron. *Trends in molecular medicine* **19**(1)**:** 40-50.

Hamperl S, Cimprich KA (2014). The contribution of co-transcriptional RNA:DNA hybrid structures to DNA damage and genome instability. *DNA repair* **19:** 84-94.

Hannan KM, Sanij E, Rothblum LI, Hannan RD, Pearson RB (2013). Dysregulation of RNA polymerase I transcription during disease. *Biochimica et biophysica acta* **1829**(3-4)**:** 342-360.

Hao le T, Burghes AH, Beattie CE (2011). Generation and Characterization of a genetic zebrafish model of SMA carrying the human SMN2 gene. *Molecular neurodegeneration* **6**(1)**:** 24.

Hao le T, Wolman M, Granato M, Beattie CE (2012). Survival motor neuron affects plastin 3 protein levels leading to motor defects. *The Journal of neuroscience : the official journal of the Society for Neuroscience* **32**(15)**:** 5074-5084.

Harding SM, Boiarsky JA, Greenberg RA (2015). ATM Dependent Silencing Links Nucleolar Chromatin Reorganization to DNA Damage Recognition. *Cell reports* **13**(2)**:** 251-259.

Hart MP, Gitler AD (2012). ALS-associated ataxin 2 polyQ expansions enhance stress-induced caspase 3 activation and increase TDP-43 pathological modifications. *The Journal of neuroscience : the official journal of the Society for Neuroscience* **32**(27)**:** 9133-9142.

Hatchi E, Skourti-Stathaki K, Ventz S, Pinello L, Yen A, Kamieniarz-Gdula K*, et al.* (2015). BRCA1 recruitment to transcriptional pause sites is required for R-loop-driven DNA damage repair. *Molecular cell* **57**(4)**:** 636-647.

Hebert MD, Szymczyk PW, Shpargel KB, Matera AG (2001). Coilin forms the bridge between Cajal bodies and SMN, the spinal muscular atrophy protein. *Genes Dev* **15**(20)**:** 2720-2729.

Heiss NS, Knight SW, Vulliamy TJ, Klauck SM, Wiemann S, Mason PJ*, et al.* (1998). X-linked dyskeratosis congenita is caused by mutations in a highly conserved gene with putative nucleolar functions. *Nature genetics* **19**(1)**:** 32-38.

Helleday T, Lo J, van Gent DC, Engelward BP (2007). DNA double-strand break repair: from mechanistic understanding to cancer treatment. *DNA repair* **6**(7)**:** 923-935.

Herrera-Moyano E, Mergui X, Garcia-Rubio ML, Barroso S, Aguilera A (2014). The yeast and human FACT chromatin-reorganizing complexes solve R-loop-mediated transcription-replication conflicts. *Genes Dev* **28**(7)**:** 735-748.

Hetman M, Pietrzak M (2012). Emerging roles of the neuronal nucleolus. *Trends in neurosciences* **35**(5)**:** 305-314.

Hill SJ, Mordes DA, Cameron LA, Neuberg DS, Landini S, Eggan K*, et al.* (2016a). Two familial ALS proteins function in prevention/repair of transcription-associated DNA damage. *Proceedings of the National Academy of Sciences of the United States of America* **113**(48)**:** E7701-E7709.

Hill SJ, Mordes DA, Cameron LA, Neuberg DS, Landini S, Eggan K*, et al.* (2016b). Two familial ALS proteins function in prevention/repair of transcription-associated DNA damage. *Proceedings of the National Academy of Sciences* **113**(48)**:** E7701-E7709.

Ho S-Y, Chao C-Y, Huang H-L, Chiu T-W, Charoenkwan P, Hwang E (2011). NeurphologyJ: An automatic neuronal morphology quantification method and its application in pharmacological discovery. *BMC Bioinformatics*

12: 230.

Hoeijmakers JH (2009). DNA damage, aging, and cancer. *The New England journal of medicine* **361**(15)**:** 1475-1485.

Hoem G, Raske CR, Garcia-Arocena D, Tassone F, Sanchez E, Ludwig AL*, et al.* (2011). CGG-repeat length threshold for FMR1 RNA pathogenesis in a cellular model for FXTAS. *Human molecular genetics* **20**(11)**:** 2161-2170.

Houtsmuller AB, Rademakers S, Nigg AL, Hoogstraten D, Hoeijmakers JH, Vermeulen W (1999). Action of DNA repair endonuclease ERCC1/XPF in living cells. *Science* **284**(5416)**:** 958-961.

Hsieh-Li HM, Chang JG, Jong YJ, Wu MH, Wang NM, Tsai CH*, et al.* (2000). A mouse model for spinal muscular atrophy. *Nature genetics* **24**(1)**:** 66-70.

Hua Y, Zhou J (2004). Survival motor neuron protein facilitates assembly of stress granules. *FEBS Lett* **572**(1-3)**:** 69-74.

Huang LC, Clarkin KC, Wahl GM (1996). Sensitivity and selectivity of the DNA damage sensor responsible for activating p53-dependent G1 arrest. *Proceedings of the National Academy of Sciences of the United States of America* **93**(10)**:** 4827-4832.

Hubers L, Valderrama-Carvajal H, Laframboise J, Timbers J, Sanchez G, Cote J (2011). HuD interacts with survival motor neuron protein and can rescue spinal muscular atrophy-like neuronal defects. *Human molecular genetics* **20**(3)**:** 553-579.

Hudson JJ, Chiang SC, Wells OS, Rookyard C, El-Khamisy SF (2012). SUMO modification of the neuroprotective protein TDP1 facilitates chromosomal single-strand break repair. *Nature communications* **3:** 733.

Huertas P, Aguilera A (2003). Cotranscriptionally formed DNA:RNA hybrids mediate transcription elongation impairment and transcription-associated recombination. *Molecular cell* **12**(3)**:** 711-721.

Hwee DT, Kennedy AR, Hartman JJ, Ryans J, Durham N, Malik FI*, et al.* (2015). The small-molecule fast skeletal troponin activator, CK-2127107, improves exercise tolerance in a rat model of heart failure. *The Journal of pharmacology and experimental therapeutics* **353**(1)**:** 159-168.

Iacono D, O'Brien R, Resnick SM, Zonderman AB, Pletnikova O, Rudow G*, et al.* (2008). Neuronal hypertrophy in asymptomatic Alzheimer disease. *Journal of neuropathology and experimental neurology* **67**(6)**:** 578-589.

Imlach Wendy L, Beck Erin S, Choi Ben J, Lotti F, Pellizzoni L, McCabe Brian D (2012). SMN Is Required for Sensory-Motor Circuit Function in Drosophila. *Cell* **151**(2)**:** 427-439.

Isaac C, Marsh KL, Paznekas WA, Dixon J, Dixon MJ, Jabs EW*, et al.* (2000). Characterization of the nucleolar gene product, treacle, in Treacher Collins syndrome. *Molecular biology of the cell* **11**(9)**:** 3061-3071.

Iwahashi CK, Yasui DH, An HJ, Greco CM, Tassone F, Nannen K*, et al.* (2006). Protein composition of the intranuclear inclusions of FXTAS. *Brain : a journal of neurology* **129**(Pt 1)**:** 256-271.

Iyama T, Wilson DM, 3rd (2013). DNA repair mechanisms in dividing and non-dividing cells. *DNA repair* **12**(8)**:** 620-636.

Jackson SP, Bartek J (2009). The DNA-damage response in human biology and disease. *Nature* **461**(7267)**:** 1071-1078.

James A, Wang Y, Raje H, Rosby R, DiMario P (2014). Nucleolar stress with and without p53. *Nucleus* **5**(5)**:** 402-426.

Jangi M, Fleet C, Cullen P, Gupta SV, Mekhoubad S, Chiao E*, et al.* (2017). SMN deficiency in severe models of spinal muscular atrophy causes widespread intron retention and DNA damage. *Proceedings of the National Academy of Sciences of the United States of America* **114**(12)**:** E2347-E2356.

Jeppesen DK, Bohr VA, Stevnsner T (2011). DNA repair deficiency in neurodegeneration. *Progress in neurobiology* **94**(2)**:** 166-200.

Johnson FB, Marciniak RA, Guarente L (1998). Telomeres, the nucleolus and aging. *Current opinion in cell biology* **10**(3)**:** 332-338.

Jones KW, Gorzynski K, Hales CM, Fischer U, Badbanchi F, Terns RM*, et al.* (2001). Direct Interaction of the Spinal Muscular Atrophy Disease Protein SMN with the Small Nucleolar RNA-associated Protein Fibrillarin. *Journal of Biological Chemistry* **276**(42)**:** 38645-38651.

Kaifer KA, Villalon E, Osman EY, Glascock JJ, Arnold LL, Cornelison DD*, et al.* (2017). Plastin-3 extends survival and reduces severity in mouse models of spinal muscular atrophy. *JCI insight* **2**(5)**:** e89970.

Kashima T, Manley JL (2003). A negative element in SMN2 exon 7 inhibits splicing in spinal muscular atrophy. *Nature Genetics* **34:** 460.

Katagiri K, Matsuzawa A, Ichijo H (2010). Regulation of apoptosis signal-regulating kinase 1 in redox signaling. *Methods in enzymology* **474:** 277-288.

Katyal S, Lee Y, Nitiss KC, Downing SM, Li Y, Shimada M*, et al.* (2014a). Aberrant topoisomerase-1 DNA lesions are pathogenic in neurodegenerative genome instability syndromes. *Nature Neuroscience* **17**(6)**:** 813–821.

Katyal S, Lee Y, Nitiss KC, Downing SM, Li Y, Shimada M*, et al.* (2014b). Aberrant topoisomerase-1 DNA lesions are pathogenic in neurodegenerative genome instability syndromes. *Nature neuroscience* **17**(6)**:** 813-821.

Kawauchi J, Mischo H, Braglia P, Rondon A, Proudfoot NJ (2008). Budding yeast RNA polymerases I and II employ parallel mechanisms of transcriptional termination. *Genes Dev* **22**(8)**:** 1082-1092.

Kedersha N, Cho MR, Li W, Yacono PW, Chen S, Gilks N*, et al.* (2000). Dynamic shuttling of TIA-1 accompanies the recruitment of mRNA to mammalian stress granules. *The Journal of cell biology* **151**(6)**:** 1257-1268.

Kedersha NL, Gupta M, Li W, Miller I, Anderson P (1999). RNA-binding proteins TIA-1 and TIAR link the phosphorylation of eIF-2 alpha to the assembly of mammalian stress granules. *The Journal of cell biology* **147**(7)**:** 1431-1442.

Keskin H, Shen Y, Huang F, Patel M, Yang T, Ashley K*, et al.* (2014). Transcript-RNA-templated DNA recombination and repair. *Nature* **515**(7527)**:** 436-439.

Kim N, Jinks-Robertson S (2012). Transcription as a source of genome instability. *Nature reviews. Genetics* **13**(3)**:** 204-214.

Kimball SR, Horetsky RL, Ron D, Jefferson LS, Harding HP (2003). Mammalian stress granules represent sites of accumulation of stalled translation initiation complexes. *American journal of physiology. Cell physiology* **284**(2)**:** C273-284.

Krichevsky AM, Kosik KS (2001). Neuronal RNA granules: a link between RNA localization and stimulation-dependent translation. *Neuron* **32**(4)**:** 683-696.

Kruhlak M, Crouch EE, Orlov M, Montano C, Gorski SA, Nussenzweig A*, et al.* (2007). The ATM repair pathway inhibits RNA polymerase I transcription in response to chromosome breaks. *Nature* **447**(7145)**:** 730-734.

Kruman, II, Wersto RP, Cardozo-Pelaez F, Smilenov L, Chan SL, Chrest FJ*, et al.* (2004). Cell cycle activation linked to neuronal cell death initiated by DNA damage. *Neuron* **41**(4)**:** 549-561.

Lam YW, Lyon CE, Lamond AI (2002). Large-Scale Isolation of Cajal Bodies from HeLa Cells. *Molecular Biology of the Cell* **13**(7)**:** 2461-2473.

Lavin MF, Delia D, Chessa L (2006). ATM and the DNA damage response. Workshop on ataxia-telangiectasia and related syndromes. *EMBO reports* **7**(2)**:** 154-160.

Le TT, Pham LT, Butchbach ME, Zhang HL, Monani UR, Coovert DD*, et al.* (2005). SMNDelta7, the major product of the centromeric survival motor neuron (SMN2) gene, extends survival in mice with spinal muscular atrophy and associates with full-length SMN. *Human molecular genetics* **14**(6)**:** 845-857.

Lee J, Hampl M, Albert P, Fine HA (2002). Antitumor activity and prolonged expression from a TRAIL-expressing adenoviral vector. *Neoplasia* **4**(4)**:** 312-323.

Lee J, Hwang YJ, Ryu H, Kowall NW, Ryu H (2014). Nucleolar dysfunction in Huntington's disease. *Biochimica et biophysica acta* **1842**(6)**:** 785-790.

Lee S, Sayin A, Cauchi RJ, Grice S, Burdett H, Baban D*, et al.* (2008). Genome-wide expression analysis of a spinal muscular atrophy model: towards discovery of new drug targets. *PloS one* **3**(1)**:** e1404.

Lee Y, McKinnon PJ (2007). Responding to DNA double strand breaks in the nervous system. *Neuroscience* **145**(4)**:** 1365-1374.

Lees-Miller SP, Meek K (2003). Repair of DNA double strand breaks by non-homologous end joining. *Biochimie* **85**(11)**:** 1161-1173.

Lefebvre S, Burglen L, Reboullet S, Clermont O, Burlet P, Viollet L*, et al.* (1995). Identification and characterization of a spinal muscular atrophy-determining gene. *Cell* **80**(1)**:** 155-165.

Leist M, Jaattela M (2001). Four deaths and a funeral: from caspases to alternative mechanisms. *Nature reviews. Molecular cell biology* **2**(8)**:** 589-598.

Li H, Custer SK, Gilson T, Hao le T, Beattie CE, Androphy EJ (2015). alpha-COP binding to the survival motor neuron protein SMN is required for neuronal process outgrowth. *Hum Mol Genet* **24**(25)**:** 7295-7307.

Li X, Manley JL (2005). Inactivation of the SR protein splicing factor ASF/SF2 results in genomic instability. *Cell* **122**(3)**:** 365-378.

Li X, Niu T, Manley JL (2007). The RNA binding protein RNPS1 alleviates ASF/SF2 depletion-induced genomic instability. *Rna* **13**(12)**:** 2108-2115.

Lieber MR, Ma Y, Pannicke U, Schwarz K (2003). Mechanism and regulation of human non-homologous DNA end-joining. *Nature reviews. Molecular cell biology* **4**(9)**:** 712-720.

Liu-Yesucevitz L, Bilgutay A, Zhang YJ, Vanderweyde T, Citro A, Mehta T*, et al.* (2010). Tar DNA binding protein-43 (TDP-43) associates with stress granules: analysis of cultured cells and pathological brain tissue. *PLoS One* **5**(10)**:** e13250.

Liu Q, Dreyfuss G (1996). A novel nuclear structure containing the survival of motor neurons protein. *EMBO J* **15**(14)**:** 3555-3565.

Lombrana R, Almeida R, Alvarez A, Gomez M (2015). R-loops and initiation of DNA replication in human cells: a missing link? *Frontiers in genetics* **6:** 158.

Loomis EW, Sanz LA, Chedin F, Hagerman PJ (2014). Transcription-associated R-loop formation across the human FMR1 CGG-repeat region. *PLoS genetics* **10**(4)**:** e1004294.

Lorson CL, Androphy EJ (1998). The Domain Encoded by Exon 2 of the Survival Motor Neuron Protein Mediates Nucleic Acid Binding. *Human molecular genetics* **7**(8)**:** 1269-1275.

Lorson CL, Hahnen E, Androphy EJ, Wirth B (1999). A single nucleotide in the SMN gene regulates splicing and is responsible for spinal muscular atrophy. *Proceedings of the National Academy of Sciences of the United States of America* **96**(11)**:** 6307-6311.

Lotti F, Imlach WL, Saieva L, Beck ES, Hao le T, Li DK*, et al.* (2012). An SMN-dependent U12 splicing event essential for motor circuit function. *Cell* **151**(2)**:** 440-454.

Lovell MA, Markesbery WR (2007). Oxidative DNA damage in mild cognitive impairment and late-stage Alzheimer's disease. *Nucleic acids research* **35**(22)**:** 7497-7504.

Lu T, Pan Y, Kao SY, Li C, Kohane I, Chan J*, et al.* (2004). Gene regulation and DNA damage in the ageing human brain. *Nature* **429**(6994)**:** 883-891.

Lunke S, El-Osta A (2013). Applicability of Histone Deacetylase Inhibition for the Treatment of Spinal Muscular Atrophy. *Neurotherapeutics : the journal of the American Society for Experimental NeuroTherapeutics*.

Machyna M, Heyn P, Neugebauer KM (2013). Cajal bodies: where form meets function. *Wiley interdisciplinary reviews. RNA* **4**(1)**:** 17-34.

Madabhushi R, Pan L, Tsai LH (2014). DNA damage and its links to neurodegeneration. *Neuron* **83**(2)**:** 266-282.

Mailand N, Bekker-Jensen S, Faustrup H, Melander F, Bartek J, Lukas C*, et al.* (2007). RNF8 ubiquitylates histones at DNA double-strand breaks and promotes assembly of repair proteins. *Cell* **131**(5)**:** 887-900.

Makarov EM, Owen N, Bottrill A, Makarova OV (2012). Functional mammalian spliceosomal complex E contains SMN complex proteins in addition to U1 and U2 snRNPs. *Nucleic acids research* **40**(6)**:** 2639-2652.

Marciniak RA, Lombard DB, Johnson FB, Guarente L (1998). Nucleolar localization of the Werner syndrome protein in human cells. *Proceedings of the National Academy of Sciences of the United States of America* **95**(12)**:** 6887-6892.

Marinello J, Bertoncini S, Aloisi I, Cristini A, Malagoli Tagliazucchi G, Forcato M*, et al.* (2016). Dynamic Effects of Topoisomerase I Inhibition on R-Loops and Short Transcripts at Active Promoters. *PLoS One* **11**(1)**:** e0147053.

Marinello J, Chillemi G, Bueno S, Manzo SG, Capranico G (2013). Antisense transcripts enhanced by camptothecin at divergent CpG-island promoters associated with bursts of topoisomerase I-DNA cleavage complex and R-loop formation. *Nucleic acids research* **41**(22)**:** 10110-10123.

Markowitz JA, Singh P, Darras BT (2012). Spinal muscular atrophy: a clinical and research update. *Pediatric neurology* **46**(1)**:** 1-12.

Martinez-Hernandez R, Soler-Botija C, Also E, Alias L, Caselles L, Gich I*, et al.* (2009). The developmental pattern of myotubes in spinal muscular atrophy indicates prenatal delay of muscle maturation. *Journal of neuropathology and experimental neurology* **68**(5)**:** 474-481.

Marvizon JC, McRoberts JA, Ennes HS, Song B, Wang X, Jinton L*, et al.* (2002). Two N-methyl-D-aspartate receptors in rat dorsal root ganglia with different subunit composition and localization. *The Journal of comparative neurology* **446**(4)**:** 325-341.

Matera AG, Frey MR (1998). Coiled bodies and gems: Janus or gemini? *American journal of human genetics* **63**(2)**:** 317-321.

McCarty DM (2008). Self-complementary AAV Vectors; Advances and Applications. *Molecular Therapy* **16**(10)**:** 1648-1656.

McGivern JV, Patitucci TN, Nord JA, Barabas MA, Stucky CL, Ebert AD (2013). Spinal muscular atrophy astrocytes exhibit abnormal calcium regulation and reduced growth factor production. *Glia* **61**(9)**:** 1418-1428.

McKinnon PJ (2009). DNA repair deficiency and neurological disease. *Nat Rev Neurosci* **10**(2)**:** 100-112.

McWhorter ML, Monani UR, Burghes AH, Beattie CE (2003). Knockdown of the survival motor neuron (Smn) protein in zebrafish causes defects in motor axon outgrowth and pathfinding. *The Journal of cell biology* **162**(5)**:** 919-931.

Meisenberg C, Ashour ME, El-Shafie L, Liao C, Hodgson A, Pilborough A*, et al.* (2016). Epigenetic changes in histone acetylation underpin resistance to the topoisomerase I inhibitor irinotecan. *Nucleic Acids Research* **pii: gkw1026**.

Melese T, Xue Z (1995). The nucleolus: an organelle formed by the act of building a ribosome. *Current opinion in cell biology* **7**(3)**:** 319-324.

Mendell J, Al-Zaidy SA, Shell R, Arnold WD, Rodino-Klapac LR, Prior TW*, et al.* (2017). AVXS-101 Phase 1 Gene Therapy Clinical Trial in SMA Type 1: Event Free Survival and Achievement of developmental milestones (CT.003). *Neurology* **88**(16 Supplement).

Mentis GZ, Blivis D, Liu W, Drobac E, Crowder ME, Kong L*, et al.* (2011). Early functional impairment of sensory-motor connectivity in a mouse model of spinal muscular atrophy. *Neuron* **69**(3)**:** 453-467.

Mercuri E, Finkel R, Montes J, Mazzone ES, Sormani MP, Main M*, et al.* (2016). Patterns of disease progression in type 2 and 3 SMA: Implications for clinical trials. *Neuromuscular disorders : NMD* **26**(2)**:** 126-131.

Meyer K, Ferraiuolo L, Schmelzer L, Braun L, McGovern V, Likhite S*, et al.* (2015). Improving single injection CSF delivery of AAV9-mediated gene therapy for SMA: a dose-response study in mice and nonhuman primates. *Molecular therapy : the journal of the American Society of Gene Therapy* **23**(3)**:** 477-487.

Miguel-Aliaga I, Culetto E, Walker DS, Baylis HA, Sattelle DB, Davies KE (1999). The Caenorhabditis Elegans Orthologue of the Human Gene Responsible for Spinal Muscular Atrophy Is a Maternal Product Critical for Germline Maturation and Embryonic Viability. *Human molecular genetics* **8**(12)**:** 2133-2143.

Millecamps S, Mallet J, Barkats M (2002). Adenoviral retrograde gene transfer in motoneurons is greatly enhanced by prior intramuscular inoculation with botulinum toxin. *Human gene therapy* **13**(2)**:** 225-232.

Mirra A, Rossi S, Scaricamazza S, Di Salvio M, Salvatori I, Valle C*, et al.* (2017). Functional interaction between FUS and SMN underlies SMA-like splicing changes in wild-type hFUS mice. *Scientific reports* **7**(1)**:** 2033.

Mischo HE, Gomez-Gonzalez B, Grzechnik P, Rondon AG, Wei W, Steinmetz L*, et al.* (2011). Yeast Sen1 helicase protects the genome from transcription-associated instability. *Molecular cell* **41**(1)**:** 21-32.

Mizuta TR, Fukita Y, Miyoshi T, Shimizu A, Honjo T (1993). Isolation of cDNA encoding a binding protein specific to 5'-phosphorylated single-stranded DNA with G-rich sequences. *Nucleic acids research* **21**(8)**:** 1761-1766.

Modesti M, Kanaar R (2001). DNA repair: spot(light)s on chromatin. *Current biology : CB* **11**(6)**:** R229-232.

Monahan Z, Shewmaker F, Pandey UB (2016). Stress granules at the intersection of autophagy and ALS. *Brain Res* **1649**(Pt B)**:** 189-200.

Monani UR, Coovert DD, Burghes AH (2000). Animal models of spinal muscular atrophy. *Human molecular genetics* **9**(16)**:** 2451-2457.

Montanaro L, Trere D, Derenzini M (2008). Nucleolus, ribosomes, and cancer. *The American journal of pathology* **173**(2)**:** 301-310.

Moreira MC, Klur S, Watanabe M, Nemeth AH, Le Ber I, Moniz JC*, et al.* (2004). Senataxin, the ortholog of a yeast RNA helicase, is mutant in ataxia-ocular apraxia 2. *Nature genetics* **36**(3)**:** 225-227.

Munoz MJ, de la Mata M, Kornblihtt AR (2010). The carboxy terminal domain of RNA polymerase II and alternative splicing. *Trends in biochemical sciences* **35**(9)**:** 497-504.

Murray LM, Comley LH, Thomson D, Parkinson N, Talbot K, Gillingwater TH (2008). Selective vulnerability of motor neurons and dissociation of pre- and post-synaptic pathology at the neuromuscular junction in mouse model of spinal muscular atrophy. *Human Molecular Genetics* **7**(17)**:** 949-962. .

Nash LA, Burns JK, Chardon JW, Kothary R, Parks RJ (2016). Spinal Muscular Atrophy: More than a Disease of Motor Neurons? *Current molecular medicine* **16**(9)**:** 779-792.

Ning K, Drepper C, Valori CF, Ahsan M, Wyles M, Higginbottom A*, et al.* (2010a). PTEN depletion rescues axonal growth defect and improve survival in SMN-deficient motor neurons *Hum Mol Genet. 2010* **19**(16)**:** 159-168.

Ning K, Drepper C, Valori CF, Ahsan M, Wyles M, Higginbottom A*, et al.* (2010b). PTEN depletion rescues axonal growth defect and improves survival in SMN-deficient motor neurons. *Human molecular genetics* **19**(16)**:** 3159-3168.

Ogino S, Leonard DG, Rennert H, Ewens WJ, Wilson RB (2002). Genetic risk assessment in carrier testing for spinal muscular atrophy. *American journal of medical genetics* **110**(4)**:** 301-307.

Olive PL, Banath JP (2006). The comet assay: a method to measure DNA damage in individual cells. *Nature protocols* **1**(1)**:** 23-29.

Olson MO (2004). Sensing cellular stress: another new function for the nucleolus? *Science's STKE : signal transduction knowledge environment* **2004**(224)**:** pe10.

Olson MO, Hingorani K, Szebeni A (2002). Conventional and nonconventional roles of the nucleolus. *International review of cytology* **219:** 199-266.

Oprea GE, Krober S, McWhorter ML, Rossoll W, Muller S, Krawczak M*, et al.* (2008). Plastin 3 is a protective modifier of autosomal recessive spinal muscular atrophy. *Science* **320**(5875)**:** 524-527.

Pagliardini S, Giavazzi A, Setola V, Lizier C, Di Luca M, DeBiasi S*, et al.* (2000). Subcellular localization and axonal transport of the survival motor neuron (SMN) protein in the developing rat spinal cord. *Human molecular genetics* **9**(1)**:** 47-56.

Parlato R, Liss B (2014). How Parkinson's disease meets nucleolar stress. *Biochimica et biophysica acta* **1842**(6)**:** 791-797.

Passini MA, Bu J, Richards AM, Kinnecom C, Sardi SP, Stanek LM*, et al.* (2011). Antisense oligonucleotides delivered to the mouse CNS ameliorate symptoms of severe spinal muscular atrophy. *Science translational medicine* **3**(72)**:** 72ra18.

Paulsen RD, Soni DV, Wollman R, Hahn AT, Yee MC, Guan A*, et al.* (2009). A genome-wide siRNA screen reveals diverse cellular processes and pathways that mediate genome stability. *Molecular cell* **35**(2)**:** 228-239.

Pederson T, Tsai RY (2009). In search of nonribosomal nucleolar protein function and regulation. *The Journal of cell biology* **184**(6)**:** 771-776.

Pedrotti S, Bielli P, Paronetto MP, Ciccosanti F, Fimia GM, Stamm S*, et al.* (2010). The splicing regulator Sam68 binds to a novel exonic splicing silencer and functions in SMN2 alternative splicing in spinal muscular atrophy. *The EMBO journal* **29**(7)**:** 1235-1247.

Pellizzoni L, Charroux B, Rappsilber J, Mann M, Dreyfuss G (2001). A functional interaction between the survival motor neuron complex and RNA polymerase II. *The Journal of cell biology* **152**(1)**:** 75-85.

Pestov DG, Lapik YR, Lau LF (2008). Assays for ribosomal RNA processing and ribosome assembly. *Current protocols in cell biology* **Chapter 22:** Unit 22 11.

Peter CJ, Evans M, Thayanithy V, Taniguchi-Ishigaki N, Bach I, Kolpak A*, et al.* (2011). The COPI vesicle complex binds and moves with survival motor neuron within axons. *Hum Mol Genet* **20**(9)**:** 1701-1711.

Poole AR, Hebert MD (2016). SMN and coilin negatively regulate dyskerin association with telomerase RNA. *Biology open* **5**(6)**:** 726-735.

Powis RA, Karyka E, Boyd P, Come J, Jones RA, Zheng Y*, et al.* (2016a). Systemic restoration of UBA1 ameliorates disease in spinal muscular atrophy. *JCI insight* **1**(11)**:** e87908.

Powis RA, Karyka E, P. B, Côme J, Jones RA, Zheng Y*, et al.* (2016b). Systemic restoration of UBA1 ameliorates disease in spinal muscular atrophy. *JCI Insight* **1**(11)**:** e87908.

Prior TW, Snyder PJ, Rink BD, Pearl DK, Pyatt RE, Mihal DC*, et al.* (2010). Newborn and carrier screening for spinal muscular atrophy. *American journal of medical genetics. Part A* **152A**(7)**:** 1608-1616.

Proudfoot NJ (2016). Transcriptional termination in mammals: Stopping the RNA polymerase II juggernaut. *Science* **352**(6291)**:** aad9926.

Qiu H, Lee S, Shang Y, Wang WY, Au KF, Kamiya S*, et al.* (2014). ALS-associated mutation FUS-R521C causes DNA damage and RNA splicing defects. *The Journal of clinical investigation* **124**(3)**:** 981-999.

Rajendra TK, Gonsalvez GB, Walker MP, Shpargel KB, Salz HK, Matera AG (2007). A Drosophila melanogaster model of spinal muscular atrophy reveals a function for SMN in striated muscle. *The Journal of cell biology* **176**(6)**:** 831-841.

Ralph GS, Radcliffe PA, Day DM, Carthy JM, Leroux MA, Lee DC*, et al.* (2005). Silencing mutant SOD1 using RNAi protects against neurodegeneration and extends survival in an ALS model. *Nature medicine* **11**(4)**:** 429-433.

Ray S, Panova T, Miller G, Volkov A, Porter AC, Russell J*, et al.* (2013). Topoisomerase IIalpha promotes activation of RNA polymerase I transcription by facilitating pre-initiation complex formation. *Nature communications* **4:** 1598.

Rieker C, Engblom D, Kreiner G, Domanskyi A, Schober A, Stotz S*, et al.* (2011). Nucleolar disruption in dopaminergic neurons leads to oxidative damage and parkinsonism through repression of mammalian target of rapamycin signaling. *The Journal of neuroscience : the official journal of the Society for Neuroscience* **31**(2)**:** 453-460.

Rindt H, Feng Z, Mazzasette C, Glascock JJ, Valdivia D, Pyles N*, et al.* (2015). Astrocytes influence the severity of spinal muscular atrophy. *Human molecular genetics* **24**(14)**:** 4094-4102.

Roda RH, Rinaldi C, Singh R, Schindler AB, Blackstone C (2014). Ataxia with oculomotor apraxia type 2 fibroblasts exhibit increased susceptibility to oxidative DNA damage. *Journal of clinical neuroscience : official journal of the Neurosurgical Society of Australasia* **21**(9)**:** 1627-1631.

Rogakou EP, Boon C, Redon C, Bonner WM (1999). Megabase chromatin domains involved in DNA double-strand breaks in vivo. *The Journal of cell biology* **146**(5)**:** 905-916.

Rossoll W, Bassell GJ (2009). Spinal muscular atrophy and a model for survival of motor neuron protein function in axonal ribonucleoprotein complexes. *Results and problems in cell differentiation* **48:** 289-326.

Rossoll W, Jablonka S, Andreassi C, Kroning AK, Karle K, Monani UR*, et al.* (2003). Smn, the spinal muscular atrophy-determining gene product, modulates axon growth and localization of beta-actin mRNA in growth cones of motoneurons. *The Journal of cell biology* **163**(4)**:** 801-812.

Rossoll W, Kroning AK, Ohndorf UM, Steegborn C, Jablonka S, Sendtner M (2002). Specific interaction of Smn, the spinal muscular atrophy determining gene product, with hnRNP-R and gry-rbp/hnRNP-Q: a role for Smn in RNA processing in motor axons? *Human molecular genetics* **11**(1)**:** 93-105.

Rubbi CP, Milner J (2003). Disruption of the nucleolus mediates stabilization of p53 in response to DNA damage and other stresses. *EMBO J* **22**(22)**:** 6068-6077.

Rudnik-Schoneborn S, Goebel HH, Schlote W, Molaian S, Omran H, Ketelsen U*, et al.* (2003). Classical infantile spinal muscular atrophy with SMN deficiency causes sensory neuronopathy. *Neurology* **60**(6)**:** 983-987.

Rudnik-Schoneborn S, Heller R, Berg C, Betzler C, Grimm T, Eggermann T*, et al.* (2008). Congenital heart disease is a feature of severe infantile spinal muscular atrophy. *Journal of medical genetics* **45**(10)**:** 635-638.

Russell J, Zomerdijk JC (2005). RNA-polymerase-I-directed rDNA transcription, life and works. *Trends in biochemical sciences* **30**(2)**:** 87-96.

Russman BS (2007). Spinal muscular atrophy: clinical classification and disease heterogeneity. *Journal of child neurology* **22**(8)**:** 946-951.

Saldi T, Cortazar MA, Sheridan RM, Bentley DL (2016). Coupling of RNA Polymerase II Transcription Elongation with Pre-mRNA Splicing. *Journal of molecular biology* **428**(12)**:** 2623-2635.

Sambrook J, Russell DW (2006). Detection of Protein-Protein Interactions Using the GST Fusion Protein Pulldown Technique. *CSH protocols* **2006**(1).

Sanchez G, Dury AY, Murray LM, Biondi O, Tadesse H, El Fatimy R*, et al.* (2013). A novel function for the survival motoneuron protein as a translational regulator. *Human molecular genetics* **22**(4)**:** 668-684.

Sanders LH, McCoy J, Hu X, Mastroberardino PG, Dickinson BC, Chang CJ*, et al.* (2014). Mitochondrial DNA damage: molecular marker of vulnerable nigral neurons in Parkinson's disease. *Neurobiology of disease* **70:** 214-223.

Sarachan Kathryn L, Valentine Kathleen G, Gupta K, Moorman Veronica R, Gledhill John M, Bernens M*, et al.* (2012). Solution structure of the core SMN–Gemin2 complex. *Biochemical Journal* **445**(3)**:** 361-370.

Sareen D, Ebert AD, Heins BM, McGivern JV, Ornelas L, Svendsen CN (2012). Inhibition of apoptosis blocks human motor neuron cell death in a stem cell model of spinal muscular atrophy. *PLoS One* **7**(6)**:** e39113.

Schmid A, DiDonato CJ (2007). Animal models of spinal muscular atrophy. *Journal of child neurology* **22**(8)**:** 1004-1012.

Schrank B, Gotz R, Gunnersen JM, Ure JM, Toyka KV, Smith AG*, et al.* (1997). Inactivation of the survival motor neuron gene, a candidate gene for human spinal muscular atrophy, leads to massive cell death in early mouse embryos. *Proceedings of the National Academy of Sciences of the United States of America* **94**(18)**:** 9920-9925.

Sendtner M (2010). Therapy development in spinal muscular atrophy. *Nature neuroscience* **13**(7)**:** 795-799.

Shababi M, Habibi J, Yang HT, Vale SM, Sewell WA, Lorson CL (2010). Cardiac defects contribute to the pathology of spinal muscular atrophy models. *Human molecular genetics* **19**(20)**:** 4059-4071.

Shav-Tal Y, Blechman J, Darzacq X, Montagna C, Dye BT, Patton JG*, et al.* (2005). Dynamic sorting of nuclear components into distinct nucleolar caps during transcriptional inhibition. *Molecular biology of the cell* **16**(5)**:** 2395-2413.

Sherr CJ, Weber JD (2000). The ARF/p53 pathway. *Current opinion in genetics & development* **10**(1)**:** 94-99.

Simic G (2008). Pathogenesis of proximal autosomal recessive spinal muscular atrophy. *Acta neuropathologica* **116**(3)**:** 223-234.

Singh NK, Singh NN, Androphy EJ, Singh RN (2006). Splicing of a critical exon of human Survival Motor Neuron is regulated by a unique silencer element located in the last intron. *Molecular and cellular biology* **26**(4)**:** 1333-1346.

Singh NN, Howell MD, Androphy EJ, Singh RN (2017a). How the discovery of ISS-N1 led to the first medical therapy for spinal muscular atrophy. *Gene therapy*.

Singh RN, Howell MD, Ottesen EW, Singh NN (2017b). Diverse role of survival motor neuron protein. *Biochimica et biophysica acta* **1860**(3)**:** 299-315.

Sirri V, Urcuqui-Inchima S, Roussel P, Hernandez-Verdun D (2008). Nucleolus: the fascinating nuclear body. *Histochemistry and cell biology* **129**(1)**:** 13-31.

Skourti-Stathaki K, Proudfoot NJ (2014). A double-edged sword: R loops as threats to genome integrity and powerful regulators of gene expression. *Genes Dev* **28**(13)**:** 1384-1396.

Skourti-Stathaki K, Proudfoot NJ, Gromak N (2011). Human senataxin resolves RNA/DNA hybrids formed at transcriptional pause sites to promote Xrn2-dependent termination. *Molecular cell* **42**(6)**:** 794-805.

Sleigh JN, Buckingham SD, Esmaeili B, Viswanathan M, Cuppen E, Westlund BM*, et al.* (2011a). A novel Caenorhabditis elegans allele, smn-1(cb131), mimicking a mild form of spinal muscular atrophy, provides a convenient drug screening platform highlighting new and pre-approved compounds. *Human molecular genetics* **20**(2)**:** 245-260.

Sleigh JN, Gillingwater TH, Talbot K (2011b). The contribution of mouse models to understanding the pathogenesis of spinal muscular atrophy. *Disease models & mechanisms* **4**(4)**:** 457-467.

Sleigh JN, Sattelle DB (2010). C. elegans models of neuromuscular diseases expedite translational research. *Translational Neuroscience* **1**(3)**:** 214-227.

Smith RA, Miller TM, Yamanaka K, Monia BP, Condon TP, Hung G*, et al.* (2006). Antisense oligonucleotide therapy for neurodegenerative disease. *The Journal of clinical investigation* **116**(8)**:** 2290-2296.

Sollier J, Cimprich KA (2015). Breaking bad: R-loops and genome integrity. *Trends in cell biology* **25**(9)**:** 514-522.

Sollier J, Stork CT, Garcia-Rubio ML, Paulsen RD, Aguilera A, Cimprich KA (2014). Transcription-coupled nucleotide excision repair factors promote R-loop-induced genome instability. *Molecular cell* **56**(6)**:** 777-785.

Sordet O, Redon CE, Guirouilh-Barbat J, Smith S, Solier S, Douarre C*, et al.* (2009). Ataxia telangiectasia mutated activation by transcription- and topoisomerase I-induced DNA double-strand breaks. *EMBO reports* **10**(8)**:** 887-893.

Stewart GS, Wang B, Bignell CR, Taylor AM, Elledge SJ (2003). MDC1 is a mediator of the mammalian DNA damage checkpoint. *Nature* **421**(6926)**:** 961-966.

Strasswimmer J, Lorson CL, Breiding DE, Chen JJ, Le T, Burghes AH*, et al.* (1999). Identification of survival motor neuron as a transcriptional activator-binding protein. *Human molecular genetics* **8**(7)**:** 1219-1226.

Stucki M, Clapperton JA, Mohammad D, Yaffe MB, Smerdon SJ, Jackson SP (2005). MDC1 directly binds phosphorylated histone H2AX to regulate cellular responses to DNA double-strand breaks. *Cell* **123**(7)**:** 1213-1226.

Tabet R, El Bitar S, Zaidan J, Dabaghian G (2017). Spinal Muscular Atrophy: The Treatment Approved. *Cureus* **9**(9)**:** e1644.

Tachi N, Kikuchi S, Kozuka N, Nogami A (2005). A new mutation of IGHMBP2 gene in spinal muscular atrophy with respiratory distress type 1. *Pediatric neurology* **32**(4)**:** 288-290.

Tadesse H, Deschenes-Furry J, Boisvenue S, Cote J (2008). KH-type splicing regulatory protein interacts with survival motor neuron protein and is misregulated in spinal muscular atrophy. *Human molecular genetics* **17**(4)**:** 506-524.

Takaku M, Tsujita T, Horikoshi N, Takizawa Y, Qing Y, Hirota K*, et al.* (2011). Purification of the human SMN-GEMIN2 complex and assessment of its stimulation of RAD51-mediated DNA recombination reactions. *Biochemistry* **50**(32)**:** 6797-6805.

Takashima H, Boerkoel CF, John J, Saifi GM, Salih MA, Armstrong D*, et al.* (2002). Mutation of TDP1, encoding a topoisomerase I-dependent DNA damage repair enzyme, in spinocerebellar ataxia with axonal neuropathy. *Nat Genet* **32:** 267-272.

Takizawa Y, Qing Y, Takaku M, Ishida T, Morozumi Y, Tsujita T*, et al.* (2010). GEMIN2 promotes accumulation of RAD51 at double-strand breaks in homologous recombination. *Nucleic acids research* **38**(15)**:** 5059-5074.

Tarabal O, Caraballo-Miralles V, Cardona-Rossinyol A, Correa FJ, Olmos G, Llado J*, et al.* (2014). Mechanisms involved in spinal cord central synapse loss in a mouse model of spinal muscular atrophy. *Journal of neuropathology and experimental neurology* **73**(6)**:** 519-535.

Terzi D, Zachariou V (2008). Adeno-associated virus-mediated gene delivery approaches for the treatment of CNS disorders. *Biotechnology Journal* **3**(12)**:** 1555-1563.

Thomas M, White RL, Davis RW (1976). Hybridization of RNA to double-stranded DNA: formation of R-loops. *Proceedings of the National Academy of Sciences of the United States of America* **73**(7)**:** 2294-2298.

Tizzano EF, Cabot C, Baiget M (1998). Cell-specific survival motor neuron gene expression during human development of the central nervous system: implications for the pathogenesis of spinal muscular atrophy. *The American journal of pathology* **153**(2)**:** 355-361.

Tsekrekou M, Stratigi K, Chatzinikolaou G (2017). The Nucleolus: In Genome Maintenance and Repair. *International journal of molecular sciences* **18**(7).

Tuduri S, Crabbe L, Conti C, Tourriere H, Holtgreve-Grez H, Jauch A*, et al.* (2009). Topoisomerase I suppresses genomic instability by preventing interference between replication and transcription. *Nature cell biology* **11**(11)**:** 1315-1324.

Uemura M, Zheng Q, Koh CM, Nelson WG, Yegnasubramanian S, De Marzo AM (2012). Overexpression of ribosomal RNA in prostate cancer is common but not linked to rDNA promoter hypomethylation. *Oncogene* **31**(10)**:** 1254-1263.

Ursic D, Chinchilla K, Finkel JS, Culbertson MR (2004). Multiple protein/protein and protein/RNA interactions suggest roles for yeast DNA/RNA helicase Sen1p in transcription, transcription-coupled DNA repair and RNA processing. *Nucleic acids research* **32**(8)**:** 2441-2452.

Valori CF, Ning K, Wyles M, Mead RJ, Grierson AJ, Shaw PJ*, et al.* (2010). Systemic delivery of scAAV9 expressing SMN prolongs survival in a model of spinal muscular atrophy. *Science translational medicine* **2**(35)**:** 35ra42.

van Gent DC, Hoeijmakers JH, Kanaar R (2001). Chromosomal stability and the DNA double-stranded break connection. *Nature reviews. Genetics* **2**(3)**:** 196-206.

van Sluis M, McStay B (2015). A localized nucleolar DNA damage response facilitates recruitment of the homology-directed repair machinery independent of cell cycle stage. *Genes Dev* **29**(11)**:** 1151-1163.

van Sluis M, McStay B (2017). Nucleolar reorganization in response to rDNA damage. *Current opinion in cell biology* **46:** 81-86.

Vanderweyde T, Youmans K, Liu-Yesucevitz L, Wolozin B (2013). Role of stress granules and RNA-binding proteins in neurodegeneration: a mini-review. *Gerontology* **59**(6)**:** 524-533.

Velma V, Carrero ZI, Cosman AM, Hebert MD (2010). Coilin interacts with Ku proteins and inhibits in vitro non-homologous DNA end joining. *FEBS Lett* **584**(23)**:** 4735-4739.

Vistbakka J, VanDuyn N, Wong G, Nass R (2012). C. elegans as a genetic model system to identify Parkinson's disease-associated therapeutic targets. *CNS & neurological disorders drug targets* **11**(8)**:** 957-964.

Vitte J, Fassier C, Tiziano FD, Dalard C, Soave S, Roblot N*, et al.* (2007). Refined characterization of the expression and stability of the SMN gene products. *The American journal of pathology* **171**(4)**:** 1269-1280.

Vitte JM, Davoult B, Roblot N, Mayer M, Joshi V, Courageot S*, et al.* (2004). Deletion of murine Smn exon 7 directed to liver leads to severe defect of liver development associated with iron overload. *The American journal of pathology* **165**(5)**:** 1731-1741.

Vousden KH (2000). p53: death star. *Cell* **103**(5)**:** 691-694.

Wahba L, Amon JD, Koshland D, Vuica-Ross M (2011). RNase H and multiple RNA biogenesis factors cooperate to prevent RNA:DNA hybrids from generating genome instability. *Molecular cell* **44**(6)**:** 978-988.

Wahl MC, Will CL, Luhrmann R (2009). The spliceosome: design principles of a dynamic RNP machine. *Cell* **136**(4)**:** 701-718.

Walker C, Herranz-Martin S, Karyka E, Liao C, Lewis K, Elsayed W*, et al.* (2017). C9orf72 expansion disrupts ATM-mediated chromosomal break repair. *Nature neuroscience* **20**(9)**:** 1225-1235.

Wang CH, Finkel RS, Bertini ES, Schroth M, Simonds A, Wong B*, et al.* (2007). Consensus statement for standard of care in spinal muscular atrophy. *Journal of child neurology* **22**(8)**:** 1027-1049.

Wang J, Haeusler AR, Simko EA (2015). Emerging role of RNA*DNA hybrids in C9orf72-linked neurodegeneration. *Cell Cycle* **14**(4)**:** 526-532.

Wang J, Wilkinson MF (2001). Deletion mutagenesis of large (12-kb) plasmids by a one-step PCR protocol. *Biotechniques* **31**(4)**:** 722-724.

Wang T, Bray SM, Warren ST (2012). New perspectives on the biology of fragile X syndrome. *Current opinion in genetics & development* **22**(3)**:** 256-263.

Wang W-Y, Pan L, Su SC, Quinn EJ, Sasaki M, Jimenez JC*, et al.* (2013a). Interaction of FUS and HDAC1 regulates DNA damage response and repair in neurons. *Nature neuroscience* **16**(10)**:** 1383-1391.

Wang WY, Pan L, Su SC, Quinn EJ, Sasaki M, Jimenez JC*, et al.* (2013b). Interaction of FUS and HDAC1 regulates DNA damage response and repair in neurons. *Nature neuroscience* **16**(10)**:** 1383-1391.

Wehner KA, Ayala L, Kim Y, Young PJ, Hosler BA, Lorson CL*, et al.* (2002). Survival motor neuron protein in the nucleolus of mammalian neurons. *Brain Research* **945**(2)**:** 160-173.

Weise S, Herrmann T, Drepper C, Jablonka S, Funk N, Klausmeyer A*, et al.* (2010). Isolation and enrichment of embryonic mouse motoneurons from the lumbar spinal cord of individual mouse embryos. *Nat Protoc.* **5**(1)**:** 31-38.

West SC (2003). Molecular views of recombination proteins and their control. *Nature reviews. Molecular cell biology* **4**(6)**:** 435-445.

Whitehead SE, Jones KW, Zhang X, Cheng X, Terns RM, Terns MP (2002). Determinants of the Interaction of the Spinal Muscular Atrophy Disease Protein SMN with the Dimethylarginine-modified Box H/ACA Small Nucleolar Ribonucleoprotein GAR1. *Journal of Biological Chemistry* **277**(50)**:** 48087-48093.

Wiese S, Herrmann T, Drepper C, Jablonka S, Funk N, Klausmeyer A*, et al.* (2010). Isolation and enrichment of embryonic mouse motoneurons from the lumbar spinal cord of individual mouse embryos. *Nature protocols* **5**(1)**:** 31-38.

Wirth B (2000). An update of the mutation spectrum of the survival motor neuron gene (SMN1) in autosomal recessive spinal muscular atrophy (SMA). *Human mutation* **15**(3)**:** 228-237.

Wishart TM, Mutsaers CA, Riessland M, Reimer MM, Hunter G, Hannam ML*, et al.* (2014). Dysregulation of ubiquitin homeostasis and β-catenin signaling promote spinal muscular atrophy. *J Clin Invest* **24**(4)**:** 1821-1834. .

Workman E, Kolb SJ, Battle DJ (2012). Spliceosomal small nuclear ribonucleoprotein biogenesis defects and motor neuron selectivity in spinal muscular atrophy. *Brain research* **1462:** 93-99.

Yamazaki T, Chen S, Yu Y, Yan B, Haertlein TC, Carrasco MA*, et al.* (2012). FUS-SMN protein interactions link the motor neuron diseases ALS and SMA. *Cell reports* **2**(4)**:** 799-806.

Young PJ, Day PM, Zhou J, Androphy EJ, Morris GE, Lorson CL (2002). A direct interaction between the survival motor neuron protein and p53 and its relationship to spinal muscular atrophy. *The Journal of biological chemistry* **277**(4)**:** 2852-2859.

Young PJ, Le TT, thi Man N, Burghes AH, Morris GE (2000). The relationship between SMN, the spinal muscular atrophy protein, and nuclear coiled bodies in differentiated tissues and cultured cells. *Experimental cell research* **256**(2)**:** 365-374.

Zarrin AA, Alt FW, Chaudhuri J, Stokes N, Kaushal D, Du Pasquier L*, et al.* (2004). An evolutionarily conserved target motif for immunoglobulin class-switch recombination. *Nature immunology* **5**(12)**:** 1275-1281.

Zerres K, Rudnik-Schoneborn S (1995). Natural history in proximal spinal muscular atrophy. Clinical analysis of 445 patients and suggestions for a modification of existing classifications. *Archives of neurology* **52**(5)**:** 518-523.

Zhang QJ, Li JJ, Lin X, Lu YQ, Guo XX, Dong EL*, et al.* (2017). Modeling the phenotype of spinal muscular atrophy by the direct conversion of human fibroblasts to motor neurons. *Oncotarget* **8**(7)**:** 10945-10953.

Zhang Z, Lotti F, Dittmar K, Younis I, Wan L, Kasim M*, et al.* (2008). SMN deficiency causes tissue-specific perturbations in the repertoire of snRNAs and widespread defects in splicing. *Cell* **133**(4)**:** 585-600.

Zhao DY, Gish G, Braunschweig U, Li Y, Ni Z, Schmitges FW*, et al.* (2016). SMN and symmetric arginine dimethylation of RNA polymerase II C-terminal domain control termination. *Nature* **529**(7584)**:** 48-53.

Zhou Y, Liu S, Ozturk A, Hicks GG (2014). FUS-regulated RNA metabolism and DNA damage repair: Implications for amyotrophic lateral sclerosis and frontotemporal dementia pathogenesis. *Rare diseases* **2:** e29515.

Zimmer AD, Koshland D (2016). Differential roles of the RNases H in preventing chromosome instability. *Proceedings of the National Academy of Sciences* **113**(43)**:** 12220-12225.

Zou J, Barahmand-pour F, Blackburn ML, Matsui Y, Chansky HA, Yang L (2004). Survival Motor Neuron (SMN) Protein Interacts with Transcription Corepressor mSin3A. *Journal of Biological Chemistry* **279**(15)**:** 14922-14928.

Zou T, Yang X, Pan D, Huang J, Sahin M, Zhou J (2011). SMN deficiency reduces cellular ability to form stress granules, sensitizing cells to stress. *Cellular and molecular neurobiology* **31**(4)**:** 541-550.

9. APPENDIX

Appendix 1: Vector maps and sequences

(a) Map of LV SMN FL plasmid

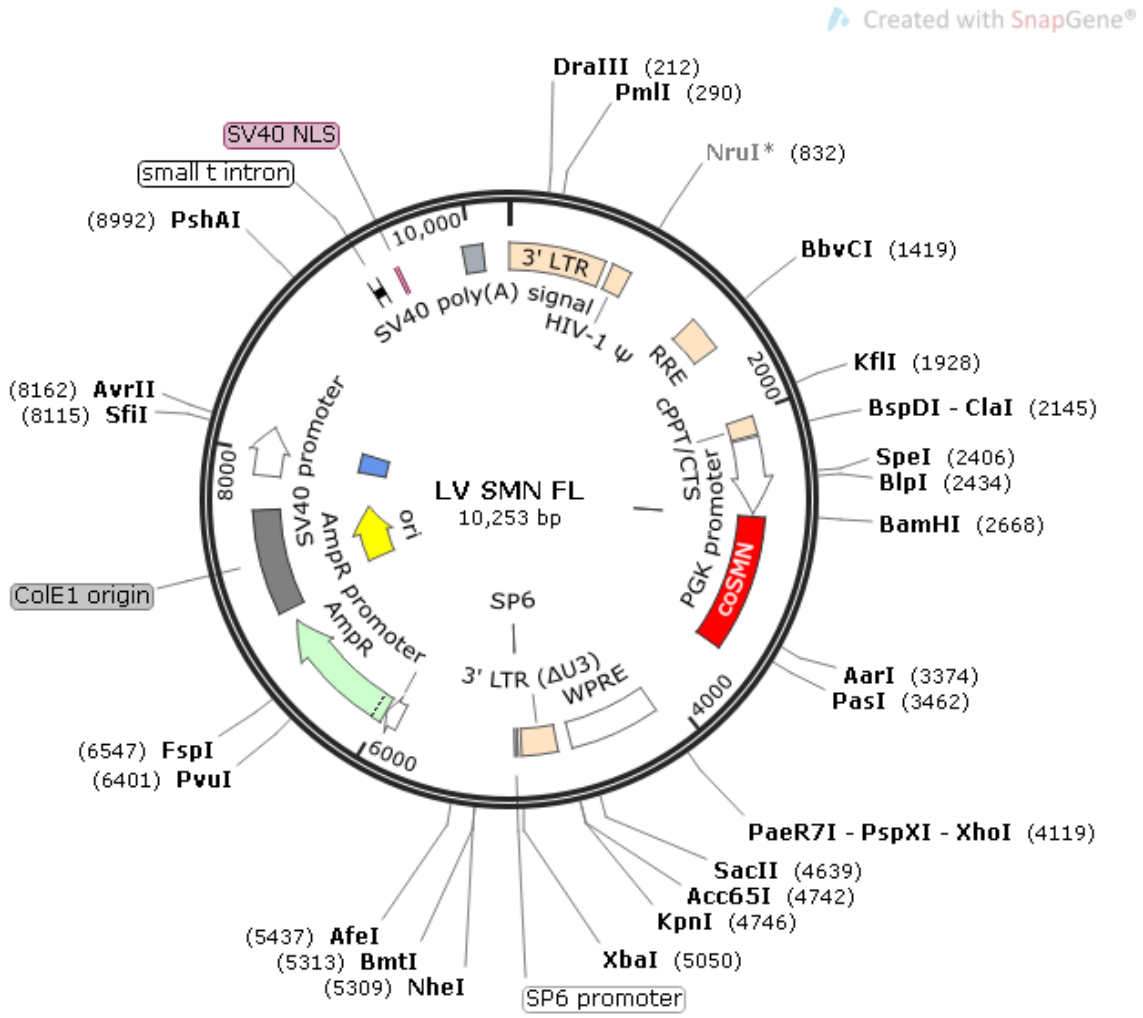

(b) Sequence of LV SMN FL plasmid

TGGAAGGGCTAATTCACTCCCAAAGAAGACAAGATATCCTTGATCTGTGGATCT
ACCACACACAAGGCTACTTCCCTGATTAGCAGAACTACACACCAGGGCCAGGG
GTCAGATATCCACTGACCTTTGGATGGTGCTACAAGCTAGTACCAGTTGAGCCA
GATAAGGTAGAAGAGGCCAATAAAGGAGAGAACACCAGCTTGTTACACCCTGT
GAGCCTGCATGGGATGGATGACCCGGAGAGAGAAGTGTTAGAGTGGAGGTTT
GACAGCCGCCTAGCATTTCATCACGTGGCCCGAGAGCTGCATCCGGAGTACTT
CAAGAACTGCTGATATCGAGCTTGCTACAAGGGACTTTCCGCTGGGGACTTTCC
AGGGAGGCGTGGCCTGGGCGGGACTGGGGAGTGGCGAGCCCTCAGATCCTG
CATATAAGCAGCTGCTTTTTGCCTGTACTGGGTCTCTCTGGTTAGACCAGATCT
GAGCCTGGGAGCTCTCTGGCTAACTAGGGAACCCACTGCTTAAGCCTCAATAA
AGCTTGCCTTGAGTGCTTCAAGTAGTGTGTGCCCGTCTGTTGTGTGACTCTGGT
AACTAGAGATCCCTCAGACCCTTTTAGTCAGTGTGGAAAATCTCTAGCAGTGGC
GCCCGAACAGGGACCTGAAAGCGAAAGGGAAACCAGAGCTCTCTCGACGCAG
GACTCGGCTTGCTGAAGCGCGCGCACGGCAAGAGGCGAGGGGCGGCGACTG
GTGAGTACGCCAAAAATTTTGACTAGCGGAGGCTAGAAGGAGAGAGATGGGTG
CGAGAGCGTCAGTATTAAGCGGGGGAGAATTAGATCGCGATGGGAAAAAATTC
GGTTAAGGCCAGGGGGAAAGAAAAAATATAAATTAAAACATATAGTATGGGCAA
GCAGGGAGCTAGAACGATTCGCAGTTAATCCTGGCCTGTTAGAAACATCAGAA
GGCTGTAGACAAATACTGGGACAGCTACAACCATCCCTTCAGACAGGATCAGA
AGAACTTAGATCATTATATAATACAGTAGCAACCCTCTATTGTGTGCATCAAAGG
ATAGAGATAAAAGACACCAAGGAAGCTTTAGACAAGATAGAGGAAGAGCAAAAC
AAAAGTAAGACCACCGCACAGCAAGCGGCCGCTGATCTTCAGACCTGGAGGAG
GAGATATGAGGGACAATTGGAGAAGTGAATTATATAAATATAAAGTAGTAAAAAT
TGAACCATTAGGAGTAGCACCCACCAAGGCAAAGAGAAGAGTGGTGCAGAGAG
AAAAAAGAGCAGTGGGAATAGGAGCTTTGTTCCTTGGGTTCTTGGGAGCAGCA
GGAAGCACTATGGGCGCAGCCTCAATGACGCTGACGGTACAGGCCAGACAATT
ATTGTCTGGTATAGTGCAGCAGCAGAACAATTTGCTGAGGGCTATTGAGGCGC
AACAGCATCTGTTGCAACTCACAGTCTGGGGCATCAAGCAGCTCCAGGCAAGA
ATCCTGGCTGTGGAAAGATACCTAAAGGATCAACAGCTCCTGGGGATTTGGGG
TTGCTCTGGAAAACTCATTTGCACCACTGCTGTGCCTTGGAATGCTAGTTGGAG
TAATAAATCTCTGGAACAGATTGGAATCACACGACCTGGATGGAGTGGGACAGA
GAAATTAACAATTACACAAGCTTAATACACTCCTTAATTGAAGAATCGCAAAACC
AGCAAGAAAAGAATGAACAAGAATTATTGGAATTAGATAAATGGGCAAGTTTGT
GGAATTGGTTTAACATAACAAATTGGCTGTGGTATATAAAATTATTCATAATGATA
GTAGGAGGCTTGGTAGGTTTAAGAATAGTTTTTGCTGTACTTTCTATAGTGAATA
GAGTTAGGCAGGGATATTCACCATTATCGTTTCAGACCCACCTCCCAACCCCGA
GGGGACCCGACAGGCCCGAAGGAATAGAAGAAGAAGGTGGAGAGAGAGACAG
AGACAGATCCATTCGATTAGTGAACGGATCTCGACGGTATCGGTTAACTTTTAA
AAGAAAAGGGGGGATTGGGGGGTACAGTGCAGGGGAAAGAATAGTAGACATAA
TAGCAACAGACATACAAACTAAAGAATTACAAAAACAAATTACAAAAATTCAAAA
TTTTATCGATGGTCGAGTACCGGGTAGGGGAGGCGCTTTTCCCAAGGCAGTCT

GGAGCATGCGCTTTAGCAGCCCCGCTGGGCACTTGGCGCTACACAAGTGGCC
TCTGGCCTCGCACACATTCCACATCCACCGGTAGGCGCCAACCGGCTCCGTTC
TTTGGTGGCCCCTTCGCGCCACCTTCTACTCCTCCCCTAGTCAGGAAGTTCCCC
CCCGCCCCGCAGCTCGCGTCGTGCAGGACGTGACAAATGGAAGTAGCACGTC
TCACTAGTCTCGTGCAGATGGACAGCACCGCTGAGCAATGGAAGCGGGTAGGC
CTTTGGGGCAGCGGCCAATAGCAGCTTTGCTCCTTCGCTTTCTGGGCTCAGAG
GCTGGGAAGGGGTGGGTCCGGGGGCGGGCTCAGGGGCGGGCTCAGGGGCG
GGGCGGGCGCCCGAAGGTCCTCCGGAGGCCCGGCATTCTGCACGCTTCAAAA
GCGCACGTCTGCCGCGCTGTTCTCCTCTTCCTCATCTCCGGGCCTTTCGACCT
CTAGGATCCaccggtGCCACCATGGCCATGAGCAGCGGCGGCTCTGGCGGCGGA
GTGCCCGAGCAGGAAGATAGCGTCCTGTTCAGGCGGGGCACCGGCCAGAGCG
ACGACAGCGACATCTGGGACGACACCGCCCTGATCAAGGCCTACGACAAGGC
CGTGGCCAGCTTCAAGCACGCCCTGAAGAACGGCGACATCTGCGAGACCAGC
GGCAAGCCCAAGACCACCCCCAAGCGGAAGCCCGCCAAGAAGAACAAGAGCC
AGAAGAAGAACACCGCCGCCAGCCTGCAGCAGTGGAAAGTGGGCGACAAGTG
CAGCGCCATCTGGTCCGAGGACGGCTGCATCTACCCCGCCACCATCGCCAGC
ATCGACTTCAAGCGGGAGACCTGCGTGGTGGTGTACACCGGCTACGGCAACC
GGGAGGAACAGAACCTGAGCGACCTGCTGTCCCCCATCTGCGAAGTGGCCAA
CAACATCGAGCAGAACGCCCAGGAAAACGAGAACGAGAGCCAAGTGTCCACC
GACGAGAGCGAGAACAGCAGAAGCCCCGGCAACAAGAGCGACAACATCAAGC
CTAAGAGCGCCCCCTGGAACAGCTTCCTGCCCCCTCCCCCCCCTATGCCTGGC
CCCAGGCTGGGCCCTGGCAAGCCCGGCCTGAAGTTCAACGGCCCTCCCCCTC
CTCCCCCACCCCCTCCACCTCACCTGCTGTCTTGCTGGCTGCCCCCCTTCCCC
AGCGGCCCTCCCATCATCCCCCCACCTCCCCCTATCTGCCCCGACAGCCTGGA
CGACGCCGACGCCCTGGGCAGCATGCTGATCAGCTGGTACATGAGCGGCTAC
CACACCGGCTATTACATGGGCTTCCGGCAGAACCAGAAAGAGGGCCGCTGCA
GCCACAGCCTGAACTGAggagaaatgctggcatagagcagcactaaatgacaccactaaagaaacga
tcagacagatctggaatgtgaagcgttatagaagataactggcctcatttcttcaaaatatcaagtgttgggaaagaaa
aaaggaagtggaatgggtaactcttcttgattaaaagttatgtaataaccaaatgcaatgtgaaatattttactggactct
attttgaaaaaccatctgtaaaagactggggtgggggtgggaggccagcacggtggtgaggcagttgagaaaatttg
aatgtggattagattttgaatgatattggataattattggtaattttatgagctgtgagaagggtgttgtagtttataaaagac
tgtcttaatttgcatacttaagcatttaggaatgaagtgttagagtgtcttaaaatgtttcaaatggtttaacaaaatgtatgt
gaggcgtatgtggcaaaatgttacagaatctaactggtggacatggctgttcattgtactgaattctgcagatatccatca
cactggcggccgCTCGAGGGAATTCCGATAATCAACCTCTGGATTACAAAATTTGTGA
AAGATTGACTGGTATTCTTAACTATGTTGCTCCTTTTACGCTATGTGGATACGCT
GCTTTAATGCCTTTGTATCATGCTATTGCTTCCCGTATGGCTTTCATTTTCTCCTC
CTTGTATAAATCCTGGTTGCTGTCTCTTTATGAGGAGTTGTGGCCCGTTGTCAG
GCAACGTGGCGTGGTGTGCACTGTGTTTGCTGACGCAACCCCCACTGGTTGGG
GCATTGCCACCACCTGTCAGCTCCTTTCCGGGACTTTCGCTTTCCCCCTCCCTA
TTGCCACGGCGGAACTCATCGCCGCCTGCCTTGCCCGCTGCTGGACAGGGGC
TCGGCTGTTGGGCACTGACAATTCCGTGGTGTTGTCGGGGAAGCTGACGTCCT
TTCCATGGCTGCTCGCCTGTGTTGCCACCTGGATTCTGCGCGGGACGTCCTTC
TGCTACGTCCCTTCGGCCCTCAATCCAGCGGACCTTCCTTCCCGCGGCCTGCT
GCCGGCTCTGCGGCCTCTTCCGCGTCTTCGCCTTCGCCCTCAGACGAGTCGGA

TCTCCCTTTGGGCCGCCTCCCCGCATCGGGAATTCGAGCTCGGTACCTTTAAA
ACCAATGACTTACAAGGCAGCTGTAAATCTTAGCCACTTTTTAAAAGAAAAGGG
GGGACTGGAAGGGCTAATTCACTCCCAACGAAAACAAAATCTGCTTTTTGCTTG
TACTGGGTCTCTCTGGTTAGACCAAATCTGAGCCTGGGAGCTCTCTGGCTAACT
AGGGAACCCACTGCTTAAGCCTCAATAAAGCTTGCCTTGAGTGCTTCAAGTAGT
GTGTGCCCGTCTGTTGTGTGACTCTGGTAACTAGAGATCCCTCAAACCCTTTTA
GTCAGTGTGGAAAATCTCTAGCAGCATCTAGAATTAATTCCGTGTATTCTATAGT
GTCACCTAAATCGTATGTGTATGATACATAAGGTTATGTATTAATTGTAGCCGCG
TTCTAACGACAATATGTACAAGCCTAATTGTGTAGCATCTGGCTTACTGAAGCA
GACCCTATCATCTCTCTCGTAAACTGCCGTCAGAGTCGGTTTGGTTGGACGAAC
CTTCTGAGTTTCTGGTAACGCCGTCCCGCACCCGGAAATGGTCAGCGAACCAA
TCAGCAGGGTCATCGCTAGCCAGATCCTCTACGCCGGACGCATCGTGGCCGG
CATCACCGGCGCCACAGGTGCGGTTGCTGGCGCCTATATCGCCGACATCACC
GATGGGGAAGATCGGGCTCGCCACTTCGGGCTCATGAGCGCTTGTTTCGGCGT
GGGTATGGTGGCAGGCCCCGTGGCCGGGGGACTGTTGGGCGCCATCTCCTTG
CATGCACCATTCCTTGCGGCGGCGGTGCTCAACGGCCTCAACCTACTACTGGG
CTGCTTCCTAATGCAGGAGTCGCATAAGGGAGAGCGTCGATATGGTGCACTCT
CAGTACAATCTGCTCTGATGCCGCATAGTTAAGCCAGCCCCGACACCCGCCAA
CACCCGCTGACGCGCCCTGACGGGCTTGTCTGCTCCCGGCATCCGCTTACAGA
CAAGCTGTGACCGTCTCCGGGAGCTGCATGTGTCAGAGGTTTTCACCGTCATC
ACCGAAACGCGCGAGACGAAAGGGCCTCGTGATACGCCTATTTTTATAGGTTAA
TGTCATGATAATAATGGTTTCTTAGACGTCAGGTGGCACTTTTCGGGGAAATGT
GCGCGGAACCCCTATTTGTTTATTTTTCTAAATACATTCAAATATGTATCCGCTC
ATGAGACAATAACCCTGATAAATGCTTCAATAATATTGAAAAAGGAAGAGTATGA
GTATTCAACATTTCCGTGTCGCCCTTATTCCCTTTTTTGCGGCATTTTGCCTTCC
TGTTTTTGCTCACCCAGAAACGCTGGTGAAAGTAAAAGATGCTGAAGATCAGTT
GGGTGCACGAGTGGGTTACATCGAACTGGATCTCAACAGCGGTAAGATCCTTG
AGAGTTTTCGCCCCGAAGAACGTTTTCCAATGATGAGCACTTTTAAAGTTCTGCT
ATGTGGCGCGGTATTATCCCGTATTGACGCCGGGCAAGAGCAACTCGGTCGCC
GCATACACTATTCTCAGAATGACTTGGTTGAGTACTCACCAGTCACAGAAAAGC
ATCTTACGGATGGCATGACAGTAAGAGAATTATGCAGTGCTGCCATAACCATGA
GTGATAACACTGCGGCCAACTTACTTCTGACAACGATCGGAGGACCGAAGGAG
CTAACCGCTTTTTTGCACAACATGGGGGATCATGTAACTCGCCTTGATCGTTGG
GAACCGGAGCTGAATGAAGCCATACCAAACGACGAGCGTGACACCACGATGCC
TGTAGCAATGGCAACAACGTTGCGCAAACTATTAACTGGCGAACTACTTACTCT
AGCTTCCCGGCAACAATTAATAGACTGGATGGAGGCGGATAAAGTTGCAGGAC
CACTTCTGCGCTCGGCCCTTCCGGCTGGCTGGTTTATTGCTGATAAATCTGGAG
CCGGTGAGCGTGGGTCTCGCGGTATCATTGCAGCACTGGGGCCAGATGGTAA
GCCCTCCCGTATCGTAGTTATCTACACGACGGGGAGTCAGGCAACTATGGATG
AACGAAATAGACAGATCGCTGAGATAGGTGCCTCACTGATTAAGCATTGGTAAC
TGTCAGACCAAGTTTACTCATATATACTTTAGATTGATTTAAAACTTCATTTTTAA
TTTAAAAGGATCTAGGTGAAGATCCTTTTTGATAATCTCATGACCAAAATCCCTT
AACGTGAGTTTTCGTTCCACTGAGCGTCAGACCCCGTAGAAAAGATCAAAGGAT
CTTCTTGAGATCCTTTTTTTCTGCGCGTAATCTGCTGCTTGCAAACAAAAAAACC

ACCGCTACCAGCGGTGGTTTGTTTGCCGGATCAAGAGCTACCAACTCTTTTTCC
GAAGGTAACTGGCTTCAGCAGAGCGCAGATACCAAATACTGTCCTTCTAGTGTA
GCCGTAGTTAGGCCACCACTTCAAGAACTCTGTAGCACCGCCTACATACCTCG
CTCTGCTAATCCTGTTACCAGTGGCTGCTGCCAGTGGCGATAAGTCGTGTCTTA
CCGGGTTGGACTCAAGACGATAGTTACCGGATAAGGCGCAGCGGTCGGGCTG
AACGGGGGGTTCGTGCACACAGCCCAGCTTGGAGCGAACGACCTACACCGAA
CTGAGATACCTACAGCGTGAGCTATGAGAAAGCGCCACGCTTCCCGAAGGGAG
AAAGGCGGACAGGTATCCGGTAAGCGGCAGGGTCGGAACAGGAGAGCGCACG
AGGGAGCTTCCAGGGGGAAACGCCTGGTATCTTTATAGTCCTGTCGGGTTTCG
CCACCTCTGACTTGAGCGTCGATTTTTGTGATGCTCGTCAGGGGGGCGGAGCC
TATGGAAAAACGCCAGCAACGCGGCCTTTTTACGGTTCCTGGCCTTTTGCTGGC
CTTTTGCTCACATGTTCTTTCCTGCGTTATCCCCTGATTCTGTGGATAACCGTAT
TACCGCCTTTGAGTGAGCTGATACCGCTCGCCGCAGCCGAACGACCGAGCGC
AGCGAGTCAGTGAGCGAGGAAGCGGAAGAGCGCCCAATACGCAAACCGCCTC
TCCCCGCGCGTTGGCCGATTCATTAATGCAGCTGTGGAATGTGTGTCAGTTAG
GGTGTGGAAAGTCCCCAGGCTCCCCAGCAGGCAGAAGTATGCAAAGCATGCAT
CTCAATTAGTCAGCAACCAGGTGTGGAAAGTCCCCAGGCTCCCCAGCAGGCAG
AAGTATGCAAAGCATGCATCTCAATTAGTCAGCAACCATAGTCCCGCCCCTAAC
TCCGCCCATCCCGCCCCTAACTCCGCCCAGTTCCGCCCATTCTCCGCCCCATG
GCTGACTAATTTTTTTTATTTATGCAGAGGCCGAGGCCGCCTCGGCCTCTGAGC
TATTCCAGAAGTAGTGAGGAGGCTTTTTTGGAGGCCTAGGCTTTTGCAAAAAGC
TTGGACACAAGACAGGCTTGCGAGATATGTTTGAGAATACCACTTTATCCCGCG
TCAGGGAGAGGCAGTGCGTAAAAAGACGCGGACTCATGTGAAATACTGGTTTT
TAGTGCGCCAGATCTCTATAATCTCGCGCAACCTATTTTCCCCTCGAACACTTTT
TAAGCCGTAGATAAACAGGCTGGGACACTTCACATGAGCGAAAAATACATCGTC
ACCTGGGACATGTTGCAGATCCATGCACGTAAACTCGCAAGCCGACTGATGCC
TTCTGAACAATGGAAAGGCATTATTGCCGTAAGCCGTGGCGGTCTGTACCGGG
TGCGTTACTGGCGCGTGAACTGGGTATTCGTCATGTCGATACCGTTTGTATTTC
CAGCTACGATCACGACAACCAGCGCGAGCTTAAAGTGCTGAAACGCGCAGAAG
GCGATGGCGAAGGCTTCATCGTTATTGATGACCTGGTGGATACCGGTGGTACT
GCGGTTGCGATTCGTGAAATGTATCCAAAAGCGCACTTTGTCACCATCTTCGCA
AAACCGGCTGGTCGTCCGCTGGTTGATGACTATGTTGTTGATATCCCGCAAGAT
ACCTGGATTGAACAGCCGTGGGATATGGGCGTCGTATTCGTCCCGCCAATCTC
CGGTCGCTAATCTTTTCAACGCCTGGCACTGCCGGGCGTTGTTCTTTTTAACTT
CAGGCGGGTTACAATAGTTTCCAGTAAGTATTCTGGAGGCTGCATCCATGACAC
AGGCAAACCTGAGCGAAACCCTGTTCAAACCCCGCTTTAAACATCCTGAAACCT
CGACGCTAGTCCGCCGCTTTAATCACGGCGCACAACCGCCTGTGCAGTCGGCC
CTTGATGGTAAAACCATCCCTCACTGGTATCGCATGATTAACCGTCTGATGTGG
ATCTGGCGCGGCATTGACCCACGCGAAATCCTCGACGTCCAGGCACGTATTGT
GATGAGCGATGCCGAACGTACCGACGATGATTTATACGATACGGTGATTGGCT
ACCGTGGCGGCAACTGGATTTATGAGTGGGCCCCGGATCTTTGTGAAGGAACC
TTACTTCTGTGGTGTGACATAATTGGACAAACTACCTACAGAGATTTAAAGCTCT
AAGGTAAATATAAAATTTTTAAGTGTATAATGTGTTAAACTACTGATTCTAATTGT
TTGTGTATTTTAGATTCCAACCTATGGAACTGATGAATGGGAGCAGTGGTGGAA

TGCCTTTAATGAGGAAAACCTGTTTTGCTCAGAAGAAATGCCATCTAGTGATGAT
GAGGCTACTGCTGACTCTCAACATTCTACTCCTCCAAAAAAGAAGAGAAAGGTA
GAAGACCCCAAGGACTTTCCTTCAGAATTGCTAAGTTTTTTGAGTCATGCTGTGT
TTAGTAATAGAACTCTTGCTTGCTTTGCTATTTACACCACAAAGGAAAAAGCTGC
ACTGCTATACAAGAAAATTATGGAAAAATATTCTGTAACCTTTATAAGTAGGCAT
AACAGTTATAATCATAACATACTGTTTTTTCTTACTCCACACAGGCATAGAGTGT
CTGCTATTAATAACTATGCTCAAAAATTGTGTACCTTTAGCTTTTTAATTTGTAAA
GGGGTTAATAAGGAATATTTGATGTATAGTGCCTTGACTAGAGATCATAATCAG
CCATACCACATTTGTAGAGCTTTTACTTGCTTTAAAAAACCTCCCACACCTCCCC
CTGAACCTGAAACATAAAATGAATGCAATTGTTGTTGTTAACTTGTTTATTGCAG
CTTATAATGGTTACAAATAAAGCAATAGCATCACAAATTTCACAAATAAAGCATTT
TTTTCACTGCATTCTAGTTGTGGTTTGTCCAAACTCATCAATGTATCTTATCATGT
GTGGATCAACTGGATAACTCAAGCTAACCAAAATCATCCCAAACTTCCCACCCC
ATACCCTATTACCACTGCCAAATTACCTGTGGTTTCATTTACTCTAAACCTGTGA
TTCCTCTGAATTATTTTCATTTTAAAGAAATTGTATTTGTTAAATATGTACTACAAA
CTTAGTAGT

(c) Map of LV SMN Δ3 plasmid

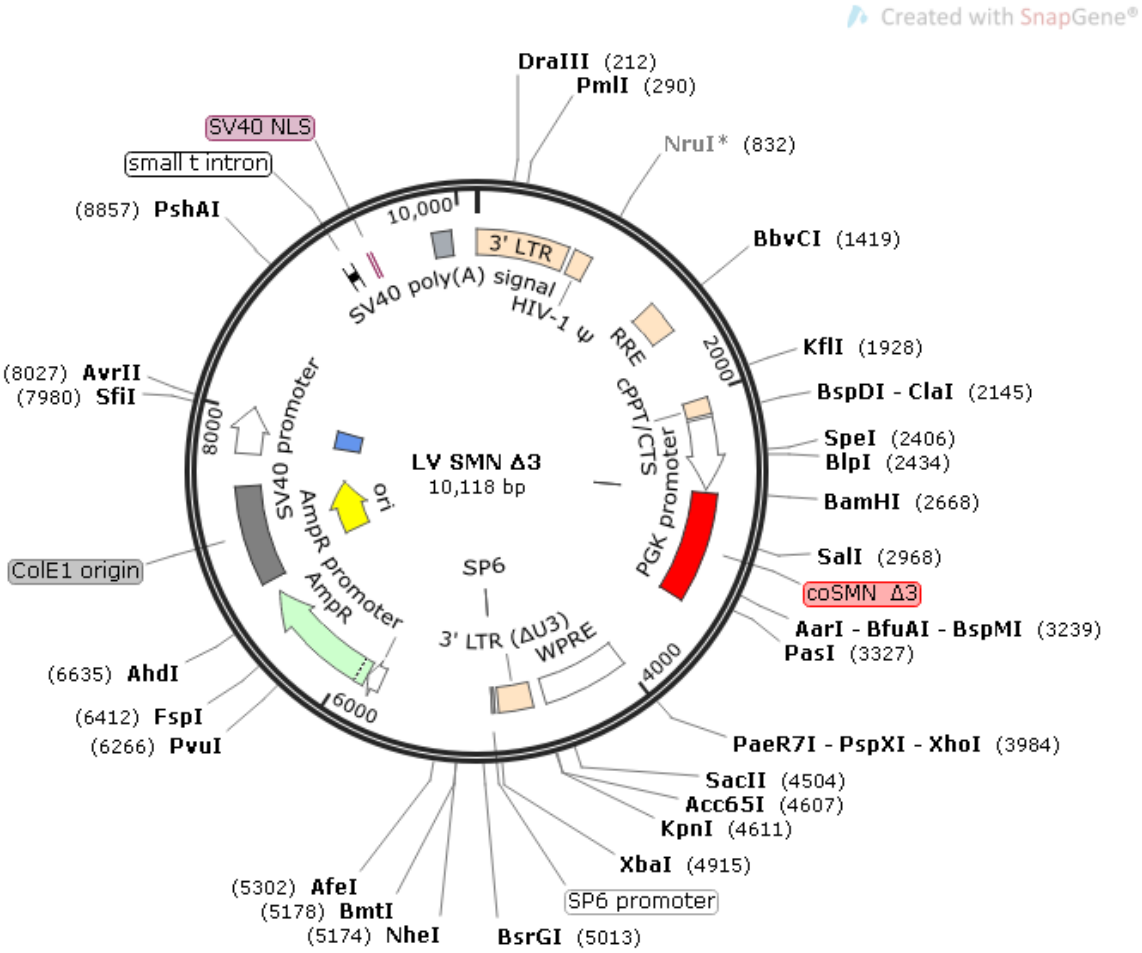

(d) Sequence of LV SMN Δ3 plasmid

TGGAAGGGCTAATTCACTCCCAAAGAAGACAAGATATCCTTGATCTGTGGATCT
ACCACACACAAGGCTACTTCCCTGATTAGCAGAACTACACACCAGGGCCAGGG
GTCAGATATCCACTGACCTTTGGATGGTGCTACAAGCTAGTACCAGTTGAGCCA
GATAAGGTAGAAGAGGCCAATAAAGGAGAGAACACCAGCTTGTTACACCCTGT
GAGCCTGCATGGGATGGATGACCCGGAGAGAGAAGTGTTAGAGTGGAGGTTT
GACAGCCGCCTAGCATTTCATCACGTGGCCCGAGAGCTGCATCCGGAGTACTT
CAAGAACTGCTGATATCGAGCTTGCTACAAGGGACTTTCCGCTGGGGACTTTCC
AGGGAGGCGTGGCCTGGGCGGGACTGGGGAGTGGCGAGCCCTCAGATCCTG
CATATAAGCAGCTGCTTTTTGCCTGTACTGGGTCTCTCTGGTTAGACCAGATCT
GAGCCTGGGAGCTCTCTGGCTAACTAGGGAACCCACTGCTTAAGCCTCAATAA
AGCTTGCCTTGAGTGCTTCAAGTAGTGTGTGCCCGTCTGTTGTGTGACTCTGGT
AACTAGAGATCCCTCAGACCCTTTTAGTCAGTGTGGAAAATCTCTAGCAGTGGC
GCCCGAACAGGGACCTGAAAGCGAAAGGGAAACCAGAGCTCTCTCGACGCAG
GACTCGGCTTGCTGAAGCGCGCGCACGGCAAGAGGCGAGGGGCGGCGACTG
GTGAGTACGCCAAAAATTTTGACTAGCGGAGGCTAGAAGGAGAGAGATGGGTG
CGAGAGCGTCAGTATTAAGCGGGGGAGAATTAGATCGCGATGGGAAAAAATTC
GGTTAAGGCCAGGGGGAAAGAAAAAATATAAATTAAAACATATAGTATGGGCAA
GCAGGGAGCTAGAACGATTCGCAGTTAATCCTGGCCTGTTAGAAACATCAGAA
GGCTGTAGACAAATACTGGGACAGCTACAACCATCCCTTCAGACAGGATCAGA
AGAACTTAGATCATTATATAATACAGTAGCAACCCTCTATTGTGTGCATCAAAGG
ATAGAGATAAAAGACACCAAGGAAGCTTTAGACAAGATAGAGGAAGAGCAAAAC
AAAAGTAAGACCACCGCACAGCAAGCGGCCGCTGATCTTCAGACCTGGAGGAG
GAGATATGAGGGACAATTGGAGAAGTGAATTATATAAATATAAAGTAGTAAAAAT
TGAACCATTAGGAGTAGCACCCACCAAGGCAAAGAGAAGAGTGGTGCAGAGAG
AAAAAAGAGCAGTGGGAATAGGAGCTTTGTTCCTTGGGTTCTTGGGAGCAGCA
GGAAGCACTATGGGCGCAGCCTCAATGACGCTGACGGTACAGGCCAGACAATT
ATTGTCTGGTATAGTGCAGCAGCAGAACAATTTGCTGAGGGCTATTGAGGCGC
AACAGCATCTGTTGCAACTCACAGTCTGGGGCATCAAGCAGCTCCAGGCAAGA
ATCCTGGCTGTGGAAAGATACCTAAAGGATCAACAGCTCCTGGGGATTTGGGG
TTGCTCTGGAAAACTCATTTGCACCACTGCTGTGCCTTGGAATGCTAGTTGGAG
TAATAAATCTCTGGAACAGATTGGAATCACACGACCTGGATGGAGTGGGACAGA
GAAATTAACAATTACACAAGCTTAATACACTCCTTAATTGAAGAATCGCAAAACC
AGCAAGAAAAGAATGAACAAGAATTATTGGAATTAGATAAATGGGCAAGTTTGT
GGAATTGGTTTAACATAACAAATTGGCTGTGGTATATAAAATTATTCATAATGATA
GTAGGAGGCTTGGTAGGTTTAAGAATAGTTTTTGCTGTACTTTCTATAGTGAATA
GAGTTAGGCAGGGATATTCACCATTATCGTTTCAGACCCACCTCCCAACCCCGA
GGGGACCCGACAGGCCCGAAGGAATAGAAGAAGAAGGTGGAGAGAGAGACAG
AGACAGATCCATTCGATTAGTGAACGGATCTCGACGGTATCGGTTAACTTTTAA
AAGAAAAGGGGGGATTGGGGGGTACAGTGCAGGGGAAAGAATAGTAGACATAA
TAGCAACAGACATACAAACTAAAGAATTACAAAAACAAATTACAAAAATTCAAAA
TTTTATCGATGGTCGAGTACCGGGTAGGGGAGGCGCTTTTCCCAAGGCAGTCT

GGAGCATGCGCTTTAGCAGCCCCGCTGGGCACTTGGCGCTACACAAGTGGCC
TCTGGCCTCGCACACATTCCACATCCACCGGTAGGCGCCAACCGGCTCCGTTC
TTTGGTGGCCCCTTCGCGCCACCTTCTACTCCTCCCCTAGTCAGGAAGTTCCCC
CCCGCCCCGCAGCTCGCGTCGTGCAGGACGTGACAAATGGAAGTAGCACGTC
TCACTAGTCTCGTGCAGATGGACAGCACCGCTGAGCAATGGAAGCGGGTAGGC
CTTTGGGGCAGCGGCCAATAGCAGCTTTGCTCCTTCGCTTTCTGGGCTCAGAG
GCTGGGAAGGGGTGGGTCCGGGGGCGGGCTCAGGGGCGGGCTCAGGGGCG
GGGCGGGCGCCCGAAGGTCCTCCGGAGGCCCGGCATTCTGCACGCTTCAAAA
GCGCACGTCTGCCGCGCTGTTCTCCTCTTCCTCATCTCCGGGCCTTTCGACCT
CTAGGATCCaccggtGCCACCATGGCCATGAGCAGCGGCGGCTCTGGCGGCGGA
GTGCCCGAGCAGGAAGATAGCGTCCTGTTCAGGCGGGGCACCGGCCAGAGCG
ACGACAGCGACATCTGGGACGACACCGCCCTGATCAAGGCCTACGACAAGGC
CGTGGCCAGCTTCAAGCACGCCCTGAAGAACGGCGACATCTGCGAGACCAGC
GGCAAGCCCAAGACCACCCCCAAGCGGAAGCCCGCCAAGAAGAACAAGAGCC
AGAAGAAGAACACCGCCGCCAGCCTGCAGCAGTGGAAAGTGgtcgacCTGTCCC
CCATCTGCGAAGTGGCCAACAACATCGAGCAGAACGCCCAGGAAAACGAGAAC
GAGAGCCAAGTGTCCACCGACGAGAGCGAGAACAGCAGAAGCCCCGGCAACA
AGAGCGACAACATCAAGCCTAAGAGCGCCCCCTGGAACAGCTTCCTGCCCCCT
CCCCCCCCTATGCCTGGCCCCAGGCTGGGCCCTGGCAAGCCCGGCCTGAAGT
TCAACGGCCCTCCCCCTCCTCCCCCACCCCCTCCACCTCACCTGCTGTCTTGC
TGGCTGCCCCCCTTCCCCAGCGGCCCTCCCATCATCCCCCCACCTCCCCCTAT
CTGCCCCGACAGCCTGGACGACGCCGACGCCCTGGGCAGCATGCTGATCAGC
TGGTACATGAGCGGCTACCACACCGGCTATTACATGGGCTTCCGGCAGAACCA
GAAAGAGGGCCGCTGCAGCCACAGCCTGAACTGAggagaaatgctggcatagagcagca
ctaaatgacaccactaaagaaacgatcagacagatctggaatgtgaagcgttatagaagataactggcctcatttctt
caaaatatcaagtgttgggaaagaaaaaaggaagtggaatgggtaactcttcttgattaaaagttatgtaataaccaa
atgcaatgtgaaatattttactggactctattttgaaaaaccatctgtaaaagactggggtgggggtgggaggccagca
cggtggtgaggcagttgagaaaatttgaatgtggattagattttgaatgatattggataattattggtaattttatgagctgt
gagaagggtgttgtagtttataaaagactgtcttaatttgcatacttaagcatttaggaatgaagtgttagagtgtcttaaa
atgtttcaaatggtttaacaaaatgtatgtgaggcgtatgtggcaaaatgttacagaatctaactggtggacatggctgtt
cattgtactgaattctgcagatatccatcacactggcggccgCTCGAGGGAATTCCGATAATCAACCT
CTGGATTACAAAATTTGTGAAAGATTGACTGGTATTCTTAACTATGTTGCTCCTT
TTACGCTATGTGGATACGCTGCTTTAATGCCTTTGTATCATGCTATTGCTTCCCG
TATGGCTTTCATTTTCTCCTCCTTGTATAAATCCTGGTTGCTGTCTCTTTATGAG
GAGTTGTGGCCCGTTGTCAGGCAACGTGGCGTGGTGTGCACTGTGTTTGCTGA
CGCAACCCCCACTGGTTGGGGCATTGCCACCACCTGTCAGCTCCTTTCCGGGA
CTTTCGCTTTCCCCCTCCCTATTGCCACGGCGGAACTCATCGCCGCCTGCCTTG
CCCGCTGCTGGACAGGGGCTCGGCTGTTGGGCACTGACAATTCCGTGGTGTT
GTCGGGGAAGCTGACGTCCTTTCCATGGCTGCTCGCCTGTGTTGCCACCTGGA
TTCTGCGCGGGACGTCCTTCTGCTACGTCCCTTCGGCCCTCAATCCAGCGGAC
CTTCCTTCCCGCGGCCTGCTGCCGGCTCTGCGGCCTCTTCCGCGTCTTCGCCT
TCGCCCTCAGACGAGTCGGATCTCCCTTTGGGCCGCCTCCCCGCATCGGGAAT
TCGAGCTCGGTACCTTTAAAACCAATGACTTACAAGGCAGCTGTAAATCTTAGC
CACTTTTTAAAAGAAAAGGGGGGACTGGAAGGGCTAATTCACTCCCAACGAAAA

CAAAATCTGCTTTTTGCTTGTACTGGGTCTCTCTGGTTAGACCAAATCTGAGCCT
GGGAGCTCTCTGGCTAACTAGGGAACCCACTGCTTAAGCCTCAATAAAGCTTG
CCTTGAGTGCTTCAAGTAGTGTGTGCCCGTCTGTTGTGTGACTCTGGTAACTAG
AGATCCCTCAAACCCTTTTAGTCAGTGTGGAAAATCTCTAGCAGCATCTAGAATT
AATTCCGTGTATTCTATAGTGTCACCTAAATCGTATGTGTATGATACATAAGGTT
ATGTATTAATTGTAGCCGCGTTCTAACGACAATATGTACAAGCCTAATTGTGTAG
CATCTGGCTTACTGAAGCAGACCCTATCATCTCTCTCGTAAACTGCCGTCAGAG
TCGGTTTGGTTGGACGAACCTTCTGAGTTTCTGGTAACGCCGTCCCGCACCCG
GAAATGGTCAGCGAACCAATCAGCAGGGTCATCGCTAGCCAGATCCTCTACGC
CGGACGCATCGTGGCCGGCATCACCGGCGCCACAGGTGCGGTTGCTGGCGCC
TATATCGCCGACATCACCGATGGGGAAGATCGGGCTCGCCACTTCGGGCTCAT
GAGCGCTTGTTTCGGCGTGGGTATGGTGGCAGGCCCCGTGGCCGGGGGACTG
TTGGGCGCCATCTCCTTGCATGCACCATTCCTTGCGGCGGCGGTGCTCAACGG
CCTCAACCTACTACTGGGCTGCTTCCTAATGCAGGAGTCGCATAAGGGAGAGC
GTCGATATGGTGCACTCTCAGTACAATCTGCTCTGATGCCGCATAGTTAAGCCA
GCCCCGACACCCGCCAACACCCGCTGACGCGCCCTGACGGGCTTGTCTGCTC
CCGGCATCCGCTTACAGACAAGCTGTGACCGTCTCCGGGAGCTGCATGTGTCA
GAGGTTTTCACCGTCATCACCGAAACGCGCGAGACGAAAGGGCCTCGTGATAC
GCCTATTTTTATAGGTTAATGTCATGATAATAATGGTTTCTTAGACGTCAGGTGG
CACTTTTCGGGGAAATGTGCGCGGAACCCCTATTTGTTTATTTTTCTAAATACAT
TCAAATATGTATCCGCTCATGAGACAATAACCCTGATAAATGCTTCAATAATATT
GAAAAAGGAAGAGTATGAGTATTCAACATTTCCGTGTCGCCCTTATTCCCTTTTT
TGCGGCATTTTGCCTTCCTGTTTTTGCTCACCCAGAAACGCTGGTGAAAGTAAA
AGATGCTGAAGATCAGTTGGGTGCACGAGTGGGTTACATCGAACTGGATCTCA
ACAGCGGTAAGATCCTTGAGAGTTTTCGCCCCGAAGAACGTTTTCCAATGATGA
GCACTTTTAAAGTTCTGCTATGTGGCGCGGTATTATCCCGTATTGACGCCGGGC
AAGAGCAACTCGGTCGCCGCATACACTATTCTCAGAATGACTTGGTTGAGTACT
CACCAGTCACAGAAAAGCATCTTACGGATGGCATGACAGTAAGAGAATTATGCA
GTGCTGCCATAACCATGAGTGATAACACTGCGGCCAACTTACTTCTGACAACGA
TCGGAGGACCGAAGGAGCTAACCGCTTTTTTGCACAACATGGGGGATCATGTA
ACTCGCCTTGATCGTTGGGAACCGGAGCTGAATGAAGCCATACCAAACGACGA
GCGTGACACCACGATGCCTGTAGCAATGGCAACAACGTTGCGCAAACTATTAA
CTGGCGAACTACTTACTCTAGCTTCCCGGCAACAATTAATAGACTGGATGGAGG
CGGATAAAGTTGCAGGACCACTTCTGCGCTCGGCCCTTCCGGCTGGCTGGTTT
ATTGCTGATAAATCTGGAGCCGGTGAGCGTGGGTCTCGCGGTATCATTGCAGC
ACTGGGGCCAGATGGTAAGCCCTCCCGTATCGTAGTTATCTACACGACGGGGA
GTCAGGCAACTATGGATGAACGAAATAGACAGATCGCTGAGATAGGTGCCTCA
CTGATTAAGCATTGGTAACTGTCAGACCAAGTTTACTCATATATACTTTAGATTG
ATTTAAAACTTCATTTTTAATTTAAAAGGATCTAGGTGAAGATCCTTTTTGATAAT
CTCATGACCAAAATCCCTTAACGTGAGTTTTCGTTCCACTGAGCGTCAGACCCC
GTAGAAAAGATCAAAGGATCTTCTTGAGATCCTTTTTTTCTGCGCGTAATCTGCT
GCTTGCAAACAAAAAAACCACCGCTACCAGCGGTGGTTTGTTTGCCGGATCAA
GAGCTACCAACTCTTTTTCCGAAGGTAACTGGCTTCAGCAGAGCGCAGATACCA
AATACTGTCCTTCTAGTGTAGCCGTAGTTAGGCCACCACTTCAAGAACTCTGTA

GCACCGCCTACATACCTCGCTCTGCTAATCCTGTTACCAGTGGCTGCTGCCAGT
GGCGATAAGTCGTGTCTTACCGGGTTGGACTCAAGACGATAGTTACCGGATAA
GGCGCAGCGGTCGGGCTGAACGGGGGGTTCGTGCACACAGCCCAGCTTGGA
GCGAACGACCTACACCGAACTGAGATACCTACAGCGTGAGCTATGAGAAAGCG
CCACGCTTCCCGAAGGGAGAAAGGCGGACAGGTATCCGGTAAGCGGCAGGGT
CGGAACAGGAGAGCGCACGAGGGAGCTTCCAGGGGGAAACGCCTGGTATCTT
TATAGTCCTGTCGGGTTTCGCCACCTCTGACTTGAGCGTCGATTTTTGTGATGC
TCGTCAGGGGGGCGGAGCCTATGGAAAAACGCCAGCAACGCGGCCTTTTTAC
GGTTCCTGGCCTTTTGCTGGCCTTTTGCTCACATGTTCTTTCCTGCGTTATCCCC
TGATTCTGTGGATAACCGTATTACCGCCTTTGAGTGAGCTGATACCGCTCGCCG
CAGCCGAACGACCGAGCGCAGCGAGTCAGTGAGCGAGGAAGCGGAAGAGCG
CCCAATACGCAAACCGCCTCTCCCCGCGCGTTGGCCGATTCATTAATGCAGCT
GTGGAATGTGTGTCAGTTAGGGTGTGGAAAGTCCCCAGGCTCCCCAGCAGGCA
GAAGTATGCAAAGCATGCATCTCAATTAGTCAGCAACCAGGTGTGGAAAGTCCC
CAGGCTCCCCAGCAGGCAGAAGTATGCAAAGCATGCATCTCAATTAGTCAGCA
ACCATAGTCCCGCCCCTAACTCCGCCCATCCCGCCCCTAACTCCGCCCAGTTC
CGCCCATTCTCCGCCCCATGGCTGACTAATTTTTTTTATTTATGCAGAGGCCGA
GGCCGCCTCGGCCTCTGAGCTATTCCAGAAGTAGTGAGGAGGCTTTTTTGGAG
GCCTAGGCTTTTGCAAAAAGCTTGGACACAAGACAGGCTTGCGAGATATGTTTG
AGAATACCACTTTATCCCGCGTCAGGGAGAGGCAGTGCGTAAAAAGACGCGGA
CTCATGTGAAATACTGGTTTTTAGTGCGCCAGATCTCTATAATCTCGCGCAACCT
ATTTTCCCCTCGAACACTTTTTAAGCCGTAGATAAACAGGCTGGGACACTTCAC
ATGAGCGAAAAATACATCGTCACCTGGGACATGTTGCAGATCCATGCACGTAAA
CTCGCAAGCCGACTGATGCCTTCTGAACAATGGAAAGGCATTATTGCCGTAAGC
CGTGGCGGTCTGTACCGGGTGCGTTACTGGCGCGTGAACTGGGTATTCGTCAT
GTCGATACCGTTTGTATTTCCAGCTACGATCACGACAACCAGCGCGAGCTTAAA
GTGCTGAAACGCGCAGAAGGCGATGGCGAAGGCTTCATCGTTATTGATGACCT
GGTGGATACCGGTGGTACTGCGGTTGCGATTCGTGAAATGTATCCAAAAGCGC
ACTTTGTCACCATCTTCGCAAAACCGGCTGGTCGTCCGCTGGTTGATGACTATG
TTGTTGATATCCCGCAAGATACCTGGATTGAACAGCCGTGGGATATGGGCGTC
GTATTCGTCCCGCCAATCTCCGGTCGCTAATCTTTTCAACGCCTGGCACTGCCG
GGCGTTGTTCTTTTTAACTTCAGGCGGGTTACAATAGTTTCCAGTAAGTATTCTG
GAGGCTGCATCCATGACACAGGCAAACCTGAGCGAAACCCTGTTCAAACCCCG
CTTTAAACATCCTGAAACCTCGACGCTAGTCCGCCGCTTTAATCACGGCGCACA
ACCGCCTGTGCAGTCGGCCCTTGATGGTAAAACCATCCCTCACTGGTATCGCA
TGATTAACCGTCTGATGTGGATCTGGCGCGGCATTGACCCACGCGAAATCCTC
GACGTCCAGGCACGTATTGTGATGAGCGATGCCGAACGTACCGACGATGATTT
ATACGATACGGTGATTGGCTACCGTGGCGGCAACTGGATTTATGAGTGGGCCC
CGGATCTTTGTGAAGGAACCTTACTTCTGTGGTGTGACATAATTGGACAAACTA
CCTACAGAGATTTAAAGCTCTAAGGTAAATATAAAATTTTTAAGTGTATAATGTGT
TAAACTACTGATTCTAATTGTTTGTGTATTTTAGATTCCAACCTATGGAACTGATG
AATGGGAGCAGTGGTGGAATGCCTTTAATGAGGAAAACCTGTTTTGCTCAGAAG
AAATGCCATCTAGTGATGATGAGGCTACTGCTGACTCTCAACATTCTACTCCTC
CAAAAAAGAAGAGAAAGGTAGAAGACCCCAAGGACTTTCCTTCAGAATTGCTAA

GTTTTTTGAGTCATGCTGTGTTTAGTAATAGAACTCTTGCTTGCTTTGCTATTTAC
ACCACAAAGGAAAAAGCTGCACTGCTATACAAGAAAATTATGGAAAAATATTCTG
TAACCTTTATAAGTAGGCATAACAGTTATAATCATAACATACTGTTTTTTCTTACT
CCACACAGGCATAGAGTGTCTGCTATTAATAACTATGCTCAAAAATTGTGTACCT
TTAGCTTTTTAATTTGTAAAGGGGTTAATAAGGAATATTTGATGTATAGTGCCTT
GACTAGAGATCATAATCAGCCATACCACATTTGTAGAGCTTTTACTTGCTTTAAA
AAACCTCCCACACCTCCCCCTGAACCTGAAACATAAAATGAATGCAATTGTTGTT
GTTAACTTGTTTATTGCAGCTTATAATGGTTACAAATAAAGCAATAGCATCACAA
ATTTCACAAATAAAGCATTTTTTTCACTGCATTCTAGTTGTGGTTTGTCCAAACTC
ATCAATGTATCTTATCATGTGTGGATCAACTGGATAACTCAAGCTAACCAAAATC
ATCCCAAACTTCCCACCCCATACCCTATTACCACTGCCAAATTACCTGTGGTTTC
ATTTACTCTAAACCTGTGATTCCTCTGAATTATTTTCATTTTAAAGAAATTGTATTT
GTTAAATATGTACTACAAACTTAGTAGT

OUTCOMES OF PHD PROGRAMME

Publications

1. Walker, C., Herranz-Martin, S., **Karyka, E**., Liao, C., Lewis, K., Elsayed, W., Lukashchuk, V., Chiang, S.C., Ray, S., Mulcahy, P.J., Jurga, M., Tsagakis, I., Iannitti, T., Chandran, J., Coldicott, I., De Vos, K.J., Hassan, M.K., Higginbottom, A., Shaw, P.J., Hautbergue, G.M., Azzouz, M., El-Khamisy, S.F., 2017. C9orf72 expansion disrupts ATM-mediated chromosomal break repair. Nature neuroscience 20, 1225-1235.
2. Hautbergue, G.M., Castelli, L.M., Ferraiuolo, L., Sanchez-Martinez, A., Cooper-Knock, J., Higginbottom, A., Lin, Y.H., Bauer, C.S., Dodd, J.E., Myszczynska, M.A., Alam, S.M., Garneret, P., Chandran, J.S., **Karyka, E**., Stopford, M.J., Smith, E.F., Kirby, J., Meyer, K., Kaspar, B.K., Isaacs, A.M., El-Khamisy, S.F., De Vos, K.J., Ning, K., Azzouz, M., Whitworth, A.J., Shaw, P.J., 2017. SRSF1-dependent nuclear export inhibition of C9ORF72 repeat transcripts prevents neurodegeneration and associated motor deficits. Nature communications 8, 16063.
3. Powis, R.A., **Karyka, E**., Boyd, P., Come, J., Jones, R.A., Zheng, Y., Szunyogova, E., Groen, E.J., Hunter, G., Thomson, D., Wishart, T.M., Becker, C.G., Parson, S.H., Martinat, C., Azzouz, M., Gillingwater, T.H., 2016. Systemic restoration of UBA1 ameliorates disease in spinal muscular atrophy. JCI insight 1, e87908.

4. Mulcahy, P.J., Binny, C., Muszynski, B., **Karyka, E**., Azzouz, M., 2015. Adeno-Associated Vectors for Gene Delivery to the Nervous System, in: Bo, X., Verhaagen, J. (Eds.), Gene Delivery and Therapy for Neurological Disorders. Springer New York, New York, NY, pp. 1-22.
5. Mulcahy, P.J., Iremonger, K., **Karyka, E**., Herranz-Martin, S., Shum, K.T., Tam, J.K., Azzouz, M., 2014. Gene therapy: a promising approach to treating spinal muscular atrophy. Human gene therapy 25, 575-586.
6. Tam, J.K.V., **Karyka, E**., Azzouz, M., 2014. Current and investigational treatments for spinal muscular atrophy. Expert Opinion on Orphan Drugs 2, 465-476.

Manuscripts under review

Jayanth S. Chandran, Paul S. Sharp, **Evangelia Karyka**, João Miguel da Conceição Alves do Cruzeiro, Ian Coldicott, Lydia Castelli, Guillaume Hautbergue, Mark Collins, and Mimoun Azzouz. Site Specific Modification of Adeno-Associated Virus Enables Both Fluorescent Imaging of Viral Particles and Identification of the Capsid Interactome.

Manuscripts in preparation

Karyka E., Liao C., Lewis K., Walker C., Herranz-Martin S., Ray S., Chiang S.H., Lukashchuk V., Iannitti T, Jones T., Ferraiuolo L., Gillingwater T., Hautbergue G., El-El-Khamisy S.[#], Azzouz M.[#]. R loop resolution reverses DNA instability associated with SMN deficiency and protects against neurodegeneration in SMA, *in preparation*

[#] Equal contribution

Presentations at conferences/symposia

Karyka E., Walker C., El-Khamisy S., Azzouz M. (2016), Defective chromosomal break repair in spinal muscular atrophy. Poster presentation. 4th RNA Metabolism in Neurological Disease, 11th Brain Research Conference. Satellite to the 2016 Meeting of the Society of Neuroscience. 10-11 November 2016, Paradise Point, San Diego, CA, USA.